Gamma-Ray Bursts

Contents

1 Topics

- GRB classification in different families with different progenitor systems.
- "Genuine short" GRBs: Possible identifications and selection effects
- The observed spectra of the P-GRBs.
- GRB prompt emission spectra below 5 keV: challenges for future missions.
- Interpretation of the ultra high energy emission from GRBs observed by Fermi, AGILE and MAGIC.
- Analysis of different families of progenitors for GRBs with different energetics.
- GRBs at redshift $z > 6$.
- GRBs originating from a multiple collapse.
- Emission from newly born neutron stars, or "neo neutron stars" (νNS).
- Induced Gravitational Collapse process for GRBs associated with supernovae.
- Redshift estimators for GRBs with no measured redshift.
- Binary Driven Hypernovae (BdHNe) as progenitor of GRBs via Induced Gravitational Collapse.
- GRB light curves as composed of different episodes.
- "Cosmic Matrix" for GRBs.
- GRB X-Ray Flares and Gamma-Ray Flares.

- GRB afterglow theory consistent with the mildly relativistic velocities inferred from the observations.
- Extended thermal emission components in GRBs.
- GRBs from merging white dwarfs.
- “Inner engine” of GRB emission.
- Quantized emission in GRBs.
- Redshift distribution of all different GRB families.
- Observations of early X-ray afterglow emission in high-redshift GRBs: implications for the νNS-rise.
- Connections between Long and Short GRB families.

2 Participants

2.1 ICRANet participants

- David Arnett
- Carlo Luciano Bianco
- Massimo Della Valle
- Li Liang
- Rahim Moradi
- Jorge Armando Rueda Hernandez
- Remo Ruffini
- Narek Sahakyan
- Gregory Vereshchagin
- Yu Wang
- She-Sheng Xue

2.2 Past collaborators

- Andrey Baranov
- Maria Grazia Bernardini (OAB, Italy)
- Joao Braga (INPE, Brazil)
- Sabrina Casanova (MPIK, Germany)

- Letizia Caito
- Pascal Chardonnet (Université de Savoie, France)
- Guido Chincarini (Università di Milano "Bicocca", Italy)
- Demetrios Christodoulou (ETH Zurich, Switzerland)
- Alessandra Corsi (INAF-IASF Roma, Italy)
- Valeri Chechetkin
- Maria Giovanna Dainotti
- Thibault Damour (IHES, France)
- Maxime Enderli
- Walter Ferrara
- Federico Fraschetti (CEA Saclay, France)
- Roberto Guida
- Vahe Gurzadyan (Yerevan Physics Institute, Armenia)
- Wen-Biao Han
- Milos Kovacevic
- Massimiliano Lattanzi (Oxford Astrophysics, UK)
- Vincenzo Liccardo
- Hendrik Ludwig
- Marco Muccino
- Nino Panagia
- Barbara Patricelli (Pisa University, Italy)
- Elena Pian
- Giovanni Battista Pisani

- Giuliano Preparata (Università di Milano, Italy)
- Daria Primorac
- Jay D. Salmonson (Livermore Lab, USA)
- Vineeth Valsan
- Jim Wilson (Livermore Lab, USA)

2.3 Ongoing collaborations

- Alexey Aksenov (ITEP, Russia)
- Lorenzo Amati (INAF-IASF Bologna, Italy)
- Ulisses Barres de Almeida (CBPF, Brazil)
- Laura Marcela Becerra Bayona (Universidad Mayor, Santiago de Chile, Chile)
- Riccardo Belvedere (ICRANet-Rio, Brazil)
- Sandip Kumar Chakrabarti (S.N. Bose National Centre and Indian Centre for Space Physics, India)
- Christian Cherubini (Università Campus Biomedico, Italy)
- Alessandro Chieffi (INAF-IASF Roma, Italy)
- Stefano Covino (OAB, Italy)
- Gustavo de Barros (UFRJ, Brazil)
- Simonetta Filippi (Università Campus Biomedico, Italy)
- Filippo Frontera (Università di Ferrara, Italy)
- Chris Fryer (Los Alamos National Laboratories, USA).
- Dafne Guetta (OAR, Italy)
- Cristiano Guidorzi (OAB, Italy)

- Stanislav Kelner (MEPhI, Russia, and MPIK, Germany)
- Marco Limongi (OAR, Italy)
- Clovis Maia (University of Brasilia, Brazil)
- Vanessa Mangano (INAF-IASF Palermo, Italy)
- Marco Marongiu (INAF - Cagliari Observatory and University of Ferrara, Italy)
- Grant Mathews (University of Notre Dame, USA)
- Taghi Mirtorabi (Alzahra University, Tehran, Iran)
- Ana Virginia Penacchioni (INPE, Brazil)
- Luis Juracy Rangel Lemos (Fundação Universidade Federal do Tocantins, Brazil)
- Felix Ryde (KTH Royal Institute of Technology, Stockholm, Sweden)
- Soroush Shakeri (Isfahan University of Technology, Iran)
- Ivan Siutsou (ICRANet-Rio, Brazil)
- Bing Zhang (University of Nevada, USA)
- Susanna Vergani (Dunsink Observatory, Ireland)
- Francesco Vissani (INFN, Italy)
- Elena Zaninoni (ICRANet-Rio, Brazil)

2.4 Students

- Yerlan Aimuratov (IRAP PhD, Kazakhstan)
- Stefano Campion (IRAP PhD, Italy)
- Yen-Chen Chen (IRAP-PhD, China-Taiwan)
- Mile Karlika (IRAP PhD, Croatia)

- Ronaldo V. Lobato (IRAP-PhD, Brazil)
- J. David Melon Fuksman (IRAP PhD, Argentina)
- Jose Fernando Rodriguez Ruiz (IRAP PhD, Colombia)
- Shurui Zhang (JIRA PhD, China)

3 Selected publications before 2005

3.1 Refereed journals

1. D. Christodoulou, R. Ruffini; "Reversible Transformations of a Charged Black Hole"; Physical Review D, 4, 3552 (1971).

   A formula is derived for the mass of a black hole as a function of its "irreducible mass", its angular momentum, and its charge. It is shown that 50% of the mass of an extreme charged black hole can be converted into energy as contrasted with 29% for an extreme rotating black hole.

2. T. Damour, R. Ruffini; "Quantum electrodynamical effects in Kerr-Newman geometries"; Physical Review Letters, 35, 463 (1975).

   Following the classical approach of Sauter, of Heisenberg and Euler and of Schwinger the process of vacuum polarization in the field of a "bare" Kerr-Newman geometry is studied. The value of the critical strength of the electromagnetic fields is given together with an analysis of the feedback of the discharge on the geometry. The relevance of this analysis for current astrophysical observations is mentioned.

3. G. Preparata, R. Ruffini, S.-S. Xue; "The dyadosphere of black holes and gamma-ray bursts"; Astronomy & Astrophysics, 338, L87 (1999).

   The "dyadosphere" has been defined as the region outside the horizon of a black hole endowed with an electromagnetic field (abbreviated to EMBH for "electromagnetic black hole") where the electromagnetic field exceeds the critical value, predicted by Heisenberg & Euler for $e^{\pm}$ pair production. In a very short time ($\sim O(\hbar/mc^2)$) a very large number of pairs is created there. We here give limits on the EMBH parameters leading to a Dyadosphere for $10M_{\odot}$ and $10^5M_{\odot}$ EMBH's, and give as well the pair densities as functions of the radial coordinate. We here assume that the pairs reach thermodynamic equilibrium with a photon gas and estimate the average energy per pair as a function of the EMBH mass. These data give the initial conditions for the analysis of an enormous pair-electromagnetic-pulse or "P.E.M. pulse" which naturally leads to relativistic expansion. Basic energy requirements for gamma ray bursts (GRB), including GRB971214 recently observed at z=3.4, can be accounted for by processes occurring in the dyadosphere. In this letter we do not address the problem of forming either the EMBH or the dyadosphere: we establish some inequalities which must be satisfied during their formation process.

4. R. Ruffini, J.D. Salmonson, J.R. Wilson, S.-S. Xue; "On the pair electromagnetic pulse of a black hole with electromagnetic structure"; Astronomy & Astrophysics, 350, 334 (1999).

   We study the relativistically expanding electron-positron pair plasma formed by the process of vacuum polarization around an electromagnetic black hole (EMBH). Such processes can occur for EMBH's with mass all the way up to $6 \times 10^5 M_\odot$. Beginning with a idealized model of a Reissner-Nordstrom EMBH with charge to mass ratio $\xi = 0.1$, numerical hydrodynamic calculations are made to model the expansion of the pair-electromagnetic pulse (PEM pulse) to the point that the system is transparent to photons. Three idealized special relativistic models have been compared and contrasted with the results of the numerically integrated general relativistic hydrodynamic equations. One of the three models has been validated: a PEM pulse of constant thickness in the laboratory frame is shown to be in excellent agreement with results of the general relativistic hydrodynamic code. It is remarkable that this precise model, starting from the fundamental parameters of the EMBH, leads uniquely to the explicit evaluation of the parameters of the PEM pulse, including the energy spectrum and the astrophysically unprecedented large Lorentz factors (up to 6×10^3 for a $10^3 M_\odot$ EMBH). The observed photon energy at the peak of the photon spectrum at the moment of photon decoupling is shown to range from 0.1 MeV to 4 MeV as a function of the EMBH mass. Correspondingly the total energy in photons is in the range of 10^{52} to 10^{54} ergs, consistent with observed gamma-ray bursts. In these computations we neglect the presence of baryonic matter which will be the subject of forthcoming publications.

5. R. Ruffini, J.D. Salmonson, J.R. Wilson, S.-S. Xue; "On the pair-electro magnetic pulse from an electromagnetic black hole surrounded by a baryonic remnant"; Astronomy & Astrophysics, 359, 855 (2000).

   The interaction of an expanding Pair-Electromagnetic pulse (PEM pulse) with a shell of baryonic matter surrounding a Black Hole with electromagnetic structure (EMBH) is analyzed for selected values of the baryonic mass at selected distances well outside the dyadosphere of an EMBH. The dyadosphere, the region in which a super critical field exists for the creation of e+e- pairs, is here considered in the special case of a Reissner-Nordstrom geometry. The interaction of the PEM pulse with the baryonic matter is described using a simplified model of a slab of constant thickness in the laboratory frame (constant-thickness approximation) as well as performing the integration of the general relativistic hydrodynamical equations. Te validation of the constant-thickness approximation, already presented in a previous paper Ruffini et al. (1999) for a PEM pulse in vacuum, is here generalized to the presence of baryonic matter. It is found that for a baryonic shell of mass-energy less than 1% of the total energy of the dyadosphere, the constant-thickness approximation is in excellent agreement with full general relativistic computations. The approximation breaks down for larger values of the baryonic shell mass, however such cases are of less interest for observed Gamma Ray Bursts (GRBs). On the basis of numerical computations of the slab model for PEM pulses, we describe (i) the properties of relativistic evolution of a PEM pulse colliding with a baryonic shell; (ii) the details of the expected emission energy and observed temperature of the associated GRBs for a given value of the EMBH mass; $10^3 M_\odot$, and for baryonic mass-energies in the range 10^{-8} to 10^{-2} the total energy of the dyadosphere.

6. C.L. Bianco, R. Ruffini, S.-S. Xue; "The elementary spike produced by a pure e+e- pair-electromagnetic pulse from a Black Hole: The PEM Pulse"; Astronomy & Astrophysics, 368, 377 (2001).

   In the framework of the model that uses black holes endowed with electromagnetic structure (EMBH) as the energy source, we study how an elementary spike appears to the detectors. We consider the simplest possible case of a pulse produced by a pure e^+e^- pair-electro-magnetic plasma, the PEM pulse, in the absence of any baryonic matter. The resulting time profiles show a *Fast-Rise-Exponential-Decay* shape, followed by a power-law tail. This is obtained without any special fitting procedure, but only by fixing the energetics of the process taking place in a given EMBH of selected mass, varying in the range from 10 to 10^3 $M_\odot$ and considering the relativistic effects to be expected in an electron-positron plasma gradually reaching transparency. Special attention is given to the contributions from all regimes with Lorentz γ factor varying from $\gamma = 1$ to $\gamma = 10^4$ in a few hundreds of the PEM pulse travel time. Although the main goal of this paper is to obtain the elementary spike intensity as a function of the arrival time, and its observed duration, some qualitative considerations are also presented regarding the expected spectrum and on its departure from the thermal one. The results of this paper will be comparable, when data will become available, with a subfamily of particularly short GRBs not followed by any afterglow. They can also be propedeutical to the study of longer bursts in presence of baryonic matter currently observed in GRBs.

7. R. Ruffini, C.L. Bianco, P. Chardonnet, F. Fraschetti, S.-S. Xue; "Relative spacetime transformations in Gamma-Ray Bursts"; The Astrophysical Journal, 555, L107 (2001).

   The GRB 991216 and its relevant data acquired from the BATSE experiment and RXTE and Chandra satellites are used as a prototypical case to test the theory linking the origin of gamma ray bursts (GRBs) to the process of vacuum polarization occurring during the formation phase of a black hole endowed with electromagnetic structure (EMBH). The relative space-time transformation paradigm (RSTT paradigm) is presented. It relates the observed signals of GRBs to their past light cones, defining the events on the worldline of the source essential for the interpretation of the data. Since GRBs present regimes with unprecedently large Lorentz γ factor, also sharply varying with time, particular attention is given to the constitutive equations relating the four time variables: the comoving time, the laboratory time, the arrival time at the detector, duly corrected by the cosmological effects. This paradigm is at the very foundation of any possible interpretation of the data of GRBs.

8. R. Ruffini, C.L. Bianco, P. Chardonnet, F. Fraschetti, S.-S. Xue; "On the interpretation of the burst structure of Gamma-Ray Bursts"; The Astrophysical Journal, 555, L113 (2001).

   Given the very accurate data from the BATSE experiment and RXTE and Chandra satellites, we use the GRB 991216 as a prototypical case to test the EMBH theory linking the origin of the energy of GRBs to the electromagnetic energy of black holes. The fit of the afterglow fixes the only two free parameters of the model and leads to a new paradigm for the interpretation of the burst structure, the IBS paradigm. It leads as well to a reconsideration of the relative roles of the afterglow and burst in GRBs by defining two new phases in this complex phenomenon: a) the injector phase, giving rise to the proper-GRB (P-GRB), and b) the beam-target phase, giving rise to the extended afterglow peak emission (E-APE) and to the afterglow. Such differentiation leads to a natural possible explanation of the bimodal distribution of GRBs observed by BATSE. The agreement with the observational data in regions extending from the horizon of the EMBH all the way out to the distant observer confirms the uniqueness of the model.

9. R. Ruffini, C.L. Bianco, P. Chardonnet, F. Fraschetti, S.-S. Xue; "On a possible Gamma-Ray Burst-Supernova time sequence"; The Astrophysical Journal, 555, L117 (2001).

   The data from the Chandra satellite on the iron emission lines in the afterglow of GRB 991216 are used to give further support for the EMBH theory, which links the origin of the energy of GRBs to the extractable energy of electromagnetic black holes (EMBHs), leading to an interpretation of the GRB-supernova correlation. Following the relative space-time transformation (RSTT) paradigm and the interpretation of the burst structure (IBS) paradigm, we introduce a paradigm for the correlation between GRBs and supernovae. The following sequence of events is shown as kinematically possible and consistent with the available data: a) the GRB-progenitor star P_1 first collapses to an EMBH, b) the proper GRB (P-GRB) and the peak of the afterglow (E-APE) propagate in interstellar space until the impact on a supernova-progenitor star P_2 at a distance $\leq 2.69 \times 10^{17}$ cm, and they induce the supernova explosion, c) the accelerated baryonic matter (ABM) pulse, originating the afterglow, reaches the supernova remnants 18.5 hours after the supernova explosion and gives rise to the iron emission lines. Some considerations on the dynamical implementation of the paradigm are presented. The concept of induced supernova explosion introduced here specifically for the GRB-supernova correlation may have more general application in relativistic astrophysics.

10. R. Ruffini, C.L. Bianco, P. Chardonnet, F. Fraschetti, S.-S. Xue; "On the physical processes which lie at the bases of time variability of GRBs"; Il Nuovo Cimento B, 116, 99 (2001).

    The relative-space-time-transformation (RSTT) paradigm and the interpretation of the burst-structure (IBS) paradigm are applied to probe the origin of the time variability of GRBs. Again GRB 991216 is used as a prototypical case, thanks to the precise data from the CGRO, RXTE and Chandra satellites. It is found that with the exception of the relatively inconspicuous but scientifically very important signal originating from the initial "proper gamma ray burst" (P-GRB), all the other spikes and time variabilities can be explained by the interaction of the accelerated-baryonic-matter pulse with inhomogeneities in the interstellar matter. This can be demonstrated by using the RSTT paradigm as well as the IBS paradigm, to trace a typical spike observed in arrival time back to the corresponding one in the laboratory time. Using these paradigms, the identification of the physical nature of the time variablity of the GRBs can be made most convincingly. It is made explicit the dependence of a) the intensities of the afterglow, b) the spikes amplitude and c) the actual time structure on the Lorentz gamma factor of the accelerated-baryonic-matter pulse. In principle it is possible to read off from the spike structure the detailed density contrast of the interstellar medium in the host galaxy, even at very high redshift.

11. R. Ruffini, C.L. Bianco, P. Chardonnet, F. Fraschetti, S.-S. Xue; "On the structures in the afterglow peak emission of gamma ray bursts"; The Astrophysical Journal, 581, L19 (2002).

    Using GRB 991216 as a prototype, it is shown that the intensity substructures observed in what is generally called the "prompt emission" in gamma ray bursts (GRBs) do originate in the collision between the accelerated baryonic matter (ABM) pulse with inhomogeneities in the interstellar medium (ISM). The initial phase of such process occurs at a Lorentz factor $\gamma \sim 310$. The crossing of ISM inhomogeneities of sizes $\Delta R \sim 10^{15}$ cm occurs in a detector arrival time interval of ~ 0.4 s implying an apparent superluminal behavior of $\sim 10^5 c$. The long lasting debate between the validity of the external shock model vs. the internal shock model for GRBs is solved in favor of the first.

12. R. Ruffini, C.L. Bianco, P. Chardonnet, F. Fraschetti, S.-S. Xue; "On the structure of the burst and afterglow of Gamma-Ray Bursts I: the radial approximation"; International Journal of Modern Physics D, 12, 173 (2003).

    We have recently proposed three paradigms for the theoretical interpretation of gamma-ray bursts (GRBs). (1) The relative space-time transformation (RSTT) paradigm emphasizes how the knowledge of the entire world-line of the source from the moment of gravitational collapse is a necessary condition in order to interpret GRB data. (2) The interpretation of the burst structure (IBS) paradigm differentiates in all GRBs between an injector phase and a beam-target phase. (3) The GRB-supernova time sequence (GSTS) paradigm introduces the concept of *induced supernova explosion* in the supernovae-GRB association. In the introduction the RSTT and IBS paradigms are enunciated and illustrated using our theory based on the vacuum polarization process occurring around an electromagnetic black hole (EMBH theory). The results are summarized using figures, diagrams and a complete table with the space-time grid, the fundamental parameters and the corresponding values of the Lorentz gamma factor for GRB 991216 used as a prototype. In the following sections the detailed treatment of the EMBH theory needed to understand the results of the three above letters is presented. We start from the considerations on the dyadosphere formation. We then review the basic hydrodynamic and rate equations, the equations leading to the relative space-time transformations as well as the adopted numerical integration techniques. We then illustrate the five fundamental eras of the EMBH theory: the self acceleration of the e^+e^- pair-electromagnetic plasma (PEM pulse), its interaction with the baryonic remnant of the progenitor star, the further self acceleration of the e^+e^- pair-electroma--gnetic radiation and baryon plasma (PEMB pulse). We then study the approach of the PEMB pulse to transparency, the emission of the proper GRB (P-GRB) and its relation to the "short GRBs". Particular attention is given to the free parameters of the theory and to the values of the thermodynamical quantities at transparency. Finally the three different regimes of the afterglow are described within the fully radiative and radial approximations: the ultrarelativistic, the relativistic and the nonrelativistic regimes. The best fit of the theory leads to an unequivocal identification of the "long GRBs" as extended emission occurring at the afterglow peak (E-APE). The relative intensities, the time separation and the hardness ratio of the P-GRB and the E-APE are used as distinctive observational test of the EMBH theory and the excellent agreement between our theoretical predictions and the observations are documented. The afterglow power-law indexes in the EMBH theory are compared and contrasted with the ones in the literature, and no beaming process is found for GRB 991216. Finally, some preliminary results relating the observed time variability of the E-APE to the inhomogeneities in the interstellar medium are presented, as well as some general considerations on the EMBH formation. The issue of the GSTS paradigm will be the object of a forthcoming publication and the relevance of the iron-lines observed in GRB 991216 is shortly reviewed. The general conclusions are then presented based on the three fundamental parameters of the EMBH theory: the dyadosphere energy, the baryonic mass of the remnant, the interstellar medium density. An in depth discussion and comparison of the EMBH theory with alternative theories is presented as well as indications of further developments beyond the radial approximation, which will be the subject of paper II in this series. Future needs for specific GRB observations are outlined.

13. R. Ruffini, C.L. Bianco, P. Chardonnet, F. Fraschetti, V. Gurzadyan, S.-S. Xue; "On the instantaneous spectrum of gamma ray bursts"; International Journal of Modern Physics D, 13, 843 (2004).

    A theoretical attempt to identify the physical process responsible for the afterglow emission of Gamma-Ray Bursts (GRBs) is presented, leading to the occurrence of thermal emission in the comoving frame of the shock wave giving rise to the bursts. The determination of the luminosities and spectra involves integration over an infinite number of Planckian spectra, weighted by appropriate relativistic transformations, each one corresponding to a different viewing angle in the past light cone of the observer. The relativistic transformations have been computed using the equations of motion of GRBs within our theory, giving special attention to the determination of the equitemporal surfaces. The only free parameter of the present theory is the "effective emitting area" in the shock wave front. A self consistent model for the observed hard-to-soft transition in GRBs is also presented. When applied to GRB 991216 a precise fit $\left(\chi^2 \simeq 1.078\right)$ of the observed luminosity in the 2–10 keV band is obtained. Similarly, detailed estimates of the observed luminosity in the 50–300 keV and in the 10–50 keV bands are obtained.

3.2 Conference proceedings

1. R. Ruffini; "Beyond the critical mass: The dyadosphere of black holes"; in "Black Holes and High Energy Astrophysics", H. sato, N. Sugiyama, Editors; p. 167; Universal Academy Press (Tokyo, Japan, 1998).

   The "dyadosphere" (from the Greek word "duas-duados" for pairs) is here defined as the region outside the horizon of a black hole endowed with an electromagnetic field (abbreviated to EMBH for "electromagnetic black hole") where the electromagnetic field exceeds the critical value, predicted by Heisenberg and Euler for e^+e^- pair production. In a very short time ($\sim O(\hbar/mc^2)$), a very large number of pairs is created there. I give limits on the EMBH parameters leading to a Dyadosphere for $10M_\odot$ and $10^5M_\odot$ EMBH's, and give as well the pair densities as functions of the radial coordinate. These data give the initial conditions for the analysis of an enormous pair-electromagnetic-pulse or "PEM-pulse" which naturally leads to relativistic expansion. Basic energy requirements for gamma ray bursts (GRB), including GRB971214 recently observed at $z = 3.4$, can be accounted for by processes occurring in the dyadosphere.

2. R. Ruffini, C.L. Bianco, P. Chardonnet, F. Fraschetti, L. Vitagliano, S.-S. Xue; "New perspectives in physics and astrophysics from the theoretical understanding of Gamma-Ray Bursts"; in "COSMOLOGY AND GRAVITATION: Xth Brazilian School of Cosmology and Gravitation; 25th Anniversary (1977-2002)", Proceedings of the Xth Brazilian School on Cosmology and Gravitation, Mangaratiba, Rio de Janeiro (Brazil), July - August 2002, M. Novello, S.E. Perez Bergliaffa, Editors; AIP Conference Proceedings, 668, 16 (2003).

   If due attention is given in formulating the basic equations for the Gamma-Ray Burst (GRB) phenomenon and in performing the corresponding quantitative analysis, GRBs open a main avenue of inquiring on totally new physical and astrophysical regimes. This program is very likely one of the greatest computational efforts in physics and astrophysics and cannot be actuated using shortcuts. A systematic approach is needed which has been highlighted in three basic new paradigms: the relative space-time transformation (RSTT) paradigm, the interpretation of the burst structure (IBS) paradigm, the GRB-supernova time sequence (GSTS) paradigm. From the point of view of fundamental physics new regimes are explored: (1) the process of energy extraction from black holes; (2) the quantum and general relativistic effects of matter-antimatter creation near the black hole horizon; (3) the physics of ultrarelativisitc shock waves with Lorentz gamma factor $\gamma > 100$. From the point of view of astronomy and astrophysics also new regimes are explored: (i) the occurrence of gravitational collapse to a black hole from a critical mass core of mass $M \gtrsim 10M_{\odot}$, which clearly differs from the values of the critical mass encountered in the study of stars "catalyzed at the endpoint of thermonuclear evolution" (white dwarfs and neutron stars); (ii) the extremely high efficiency of the spherical collapse to a black hole, where almost 99.99% of the core mass collapses leaving negligible remnant; (iii) the necessity of developing a fine tuning in the final phases of thermonuclear evolution of the stars, both for the star collapsing to the black hole and the surrounding ones, in order to explain the possible occurrence of the "induced gravitational collapse". New regimes are as well encountered from the point of view of nature of GRBs: (I) the basic structure of GRBs is uniquely composed by a proper-GRB (P-GRB) and the afterglow; (II) the long bursts are then simply explained as the peak of the afterglow (the E-APE) and their observed time variability is explained in terms of inhomogeneities in the interstellar medium (ISM); (III) the short bursts are identified with the P-GRBs and the crucial information on general relativistic and vacuum polarization effects are encoded in their spectra and intensity time variability. A new class of space missions to acquire information on such extreme new regimes are urgently needed.

3. R. Ruffini, C.L. Bianco, P. Chardonnet, F. Fraschetti, S.-S. Xue; "The EMBH Model in GRB 991216 and GRB 980425"; in Proceedings of "Third Rome Workshop on Gamma-Ray Burst in the Afterglow Era", 17-20 September 2002; M. Feroci, F. Frontera, N. Masetti, L. Piro, Editors; ASP Conference Series, 312, 349 (2004).

   This is a summary of the two talks presented at the Rome GRB meeting by C.L. Bianco and R. Ruffini. It is shown that by respecting the Relative Space-Time Transformation (RSTT) paradigm and the Interpretation of the Burst Structure (IBS) paradigm, important inferences are possible: a) in the new physics occurring in the energy sources of GRBs, b) on the structure of the bursts and c) on the composition of the interstellar matter surrounding the source.

4. M.G. Bernardini, C.L. Bianco, P. Chardonnet, F. Fraschetti, R. Ruffini, S.-S. Xue; "A New Astrophysical 'Triptych': GRB030329/SN2003dh/URCA-2"; in "GAMMA-RAY BURSTS: 30 YEARS OF DISCOVERY", Proceedings of the Los Alamos "Gamma Ray Burst Symposium", Santa Fe, New Mexico, 8 – 12 September 2003, E.E. Fenimore, M. Galassi, Editors; AIP Conference Proceedings, 727, 312 (2004).

   We analyze the data of the Gamma-Ray Burst/Supernova GRB030329/SN2003dh system obtained by HETE-2, R-XTE, XMM and VLT within our theory for GRB030329. By fitting the only three free parameters of the EMBH theory, we obtain the luminosity in fixed energy bands for the prompt emission and the afterglow. Since the Gamma-Ray Burst (GRB) analysis is consistent with a spherically symmetric expansion, the energy of GRB030329 is $E = 2.1 \times 10^{52}$ erg, namely $\sim 2 \times 10^3$ times larger than the Supernova energy. We conclude that either the GRB is triggering an induced-supernova event or both the GRB and the Supernova are triggered by the same relativistic process. In no way the GRB can be originated from the supernova. We also evidence that the XMM observations, much like in the system GRB980425/SN1998bw, are not part of the GRB afterglow, as interpreted in the literature, but are associated to the Supernova phenomenon. A dedicated campaign of observations is needed to confirm the nature of this XMM source as a newly born neutron star cooling by generalized URCA processes.

5. F. Fraschetti, M.G. Bernardini, C.L. Bianco, P. Chardonnet, R. Ruffini, S.-S. Xue; "The GRB980425-SN1998bw Association in the EMBH Model"; in "GAMMA-RAY BURSTS: 30 YEARS OF DISCOVERY", Proceedings of the Los Alamos "Gamma Ray Burst Symposium", Santa Fe, New Mexico, 8 – 12 September 2003, E.E. Fenimore, M. Galassi, Editors; AIP Conference Proceedings, 727, 424 (2004).

   Our GRB theory, previously developed using GRB 991216 as a prototype, is here applied to GRB 980425. We fit the luminosity observed in the 40–700 keV, 2–26 keV and 2–10 keV bands by the BeppoSAX satellite. In addition the supernova SN1998bw is the outcome of an "induced gravitational collapse" triggered by GRB 980425, in agreement with the GRB-Supernova Time Sequence (GSTS) paradigm. A further outcome of this astrophysically exceptional sequence of events is the formation of a young neutron star generated by the SN1998bw event. A coordinated observational activity is recommended to further enlighten the underlying scenario of this most unique astrophysical system.

6. A. Corsi, M.G. Bernardini, C.L. Bianco, P. Chardonnet, F. Fraschetti, R. Ruffini, S.-S. Xue; "GRB 970228 Within the EMBH Model"; in "GAMMA-RAY BURSTS: 30 YEARS OF DISCOVERY", Proceedings of the Los Alamos "Gamma Ray Burst Symposium", Santa Fe, New Mexico, 8 – 12 September 2003, E.E. Fenimore, M. Galassi, Editors; AIP Conference Proceedings, 727, 428 (2004).

   We consider the gamma-ray burst of 1997 February 28 (GRB 970228) within the ElectroMagnetic Black Hole (EMBH) model. We first determine the value of the two free parameters that characterize energetically the GRB phenomenon in the EMBH model, that is to say the dyadosphere energy, $E_{dya} = 5.1 \times 10^{52}$ ergs, and the baryonic remnant mass M_B in units of E_{dya}, $B = M_B c^2 / E_{dya} = 3.0 \times 10^{-3}$. Having in this way estimated the energy emitted during the beam-target phase, we evaluate the role of the InterStellar Medium (ISM) number density (n_{ISM}) and of the ratio $\mathcal{R}$ between the effective emitting area and the total surface area of the GRB source, in reproducing the observed profiles of the GRB 970228 prompt emission and X-ray (2-10 keV energy band) afterglow. The importance of the ISM distribution three-dimensional treatment around the central black hole is also stressed in this analysis.

4 Publications (2005–2024)

4.1 Refereed journals

1. R. Ruffini, C.L. Bianco, P. Chardonnet, F. Fraschetti, V. Gurzadyan, S.-S. Xue; "Emergence of a filamentary structure in the fireball from GRB spectra"; International Journal of Modern Physics D, 14, 97 (2005).

   It is shown that the concept of a fireball with a definite filamentary structure naturally emerges from the analysis of the spectra of Gamma-Ray Bursts (GRBs). These results, made possible by the recently obtained analytic expressions of the equitemporal surfaces in the GRB afterglow, depend crucially on the single parameter R describing the effective area of the fireball emitting the X-ray and gamma-ray radiation. The X-ray and gamma-ray components of the afterglow radiation are shown to have a thermal spectrum in the co-moving frame of the fireball and originate from a stable shock front described self-consistently by the Rankine-Hugoniot equations. Precise predictions are presented on a correlation between spectral changes and intensity variations in the prompt radiation verifiable, e.g., by the Swift and future missions. The highly variable optical and radio emission depends instead on the parameters of the surrounding medium. The GRB 991216 is used as a prototype for this model.

2. R. Ruffini, M.G. Bernardini, C.L. Bianco, P. Chardonnet, F. Fraschetti, V. Gurzadyan, M. Lattanzi, L. Vitagliano, S.-S. Xue; "Extracting energy from black holes: 'long' and 'short' GRBs and their astrophysical settings"; Il Nuovo Cimento C, 28, 589 (2005).

   The introduction of the three interpretational paradigms for Gamma-Ray Bursts (GRBs) and recent progress in understanding the X- and gamma-ray luminosity in the afterglow allow us to make assessments about the astrophysical settings of GRBs. In particular, we evidence the distinct possibility that some GRBs occur in a binary system. This subclass of GRBs manifests itself in a "tryptich": one component formed by the collapse of a massive star to a black hole, which originates the GRB; a second component by a supernova and a third one by a young neutron star born in the supernova event. Similarly, the understanding of the physics of quantum relativistic processes during the gravitational collapse makes possible precise predictions about the structure of short GRBs.

3. M.G. Bernardini, C.L. Bianco, P. Chardonnet, F. Fraschetti, R. Ruffini, S.-S. Xue; "Theoretical interpretation of luminosity and spectral properties of GRB 031203"; The Astrophysical Journal, 634, L29 (2005).

   The X-ray and gamma-ray observations of the source GRB 031203 by INTEGRAL are interpreted within our theoretical model. In addition to a complete spacetime parameterization of the GRB, we specifically assume that the afterglow emission originates from a thermal spectrum in the comoving frame of the expanding baryonic matter shell. By determining the two free parameters of the model and estimating the density and filamentary structure of the ISM, we reproduce the observed luminosity in the 20-200 keV energy band. As in previous sources, the prompt radiation is shown to coincide with the peak of the afterglow, and the luminosity substructure is shown to originate in the filamentary structure of the ISM. We predict a clear hard-to-soft behavior in the instantaneous spectra. The time-integrated spectrum over 20 s observed by INTEGRAL is well fitted. Despite the fact that this source has been considered "unusual", it appears to us to be a normal low-energy GRB.

4. R. Ruffini, M.G. Bernardini, C.L. Bianco, P. Chardonnet, F. Fraschetti, S.-S. Xue; Evidence for isotropic emission in GRB991216; Advances in Space Research, 38, 1291 (2006).

   The issue of the possible presence or absence of jets in GRBs is here re-examined for GRB991216. We compare and contrast our theoretically predicted afterglow luminosity in the 2–10 keV band for spherically symmetric versus jetted emission. At these wavelengths the jetted emission can be excluded and data analysis confirms spherical symmetry. These theoretical fits are expected to be improved by the forthcoming data of the Swift mission.

5. R. Ruffini, M.G. Bernardini, C.L. Bianco, P. Chardonnet, F. Fraschetti, R. Guida, S.-S. Xue; "GRB 050315: A step toward understanding the uniqueness of the overall GRB structure"; The Astrophysical Journal, 645, L109 (2006).

Using the Swift data of GRB 050315, we are making progress toward understanding the uniqueness of our theoretically predicted gamma-ray burst (GRB) structure, which is composed of a proper GRB (P-GRB), emitted at the transparency of an electron-positron plasma with suitable baryon loading, and an afterglow comprising the so-called prompt emission due to external shocks. Thanks to the Swift observations, the P-GRB is identified, and for the first time we can theoretically fit detailed light curves for selected energy bands on a continuous timescale ranging over 106 s. The theoretically predicted instantaneous spectral distribution over the entire afterglow is presented, confirming a clear hard-to-soft behavior encompassing, continuously, the "prompt emission" all the way to the latest phases of the afterglow.

6. C.L. Bianco, L. Caito, R. Ruffini; "Theoretical interpretation of GRB 011121"; Il Nuovo Cimento B, 121, 1441 (2006).

   GRB011121 is analyzed as a prototype to understand the "flares" recently observed by Swift in the afterglow of many GRB sources. Detailed theoretical computation of the GRB011121 light curves in selected energy bands are presented and compared and contrasted with observational BeppoSAX data.

7. R. Ruffini, M.G. Bernardini, C.L. Bianco, P. Chardonnet, F. Fraschetti, R. Guida, S.-S. Xue; "GRB 050315: A step toward the uniqueness of the overall GRB structure"; Il Nuovo Cimento B, 121, 1367 (2006).

   Using the *Swift* data of GRB 050315, we progress on the uniqueness of our theoretically predicted Gamma-Ray Burst (GRB) structure as composed by a proper-GRB (P-GRB), emitted at the transparency of an electron-positron plasma with suitable baryon loading, and an afterglow comprising the so called "prompt emission" as due to external shocks. Thanks to the *Swift* observations, we can theoretically fit detailed light curves for selected energy bands on a continuous time scale ranging over 10^6 seconds. The theoretically predicted instantaneous spectral distribution over the entire afterglow confirms a clear hard-to-soft behavior encompassing, continuously, the "prompt emission" all the way to the latest phases of the afterglow. Consequences of the instrumental threshold on the definition of "short" and "long" GRBs are discussed.

8. M.G. Bernardini, C.L. Bianco, L. Caito, P. Chardonnet, A. Corsi, M.G. Dainotti, F. Fraschetti, R. Guida, R. Ruffini, S.-S. Xue; GRB970228 as a prototype for short GRBs with afterglow; Il Nuovo Cimento B, 121, 1439 (2006).

GRB970228 is analyzed as a prototype to understand the relative role of short GRBs and their associated afterglows, recently observed by Swift and HETE-II. Detailed theoretical computation of the GRB970228 light curves in selected energy bands are presented and compared with observational BeppoSAX data.

9. M.G. Dainotti, M.G. Bernardini, C.L. Bianco, L. Caito, R. Guida, R. Ruffini; "GRB060218 and GRBs associated with Supernovae Ib/c"; Astronomy & Astrophysics, 471, L29 (2007).

   Context: The *Swift* satellite has given continuous data in the range 0.3–150 keV from 0 s to 10^6 s for GRB060218 associated with SN2006aj. This Gamma-Ray Burst (GRB) which has an unusually long duration ($T_{90} \sim 2100$ s) fulfills the Amati relation. These data offer the opportunity to probe theoretical models for GRBs connected with Supernovae (SNe).
   Aims: We plan to fit the complete γ- and X-ray light curves of this long duration GRB, including the prompt emission, in order to clarify the nature of the progenitors and the astrophysical scenario of the class of GRBs associated with SNe Ib/c.
   Methods: We apply our "fireshell" model based on the formation of a black hole, giving the relevant references. It is characterized by the precise equations of motion and equitemporal surfaces and by the role of thermal emission.
   Results: The initial total energy of the electron-positron plasma $E_{e^\pm}^{tot} = 2.32 \times 10^{50}$ erg has a particularly low value, similar to the other GRBs associated with SNe. For the first time, we observe a baryon loading $B = 10^{-2}$ which coincides with the upper limit for the dynamical stability of the fireshell. The effective CircumBurst Medium (CBM) density shows a radial dependence $n_{cbm} \propto r^{-\alpha}$ with $1.0 \lesssim \alpha \lesssim 1.7$ and monotonically decreases from 1 to 10^{-6} particles/cm^3. This behavior is interpreted as being due to a fragmentation in the fireshell. Analogies with the fragmented density and filling factor characterizing Novae are outlined. The fit presented is particularly significant in view of the complete data set available for GRB060218 and of the fact that it fulfills the Amati relation.
   Conclusions: We fit GRB060218, usually considered as an X-Ray Flash (XRF), as a "canonical GRB" within our theoretical model. The smallest possible black hole, formed by the gravitational collapse of a neutron star in a binary system, is consistent with the especially low energetics of the class of GRBs associated with SNe Ib/c. We provide the first evidence for a fragmentation in the fireshell. This fragmentation is crucial in explaining both the unusually large T_{90} and the consequently inferred abnormally low value of the CBM effective

density.

10. M.G. Bernardini, C.L. Bianco, L. Caito, M.G. Dainotti, R. Guida, R. Ruffini; "GRB970228 and a class of GRBs with an initial spikelike emission"; Astronomy & Astrophysics, 474, L13 (2007).

    Context: The discovery by *Swift* and HETE-2 of an afterglow emission associated possibly with short GRBs opened the new problematic of their nature and classification. This issue has been further enhanced by the observation of GRB060614 and by a new analysis of the BATSE catalog which led to the identification of a new class of GRBs with "an occasional softer extended emission lasting tenths of seconds after an initial spikelike emission".
    Aims: We plan a twofold task: a) to fit this new class of "hybrid" sources within our "canonical GRB" scenario, where all GRBs are generated by a "common engine" (i.e. the gravitational collapse to a black hole); b) to propose GRB970228 as the prototype of the above mentioned class, since it shares the same morphology and observational features.
    Methods: We analyze *Beppo*SAX data on GRB970228 within the "fireshell" model and we determine the parameters describing the source and the CircumBurst Medium (CBM) needed to reproduce its light curves in the 40–700 keV and 2–26 keV energy bands.
    Results: We find that GRB970228 is a "canonical GRB", like e.g. GRB050315, with the main peculiarity of a particularly low average density of the CBM $\langle n_{cbm} \rangle \sim 10^{-3}$ particles/cm^3. We also simulate the light curve corresponding to a rescaled CBM density profile with $\langle n_{cbm} \rangle = 1$ particle/cm^3. From such a comparison it follows that the total time-integrated luminosity is a faithful indicator of the nature of GRBs, contrary to the peak luminosity which is merely a function of the CBM density.
    Conclusions: We call attention on discriminating the short GRBs between the "genuine" and the "fake" ones. The "genuine" ones are intrinsically short, with baryon loading $B \lesssim 10^{-5}$, as stated in our original classification. The "fake" ones, characterized by an initial spikelike emission followed by an extended emission lasting tenths of seconds, have a baryon loading $10^{-4} \lesssim B \leq 10^{-2}$. They are observed as such only due to an underdense CBM consistent with a galactic halo environment which deflates the afterglow intensity.

11. R. Guida, M.G. Bernardini, C.L. Bianco, L. Caito, M.G. Dainotti, R. Ruffini; "The Amati relation in the "fireshell" model"; Astronomy & Astrophysics, 487, L37 (2008).

Context: The cosmological origin of gamma-ray bursts (GRBs) has been firmly established, with redshifts up to $z = 6.29$. They are possible candidates for use as "distance indicators" for testing cosmological models in a redshift range hardly achievable by other cosmological probes. Asserting the validity of the empirical relations among GRB observables is now crucial for their calibration.
Aims: Motivated by the relation proposed by Amati and collaborators, we look within the "fireshell" model for a relation between the peak energy E_p of the νF_ν total time-integrated spectrum of the afterglow and the total energy of the afterglow E_{aft}, which in our model encompasses and extends the prompt emission.
Methods: The fit within the fireshell model, as for the "canonical" GRB050315, uses the complete arrival time coverage given by the Swift satellite. It is performed simultaneously, self-consistently, and recursively in the four BAT energy bands (15–25 keV, 25–50 keV, 50–100 keV, and 100-150 keV), as well as in the XRT one (0.2–10 keV). It uniquely determines the two free parameters characterizing the GRB source, the total energy $E_{tot}^{e^\pm}$ of the $e^\pm$ plasma and its baryon loading B, as well as the effective CircumBurst Medium (CBM) distribution. We can then build two sets of "gedanken" GRBs varying the total energy of the electron-positron plasma $E_{tot}^{e^\pm}$ and keeping the same baryon loading B of GRB050315. The first set assumes the one obtained in the fit of GRB050315 for the effective CBM density. The second set assumes instead a constant CBM density equal to the average value of the GRB050315 prompt phase.
Results: For the first set of "gedanken" GRBs we find a relation $E_p \propto (E_{aft})^a$, with $a = 0.45 \pm 0.01$, whose slope strictly agrees with the Amati one. Such a relation, in the limit $B \to 10^{-2}$, coincides with the Amati one. Instead, no correlation is found in the second set of "gedanken" GRBs.
Conclusions: Our analysis excludes the proper GRB (P-GRB) from the prompt emission, extends all the way to the latest afterglow phases, and is independent of the assumed cosmological model, since all "gedanken" GRBs are at the same redshift. The Amati relation, on the other hand, includes the P-GRB, focuses only on the prompt emission, being therefore influenced by the instrumental threshold that fixes the end of the prompt emission, and depends on the assumed cosmology. This might explain the intrinsic scatter observed in the Amati relation.

12. L. Caito, M.G. Bernardini, C.L. Bianco, M.G. Dainotti, R. Guida, R. Ruffini; "GRB060614: a "fake" short GRB from a merging binary system"; Astronomy & Astrophysics, 489, 501 (2009).

Context: GRB060614 observations by VLT and by Swift have infringed the traditionally accepted gamma-ray burst (GRB) collapsar scenario that purports the origin of all long duration GRBs from supernovae (SN). GRB060614 is the first nearby long duration GRB clearly not associated with a bright Ib/c SN. Moreover, its duration ($T_{90} \sim 100$ s) makes it hardly classifiable as a short GRB. It presents strong similarities with GRB970228, the prototype of a new class of "fake" short GRBs that appear to originate from the coalescence of binary neutron stars or white dwarfs spiraled out into the galactic halo. *Aims*: Within the "canonical" GRB scenario based on the "fireshell" model, we test if GRB060614 can be a "fake" or "disguised" short GRB. We model the traditionally termed "prompt emission" and discriminate the signal originating from the gravitational collapse leading to the GRB from the process occurring in the circumburst medium (CBM). *Methods*: We fit GRB060614 light curves in Swift's BAT ($15-150$ keV) and XRT ($0.2-10$ keV) energy bands. Within the fireshell model, light curves are formed by two well defined and different components: the proper-GRB (P-GRB), emitted when the fireshell becomes transparent, and the extended afterglow, due to the interaction between the leftover accelerated baryonic and leptonic shell and the CBM. *Results*: We determine the two free parameters describing the GRB source within the fireshell model: the total $e^{\pm}$ plasma energy ($E_{tot}^{e^{\pm}} = 2.94 \times 10^{51}$erg) and baryon loading ($B = 2.8 \times 10^{-3}$). A small average CBM density $\sim 10^{-3}$ particles/cm^3 is inferred, typical of galactic halos. The first spikelike emission is identified with the P-GRB and the following prolonged emission with the extended afterglow peak. We obtain very good agreement in the BAT ($15-150$ keV) energy band, in what is traditionally called "prompt emission", and in the XRT ($0.2-10$ keV) one. *Conclusions*: The *anomalous* GRB060614 finds a natural interpretation within our canonical GRB scenario: it is a "disguised" short GRB. The total time-integrated extended afterglow luminosity is greater than the P-GRB one, but its peak luminosity is smaller since it is deflated by the peculiarly low average CBM density of galactic halos. This result points to an old binary system, likely formed by a white dwarf and a neutron star, as the progenitor of GRB060614 and well justifies the absence of an associated SN Ib/c. Particularly important for further studies of the final merging process are the temporal structures in the P-GRB down to 0.1 s.

13. M.G. Bernardini, C.L. Bianco, L. Caito, M.G. Dainotti, R. Guida, R. Ruffini; "GRB970228 in the "canonical GRB" scenario"; Journal of the Korean Physical Society, 56, 1575 (2010).

Within the "fireshell" model, we define a "canonical GRB" light curve with two sharply different components: the proper-GRB (P-GRB), emitted when the optically thick fireshell of an electron-positron plasma originating from the phenomenon reaches transparency, and the afterglow, emitted due to the collision between the remaining optically thin fireshell and the circumburst medium (CBM). On the basis of the recent understanding of GRB970228 as the prototype for a new class of GRBs with "an occasional softer extended emission lasting tenths of seconds after an initial spikelike emission", we outline our "canonical GRB" scenario, originating from the gravitational collapse to a black hole, with special emphasis on the discrimination between "genuine" and "fake" short GRBs. Furthermore, we investigate how the GRB970228 analysis provides a theoretical explanation for the apparent absence of such a correlation for the GRBs belonging to this new class.

14. L. Caito, M.G. Bernardini, C.L. Bianco, M.G. Dainotti, R. Guida, R. Ruffini; "GRB060614: a preliminary result"; Journal of the Korean Physical Society, 56, 1579 (2010).

    The explosion of GRB 060614 produced a deep break in the GRB scenario and opened new horizons of investigation because it can't be traced back to any traditional scheme of classification. In fact, it manifests peculiarities both of long bursts and of short bursts, and above all, it is the first case of a long-duration near GRB without any bright Ib/c associated Supernova. We will show that, in our canonical GRB scenario, this "anomalous" situation finds a natural interpretation and allows us to discuss a possible variation in the traditional classification scheme, introducing a distinction between "genuine" and "fake" short bursts.

15. M.G. Dainotti, M.G. Bernardini, C.L. Bianco, L. Caito, R. Guida, R. Ruffini; "The astrophysical trypthic: GRB, SN and URCA can be extended to GRB060218?"; Journal of the Korean Physical Society, 56, 1588 (2010).

    The *Swift* satellite has given continuous data in the range 0.3–150 keV from 0 s to 10^6 s for GRB060218 associated with SN2006aj. This GRB is the fourth GRB spectroscopically associated with SNe after the cases of GRB980425-SN1998bw, GRB031203-SN2003lw, GRB 030329-SN2003dh. It has an unusually long duration ($T_{90} \sim 2100$ s). These data offer the opportunity to probe theoretical models for Gamma-Ray Bursts (GRBs) connected with Supernovae (SNe). We plan to fit the complete γ- and X-ray light curves of this long duration GRB, including the prompt emission, in order to clarify the nature of the progenitors and the astrophysical scenario of the class of GRBs associated to SNe Ib/c. We apply our "fireshell" model based on the formation of a black hole, giving the relevant references. The initial total energy of the electron-positron plasma $E^{tot}_{e^{\pm}} = 2.32 \times 10^{50}$ erg has a particularly low value similarly to the other GRBs associated with SNe. For the first time we observe a baryon loading $B = 10^{-2}$ which coincides with the upper limit for the dynamical stability of the fireshell. The effective CircumBurst Medium (CBM) density shows a radial dependence $n_{cbm} \propto r^{-\alpha}$ with $1.0 \lesssim \alpha \lesssim 1.7$ and monotonically decreases from 1 to 10^{-6} particles/cm^3. Such a behavior is interpreted as due to a fragmentation in the fireshell. Such a fragmentation is crucial in explaining both the unusually large T_{90} and the consequently inferred abnormal low value of the CBM effective density. We fit GRB060218, usually considered as an X-Ray Flash (XRF), as a "canonical GRB" within our theoretical model. The smallest possible black hole, formed by the gravitational collapse of a neutron star in a binary system, is consistent with the especially low energetics of the class of GRBs associated with SNe Ib/c. We present the URCA process and the connection between the GRBs associated with SNe extended also to the case of GRB060218.

16. L. Izzo, M.G. Bernardini, C.L. Bianco, L. Caito, B. Patricelli, R. Ruffini; "GRB 090423 at Redshift 8.1: a Theoretical Interpretation"; Journal of the Korean Physical Society, 57, 551 (2010).

    GRB 090423 is the farthest gamma ray burst ever observed, with a redshift of about 8.1. We present within the fireshell scenario a complete analysis of this GRB. We model the prompt emission and the first rapid flux decay of the afterglow emission as being to the canonical emission of the interaction in the interval $0 \leq t \leq 440$ s by using accelerated baryonic matter with the circumburst medium. After the data reduction of the Swift data in the BAT (15 - 150 keV) and XRT (0.2 - 10 keV) energy bands, we interpret the light curves and the spectral distribution in the context of the fireshell scenario. We also confirm in this source the existence of a second component, a plateau phase, as being responsible for the late emission in the X-ray light curve. This extra component originates from the fact that the ejecta have a range of the bulk Lorentz Γ factor, which starts to interact each other ejecta at the start of the plateau phase.

17. L. Caito, L. Amati, M.G. Bernardini, C.L. Bianco, G. De Barros, L. Izzo, B. Patricelli, R. Ruffini; "GRB 071227: an additional case of a disguised

short burst"; Astronomy & Astrophysics, 521, A80 (2010).

Context: Observations of gamma-ray bursts (GRBs) have shown an hybridization between the two classes of long and short bursts. In the context of the fireshell model, the GRB light curves are formed by two different components: the *proper* GRB (P-GRB) and the extended afterglow. Their relative intensity is linked to the fireshell baryon loading B. The GRBs with P-GRB predominance are the short ones, the remainders are long. A new family of *disguised* short bursts has been identified: long bursts with a protracted low instantaneous luminosity due to a low density CircumBurst Medium (CBM). In the 15–150 keV energy band GRB 071227 exhibits a short duration (about 1.8s) spike-like emission followed by a very soft extended tail up to one hundred seconds after the trigger. It is a faint ($E_{iso} = 5.8 \times 10^{50}$) nearby GRB ($z = 0.383$) that does not have an associated type Ib/c bright supernova (SN). For these reasons, GRB 071227 has been classified as a short burst not fulfilling the Amati relation holding for long burst. *Aims:* We check the classification of GRB 071227 provided by the fireshell model. In particular, we test whether this burst is another example of a *disguised* short burst, after GRB 970228 and GRB 060614, and, for this reason, whether it fulfills the Amati relation. *Methods:* We simulate GRB 071227 light curves in the *Swift* BAT 15–50 keV bandpass and in the XRT (0.3–10 keV) energy band within the fireshell model. *Results:* We perform simulations of the tail in the 15–50 keV bandpass, as well as of the first part of the X-ray afterglow. This infers that: $E_{tot}^{e^\pm} = 5.04 \times 10^{51}$ erg, $B = 2.0 \times 10^{-4}$, $E_{P-GRB}/E_{aft} \sim 0.25$, and $\langle n_{cbm} \rangle = 3.33$ particles/cm^3. These values are consistent with those of "long duration" GRBs. We interpret the observed energy of the first hard emission by identifying it with the P-GRB emission. The remaining long soft tail indeed fulfills the Amati relation. *Conclusions:* Previously classified as a short burst, GRB 071227 on the basis of our analysis performed in the context of the fireshell scenario represents another example of a *disguised* short burst, after GRB 970228 and GRB 060614. Further confirmation of this result is that the soft tail of GRB 071227 fulfills the Amati relation.

18. M.G. Bernardini, C.L. Bianco, L. Caito, L. Izzo, B. Patricelli, R. Ruffini; "Analysis of GRB060607A within the fireshell model: prompt emission, X-ray flares and late afterglow phase"; Astronomy & Astrophysics, submitted to.

    Context: GRB060607A is a very distant ($z = 3.082$) and energetic event ($E_{iso} \sim 10^{53}$ erg). Its main peculiarity is that the peak of the near-infrared (NIR) afterglow has been observed with the REM robotic telescope. This NIR peak has been interpreted as the afterglow onset within the fireball forward shock model, and the initial Lorentz gamma factor of the emitting system has been inferred. *Aims*: We analyze GRB060607A within the fireshell model. We emphasize the central role of the prompt emission in determining the initial Lorentz gamma factor of the extended afterglow and we interpret the X-ray flares as produced by the interaction of the optically thin fireshell with overdense CircumBurst Medium (CBM) clumps. *Methods*: We deal only with the Swift BAT and XRT observations, that are the basic contribution to the GRB emission and that are neglected in the treatment adopted in the current literature. The numerical modeling of the fireshell dynamics allows to calculate all its characteristic quantities, in particular the exact value of the Lorentz gamma factor at the transparency. *Results*: We show that the theoretically computed prompt emission light curves are in good agreement with the observations in all the *Swift* BAT energy bands as well as the spectra integrated over different time intervals. The flares observed in the decaying phase of the X-ray afterglow are also reproduced by the same mechanism, but in a region in which the typical dimensions of the clumps are smaller than the visible area of the fireshell and most energy lies in the X-ray band due to the hard-to-soft evolution. *Conclusions*: We show that it is possible to obtain flares with $\Delta t/t$ compatible with the observations when the three-dimensional structure of the CBM clumps is duly taken into account. We stop our analysis at the beginning of the X-ray plateau phase, since we suppose this originates from the instabilities developed in the collision between different subshells within a structured fireshell.

19. G. de Barros, M. G. Bernardini, C.L. Bianco, L. Caito, L. Izzo, B. Patricelli, R. Ruffini; "On the nature of GRB 050509b: a disguised short GRB"; Astronomy & Astrophyscs, 529, A130 (2011)

    Context: GRB 050509b, detected by the *Swift* satellite, is the first case where an X-ray afterglow has been observed associated with a short gamma-ray burst (GRB). Within the fireshell model, the canonical GRB light curve presents two different components: the proper-GRB (P-GRB) and the extended afterglow. Their relative intensity is a function of the fireshell baryon loading parameter B and of the CircumBurst Medium (CBM) density (n_{CBM}). In particular, the traditionally called short GRBs can be either "genuine" short GRBs (with $B \lesssim 10^{-5}$, where the P-GRB is energetically predominant) or "disguised" short GRBs (with $B \gtrsim 3.0 \times 10^{-4}$ and $n_{CBM} \ll 1$, where the extended afterglow is energetically predominant). *Aims*: We verify whether GRB 050509b can be classified as a "genuine" short or a "disguised" short GRB, in the fireshell model. *Methods*: We investigate two alternative scenarios. In the first, we start from the assumption that this GRB is a "genuine" short burst. In the second attempt, we assume that this GRB is a "disguised" burst. *Results*: If GRB 050509b were a genuine short GRB, there should initially be very hard emission which is ruled out by the observations. The analysis that assumes that this is a disguised short GRB is compatible with the observations. The theoretical model predicts a value of the extended afterglow energy peak that is consistent with the Amati relation. *Conclusions*: GRB 050509b cannot be classified as a "genuine" short GRB. The observational data are consistent with a "disguised" short GRB classification, i.e., a long burst with a weak extended afterglow "deflated" by the low density of the CBM. We expect that all short GRBs with measured redshifts are disguised short GRBs because of a selection effect: if there is enough energy in the afterglow to measure the redshift, then the proper GRB must be less energetic than the afterglow. The Amati relation is found to be fulfilled only by the extended afterglow excluding the P-GRB.

20. L. Caito, M.G. Bernardini, C.L. Bianco, L. Izzo, B. Patricelli, R. Ruffini; "GRB 071227: another disguised short burst"; International Journal of Modern Physics D, 20, 1931 (2011).

Observations of Gamma-ray Bursts (GRBs) put forward in the recent years have revealed, with increasing evidence, that the historical classification between long and short bursts has to be revised. Within the Fireshell scenario, both short and long bursts are canonical bursts, consisting of two different phases. First, a Proper-GRB (P-GRB), that is the emission of photons at the transparency of the fireshell. Then, the Extended Afterglow, multiwavelength emission due to the interacion of the baryonic remnants of the fireshell with the CircumBurst Medium (CBM). We discriminate between long and short bursts by the amount of energy stored in the first phase with respect to the second one. Within the Fireshell scenario, we have introduced a third intermediate class: the disguised GRBs. They appear like short bursts, because their morphology is characterized by a first, short, hard episode and a following deflated tail, but this last part — coincident with the peak of the afterglow — is energetically predominant. The origin of this peculiar kind of sources is inferred to a very low average density of the environment (of the order of 10^{-3}). After GRB 970228 and GRB 060614, we find in GRB 071227 a third example of disguised burst.

21. L. Izzo, M.G. Bernardini, C.L. Bianco, L. Caito, B. Patricelli, L.J. Rangel Lemos, R. Ruffini; "GRB 080916C and the high-energy emission in the fireshell scenario"; International Journal of Modern Physics D, 20, 1949 (2011).

    In this paper we discuss a possible explanation for the high energy emission (up to $\sim$ GeV) seen in GRB 080916C. We propose that the GeV emission is originated by the collision between relativistic baryons in the fireshell after the transparency and the nucleons located in molecular clouds near the burst site. This collision should give rise pion production, whose immediate decay provides high energy photons, neutrinos and leptons. Using a public code (SYBILL) we simulate these relativistic collisions in their simple form, so that we can draw our preliminar results in this paper. We will present moreover our hypothesis that the delayed onset of this emission identifies in a complete way the P-GRB emission.

22. B. Patricelli, M.G. Bernardini, C.L. Bianco, L. Caito, L. Izzo, R. Ruffini, G. Vereshchagin; "A new spectral energy distribution of photons in the fireshell model of GRBs"; International Journal of Modern Physics D, 20, 1983 (2011).

    The analysis of various Gamma-Ray Bursts (GRBs) having a low energetics (an isotropic energy $E_{iso} \lesssim 10^{53}$ ergs) within the fireshell model has shown how the $N(E)$ spectrum of their prompt emission can be reproduced in a satisfactory way by a convolution of thermal spectra. Nevertheless, from the study of very energetic bursts ($E_{iso} \lesssim 10^{54}$ ergs) such as, for example, GRB 080319B, some discrepancies between the numerical simulations and the observational data have been observed. We investigate a different spectrum of photons in the comoving frame of the fireshell in order to better reproduce the spectral properties of GRB prompt emission within the fireshell model. We introduce a phenomenologically modified thermal spectrum: a thermal spectrum characterized by a different asymptotic power-law index in the low energy region. Such an index depends on a free parameter α, so that the pure thermal spectrum corresponds to the case $\alpha = 0$. We test this spectrum by comparing the numerical simulations with the observed prompt emission spectra of various GRBs. From this analysis it has emerged that the observational data can be correctly reproduced by assuming a modified thermal spectrum with $\alpha = -1.8$.

23. A.V. Penacchioni, R. Ruffini, L. Izzo, M. Muccino, C.L. Bianco, L. Caito, B. Patricelli, L. Amati; "Evidence for a proto-black hole and a double

astrophysical component in GRB 101023"; Astronomy & Astrophysics, 538, A58 (2012).

Context: It has been recently shown that GRB 090618, observed by AGILE, Coronas Photon, Fermi, Konus, Suzaku and Swift, is composed of two very different components: episode 1, lasting 50 s, shows a thermal plus power-law spectrum with a characteristic temperature evolving in time as a power law; episode 2 (the remaining 100 s) is a canonical long GRB. We have associated episode 1 to the progenitor of a collapsing bare core leading to the formation of a black hole: what was defined as a "proto black hole". *Aims*: In precise analogy with GRB 090618 we aim to analyze the 89s of the emission of GRB 101023, observed by Fermi, Gemini, Konus and Swift, to see if there are two different episodes: the first one presenting a characteristic black-body temperature evolving in time as a broken power law, and the second one consistent with a canonical GRB. *Methods*: To obtain information on the spectra, we analyzed the data provided by the GBM detector onboard the Fermi satellite, and we used the heasoft package XSPEC and RMFIT to obtain their spectral distribution. We also used the numerical code GRBsim to simulate the emission in the context of the fireshell scenario for episode 2. *Results*: We confirm that the first episode can be well fit by a black body plus power-law spectral model. The temperature changes with time following a broken power law, and the photon index of the power-law component presents a soft-to-hard evolution. We estimate that the radius of this source increases with time with a velocity of $1.5 \times 10^4 km/s$. The second episode appears to be a canonical GRB. By using the Amati and the Atteia relations, we determined the cosmological redshift, $z \sim 0.9 \pm 0.084(stat.) \pm 0.2(sys.)$. The results of GRB 090618 are compared and contrasted with the results of GRB 101023. Particularly striking is the scaling law of the soft X-ray component of the afterglow. *Conclusions*: We identify GRB 090618 and GRB 101023 with a new family of GRBs related to a single core collapse and presenting two astrophysical components: a first one related to the proto-black hole prior to the process of gravitational collapse (episode 1), and a second one, which is the canonical GRB (episode 2) emitted during the formation of the black hole. For the first time we are witnessing the process of a black hole formation from the instants preceding the gravitational collapse up to the GRB emission. This analysis indicates progress towards developing a GRB distance indicator based on understanding the P-GRB and the prompt emission, as well as the soft X-ray behavior of the late afterglow.

24. R. Negreiros, R. Ruffini, C. L. Bianco, J. A. Rueda; "Cooling of young

neutron stars in GRB associated to supernovae"; Astronomy & Astrophysics, 540, A12 (2012).

Context: The traditional study of neutron star cooling has been generally applied to quite old objects such as the Crab Pulsar (957 years) or the central compact object in Cassiopeia A (330 years) with an observed surface temperature $\sim 10^6$ K. However, recent observations of the late ($t = 10^8$–10^9 s) emission of the supernovae (SNe) associated to GRBs (GRB-SN) show a distinctive emission in the X-ray regime consistent with temperatures $\sim 10^7$–10^8 K. Similar features have been also observed in two Type Ic SNe SN 2002ap and SN 1994I that are not associated to GRBs. *Aims*: We advance the possibility that the late X-ray emission observed in GRB-SN and in isolated SN is associated to a hot neutron star just formed in the SN event, here defined as a neo-neutron star. *Methods*: We discuss the thermal evolution of neo-neutron stars in the age regime that spans from ~ 1 minute (just after the proto-neutron star phase) all the way up to ages < 10–100 yr. We examine critically the key factor governing the neo-neutron star cooling with special emphasis on the neutrino emission. We introduce a phenomenological heating source, as well as new boundary conditions, in order to mimic the high temperature of the atmosphere for young neutron stars. In this way we match the neo-neutron star luminosity to the observed late X-ray emission of the GRB-SN events: URCA-1 in GRB980425-SN1998bw, URCA-2 in GRB030329-SN2003dh, and URCA-3 in GRB031203-SN2003lw. *Results*: We identify the major role played by the neutrino emissivity in the thermal evolution of neo-neutron stars. By calibrating our additional heating source at early times to $\sim 10^{12}$–10^{15} erg/g/s, we find a striking agreement of the luminosity obtained from the cooling of a neo-neutron stars with the prolonged ($t = 10^8$–10^9 s) X-ray emission observed in GRB associated with SN. It is therefore appropriate a revision of the boundary conditions usually used in the thermal cooling theory of neutron stars, to match the proper conditions of the atmosphere at young ages. The traditional thermal processes taking place in the crust might be enhanced by the extreme high-temperature conditions of a neo-neutron star. Additional heating processes that are still not studied within this context, such as e^+e^- pair creation by overcritical fields, nuclear fusion, and fission energy release, might also take place under such conditions and deserve further analysis. *Conclusions*: Observation of GRB-SN has shown the possibility of witnessing the thermal evolution of neo-neutron stars. A new campaign of dedicated observations is recommended both of GRB-SN and of isolated Type Ic SN.

25. L. Izzo, R. Ruffini, A.V. Penacchioni, C.L. Bianco, L. Caito, S.K. Chakrabarti, J.A. Rueda, A. Nandi, B. Patricelli; "A double component in GRB 090618: a proto-black hole and a genuinely long gamma-ray burst"; Astronomy & Astrophysics, 543, A10 (2012).

    Context: The joint X-ray and gamma-ray observations of GRB 090618 by very many satellites offer an unprecedented possibility of testing crucial aspects of theoretical models. In particular, they allow us to test (a) in the process of gravitational collapse, the formation of an optically thick e+e.-baryon plasma self-accelerating to Lorentz factors in the range $200 < \Gamma < 3000$; (b) its transparency condition with the emission of a component of 10^{53-54} baryons in the TeV region and (c) the collision of these baryons with the circumburst medium (CBM) clouds, characterized by dimensions of 10^{15-16} cm. In addition, these observations offer the possibility of testing a new understanding of the thermal and power-law components in the early phase of this GRB. *Aims*: We test the fireshell model of GRBs in one of the closest ($z = 0.54$) and most energetic ($E_{iso} = 2.90 \times 10^{53}$ erg) GRBs, namely GRB 090618. It was observed at ideal conditions by several satellites, namely *Fermi*, *Swift*, Konus-WIND, AGILE, RT-2, and Suzaku, as well as from on-ground optical observatories. *Methods*: We analyzed the emission from GRB 090618 using several spectral models, with special attention to the thermal and power-law components. We determined the fundamental parameters of a canonical GRB within the context of the fireshell model, including the identification of the total energy of the e^+e^- plasma, E_{tot}^{e+e-}, the proper GRB (P-GRB), the baryon load, the density and structure of the CBM. *Results*: We find evidence of the existence of two different episodes in GRB 090618. The first episode lasts 50 s and is characterized by a spectrum consisting of a thermal component, which evolves between $kT = 54$ keV and $kT = 12$ keV, and a power law with an average index $\gamma = 1.75 \pm 0.04$. The second episode, which lasts for ~ 100 s, behaves as a canonical long GRB with a Lorentz gamma factor at transparency of $\Gamma = 495$, a temperature at transparency of 29.22 keV and with a characteristic size of the surrounding clouds of $R_{cl} \sim 10^{15-16}$ cm and masses of $\sim 10^{22-24}$ g. *Conclusions*: We support the recently proposed two-component nature of GRB 090618, namely, episode 1 and episode 2, with a specific theoretical analysis.We furthermore illustrate that episode 1 cannot be considered to be either a GRB or a part of a GRB event, but it appears to be related to the progenitor of the collapsing bare core, leading to the formation of the black hole, which we call a "proto-black hole". Thus, for the first time, we are witnessing the process of formation of a black hole from the phases just preceding the gravitational collapse all the way up to the GRB emission.

26. B. Patricelli, M.G. Bernardini, C.L. Bianco, L. Caito, G. De Barros, L. Izzo, R. Ruffini, G.V. Vereshchagin; "Analysis of GRB 080319B and GRB 050904 within the Fireshell Model: Evidence for a Broader Spectral Energy Distribution"; The Astrophysical Journal, 756, 16 (2012).

    The observation of GRB 080319B, with an isotropic energy $E_{iso} = 1.32 \times 10^{54}$ erg, and GRB 050904, with $E_{iso} = 1.04 \times 10^{54}$ erg, offers the possibility of studying the spectral properties of the prompt radiation of two of the most energetic Gamma Ray Bursts (GRBs). This allows us to probe the validity of the fireshell model for GRBs beyond 10^{54} erg, well outside the energy range where it has been successfully tested up to now (10^{49}–10^{53} erg). We find that in the low energy region, the prompt emission spectra observed by *Swift* BAT reveals more power than theoretically predicted. The opportunities offered by these observations to improve the fireshell model are outlined in this paper. One of the distinguishing features of the fireshell model is that it relates the observed GRB spectra to the spectrum in the comoving frame of the fireshell. Originally, a fully radiative condition and a comoving thermal spectrum were adopted. An additional power-law in the comoving thermal spectrum is required due to the discrepancy of the theoretical and observed light curves and spectra in the fireshell model for GRBs 080319B and 050904. A new phenomenological parameter α is correspondingly introduced in the model. We perform numerical simulations of the prompt emission in the *Swift* BAT bandpass by assuming different values of α within the fireshell model. We compare them with the GRB 080319B and GRB 050904 observed time-resolved spectra, as well as with their time-integrated spectra and light curves. Although GRB 080319B and GRB 050904 are at very different redshifts (z=0.937 and z=6.29 respectively), a value of $\alpha = -1.8$ leads for both of them to a good agreement between the numerical simulations and the observed BAT light curves, time-resolved and time-integrated spectra. Such a modified spectrum is also consistent with the observations of previously analyzed less energetic GRBs and reasons for this additional agreement are given. Perspectives for future low energy missions are outlined.

27. M. Muccino, R. Ruffini, C.L. Bianco, L. Izzo, A.V. Penacchioni; "GRB 090227B: The missing link between the genuine short and long GRBs"; The Astrophysical Journal, 763, 125 (2013).

The time-resolved spectral analysis of GRB 090227B, made possible by the *Fermi*-GBM data, allows to identify in this source the missing link between the genuine short and long GRBs. Within the Fireshell model of the Gamma-Ray Bursts (GRBs) we predict genuine short GRBs: bursts with the same inner engine of the long bursts but endowed with a severely low value of the Baryon load, $B \lesssim 5 \times 10^{-5}$. A first energetically predominant emission occurs at the transparency of the e^+e^- plasma, the Proper-GRB (P-GRB), followed by a softer emission, the extended afterglow. The typical separation between the two emissions is expected to be of the order of 10^{-3} – 10^{-2} s. We identify the P-GRB of GRB 090227B in the first 96 ms of emission, where a thermal component with the temperature $kT = (517 \pm 28)$ keV and a flux comparable with the non thermal part of the spectrum is observed. This non thermal component as well as the subsequent emission, where there is no evidence for a thermal spectrum, is identified with the extended afterglow. We deduce a theoretical cosmological redshift $z = 1.61 \pm 0.14$. We then derive the total energy $E^{tot}_{e^+e^-} = (2.83 \pm 0.15) \times 10^{53}$ ergs, the Baryon load $B = (4.13 \pm 0.05) \times 10^{-5}$, the Lorentz Γ factor at transparency $\Gamma_{tr} = (1.44 \pm 0.01) \times 10^4$, and the intrinsic duration $\Delta t' \sim 0.35$ s. We also determine the average density of the CircumBurst Medium (CBM), $\langle n_{CBM} \rangle = (1.90 \pm 0.20) \times 10^{-5}$ particles/cm^3. There is no evidence of beaming in the system. In view of the energetics and of the Baryon load of the source, as well as of the low interstellar medium and of the intrinsic time scale of the signal, we identify the GRB progenitor as a binary neutron star. From the recent progress in the theory of neutron stars, we obtain masses of the stars $m_1 = m_2 = 1.34 M_\odot$ and their corresponding radii $R_1 = R_2 = 12.24$ km and thickness of their crusts ~ 0.47 km, consistent with the above values of the Baryon load, of the energetics and of the time duration of the event.

28. A.V. Penacchioni, R. Ruffini, C.L. Bianco, L. Izzo, M. Muccino, G.B. Pisani, J.A. Rueda; "GRB 110709B in the induced gravitational collapse paradigm"; Astronomy & Astrophysics, 551, A133 (2013).

    Context: GRB 110709B is the first source for which *Swift* BAT triggered twice, with a time separation of ~ 10 minutes. The first emission (called here Episode 1) goes from 40 s before the first trigger up to 60 s after it. The second emission (hereafter Episode 2) goes from 35 s before the second trigger to 100 s after it. These features reproduce the ones of GRB 090618, which has been recently interpreted within the Induced Gravitational Collapse paradigm (IGC). In line with this paradigm we assume the progenitor to be a close binary system composed of a core of an evolved star and a Neutron Star (NS). The evolved star explodes as a Supernova (SN) and ejects material that is partially accreted by the NS. We identify this process with Episode 1. The accretion process brings the NS over its critical mass, thus gravitationally collapsing to a BH. This process leads to the GRB emission, Episode 2. The double trigger has given for the first time the possibility to have a coverage of the X-ray emission observed by XRT both prior to and during the prompt phase of GRB 110709B. *Aims*: We analyze the spectra and time variability of Episode 1 and 2 and compute the relevant parameters of the binary progenitor, as well as the astrophysical parameters both in the SN and the GRB phase in the IGC paradigm. *Methods*: We perform a time-resolved spectral analysis of Episode 1 by fitting the spectrum with a blackbody (BB) plus a power-law (PL) spectral model. From the BB fluxes and temperatures of Episode 1 and the luminosity distance d_L, we evaluate the evolution with time of the radius of the BB emitter, associated here to the evolution of the SN ejecta. We analyze Episode 2 within the Fireshell model, identifying the Proper-GRB (P-GRB) and simulating the light curve and spectrum. We establish the redshift to be $z = 0.75$, following the phenomenological methods by Amati, by Yonetoku and by Grupe, and our analysis of the late X-ray afterglow. It is most remarkable that the determination of the cosmological redshift on the ground of the scaling of the late X-ray afterglow, already verified in GRB 090618 and GRB 101023, is again verified by this analysis. *Results*: We find for Episode 1 a temperature of the BB component that evolves with time following a broken PL, with the slope of the PL at early times $\alpha = 0$ (constant function) and the slope of the PL at late times $\beta = -4 \pm 2$. The break occurs at $t = 41.21$ s. The total energy of Episode 1 is $E_{iso}^{(1)} = 1.42 \times 10^{53}$ erg. The total energy of Episode 2 is $E_{iso}^{(2)} = 2.43 \times 10^{52}$ erg. We find at transparency a Lorentz factor $\Gamma \sim 1.73 \times 10^2$, laboratory radius of 6.04×10^{13} cm, P-GRB observed temperature $kT_{P-GRB} = 12.36$ keV, baryon load $B = 5.7 \times 10^{-3}$ and P-GRB energy of $E_{P-GRB} = 3.44 \times 10^{50}$ erg. We find a remarkable coincidence of the cosmological redshift by the scaling of the XRT data and with three other phenomenological methods. *Conclusions*: We interpret GRB 110709B as a member of the IGC sources, together with GRB 970828, GRB 090618 and GRB 101023. The existence of the XRT data during the prompt phase of the emission of GRB 110709B (Episode 2) offers an unprecedented tool for improving the diagnostic of GRBs emission.

29. G.B. Pisani, L. Izzo, R. Ruffini, C.L. Bianco, M. Muccino, A.V. Penacchioni, J.A. Rueda, Y. Wang; "Novel distance indicator for gamma-ray bursts associated with supernovae"; Astronomy & Astrophysics, 552,

L5 (2013).

Context: In recent years it has been proposed that the temporal coincidence of a Gamma Ray Burst (GRB) and a type Ib/c supernova (SN) can be explained by the concept of Induced Gravitational Collapse (IGC) of a Neutron Star (NS) to a Black Hole (BH) by accretion of matter ejected by a SN Ib/c. This scenario reveals a possible common behavior in the late time X-ray emission of this subclass of GRBs. *Aims*: We want to test if such a common behavior can actually be present in the sources belonging to this GRB sub-class and if this may lead to a redshift estimator for these sources. *Methods*: We build a sample of GRBs belonging to this sub-class, and we rescale the X-ray light curves of all of them both in time and in flux to a common cosmological redshift. *Results*: We found that the X-ray light curves of all the GRBs of the sample with a measured redshift present a common late time behavior when rescaled to a common redshift $z = 1$. We then use this result to estimate the redshift of the GRBs of the sample with no measured redshift. *Conclusions*: The common behavior in the late decay of the X-ray light curves of the GRBs of the sample points to a common physical mechanism in this particular phase of the GRB emission, possibly related to the SN process. This scenario may represent an invaluable tool to estimate the redshift of GRBs belonging to this sub-class of events. More GRBs are therefore needed in order to enlarge the subclass and to make more stringent constraints on the redshift estimates performed with this method for GRBs pertaining to this class.

30. C.L. Bianco, M. G. Bernardini, L. Caito, G. De Barros, L. Izzo, M. Muccino, B. Patricelli, A.V. Penacchioni, G.B. Pisani, R. Ruffini; "The canonical GRB scenario"; Il Nuovo Cimento C, 36 s01, 21 (2013).

    The canonical GRB scenario implied by the fireshell model is briefly summarized.

31. A.V. Penacchioni, R. Ruffini, L. Izzo, M. Muccino, C.L. Bianco, L. Caito, B. Patricelli; "Evidences for a double component in the emission of GRB 101023"; Il Nuovo Cimento C, 36 s01, 117 (2013).

    In this work we present the results of the analysis of GRB 101023 in the fireshell scenario. Its redshift is not known, so we attempted to infer it from the Amati Relation, obtaining $z = 0.9$. Its light curve presents a double emission, which makes it very similar to the already studied GRB 090618. We called each part Episode 1 and Episode 2. We performed a time-resolved spectral analysis with RMFIT using different spectral models, and fitted the light curve with a numerical code integrating the fireshell equations of motion. We used Fermi GBM data to build the light curve, in particular the second NaI detector, in the range (8.5–1000 keV). We considered different hypotheses regarding which part of the light curve could be the GRB and performed the analysis of all of them. We noticed a great variation of the temperature with time in the first episode, as well as almost no variation of the progenitor radius. We found that the first emission does not match the requirements for a GRB, while the second part perfectly agrees with being a canonical GRB, with a P-GRB lasting 4 s.

32. M. Muccino, R. Ruffini, C.L. Bianco, L. Izzo, A.V. Penacchioni, G.B. Pisani; "GRB 090510: A Disguised Short Gamma-Ray Burst with the Highest Lorentz Factor and Circumburst Medium"; The Astrophysical Journal, 772, 62 (2013).

    GRB 090510, observed both by Fermi and AGILE satellites, is the first bright short-hard Gamma-Ray Burst (GRB) with an emission from the keV up to the GeV energy range. Within the Fireshell model, we interpret the faint precursor in the light curve as the emission at the transparency of the expanding e^+e^- plasma: the Proper-GRB (P-GRB). From the observed isotropic energy we assume a total plasma energy $E^{tot}_{e^+e^-} = (1.10 \pm 0.06) \times 10^{53}$erg and derive a Baryon load $B = (1.45 \pm 0.28) \times 10^{-3}$ and a Lorentz factor at transparency $\Gamma_{tr} = (6.7 \pm 1.6) \times 10^2$. The main emission $\sim$ 0.4s after the initial spike is interpreted as the extended afterglow, due to the interaction of the ultrarelativistic baryons with the CircumBurst Medium (CBM). Using the condition of fully radiative regime, we infer a CBM average spherically symmetric density of $\langle n_{CBM} \rangle = (1.85 \pm 0.14) \times 10^3$ particles/cm^3, one of the highest found in the Fireshell model. The value of the filling factor, $1.5 \times 10^{-10} \leq \mathcal{R} \leq 3.8 \times 10^{-8}$, leads to the estimate of filaments with densities $n_{fil} = n_{CBM}/\mathcal{R} \approx (10^6 - 10^{14})$ particles/cm^3. The sub-MeV and the MeV emissions are well reproduced. When compared to the canonical GRBs with $\langle n_{CBM} \rangle \approx 1$ particles/cm^3 and to the disguised short GRBs with $\langle n_{CBM} \rangle \approx 10^{-3}$ particles/cm^3, the case of GRB 090510 leads to the existence of a new family of bursts exploding in an over-dense galactic region with $\langle n_{CBM} \rangle \approx 10^3$ particles/cm^3. The joint effect of the high Γ_{tr} and the high density compresses in time and "inflates" in intensity the extended afterglow, making it appear as a short burst, which we here define as "disguised short GRB by excess". The determination of the above parameters values may represent an important step towards the explanation of the GeV emission.

33. R. Ruffini, M. Muccino, C.L. Bianco, M. Enderli, L. Izzo, M. Kovacevic, A.V. Penacchioni, G.B. Pisani, J.A. Rueda, Y. Wang; "On Binary Driven Hypernovae and their nested late X-ray emission"; Astronomy & Astrophysics, 565, L10 (2014).

    Context: The induced gravitational collapse (IGC) paradigm addresses the very energetic (10^{52}–10^{54} erg) long gamma-ray bursts (GRBs) associated to supernovae (SNe). Unlike the traditional "collapsar" model, an evolved FeCO core with a companion neutron star (NS) in a tight binary system is considered as the progenitor. This special class of sources, here named "binary driven hypernovae" (BdHNe), presents a composite sequence composed of four different episodes with precise spectral and luminosity features.
    Aims: We first compare and contrast the steep decay, the plateau, and the power-law decay of the X-ray luminosities of three selected BdHNe (GRB 060729, GRB 061121, and GRB 130427A). Second, to explain the different sizes and Lorentz factors of the emitting regions of the four episodes, for definiteness, we use the most complete set of data of GRB 090618. Finally, we show the possible role of r-process, which originates in the binary system of the progenitor.
    Methods: We compare and contrast the late X-ray luminosity of the above three BdHNe. We examine correlations between the time at the starting point of the constant late power-law decay t_a^*, the average prompt luminosity $\langle L_{iso} \rangle$, and the luminosity at the end of the plateau L_a. We analyze a thermal emission ($\sim$ 0.97–0.29 keV), observed during the X-ray steep decay phase of GRB 090618.
    Results: The late X-ray luminosities of the three BdHNe, in the rest-frame energy band 0.3–10 keV, show a precisely constrained "nested" structure. In a space-time diagram, we illustrate the different sizes and Lorentz factors of the emitting regions of the three episodes. For GRB 090618, we infer an initial dimension of the thermal emitter of $\sim 7 \times 10^{12}$ cm, expanding at $\Gamma \approx 2$. We find tighter correlations than the Dainotti-Willingale ones.
    Conclusions: We confirm a constant slope power-law behavior for the late X-ray luminosity in the source rest frame, which may lead to a new distance indicator for BdHNe. These results, as well as the emitter size and Lorentz factor, appear to be inconsistent with the traditional afterglow model based on synchrotron emission from an ultra-relativistic ($\Gamma \sim 10^2$–10^3) collimated jet outflow. We argue, instead, for the possible role of r-process, originating in the binary system, to power the mildly relativistic X-ray source.

34. R. Ruffini, L. Izzo, M. Muccino, G.B. Pisani, J.A. Rueda, Y. Wang, C. Barbarino, C.L. Bianco, M. Enderli, M. Kovacevic; "Induced gravitational collapse at extreme cosmological distances: the case of GRB 090423"; Astronomy & Astrophysics, 569, A39 (2014).

    Context: The induced gravitational collapse (IGC) scenario has been introduced in order to explain the most energetic gamma ray bursts (GRBs), $E_{iso} = 10^{52} - 10^{54}$ erg, associated with type Ib/c supernovae (SNe). It has led to the concept of binary-driven hypernovae (BdHNe) originating in a tight binary system composed by a FeCO core on the verge of a SN explosion and a companion neutron star (NS). Their evolution is characterized by a rapid sequence of events: 1) The SN explodes, giving birth to a new NS (νNS). The accretion of SN ejecta onto the companion NS increases its mass up to the critical value; 2) The consequent gravitational collapse is triggered, leading to the formation of a black hole (BH) with GRB emission; 3) A novel feature responsible for the emission in the GeV, X-ray, and optical energy range occurs and is characterized by specific power-law behavior in their luminosity evolution and total spectrum; 4) The optical observations of the SN then occurs.
    Aims: We investigate whether GRB 090423, one of the farthest observed GRB at $z = 8.2$, is a member of the BdHN family.
    Methods: We compare and contrast the spectra, the luminosity evolution, and the detectability in the observations by *Swift* of GRB 090423 with the corresponding ones of the best known BdHN case, GRB 090618.
    Results: Identification of constant slope power-law behavior in the late X-ray emission of GRB 090423 and its overlapping with the corresponding one in GRB 090618, measured in a common rest frame, represents the main result of this article. This result represents a very significant step on the way to using the scaling law properties, proven in Episode 3 of this BdHN family, as a cosmological standard candle.
    Conclusions: Having identified GRB 090423 as a member of the BdHN family, we can conclude that SN events, leading to NS formation, can already occur already at $z = 8.2$, namely at 650 Myr after the Big Bang. It is then possible that these BdHNe originate stem from 40-60 $M_\odot$ binaries. They are probing the Population II stars after the completion and possible disappearance of Population III stars.

35. M. Muccino, C.L. Bianco, L. Izzo, Y. Wang, M. Enderli, M. Kovacevic, G.B. Pisani, A.V. Penacchioni, R. Ruffini; "The Genuine Short GRB 090227B and the Disguised by Excess GRB 090510"; Gravitation and

Cosmology, 20, 197 (2014).

GRB 090227B and GRB 090510, traditionally classified as short gamma-ray Bursts (GRBs), indeed originate from different systems. For GRB 090227B we inferred a total energy of the e^+e^- plasma $E^{tot}_{e^+e^-} = (2.83 \pm 0.15) \times 10^{53}$ erg, a baryon load of $B = (4.1 \pm 0.05) \times 10^{-5}$, and a CircumBurst Medium (CBM) average density $\langle n_{CBM} \rangle = (1.90 \pm 0.20) \times 10^{-5}$ cm^{-3}. From these results we have assumed the progenitor of this burst to be a symmetric neutron stars (NSs) merger with masses $m = 1.34 M_\odot$, radii $R = 12.24$ km. GRB 090510, instead, has $E^{tot}_{e^+e^-} = (1.10 \pm 0.06) \times 10^{53}$ erg, $B = (1.45 \pm 0.28) \times 10^{-3}$, implying a Lorentz factor at transparency of $\Gamma = (6.7 \pm 1.7) \times 10^2$, which are characteristic of the long GRB class, and a very high CBM density, $\langle n_{CBM} \rangle = (1.85 \pm 0.14) \times 10^3$ cm^{-3}. The joint effect of the high values of Γ and of $\langle n_{CBM} \rangle$ compresses in time and "inflates" in intensity in an extended afterglow, making appear GRB 090510 as a short burst, which we here define as "disguised short GRB by excess" occurring an overdense region with 10^3 cm^{-3}.

36. M. Muccino, C.L. Bianco, L. Izzo, Y. Wang, M. Enderli, G.B. Pisani, A.V. Penacchioni, R. Ruffini; "Two short bursts originating from different astrophysical systems: The genuine short GRB 090227B and the disguised short GRB 090510 by excess"; Journal of the Korean Physical Society, 65, 865 (2014).

    GRB 090227B and GRB 090510 are two gamma-ray bursts (GRBs) traditionally classified as short bursts. The major outcome of our analysis is that they indeed originate from different systems. In the case of GRB 090227B, from the inferred values of the total energy of the e^+e^- plasma, $E^{tot}_{e^+e^-} = (2.83 \pm 0.15) \times 10^{53}$ erg, the engulfed baryonic mass M_B, expressed as $B = M_B c^2 / E^{tot}_{e^+e^-} = (4.1 \pm 0.05) \times 10^{-5}$, and the circumburst medium (CBM) average density, $\langle n_{CBM} \rangle = (1.90 \pm 0.20) \times 10^{-5}$ cm^{-3}, we have assumed the progenitor of this burst to be a symmetric neutron star (NS) merger with masses $m = 1.34 M_\odot$, radii $R = 12.24$ km, and crustal thicknesses of ~ 0.47 km. In the case of GRB 090510, we have derived the total plasma energy, $E^{tot}_{e^+e^-} = (1.10 \pm 0.06) \times 10^{53}$ erg, the Baryon load, $B = (1.45 \pm 0.28) \times 10^{-3}$, and the Lorentz factor at transparency, $\Gamma = (6.7 \pm 1.7) \times 10^2$, which are characteristic of the long GRB class, as well as a very high CBM density, $\langle n_{CBM} \rangle = (1.85 \pm 0.14) \times 10^3$ cm^{-3}. The joint effect of the high values of Γ and $\langle n_{CBM} \rangle$ compresses in time and "inflates" in intensity the extended afterglow, making GRB 090510 appear to be a short burst, which we here define as a "disguised short GRB by excess", occurring in an overdense region with 10^3 cm^{-3}.

37. R. Ruffini, Y. Wang, M. Kovacevic, C.L. Bianco, M. Enderli, M. Muccino, A.V. Penacchioni, G.B. Pisani, J. Rueda; "GRB 130427A and SN 2013cq: A Multi-wavelength Analysis of An Induced Gravitational Collapse Event"; The Astrophysical Journal, 798, 10 (2015).

    We have performed our data analysis of the observations by *Swift*, *NuStar* and *Fermi* satellites in order to probe the induced gravitational collapse (IGC) paradigm for GRBs associated with supernovae (SNe), in the "terra incognita" of GRB 130427A. We compare and contrast our data analysis with those in the literature. We have verified that the GRB 130427A conforms to the IGC paradigm by examining the power law behavior of the luminosity in the early 10^4 s of the XRT observations. This has led to the identification of the four different episodes of the "binary driven hypernovae" (BdHNe) and to the prediction, on May 2, 2013, of the occurrence of SN 2013cq, duly observed in the optical band on May 13, 2013. The exceptional quality of the data has allowed the identification of novel features in *Episode 3* including: a) the confirmation and the extension of the existence of the recently discovered "nested structure" in the late X-ray luminosity in GRB 130427A, as well as the identification of a spiky structure at 10^2 s in the cosmological rest-frame of the source; b) a power law emission of the GeV luminosity light curve and its onset at the end of *Episode 2*; c) different Lorentz Γ factors for the emitting regions of the X-ray and GeV emissions in this *Episode 3*. These results make it possible to test the details of the physical and astrophysical regimes at work in the BdHNe: 1) a newly born neutron star and the supernova ejecta, originating in *Episode 1*, 2) a newly formed black hole originating in *Episode 2*, and 3) the possible interaction among these components, observable in the standard features of *Episode 3*.

38. M. Muccino, R. Ruffini, C.L. Bianco, M. Enderli, M. Kovacevic, L. Izzo, A.V. Penacchioni, G.B. Pisani, J.A. Rueda, Y. Wang; "On binary driven hypernovae and their nested late X-ray emission"; Astronomy Reports, 59, 581 (2015).

    The induced gravitational collapse (IGC) paradigm addresses energetic (10^{52}–10^{54} erg), long gamma-ray bursts (GRBs) associated to supernovae (SNe) and proposes as their progenitors tight binary systems composed of an evolved FeCO core and a companion neutron star (NS). Their emission is characterized by four specific episodes: Episode 1, corresponding to the on-set of the FeCO

SN explosion and the accretion of the ejecta onto the companion NS; Episode 2, related the collapse of the companion NS to a black hole (BH) and to the emission of a long GRB; Episode 3, observed in X-rays and characterized by a steep decay, a plateau phase and a late power-law decay; Episode 4, corresponding to the optical SN emission due to the ^{56}Ni decay. We focus on Episode 3 and we show that, from the thermal component observed during the steep decay of the prototype GRB 090618, the emission region has a typical dimension of $\sim 10^{13}$ cm, which is inconsistent with the typical size of the emitting region of GRBs, e.g., $\sim 10^{16}$ cm. We propose, therefore, that the X-ray afterglow emission originates from a spherically symmetric SN ejecta expanding at $\Gamma \sim 2$ or, possibly, from the accretion onto the newly formed black hole, and we name these systems "binary driven hypernovae" (BdHNe). This interpretation is alternative to the traditional afterglow model based on the GRB synchrotron emission from a collimated jet outflow, expanding at ultra-relativistic Lorentz factor of $\Gamma \sim 10^2 - 10^3$ and originating from the collapse of a single object. We show then that the rest-frame energy band 0.3–10 keV X-ray luminosities of three selected BdHNe, GRB 060729, GRB 061121, and GRB 130427A, evidence a precisely constrained "nested" structure and satisfy precise scaling laws between the average prompt luminosity, $< L_{iso} >$, and the luminosity at the end of the plateau, L_a, as functions of the time at the end of the plateau. All these features extend the applicability of the "cosmic candle" nature of Episode 3. The relevance of r-process in fulfilling the demanding scaling laws and the nested structure are indicated.

39. R. Ruffini, J.A. Rueda, C. Barbarino, C. L. Bianco, H. Dereli, M. Enderli, L. Izzo, M. Muccino, A.V. Penacchioni, G.B. Pisani, Y. Wang; "Induced Gravitational Collapse in the BATSE era: the case of GRB 970828"; Astronomy Reports, 59, 626 (2015).

    Following the recently established "Binary-driven HyperNova" (BdHN) paradigm, we here interpret GRB 970828 in terms of the four episodes typical of such a model. The "Episode 1", up to 40 s after the trigger time t_0, with a time varying thermal emission and a total energy of $E_{iso,1st} = 2.60 \times 10^{53}$ erg, is interpreted as due to the onset of an hyper-critical accretion process onto a companion neutron star, triggered by the companion star, an FeCO core approaching a SN explosion. The "Episode 2", observed up t_0+90 s, is interpreted as a canonical gamma ray burst, with an energy of $E^{e^+e^-}_{tot} = 1.60 \times 10^{53}$ erg, a baryon load of $B = 7 \times 10^{-3}$ and a bulk Lorentz factor at transparency of $\Gamma = 142.5$. From this Episode 2, we infer that the GRB exploded in an environment with a large average particle density $\langle n \rangle \approx 10^3$ particles/cm^3 and dense clouds characterized by typical dimensions of $(4 \div 8) \times 10^{14}$ cm and $\delta n/n \sim 10$. The "Episode 3" is identified from t_0+90 s all the way up to 10^{5-6} s: despite the paucity of the early X-ray data, typical in the BATSE, pre-Swift era, we find extremely significant data points in the late X-ray afterglow emission of GRB 970828, which corresponds to the ones observed in all BdHNe sources. The "Episode 4", related to the Supernova emission, does not appear to be observable in this source, due to the presence of darkening from the large density of the GRB environment, also inferred from the analysis of the Episode 2.

40. Y. Wang, R. Ruffini, M. Kovacevic, C.L. Bianco, M. Enderli, M. Muccino, A.V. Penacchioni, G.B. Pisani, J.A. Rueda; "Predicting supernova associated to gamma-ray burst 130427a"; Astronomy Reports, 59, 667 (2015).

    Binary systems constituted by a neutron star and a massive star are not rare in the universe. The Induced Gravitational Gamma-ray Burst (IGC) paradigm interprets Gamma-ray bursts as the outcome of a neutron star that collapses into a black hole due to the accretion of the ejecta coming from its companion massive star that underwent a supernova event. GRB 130427A is one of the most luminous GRBs ever observed, of which isotropic energy exceeds 10^{54} erg. And it is within one of the few GRBs obtained optical, X-ray and GeV spectra simultaneously for hundreds of seconds, which provides an unique opportunity so far to understand the multi-wavelength observation within the IGC paradigm, our data analysis found low Lorentz factor blackbody emission in the Episode 3 and its X-ray light curve overlaps typical IGC Golden Sample, which comply to the IGC mechanisms. We consider these findings as clues of GRB 130427A belonging to the IGC GRBs. We predicted on GCN the emergence of a supernova on May 2, 2013, which was later successfully detected on May 13, 2013.

41. R. Ruffini, M. Muccino, M. Kovacevic, F.G. Oliveira, J.A. Rueda, C.L. Bianco, M. Enderli, A.V. Penacchioni, G.B. Pisani, Y. Wang, E. Zaninoni; "GRB 140619B: a short GRB from a binary neutron star merger leading to black hole formation"; The Astrophysical Journal, 808, 190 (2015).

    We show the existence of two families of short GRBs, both originating from the merger of binary neutron stars (NSs): family-1 with $E_{iso} < 10^{52}$ erg, leading to a massive NS as the merged core, and family-2 with $E_{iso} > 10^{52}$ erg, leading to a black hole (BH). Following the identification of the prototype

GRB 090227B, we present the details of a new example of family-2 short burst: GRB 140619B. From the spectral analysis of the early ~ 0.2 s, we infer an observed temperature $kT = (324 \pm 33)$ keV of the e^+e^--plasma at transparency (P-GRB), a theoretically derived redshift $z = 2.67 \pm 0.37$, a total burst energy $E^{tot}_{e^+e^-} = (6.03 \pm 0.79) \times 10^{52}$ erg, a rest-frame peak energy $E_{p,i} = 4.7$ MeV, and a baryon load $B = (5.52 \pm 0.73) \times 10^{-5}$. We also estimate the corresponding emission of gravitational waves. Two additional examples of family-2 short bursts are identified: GRB 081024B and GRB 090510, remarkable for its well determined cosmological distance. We show that marked differences exist in the nature of the afterglows of these two families of short bursts: family-2 bursts, leading to BH formation, consistently exhibit high energy emission following the P-GRB emission; family-1 bursts, leading to the formation of a massive NS, should never exhibit high energy emission. We also show that both the families fulfill an $E_{p,i}$–E_{iso} relation with slope $\gamma = 0.59 \pm 0.07$ and a normalization constant incompatible with the one for long GRBs. The observed rate of such family-2 events is $\rho_0 = \left(2.1^{+2.8}_{-1.4}\right) \times 10^{-4}\mathrm{Gpc}^{-3}\mathrm{yr}^{-1}$.

42. R. Ruffini, Y. Aimuratov, C.L. Bianco, M. Enderli, M. Kovacevic, R. Moradi, M. Muccino, A.V. Penacchioni, G.B. Pisani, J.A. Rueda, Y. Wang; "Induced gravitational collapse in FeCO Core-Neutron star binaries and Neutron star-Neutron star binary mergers"; International Journal of Modern Physics A, 30, 1545023 (2015).

    We review the recent progress in understanding the nature of gamma-ray bursts (GRBs). The occurrence of GRB is explained by the Induced Gravitational Collapse (IGC) in FeCO Core-Neutron star binaries and Neutron star-Neutron star binary mergers, both processes occur within binary system progenitors. Making use of this most unexpected new paradigm, with the fundamental implications by the neutron star (NS) critical mass, we find that different initial configurations of binary systems lead to different GRB families with specific new physical predictions confirmed by observations.

43. R. Ruffini, M. Muccino, Y. Aimuratov, C.L. Bianco, C. Cherubini, M. Enderli, M. Kovacevic, R. Moradi, A.V. Penacchioni, G.B. Pisani, J.A. Rueda, Y. Wang; "GRB 090510: A genuine short-GRB from a binary neutron star coalescing into a Kerr-Newman black hole"; The Astrophysical Journal, 831, 178 (2016).

    In a new classification of merging binary neutron stars (NSs) we separate short gamma-ray bursts (GRBs) in two sub-classes. The ones with $E_{\rm iso} \lesssim 10^{52}$ erg coalesce to form a massive NS and are indicated as short gamma-ray flashes (S-GRFs). The hardest, with $E_{\rm iso} \gtrsim 10^{52}$ erg, coalesce to form a black hole (BH) and are indicated as genuine short-GRBs (S-GRBs). Within the fireshell model, S-GRBs exhibit three different components: the P-GRB emission, observed at the transparency of a self-accelerating baryon-e^+e^- plasma; the prompt emission, originating from the interaction of the accelerated baryons with the circumburst medium; the high-energy (GeV) emission, observed after the P-GRB and indicating the formation of a BH. GRB 090510 gives the first evidence for the formation of a Kerr BH or, possibly, a Kerr-Newman BH. Its P-GRB spectrum can be fitted by a convolution of thermal spectra whose origin can be traced back to an axially symmetric dyadotorus. A large value of the angular momentum of the newborn BH is consistent with the large energetics of this S-GRB, which reach in the 1–10000 keV range $E_{\rm iso} = (3.95 \pm 0.21) \times 10^{52}$ erg and in the 0.1–100 GeV range $E_{\rm LAT} = (5.78 \pm 0.60) \times 10^{52}$ erg, the most energetic GeV emission ever observed in S-GRBs. The theoretical redshift $z_{\rm th} = 0.75 \pm 0.17$ that we derive from the fireshell theory is consistent with the spectroscopic measurement $z = 0.903 \pm 0.003$, showing the self-consistency of the theoretical approach. All S-GRBs exhibit GeV emission, when inside the *Fermi*-LAT field of view, unlike S-GRFs, which never evidence it. The GeV emission appears to be the discriminant for the formation of a BH in GRBs, confirmed by their observed overall energetics.

44. Ruffini, R.; Rueda, J. A.; Muccino, M.; Aimuratov, Y.; Becerra, L. M.; Bianco, C. L.; Kovacevic, M.; Moradi, R.; Oliveira, F. G.; Pisani, G. B.; Wang, Y.; On the classification of GRBs and their occurrence rates; The Astrophysical Journal, 832, 136 (2016).

    There is mounting evidence for the binary nature of the progenitors of gamma-ray bursts (GRBs). For a long GRB, the induced gravitational collapse (IGC) paradigm proposes as progenitor, or "in-state", a tight binary system composed of a carbon-oxygen core ($CO_{\rm core}$) undergoing a supernova (SN) explosion which triggers hypercritical accretion onto a neutron star (NS) companion. For a short GRB, a NS-NS merger is traditionally adopted as the progenitor. We divide long and short GRBs into two sub-classes, depending on whether or not a black hole (BH) is formed in the merger or in the hypercritical accretion process exceeding the NS critical mass. For long bursts, when no BH is formed we have the sub-class of X-ray flashes (XRFs), with isotropic energy $E_{iso} \lesssim 10^{52}$ erg and rest-frame spectral peak energy $E_{p,i} \lesssim 200$ keV. When a BH is formed we have the sub-class of binary-driven hypernovae (BdHNe), with $E_{iso} \gtrsim 10^{52}$ erg and $E_{p,i} \gtrsim 200$ keV. In analogy, short bursts are similarly divided into two sub-classes. When no BH is formed, short gamma-ray flashes (S-GRFs) occur, with $E_{iso} \lesssim 10^{52}$ erg and $E_{p,i} \lesssim 2$ MeV. When a BH is formed, the authentic short GRBs (S-GRBs) occur, with $E_{iso} \gtrsim 10^{52}$ erg and $E_{p,i} \gtrsim 2$ MeV. We give examples and observational signatures of these four sub-classes and their rate of occurrence. From their respective rates it is possible that "in-states" of S-GRFs and S-GRBs originate from the "out-states" of XRFs. We indicate two additional progenitor systems: white dwarf-NS and BH-NS. These systems have hybrid features between long and short bursts. In the case of S-GRBs and BdHNe evidence is given of the coincidence of the onset of the high energy GeV emission with the birth of a Kerr BH.

45. Becerra, L.; Bianco, C. L.; Fryer, C. L.; Rueda, J. A.; Ruffini, R.; On the induced gravitational collapse scenario of gamma-ray bursts associated with supernovae; The Astrophysical Journal, 833, 107 (2016).

    Following the induced gravitational collapse (IGC) paradigm of gamma-ray bursts (GRBs) associated with type Ib/c supernovae, we present numerical simulations of the explosion of a carbon-oxygen (CO) core in a binary system with a neutron-star (NS) companion. The supernova ejecta trigger a *hypercritical* accretion process onto the NS thanks to a copious neutrino emission and the trapping of photons within the accretion flow. We show that temperatures 1–10 MeV develop near the NS surface, hence electron-positron annihilation into neutrinos becomes the main cooling channel leading to accretion rates 10^{-9}–10^{-1} $M_\odot$ s^{-1} and neutrino luminosities 10^{43}–10^{52} erg s^{-1} (the shorter the orbital period the higher the accretion rate). We estimate the maximum orbital period, $P_{\rm max}$, as a function of the NS initial mass, up to which the NS companion can reach by hypercritical accretion the critical mass for gravitational collapse leading to black-hole (BH) formation. We then estimate the effects of the accreting and orbiting NS companion onto a novel geometry of the supernova ejecta density profile. We present the results of a 1.4×10^7 particle simulation which show that the NS induces accentuated asymmetries in the ejecta density around the orbital plane. We elaborate on the observables associated with the above features of the IGC process. We apply this framework to specific GRBs: we find that X-ray flashes (XRFs) and binary-driven hypernovae (BdHNe) are produced in binaries with $P > P_{\rm max}$ and $P < P_{\rm max}$, respectively. We analyze in detail the case of XRF 060218.

46. Pisani, G. B.; Ruffini, R.; Aimuratov, Y.; Bianco, C. L.; Kovacevic, M.;

Moradi, R.; Muccino, M.; Penacchioni, A. V.; Rueda, J. A.; Shakeri, S.; Wang, Y.; On the universal late X-ray emission of binary-driven hypernovae and its possible collimation; The Astrophysical Journal, 833, 159 (2016).

It has been previously discovered a universal power-law behaviour of the late X-ray emission (LXRE) of a "golden sample" (GS) of six long energetic GRBs, when observed in the rest-frame of the source. This remarkable feature, independent on the different isotropic energy (E_{iso}) of each GRB, has been used to estimate the cosmological redshift of some long GRBs. This analysis is here extended to a new class of 161 long GRBs, all with $E_{iso} > 10^{52}$ erg. These GRBs are indicated as binary-driven hypernovae (BdHNe) in view of their progenitors: a tight binary systems composed of a carbon-oxigen core (CO_{core}) and a neutron star (NS) undergoing an induced gravitational collapse (IGC) to a black hole (BH) triggered by the CO_{core} explosion as a supernova (SN). We confirm the universal behaviour of the LXRE for the "enlarged sample" (ES) of 161 BdHNe observed up to the end of 2015, assuming a double-cone emitting region. We obtain a distribution of half-opening angles peaking at $\theta = 17.62^{\circ}$, with mean value 30.05°, and a standard deviation 19.65°. This, in turn, leads to the possible establishment of a new cosmological candle. Within the IGC model, such universal LXRE behaviour is only indirectly related to the GRB and originates from the SN ejecta, of a standard constant mass, being shocked by the GRB emission. The fulfillment of the universal relation in the LXRE and its independence of the prompt emission, further confirmed in this article, establishes a crucial test for any viable GRB model.

47. Y. Aimuratov, R. Ruffini, M. Muccino, C.L. Bianco, A.V. Penacchioni, G.B. Pisani, D. Primorac, J.A. Rueda, Y. Wang; GRB 081024B and GRB 140402A: Two Additional Short GRBs from Binary Neutron Star Mergers; The Astrophysical Journal, 844, 83 (2017).

    Theoretical and observational evidences have been recently gained for a twofold classification of short bursts: 1) short gamma-ray flashes (S-GRFs), with isotropic energy $E_{iso} < 10^{52}$ erg and no BH formation, and 2) the authentic short gamma-ray bursts (S-GRBs), with isotropic energy $E_{iso} > 10^{52}$ erg evidencing a BH formation in the binary neutron star merging process. The signature for the BH formation consists in the on-set of the high energy (0.1–100 GeV) emission, coeval to the prompt emission, in all S-GRBs. No GeV emission is expected nor observed in the S-GRFs. In this paper we present two additional S-GRBs, GRB 081024B and GRB 140402A, following the already identified S-GRBs, i.e., GRB 090227B, GRB 090510 and GRB 140619B. We also return on the absence of the GeV emission of the S-GRB 090227B, at an angle of 71° from the *Fermi*-LAT boresight. All the correctly identified S-GRBs correlate to the high energy emission, implying no significant presence of beaming in the GeV emission. The existence of a common power-law behavior in the GeV luminosities, following the BH formation, when measured in the source rest-frame, points to a commonality in the mass and spin of the newly-formed BH in all S-GRBs.

48. J.A. Rueda, Y. Aimuratov, U. Barres de Almeida, L.M. Becerra, C.L. Bianco, C. Cherubini, S. Filippi, M. Karlica, M. Kovacevic, J.D. Melon Fuksman, R. Moradi, M. Muccino, A.V. Penacchioni, G.B. Pisani, D. Primorac, R. Ruffini, N. Sahakyan, S. Shakeri, Y. Wang; The binary systems associated with short and long gamma-ray bursts and their detectability; International Journal of Modern Physics D, 26, 1730016 (2017).

    Short and long-duration gamma-ray bursts (GRBs) have been recently subclassified into seven families according to the binary nature of their progenitors. For short GRBs, mergers of neutron star binaries (NS–NS) or neutron star-black hole binaries (NS-BH) are proposed. For long GRBs, the induced gravitational collapse (IGC) paradigm proposes a tight binary system composed of a carbon–oxygen core (COcore) and a NS companion. The explosion of the COcore as supernova (SN) triggers a hypercritical accretion process onto the NS companion which might reach the critical mass for the gravitational collapse to a BH. Thus, this process can lead either to a NS-BH or to NS–NS depending on whether or not the accretion is sufficient to induce the collapse of the NS into a BH. We shall discuss for the above compact object binaries: (1) the role of the NS structure and the equation-of-state on their final fate; (2) their occurrence rates as inferred from the X and gamma-ray observations; (3) the expected number of detections of their gravitational wave (GW) emission by the Advanced LIGO interferometer.

49. R. Ruffini, Y. Aimuratov, L.M. Becerra, C.L. Bianco, M. Karlica, M. Kovacevic, J.D. Melon Fuksman, R. Moradi, M. Muccino, A.V. Penacchioni, G.B. Pisani, D. Primorac, J.A. Rueda, S. Shakeri, G.V. Vereshchagin, Y. Wang, S.-S. Xue; The cosmic matrix in the 50th anniversary of relativistic astrophysics; International Journal of Modern Physics D, 26, 1730019 (2017).

Our concept of induced gravitational collapse (IGC paradigm) starting from a supernova occurring with a companion neutron star, has unlocked the understanding of seven different families of gamma ray bursts (GRBs), indicating a path for the formation of black holes in the universe. An authentic laboratory of relativistic astrophysics has been unveiled in which new paradigms have been introduced in order to advance knowledge of the most energetic, distant and complex systems in our universe. A novel cosmic matrix paradigm has been introduced at a relativistic cosmic level, which parallels the concept of an S-matrix introduced by Feynmann, Wheeler and Heisenberg in the quantum world of microphysics. Here the "in" states are represented by a neutron star and a supernova, while the "out" states, generated within less than a second, are a new neutron star and a black hole. This novel field of research needs very powerful technological observations in all wavelengths ranging from radio through optical, X-ray and gamma ray radiation all the way up to ultra-high-energy cosmic rays.

50. R. Ruffini, Y. Wang, Y. Aimuratov, U. Barres de Almeida, L.M. Becerra, C.L. Bianco, Y.C. Chen, M. Karlica, M. Kovacevic, L. Li, J.D. Melon Fuksman, R. Moradi, M. Muccino, A.V. Penacchioni, G.B. Pisani, D. Primorac, J.A. Rueda, S. Shakeri, G.V. Vereshchagin, S.-S. Xue; Early X-Ray Flares in GRBs; The Astrophysical Journal, 852, 53 (2018).

    We analyze the early X-ray flares in the GRB "flare-plateau-afterglow" (FPA) phase observed by Swift-XRT. The FPA occurs only in one of the seven GRB subclasses: the binary-driven hypernovae (BdHNe). This subclass consists of long GRBs with a carbon-oxygen core and a neutron star (NS) binary companion as progenitors. The hypercritical accretion of the supernova (SN) ejecta onto the NS can lead to the gravitational collapse of the NS into a black hole. Consequently, one can observe a GRB emission with isotropic energy $E_{iso} \gtrsim 10^{52}$ erg, as well as the associated GeV emission and the FPA phase. Previous work had shown that gamma-ray spikes in the prompt emission occur at $\sim 10^{15}$–10^{17} cm with Lorentz gamma factor $\Gamma \sim 10^2$–10^3. Using a novel data analysis we show that the time of occurrence, duration, luminosity and total energy of the X-ray flares correlate with E_{iso}. A crucial feature is the observation of thermal emission in the X-ray flares that we show occurs at radii $\sim 10^{12}$ cm with $\Gamma \lesssim 4$. These model independent observations cannot be explained by the "fireball" model, which postulates synchrotron and inverse Compton radiation from a single ultra relativistic jetted emission extending from the prompt to the late afterglow and GeV emission phases. We show that in BdHNe a collision between the GRB and the SN ejecta occurs at $\simeq 10^{10}$ cm reaching transparency at $\sim 10^{12}$ cm with $\Gamma \lesssim 4$. The agreement between the thermal emission observations and these theoretically derived values validates our model and opens the possibility of testing each BdHN episode with the corresponding Lorentz gamma factor.

51. R. Ruffini, J. Rodriguez, M. Muccino, J.A. Rueda, Y. Aimuratov, U. Barres de Almeida, L.M. Becerra, C.L. Bianco, C. Cherubini, S. Filippi, D. Gizzi, M. Kovacevic, R. Moradi, F.G. Oliveira, G.B. Pisani, Y. Wang; On the Rate and on the Gravitational Wave Emission of Short and Long GRBs; The Astrophysical Journal, 859, 30 (2018).

    On the ground of the large number of gamma-ray bursts (GRBs) detected with cosmological redshift, we classified GRBs in seven subclasses, all with binary progenitors which emit gravitational waves (GWs). Each binary is composed of combinations of carbon-oxygen cores (COcore), neutron stars (NSs), black holes (BHs), and white dwarfs (WDs). The long bursts, traditionally assumed to originate from a BH with an ultrarelativistic jetted emission, not emitting GWs, have been subclassified as (I) X-ray flashes (XRFs), (II) binary-driven hypernovae (BdHNe), and (III) BH-supernovae (BH-SNe). They are framed within the induced gravitational collapse paradigm with a progenitor COcore-NS/BH binary. The SN explosion of the COcore triggers an accretion process onto the NS/BH. If the accretion does not lead the NS to its critical mass, an XRF occurs, while when the BH is present or formed by accretion, a BdHN occurs. When the binaries are not disrupted, XRFs lead to NS-NS and BdHNe lead to NS-BH. The short bursts, originating in NS-NS, are subclassified as (IV) short gamma-ray flashes (S-GRFs) and (V) short GRBs (S-GRBs), the latter when a BH is formed. There are (VI) ultrashort GRBs (U-GRBs) and (VII) gamma-ray flashes (GRFs) formed in NS-BH and NS-WD, respectively. We use the occurrence rate and GW emission of these subclasses to assess their detectability by Advanced LIGO-Virgo, eLISA, and resonant bars. We discuss the consequences of our results in view of the announcement of the LIGO/Virgo Collaboration of the source GW 170817 as being originated by an NS-NS.

52. J.A. Rueda, R. Ruffini, Y. Wang, Y. Aimuratov, U. Barres de Almeida, C.L. Bianco, Y.-C. Chen, R.V. Lobato, C. Maia, D. Primorac, R. Moradi, J. Rodriguez; GRB 170817A-GW170817-AT 2017gfo and the observations of NS-NS, NS-WD and WD-WD mergers; Journal of Cosmology and Astroparticle Physics, 10, 006 (2018).

The LIGO-Virgo Collaboration has announced the detection of GW170817 and has associated it with GRB 170817A . These signals have been followed after 11 hours by the optical and infrared emission of AT 2017gfo. The origin of this complex phenomenon has been attributed to a neutron star-neutron star (NS-NS) merger. In order to probe this association we confront our current understanding of the gravitational waves and associated electromagnetic radiation with four observed GRBs originating in binaries composed of different combinations NSs and white dwarfs (WDs). We consider 1) GRB 090510 the prototype of NS-NS merger leading to a black hole (BH); 2) GRB 130603B the prototype of a NS-NS merger leading to massive NS (MNS) with an associated kilonova; 3) GRB 060614 the prototype of a NS-WD merger leading to a MNS with an associated kilonova candidate; 4) GRB 170817A the prototype of a WD-WD merger leading to massive WD with an associated AT 2017gfo-like emission. None of these systems support the above mentioned association. The clear association between GRB 170817A and AT 2017gfo has led to introduce a new model based on a new subfamily of GRBs originating from WD-WD mergers. We show how this novel model is in agreement with the exceptional observations in the optical, infrared, X- and gamma-rays of GRB 170817A-AT 2017gfo.

53. R. Ruffini, M. Karlica, N. Sahakyan, J.A. Rueda, Y. Wang, G.W. Mathews, C.L. Bianco, M. Muccino; A GRB Afterglow Model Consistent with Hypernova Observations; The Astrophysical Journal, 869, 101 (2018).

We describe the afterglows of the long gamma-ray-burst (GRB) 130427A within the context of a binary-driven hypernova. The afterglows originate from the interaction between a newly born neutron star (νNS), created by an Ic supernova (SN), and a mildly relativistic ejecta of a hypernova (HN). Such an HN in turn results from the impact of the GRB on the original SN Ic. The mildly relativistic expansion velocity of the afterglow ($\Gamma \sim 3$) is determined, using our model-independent approach, from the thermal emission between 196 and 461 s. The power law in the optical and X-ray bands of the afterglow is shown to arise from the synchrotron emission of relativistic electrons in the expanding magnetized HN ejecta. Two components contribute to the injected energy: the kinetic energy of the mildly relativistic expanding HN and the rotational energy of the fast-rotating highly magnetized ?NS. We reproduce the afterglow in all wavelengths from the optical (10^{14} Hz) to the X-ray band (10^{19} Hz) over times from 604 s to 5.18×10^6 s relative to the Fermi-GBM trigger. Initially, the emission is dominated by the loss of kinetic energy of the HN component.

After 10^5 s the emission is dominated by the loss of rotational energy of the νNS, for which we adopt an initial rotation period of 2 ms and a dipole plus quadrupole magnetic field of $\lesssim 7 \times 10^{12}$ G or $\sim 10^{14}$ G. This scenario with a progenitor composed of a COcore and an NS companion differs from the traditional ultra-relativistic-jetted treatments of the afterglows originating from a single black hole.

54. R. Ruffini, L.M. Becerra, C.L. Bianco, Y.-C. Chen, M. Karlica, M. Kovacevic, J.D. Melon Fuksman, R. Moradi, M. Muccino, G.B. Pisani, D. Primorac, J.A. Rueda, G.V. Vereshchagin, Y. Wang, S.-S. Xue; On the ultra-relativistic Prompt Emission (UPE), the Hard and Soft X-ray Flares, and the extended thermal emission (ETE) in GRB 151027A; The Astrophysical Journal, 869, 151 (2018).

    We analyze GRB 151027A within the binary-driven hypernova approach, with a progenitor of a carbon–oxygen core on the verge of a supernova (SN) explosion and a binary companion neutron star (NS). The hypercritical accretion of the SN ejecta onto the NS leads to its gravitational collapse into a black hole (BH), to the emission of the gamma-ray burst (GRB), and to a copious e+e- plasma. The impact of this e+e- plasma on the SN ejecta explains the early soft X-ray flare observed in long GRBs. Here, we apply this approach to the ultra-relativistic prompt emission (UPE) and to the hard X-ray flares. We use GRB 151027A as a prototype. From the time-integrated and the time-resolved analysis, we identify a double component in the UPE and confirm its ultra-relativistic nature. We confirm the mildly relativistic nature of the soft X-ray flare, of the hard X-ray flare, and of the extended thermal emission (ETE). We show that the ETE identifies the transition from an SN to a hypernova (HN). We then address the theoretical justification of these observations by integrating the hydrodynamical propagation equations of the e+e- into the SN ejecta, with the latter independently obtained from 3D smoothed particle hydrodynamics simulations. We conclude that the UPE, the hard X-ray flare, and the soft X-ray flare do not form a causally connected sequence. Within our model, they are the manifestation of the same physical process of the BH formation as seen through different viewing angles, implied by the morphology and the ~ 300 s rotation period of the HN ejecta.

55. R. Moradi, R. Ruffini, C.L. Bianco, Y.-C. Chen, M. Karlica, J.D. Melon Fuksman, D. Primorac, J.A. Rueda, S. Shakeri, Y. Wang, S.-S. Xue; Relativistic Behavior and Equitemporal Surfaces in Ultra-Relativistic Prompt

Emission Phase of Gamma-Ray Bursts; Astronomy Reports, 62, 905 (2018).

In this work we study a role of baryon load and interstellar medium density to explain the nature of peaks in the ultra-relativistic prompt emission (UPE) phase of Gamma-ray Bursts (GRBs). We study the behavior of their Γ Lorenz factor fromthe moment of transparency all the way up to interstellar medium. We finally study the characteristic of equitemporal surfaces in the UPE phase.

56. D. Primorac, M. Muccino, R. Moradi, Y. Wang, J.D. Melon Fuksman, R. Ruffini, C.L. Bianco, J.A. Rueda; Structure of the Prompt Emission of GRB 151027A Within the Fireshell Model; Astronomy Reports, 62, 933 (2018).

    Long gamma-ray burst GRB 151027A was observed by all three detectors on-board the Swift spacecraft, and many more, including MAXI, Konus-Wind and Fermi GBM/LAT instruments. This revealed a complex structure of the prompt and afterglow emission, consisting of a double-peak gammaray prompt with a quiescent period and a HRF/SXF within the X-ray afterglow, together with multiple BB components seen within the time-resolved spectral analysis. These features, within the fireshell model, are interpreted as the manifestation of the same physical process viewed at different angles with respect to the HN ejecta. Here we present the time-resolved and time-integrated spectral analysis used to determine the energy of the e-e+ plasma E_{tot} and the baryon load B. These quantities describe the dynamics of the fireshell up to the transparency point. We proceed with the light-curve simulation from which CBM density values and its inhomogeneities are deduced. We also investigate the properties of GRB 140206A, whose prompt emission exhibits a similar structure.

57. Y. Wang, J.A. Rueda, R. Ruffini, C.L. Bianco, L.M. Becerra, L. Li, M. Karlica; Two Predictions of Supernova: GRB 130427A/SN 2013cq and GRB 180728A/SN 2018fip; The Astrophysical Journal, 874, 39 (2019).

    On 2018 July 28, GRB 180728A triggered *Swift* satellites and, soon after the determination of the redshift, we identified this source as a type II binary-driven hypernova (BdHN II) in our model. Consequently, we predicted the appearance time of its associated supernova (SN), which was later confirmed as SN 2018fip. A BdHN II originates in a binary composed of a carbon-oxygen core (CO_{core}) undergoing SN, and the SN ejecta hypercritically accrete onto a companion neutron star (NS). From the time of the SN shock breakout to the time when the hypercritical accretion starts, we infer the binary separation

$\simeq 3 \times 10^{10}$ cm. The accretion explains the prompt emission of isotropic energy $\simeq 3 \times 10^{51}$ erg, lasting ~ 10 s, and the accompanying observed blackbody emission from a thermal convective instability bubble. The new neutron star (νNS) originating from the SN powers the late afterglow from which a νNS initial spin of 2.5 ms is inferred. We compare GRB 180728A with GRB 130427A, a type I binary-driven hypernova (BdHN I) with isotropic energy $> 10^{54}$ erg. For GRB 130427A we have inferred an initially closer binary separation of $\simeq 10^{10}$ cm, implying a higher accretion rate leading to the collapse of the NS companion with consequent black hole formation, and a faster, 1 ms spinning νNS. In both cases, the optical spectra of the SNe are similar, and not correlated to the energy of the gamma-ray burst. We present three-dimensional smoothed-particle-hydrodynamic simulations and visualisations of the BdHNe I and II.

58. J.A. Rueda, R. Ruffini, Y. Wang, C.L. Bianco, J.M. Blanco-Iglesias, M. Karlica, P. Lorén-Aguilar, R. Moradi, N. Sahakyan; Electromagnetic emission of white dwarf binary mergers; Journal of Cosmology and Astroparticle Physics, 03, 044 (2019).

    It has been recently proposed that the ejected matter from white dwarf (WD) binary mergers can produce transient, optical and infrared emission similar to the "kilonovae" of neutron star (NS) binary mergers. To confirm this we calculate the electromagnetic emission from WD-WD mergers and compare with kilonova observations. We simulate WD-WD mergers leading to a massive, fast rotating, highly magnetized WD with an adapted version of the smoothed-particle-hydrodynamics (SPH) code Phantom. We thus obtain initial conditions for the ejecta such as escape velocity, mass and initial position and distribution. The subsequent thermal and dynamical evolution of the ejecta is obtained by integrating the energy-conservation equation accounting for expansion cooling and a heating source given by the fallback accretion onto the newly-formed WD and its magneto-dipole radiation. We show that magnetospheric processes in the merger can lead to a prompt, short gamma-ray emission of up to $\approx 10^{46}$ erg in a timescale of 0.1–1 s. The bulk of the ejecta initially expands non-relativistically with velocity 0.01 c and then it accelerates to 0.1 c due to the injection of fallback accretion energy. The ejecta become transparent at optical wavelengths around ~ 7 days post-merger with a luminosity 10^{41}–10^{42} erg s^{-1}. The X-ray emission from the fallback accretion becomes visible around $\sim$ 150–200 day post-merger with a luminosity of 10^{39} erg s^{-1}. We also predict the post-merger time at which the central WD should appear as a pulsar depending on the value of the magnetic field and rotation period.

59. J.A. Rueda, R. Ruffini, Y. Wang; Induced Gravitational Collapse, Binary-Driven Hypernovae, Long Gramma-ray Bursts and Their Connection with Short Gamma-ray Bursts; Universe, 5, 110 (2019).

There is increasing observational evidence that short and long Gamma-ray bursts (GRBs) originate in different subclasses, each one with specific energy release, spectra, duration, etc, and all of them with binary progenitors. The binary components involve carbon-oxygen cores (CO_{core}), neutron stars (NSs), black holes (BHs), and white dwarfs (WDs). We review here the salient features of the specific class of binary-driven hypernovae (BdHNe) within the induced gravitational collapse (IGC) scenario for the explanation of the long GRBs. The progenitor is a CO_{core}-NS binary. The supernova (SN) explosion of the CO_{core}, producing at its center a new NS (νNS), triggers onto the NS companion a hypercritical, i.e., highly super-Eddington accretion process, accompanied by a copious emission of neutrinos. By accretion the NS can become either a more massive NS or reach the critical mass for gravitational collapse with consequent formation of a BH. We summarize the results on this topic from the first analytic estimates in 2012 all the way up to the most recent three-dimensional (3D) smoothed-particle-hydrodynamics (SPH) numerical simulations in 2018. Thanks to these results it is by now clear that long GRBs are richer and more complex systems than thought before. The SN explosion and its hypercritical accretion onto the NS explain the X-ray precursor. The feedback of the NS accretion, the NS collapse and the BH formation produce asymmetries in the SN ejecta, implying the necessity of a 3D analysis for GRBs. The newborn BH, the surrounding matter and the magnetic field inherited from the NS, comprises the *inner engine* from which the GRB electron-positron (e^+e^-) plasma and the high-energy emission are initiated. The impact of the e^+e^- on the asymmetric ejecta transforms the SN into a hypernova (HN). The dynamics of the plasma in the asymmetric ejecta leads to signatures depending on the viewing angle. This explains the ultrarelativistic prompt emission in the MeV domain and the mildly-relativistic flares in the early afterglow in the X-ray domain. The feedback of the νNS pulsar-like emission on the HN explains the X-ray late afterglow and its power-law regime. All of the above is in contrast with a simple GRB model attempting to explain the entire GRB with the kinetic energy of an ultrarelativistic jet extending through all of the above GRB phases, as traditionally proposed in the "collapsar-fireball" model. In addition, BdHNe in their different flavors lead to νNS-NS or νNS-BH binaries. The gravitational wave emission drives these binaries to merge producing short GRBs. It is thus established a previously unthought interconnection between long and short GRBs and their occurrence rates. This needs to be accounted for in the cosmological evolution of binaries within population synthesis models for the formation of compact-object binaries.

60. R. Ruffini, J.D. Melon Fuksman, G.V. Vereshchagin; On the role of a cavity in the hypernova ejecta of GRB 190114C; The Astrophysical Journal, 883, 191 (2019).

    Within the binary-driven hypernova I (BdHN I) scenario, the gamma-ray burst GRB190114C originates in a binary system composed of a massive carbon-oxygen core (CO_{core}), and a binary neutron star (NS) companion. As the CO_{core} undergoes a supernova explosion with the creation of a new neutron star (νNS), hypercritical accretion occurs onto the companion binary neutron star until it exceeds the critical mass for gravitational collapse. The formation of a black hole (BH) captures 10^{57} baryons by enclosing them within its horizon, and thus a cavity of approximately 10^{11} cm is formed around it with initial density 10^{-7} g/cm^3. A further depletion of baryons in the cavity originates from the expansion of the electron-positron-photon ($e^+e^-\gamma$) plasma formed at the collapse, reaching a density of 10^{-14} g/cm^3 by the end of the interaction. It is demonstrated here using an analytical model complemented by a hydrodynamical numerical simulation that part of the $e^+e^-\gamma$ plasma is reflected off the walls of the cavity. The consequent outflow and its observed properties are shown to coincide with the featureless emission occurring in a time interval of duration t_{rf}, measured in the rest frame of the source, between 11 and 20 s of the GBM observation. Moreover, similar features of the GRB light curve were previously observed in GRB 090926A and GRB 130427A, all belonging to the BdHN I class. This interpretation supports the general conceptual framework presented in R. Ruffini et al. and guarantees that a low baryon density is reached in the cavity, a necessary condition for the operation of the "*inner engine*" of the GRB presented in an accompanying article.

61. R. Ruffini, R. Moradi, J.A. Rueda, L.M. Becerra, C.L. Bianco, C. Cherubini, S. Filippi, Y.C. Chen, M. Karlica, N. Sahakyan, Y. Wang, S.-S. Xue; On the GeV Emission of the Type I BdHN GRB 130427A; The Astrophysical Journal, 886, 82 (2019).

    We propose that the *inner engine* of a type I binary-driven hypernova (BdHN) is composed of a Kerr black hole (BH) in a non-stationary state, embedded in a uniform magnetic field B_0 aligned with the BH rotation axis, and surrounded by an ionized plasma of extremely low density of 10^{-14} g cm^{-3}. Using GRB 130427A as a prototype we show that this *inner engine* acts in a sequence of *elementary impulses*. Electrons are accelerated to ultra-relativistic energy near the BH horizon and, propagating along the polar axis, $\theta = 0$, they can reach energies of $\sim 10^{18}$ eV, and partially contribute to ultra-high energy cosmic rays (UHECRs). When propagating with $\theta \neq 0$ through the magnetic field B_0 they give origin by synchrotron emission to GeV and TeV radiation. The mass of BH, $M = 2.3 M_\odot$, its spin, $\alpha = 0.47$, and the value of magnetic field $B_0 = 3.48 \times 10^{10}$ G, are determined self-consistently in order to fulfill the energetic and the transparency requirement. The repetition time of each elementary impulse of energy $\mathcal{E} \sim 10^{37}$ erg, is $\sim 10^{-14}$ s at the beginning of the process, then slowly increasing with time evolution. In principle, this "*inner engine*" can operate in a GRB for thousands of years. By scaling the BH mass and the magnetic field the same "*inner engine*" can describe active galactic nuclei (AGN).

62. L. Li; Thermal Components in Gamma-ray Bursts. II. Constraining the Hybrid Jet Model; The Astrophysical Journal, 894, 100 (2020).

    In explaining the physical origin of the jet composition of gamma-ray bursts (GRBs), a more general picture, i.e. the hybrid jet model (which introduced another magnetization parameter σ_0 on the basis of the traditional fireball model), has been well studied in Gao & Zhang. However, it still has not yet been applied to a large GRB sample. Here, we first employ the "top-down" approach of Gao & Zhang to diagnose the photosphere properties at the central engine to see how the hybrid model can account for the observed data as well, through applying a *Fermi* GRB sample (eight bursts) with the detected photosphere component, as presented in Li (our Paper I). We infer all physical parameters of a hybrid problem with three typical values of the radius of the jet base (r_0 = 10^7, 10^8, and 10^9 cm). We find that the dimensionless entropy for all the bursts shows $\eta \gg 1$ while the derived (1+σ_0) for five bursts (GRB 081224, GRB 110721A, GRB 090719, GRB 100707, and GRB 100724) is larger than unity, indicating that in addition to a hot fireball component, another cold Poynting-flux component may also play an important role. Our analysis also shows that in a few time bins for all r_0 in GRB 081224 and GRB 110721A, the magnetization parameter at $\sim 10^{15}$cm (1+σ_{r15}) is greater than unity, which implies that internal-collision-induced magnetic reconnection and turbulence may be the mechanism to power the nonthermal emission, rather than internal shocks. We conclude that the majority of bursts (probably all) can be well explained by the hybrid jet problem.

63. J.A. Rueda, R. Ruffini, M. Karlica, R. Moradi, Y. Wang; Magnetic fields and afterglows of bdhne: inferences from grb 130427a, grb 160509a, grb 160625b, grb 180728a, and grb 190114c; The Astrophysical Journal, 893, 148 (2020).

    GRB 190114C is the first binary-driven hypernova (BdHN) fully observed from the initial supernova appearance to the final emergence of the optical SN signal. It offers an unprecedented testing ground for the BdHN theory and it is here determined and further extended to additional gamma-ray bursts (GRBs). BdHNe comprise two subclasses of long GRBs with progenitors a binary system composed of a carbon-oxygen star (CO_{core}) and a neutron star (NS) companion. The CO_{core} explodes as a SN leaving at its center a newborn NS (νNS). The SN ejecta hypercritically accretes both on the νNS and the NS companion. BdHNe I are the tightest binaries where the accretion leads the companion NS to gravitational collapse into a black hole (BH). In BdHN II the accretion onto the NS is lower, so there is no BH formation. We observe the same structure of the afterglow for GRB 190114C and other selected examples of BdHNe I (GRB 130427A, GRB 160509A, GRB 160625B) and for BdHN II (GRB 180728A). In all the cases the explanation of the afterglow is reached via the synchrotron emission powered by the νNS: their magnetic fields structures and their spin are determined. For BdHNe I, we discuss the properties of the magnetic field embedding the newborn BH, inherited from the collapsed NS and amplified during the gravitational collapse process, and surrounded by the SN ejecta.

64. J.A. Rueda, R. Ruffini; The blackholic quantum; European Physical Journal C, 80, 300 (2020).

    We show that the high-energy emission of GRBs originates in the *inner engine*: a Kerr black hole (BH) surrounded by matter and a magnetic field B_0. It radiates a sequence of discrete events of particle acceleration, each of energy $\mathcal{E} = \hbar\,\Omega_{\rm eff}$, the *blackholic quantum*, where $\Omega_{\rm eff} = 4(m_{\rm Pl}/m_n)^8 (c\,a/G\,M)(B_0^2/\rho_{\rm Pl})\Omega_+$. Here M, $a = J/M$, $\Omega_+ = c^2\partial M/\partial J = (c^2/G)\,a/(2Mr_+)$ and r_+ are the BH mass, angular momentum per unit mass, angular velocity and horizon; m_n is the neutron mass, $m_{\rm Pl}$, $\lambda_{\rm Pl} = \hbar/(m_{\rm Pl}c)$ and $\rho_{\rm Pl} = m_{\rm Pl}c^2/\lambda_{\rm Pl}^3$, are the Planck mass, length and energy density. Here and in the following use CGS-Gaussian units. The timescale of each process is $\tau_{\rm el} \sim \Omega_+^{-1}$, along the rotation axis, while it is much shorter off-axis owing to energy losses such as synchrotron radiation. We show an analogy with the Zeeman and Stark effects, properly scaled from microphysics to macrophysics, that allows us to define the *BH magneton*,

$\mu_{\rm BH} = (m_{\rm Pl}/m_n)^4 (c\,a/G\,M) e\,\hbar/(Mc)$. We give quantitative estimates for GRB 130427A adopting $M = 2.3\ M_\odot$, $c\,a/(G\,M) = 0.47$ and $B_0 = 3.5 \times 10^{10}$ G. Each emitted *quantum*, $\mathcal{E} \sim 10^{37}$ erg, extracts only 10^{-16} times the BH rotational energy, guaranteeing that the process can be repeated for thousands of years. The *inner engine* can also work in AGN as we here exemplified for the supermassive BH at the center of M87.

65. B. Zhang, Y. Wang, L. Li; Dissecting the Energy Budget of a Gamma-Ray Burst Fireball; The Astrophysical Journal Letters, 909, L3 (2021)

66. L. Li, B. Zhang; Testing the High-latitude Curvature Effect of Gamma-Ray Bursts with Fermi Data: Evidence of Bulk Acceleration in Prompt Emission; The Astrophysical Journal Supplement Series, 253, 43 (2021)

67. L. Li, F. Ryde, A. Pe'er, H.-F. Yu, Z. Acuner; The Astrophysical Journal Supplement Series; 254, 35 (2021)

68. Y. Wang; Do All Long-duration Gamma-Ray Bursts Emit GeV Photons?; The Astrophysical Journal, 913, 86 (2021)

69. L. Li; Searching for Observational Evidence for Binary Star Systems in Gamma-ray Bursts; Astronomy Reports, 65, 973 (2021)

70. Y. Wang; Gamma-Ray Burst from Binary Star: Neutron Star and Carbon–Oxygen Core; Astronomy Reports, 65, 1077 (2021)

71. R. Ruffini; Discovery of the Moment of Formation of the Black Hole in GRB 190114C; Astronomy Reports, 65, 1030 (2021)

72. R. Ruffini, R. Moradi, J.A. Rueda, L. Li, N. Sahakyan, Y.-C. Chen, Y. Wang, Y. Aimuratov, L. Becerra, C.L. Bianco, C. Cherubini, S. Filippi, M. Karlica, G.J. Mathews, M. Muccino, G.B. Pisani, S.-S. Xue; The morphology of the X-ray afterglows and of the jetted GeV emission in long GRBs; Monthly Notices of the Royal Astronomical Society, 504, 5301 (2021)

73. R. Moradi, J.?A. Rueda, R. Ruffini, Liang Li, C.?L. Bianco, S. Campion, C. Cherubini, S. Filippi, Y. Wang, and S.?S. Xue; Nature of the ultrarelativistic prompt emission phase of GRB 190114C; Phys. Rev. D, 104, 063043 (2021)

74. R. Moradi, J.A. Rueda, R. Ruffini and Y. Wang; The newborn black hole in GRB 191014C proves that it is alive; Astronomy & Astrophysics, 649, A75 (2021)

75. Xu, Fan, Geng, Jin-Jun, Wang, Xu, Li, Liang, Huang, Yong-Feng, "Is the birth of PSR J0538+2817 accompanied by a gamma-ray burst?"; Monthly Notices of the Royal Astronomical Society, 509, 4916 (2022)

76. Li, Liang; "Standard GRB Spectral Models "Misused"?"; The Astrophysical Journal, 941, 27 (2022)

77. Marongiu, M.; Guidorzi, C., Stratta, G., Gomboc, A., Jordana-Mitjans, N., Dichiara, S., Kobayashi, S., Kopa?, D., Mundell, C. G.; "Radio data challenge the broadband modelling of GRB 160131A afterglow"; Astronomy & Astrophysics, 658, A11 (2022)

78. Li, Liang; Rueda, J. A. ; Moradi, R.; Wang, Y. ; Xue, S. S. ; Ruffini, R.; "Self-similarities and Power Laws in the Time-resolved Spectra of GRB 190114C, GRB 130427A, GRB 160509A, and GRB 160625B"; The Astrophysical Journal, 945, 10 (2023)

79. Aimuratov, Y.; Becerra, L. M.; Bianco, C. L.; Cherubini, C.; Della Valle, M.; Filippi, S.; Li, Liang; Moradi, R.; Rastegarnia, F. ; Rueda, J. A.; Ruffini, R.; Sahakyan, N.; Wang, Y.; Zhang, S. R.; "GRB-SN Association within the Binary-driven Hypernova Model"; The Astrophysical Journal, 955, 93 (2023)

80. C.L. Bianco, M.T. Mirtorabi, R. Moradi, F. Rastegarnia, J.A. Rueda, R. Ruffini, Y. Wang, M. Della Valle, L. Li, S.R. Zhang; "Probing Electromagnetic Gravitational-wave Emission Coincidence in a Type I Binary-driven Hypernova Family of Long Gamma-Ray Bursts at Very High Redshift"; The Astrophysical Journal, 966, 219 (2024)

81. J.A. Rueda, L. Becerra, C.L. Bianco, M. Della Valle, C.L. Fryer, C. Guidorzi, R. Ruffini; "Long and short GRB connection"; Phys. Rev. D, 111, 023010 (2025)

82. R. Ruffini, C.L. Bianco, L. Li, M.T. Mirtorabi, R. Moradi, F. Rastegar Nia, J.A. Rueda, S.R. Zhang, Y. Wang; "Ten Supernova-rise in Binary Driven Gamma-ray Bursts"; eprint arXiv:2405.08231 (2024)

4.2 Conference proceedings

1. R. Ruffini, M.G. Bernardini, C.L. Bianco, P. Chardonnet, F. Fraschetti, V. Gurzadyan, L. Vitagliano, S.-S. Xue; "The Blackholic energy: long and short Gamma-Ray Bursts (New perspectives in physics and astrophysics from the theoretical understanding of Gamma-Ray Bursts, II)"; in Proceedings of the XIth Brazilian School on Cosmology and Gravitation, Mangaratiba, Rio de Janeiro (Brazil), July – August 2004, M. Novello, S.E. Perez Bergliaffa, Editors; AIP Conference Proceedings, 782, 42 (2005).

   We outline the confluence of three novel theoretical fields in our modeling of Gamma-Ray Bursts (GRBs): 1) the ultrarelativistic regime of a shock front expanding with a Lorentz gamma factor $\sim$ 300; 2) the quantum vacuum polarization process leading to an electron-positron plasma originating the shock front; and 3) the general relativistic process of energy extraction from a black hole originating the vacuum polarization process. There are two different classes of GRBs: the long GRBs and the short GRBs. We here address the issue of the long GRBs. The theoretical understanding of the long GRBs has led to the detailed description of their luminosities in fixed energy bands, of their spectral features and made also possible to probe the astrophysical scenario in which they originate. We are specially interested, in this report, to a subclass of long GRBs which appear to be accompanied by a supernova explosion. We are considering two specific examples: GRB980425/SN1998bw and GRB030329/SN2003dh. While these supernovae appear to have a standard energetics of 10^{49} ergs, the GRBs are highly variable and can have energetics 10^4 – 10^5 times larger than the ones of the supernovae. Moreover, many long GRBs occurs without the presence of a supernova. It is concluded that in no way a GRB can originate from a supernova. The precise theoretical understanding of the GRB luminosity we present evidence, in both these systems, the existence of an independent component in the X-ray emission, usually interpreted in the current literature as part of the GRB afterglow. This component has been observed by Chandra and XMM to have a strong decay on scale of months. We have named here these two sources respectively URCA-1 and URCA-2, in honor of the work that George Gamow and Mario Shoenberg did in 1939 in this town of Urca identifying the basic mechanism, the Urca processes, leading to the process of gravitational collapse and the formation of a neutron star and a supernova. The further hypothesis is considered to relate this X-ray source to a neutron star, newly born in the Supernova. This hypothesis should be submitted to further theoretical and observational investigation. Some theoretical developments to clarify the astrophysical origin of this new scenario are outlined. We turn then to the theoretical developments in the short GRBs: we first report some progress in the understanding the dynamical phase of collapse, the mass-energy formula and the extraction of blackholic energy which have been motivated by the analysis of the short GRBs. In this context progress has also been accomplished on establishing an absolute lower limit to the irreducible mass of the black hole as well as on some critical considerations about the relations of general relativity and the second law of thermodynamics. We recall how this last issue has been one of the most debated in theoretical physics in the past thirty years due to the work of Bekenstein and Hawking. Following these conceptual progresses we analyze the vacuum polarization process around an overcritical collapsing shell. We evidence the existence of a separatrix and a dyadosphere trapping surface in the dynamics of the electron-positron plasma generated during the process of gravitational collapse. We then analyze, using recent progress in the solution of the Vlasov-Boltzmann-Maxwell system, the oscillation regime in the created electron-positron plasma and their rapid convergence to a thermalized spectrum. We conclude by making precise predictions for the spectra, the energy fluxes and characteristic time-scales of the radiation for short-bursts. If the precise luminosity variation and spectral hardening of the radiation we have predicted will be confirmed by observations of short-bursts, these systems will play a major role as standard candles in cosmology. These considerations will also be relevant for the analysis of the long-bursts when the baryonic matter contribution will be taken into account.

2. R. Ruffini, M.G. Bernardini, C.L. Bianco, P. Chardonnet, F. Fraschetti, V. Gurzadyan, L. Vitagliano, S.-S. Xue; "Black hole physics and astrophysics: The GRB-Supernova connection and URCA-1 – URCA-2"; in Proceedings of the Tenth Marcel Grossmann Meeting on General Relativity, Rio de Janeiro, Brazil, July 2003, M. Novello, S.E. Perez-Bergliaffa, Editors; p. 369; World Scientific, (Singapore, 2006).

   We outline the confluence of three novel theoretical fields in our modeling of Gamma-Ray Bursts (GRBs): 1) the ultrarelativistic regime of a shock front expanding with a Lorentz gamma factor ~ 300; 2) the quantum vacuum polarization process leading to an electron-positron plasma originating the shock front; and 3) the general relativistic process of energy extraction from a black hole originating the vacuum polarization process. There are two different classes of GRBs: the long GRBs and the short GRBs. We here address the issue of the long GRBs. The theoretical understanding of the long GRBs has led to the detailed description of their luminosities in fixed energy bands, of their spectral features and made also possible to probe the astrophysical scenario in which they originate. We are specially interested, in this report, to a subclass of long GRBs which appear to be accompanied by a supernova explosion. We are considering two specific examples: GRB980425/SN1998bw and GRB030329/SN2003dh. While these supernovae appear to have a standard energetics of 10^{49} ergs, the GRBs are highly variable and can have energetics 10^4 – 10^5 times larger than the ones of the supernovae. Moreover, many long GRBs occurs without the presence of a supernova. It is concluded that in no way a GRB can originate from a supernova. The precise theoretical understanding of the GRB luminosity we present evidence, in both these systems, the existence of an independent component in the X-ray emission, usually interpreted in the current literature as part of the GRB afterglow. This component has been observed by Chandra and XMM to have a strong decay on scale of months. We have named here these two sources respectively URCA-1 and URCA-2, in honor of the work that George Gamow and Mario Shoenberg did in 1939 in this town of Urca identifying the basic mechanism, the Urca processes, leading to the process of gravitational collapse and the formation of a neutron star and a supernova. The further hypothesis is considered to relate this X-ray source to a neutron star, newly born in the Supernova. This hypothesis should be submitted to further theoretical and observational investigation. Some theoretical developments to clarify the astrophysical origin of this new scenario are outlined.

3. M.G. Bernardini, C.L. Bianco, P. Chardonnet, F. Fraschetti, R. Ruffini, S.-S. Xue; "General features of GRB 030329 in the EMBH model"; in Proceedings of the Tenth Marcel Grossmann Meeting on General Relativity, Rio de Janeiro, Brazil, July 2003, M. Novello, S.E. Perez-Bergliaffa, Editors; p. 2459; World Scientific, (Singapore, 2006).

   GRB 030329 is considered within the EMBH model. We determine the three free parameters and deduce its luminosity in given energy bands comparing it with the observations. The observed substructures are compared with the predictions of the model: by applying the result that substructures observed in the extended afterglow peak emission (E-APE) do indeed originate in the collision of the accelerated baryonic matter (ABM) pulse with the inhomogeneities in the interstellar medium around the black-hole, masks of density inhomogeneities are considered in order to reproduce the observed temporal substructures. The induced supernova concept is applied to this system and the general consequences that we are witnessing are the formation of a cosmological thriptych of a black hole originating the GRB 030329, the supernova SN2003dh and a young neutron star. Analogies to the system GRB 980425–SN1998bw are outlined.

4. R. Ruffini, M.G. Bernardini, C.L. Bianco, P. Chardonnet, A. Corsi, F. Fraschetti, S.-S. Xue; "GRB 970228 and its associated Supernova in the EMBH model"; in Proceedings of the Tenth Marcel Grossmann Meeting on General Relativity, Rio de Janeiro, Brazil, July 2003, M. Novello, S.E. Perez-Bergliaffa, Editors; p. 2465; World Scientific, (Singapore, 2006).

   The γ-ray burst of 1997 February 28 is analyzed within the Electromagnetic Black Hole model. We first estimate the value of the total energy deposited in the dyadosphere, E_{dya}, and the amount of baryonic matter left over by the EMBH progenitor star, $B = M_B c^2 / E_{dya}$. We then consider the role of the interstellar medium number density n_{ISM} and of the ratio R between the effective emitting area and the total surface area of the γ-ray burst source, in reproducing the prompt emission and the X-ray afterglow of this burst. Some considerations are also done concerning the possibility of explaining, within the theory, the observed evidence for a supernova in the optical afterglow.

5. F. Fraschetti, M.G. Bernardini, C.L. Bianco, P. Chardonnet, R. Ruffini, S.-S. Xue; "Inferences on the ISM structure around GRB980425 and GRB980425-SN1998bw association in the EMBH Model"; in Proceedings of the Tenth Marcel Grossmann Meeting on General Relativity, Rio de Janeiro, Brazil, July 2003, M. Novello, S.E. Perez-Bergliaffa, Editors; p. 2451; World Scientific, (Singapore, 2006).

   We determine the four free parameters within the EMBH model for GRB 980425 and deduce its luminosity in given energy bands, its spectra and its time variability in the prompt radiation. We compute the basic kinematical parameters of GRB 980425. In the extended afterglow peak emission the Lorentz γ factor is lower than the critical value 150 which has been found in Ruffini et al. (2002) to be necessary in order to perform the tomography of the ISM surrounding the GRB as suggested by Dermer & Mitman (1999). The detailed structure of the density inhomogeneities as well as the effects of radial apparent superluminal effects are evaluated within the EMBH model. Under the assumption that the energy distribution of emitted radiation is thermal in the comoving frame, time integrated spectra of EMBH model for prompt emission are computed. The induced supernova concept is applied to this system and general consequences on the astrophysical and cosmological scenario are derived.

6. R. Ruffini, M.G. Bernardini, C.L. Bianco, P. Chardonnet, F. Fraschetti, R. Guida, S.-S. Xue; "GRB 050315: A step in the proof of the uniqueness of the overall GRB structure"; in "GAMMA-RAY BURSTS IN THE SWIFT ERA: Sixteenth Maryland Astrophysics Conference", Washington, DC, USA, November 29th – December 2nd 2005, Stephen S. Holt, Neil Gehrels, John A. Nousek, Editors; AIP Conference Proceedings, 836, 103 (2006).

   Using the Swift data of GRB 050315, we progress in proving the uniqueness of our theoretically predicted Gamma-Ray Burst (GRB) structure as composed by a proper-GRB, emitted at the transparency of an electron-positron plasma with suitable baryon loading, and an afterglow comprising the "prompt radiation" as due to external shocks. Detailed light curves for selected energy bands are theoretically fitted in the entire temporal region of the Swift observations ranging over 10^6 seconds.

7. R. Ruffini, M.G. Bernardini, C.L. Bianco, P. Chardonnet, F. Fraschetti, S.-S. Xue; "Theoretical Interpretation of GRB 031203 and URCA-3"; in "Relativistic Astrophysics and Cosmology - Einstein's Legacy", B. Aschenbach, V. Burwitz, G. Hasinger, B. Leibundgut, Editors; Springer-Verlag (2007).

8. R. Ruffini, M.G. Bernardini, C.L. Bianco, L. Caito, P. Chardonnet, M.G. Dainotti, F. Fraschetti, R. Guida, M. Rotondo, G. Vereshchagin, L. Vita--gliano, S.-S. Xue; "The Blackholic energy and the canonical Gamma-Ray Burst"; in Proceedings of the XIIth Brazilian School on Cosmology and Gravitation, Mangaratiba, Rio de Janeiro (Brazil), September 2006, M. Novello, S.E. Perez Bergliaffa, Editors; AIP Conference Proceedings, 910, 55 (2007).

   Gamma-Ray Bursts (GRBs) represent very likely "the" most extensive computational, theoretical and observational effort ever carried out successfully in physics and astrophysics. The extensive campaign of observation from space based X-ray and γ-ray observatory, such as the *Vela*, CGRO, BeppoSAX, HETE-II, INTEGRAL, *Swift*, R-XTE, *Chandra*, XMM satellites, have been matched by complementary observations in the radio wavelength (e.g. by the VLA) and in the optical band (e.g. by VLT, Keck, ROSAT). The net result is unprecedented accuracy in the received data allowing the determination of the energetics, the time variability and the spectral properties of these GRB sources. The very fortunate situation occurs that these data can be confronted with a mature theoretical development. Theoretical interpretation of the above data allows progress in three different frontiers of knowledge: **a)** the ultrarelativistic regimes of a macroscopic source moving at Lorentz gamma factors up to ~ 400; **b)** the occurrence of vacuum polarization process verifying some of the yet untested regimes of ultrarelativistic quantum field theories; and **c)** the first evidence for extracting, during the process of gravitational collapse leading to the formation of a black hole, amounts of energies up to 10^{55} ergs of blackholic energy — a new form of energy in physics and astrophysics. We outline how this progress leads to the confirmation of three interpretation paradigms for GRBs proposed in July 2001. Thanks mainly to the observations by *Swift* and the optical observations by VLT, the outcome of this analysis points to the existence of a "canonical" GRB, originating from a variety of different initial astrophysical scenarios. The communality of these GRBs appears to be that they all are emitted in the process of formation of a black hole with a negligible value of its angular momentum. The following sequence of events appears to be canonical: the vacuum polarization process in the dyadosphere with the creation of the optically thick self accelerating electron-positron plasma; the engulfment of baryonic mass during the plasma expansion; adiabatic expansion of the optically thick "fireshell" of electron-positron-baryon plasma up to the transparency; the interaction of the accelerated baryonic matter with the interstellar medium (ISM). This leads to the canonical GRB composed of a proper GRB (P-GRB), emitted at the moment of transparency, followed by an extended afterglow. The sole parameters in this scenario are the total energy of the dyadosphere E_{dya}, the fireshell baryon loading M_B defined by the dimensionless parameter $B \equiv M_B c^2 / E_{dya}$, and the ISM filamentary distribution around the source. In the limit $B \to 0$ the total energy is radiated in the P-GRB with a vanishing contribution in the afterglow. In this limit, the canonical GRBs explain as well the short GRBs. In these lecture notes we systematically outline the main results of our model comparing and contrasting them with the ones in the current literature. In both cases, we have limited ourselves to review already published results in refereed publications. We emphasize as well the role of GRBs in testing yet unexplored grounds in the foundations of general relativity and relativistic field theories.

9. R. Ruffini, M.G. Bernardini, C.L. Bianco, L. Caito, P. Chardonnet, M.G. Dainotti, F. Fraschetti, R. Guida, G. Vereshchagin, S.-S. Xue; "The role of GRB 031203 in clarifying the astrophysical GRB scenario"; in Proceedings of the 6^{th} Integral Workshop - The Obscured Universe, Moscow, (Russia), July 2006, S. Grebenev, R. Sunyaev, C. Winkler, A. Parmar, L. Ouwehand, Editors; ESA Special Publication, SP-622, 561 (2007).

   The luminosity and the spectral distribution of the afterglow of GRB 031203 have been presented within our theoretical framework, which envisages the GRB structure as composed by a proper-GRB, emitted at the transparency of an electron-positron plasma with suitable baryon loading, and an afterglow comprising the "prompt emission" as due to external shocks. In addition to the GRB emission, there appears to be a prolonged soft X-Ray emission lasting for 10^6–10^7 seconds followed by an exponential decay. This additional source has been called by us URCA-3. It is urgent to establish if this component is related to the GRB or to the Supernova (SN). In this second case, there are two possibilities: either the interaction of the SN ejecta with the interstellar medium or, possibly, the cooling of a young neutron star formed in the SN 2003lw process. The analogies and the differences between this triptych GRB 031203 / SN 2003lw / URCA-3 and the corresponding ones GRB 980425 / SN 1998bw / URCA-1 and GRB 030329 / SN 2003dh / URCA-2, as well as GRB 060218 / SN 2006aj are discussed.

10. M.G. Bernardini, C.L. Bianco, L. Caito, M.G. Dainotti, R. Guida, R. Ruffini; "GRB970228 and the class of GRBs with an initial spikelike emission: do they follow the Amati relation?"; in Relativistic Astrophysics – Proceedings of the 4^{th} Italian-Sino Workshop, Pescara (Italy), July 2007, C.L. Bianco, S.-S. Xue, Editors; AIP Conference Proceedings, 966, 7 (2008).

    On the basis of the recent understanding of GRB050315 and GRB060218, we return to GRB970228, the first Gamma-Ray Burst (GRB) with detected afterglow. We proposed it as the prototype for a new class of GRBs with "an occasional softer extended emission lasting tenths of seconds after an initial spikelike emission". Detailed theoretical computation of the GRB970228 light curves in selected energy bands for the prompt emission are presented and compared with observational *Beppo*SAX data. From our analysis we conclude that GRB970228 and likely the ones of the above mentioned new class of GRBs are "canonical GRBs" have only one peculiarity: they exploded in a galactic environment, possibly the halo, with a very low value of CBM density. Here we investigate how GRB970228 unveils another peculiarity of this class of GRBs: they do not fulfill the "Amati relation". We provide a theoretical explanation within the fireshell model for the apparent absence of such correlation for the GRBs belonging to this new class.

11. C.L. Bianco, M.G. Bernardini, L. Caito, M.G. Dainotti, R. Guida, R. Ruffini; "The "Fireshell" Model and the "Canonical" GRB Scenario; in Relativistic Astrophysics – Proceedings of the 4^{th} Italian-Sino Workshop, Pescara (Italy), July 2007, C.L. Bianco, S.-S. Xue, Editors; AIP Conference Proceedings, 966, 12 (2008).

    In the "fireshell" model we define a "canonical GRB" light curve with two sharply different components: the Proper-GRB (P-GRB), emitted when the optically thick fireshell of electron-positron plasma originating the phenomenon reaches transparency, and the afterglow, emitted due to the collision between the remaining optically thin fireshell and the CircumBurst Medium (CBM). We outline our "canonical GRB" scenario, originating from the gravitational collapse to a black hole, with a special emphasis on the discrimination between "genuine" and "fake" short GRBs.

12. L. Caito, M.G. Bernardini, C.L. Bianco, M.G. Dainotti, R. Guida, R. Ruffini; "GRB 060614: A Progress Report"; in Relativistic Astrophysics – Proceedings of the 4^{th} Italian-Sino Workshop, Pescara (Italy), July 2007, C.L. Bianco, S.-S. Xue, Editors; AIP Conference Proceedings, 966, 16 (2008).

    The explosion of GRB 060614, detected by the Swift satellite, produced a deep break in the GRB scenario opening new horizons of investigation, because it can't be traced back to any traditional scheme of classification. In fact, it manifests peculiarities both of long bursts and of short bursts. Above all, it is the first case of long duration near GRB without any bright Ib/c associated Supernova. We will show that, in our canonical GRB scenario, this "anomalous" situation finds a natural interpretation and allows us to discuss a possible variation to the traditional classification scheme, introducing the distinction between "genuine" and "fake" short bursts.

13. M.G. Dainotti, M.G. Bernardini, C.L. Bianco, L. Caito, R. Guida, R. Ruffini; "GRB 060218 and the Binaries as Progenitors of GRB-SN Systems"; in Relativistic Astrophysics – Proceedings of the 4^{th} Italian-Sino Workshop, Pescara (Italy), July 2007, C.L. Bianco, S.-S. Xue, Editors; AIP Conference Proceedings, 966, 25 (2008).

We study the Gamma-Ray Burst (GRB) 060218: a particularly close source at $z = 0.033$ with an extremely long duration, namely $T_{90} \sim 2000$ s, related to SN 2006aj. This source appears to be a very soft burst, with a peak in the spectrum at 4.9 keV, therefore interpreted as an X-Ray Flash (XRF). It fullfills the Amati relation. I present the fitting procedure, which is time consuming. In order to show its sensitivity I also present two examples of fits with the same value of B and different value of $E^{tot}_{e^{\pm}}$. We fit the X- and γ-ray observations by *Swift* of GRB 060218 in the 0.1–150 keV energy band during the entire time of observations from 0 all the way to 10^6 s within a unified theoretical model. The free parameters of our theory are only three, namely the total energy $E^{tot}_{e\pm}$ of the $e^{\pm}$ plasma, its baryon loading $B \equiv M_B c^2/E^{tot}_{e\pm}$, as well as the CircumBurst Medium (CBM) distribution. We justify the extremely long duration of this GRB by a total energy $E^{tot}_{e\pm} = 2.32 \times 10^{50}$ erg, a very high value of the baryon loading $B = 1.0 \times 10^{-2}$ and the effective CircumBurst Medium (CBM) density which shows a radial dependence $n_{cbm} \propto r^{-\alpha}$ with $1.0 \leq \alpha \leq 1.7$ and monotonically decreases from 1 to 10^{-6} particles/cm^3. We recall that this value of the B parameter is the highest among the sources we have analyzed and it is very close to its absolute upper limit expected. By our fit we show that there is no basic differences between XRFs and more general GRBs. They all originate from the collapse process to a black hole and their difference is due to the variability of the three basic parameters within the range of full applicability of the theory. We also think that the smallest possible black hole, formed by the gravitational collapse of a neutron star in a binary system, is consistent with the especially low energetics of the class of GRBs associated with SNe Ib/c.

14. R. Guida, M.G. Bernardini, C.L. Bianco, L. Caito, M.G. Dainotti, R. Ruffini; "The Amati Relation within the Fireshell Model"; in Relativistic Astrophysics – Proceedings of the 4^{th} Italian-Sino Workshop, Pescara (Italy), July 2007, C.L. Bianco, S.-S. Xue, Editors; AIP Conference Proceedings, 966, 46 (2008).

    In this work we show the existence of a spectral-energy correlation within our "fireshell" model for GRBs. The free parameters of the model are the total energy $E^{e\pm}_{tot}$ of the $e^{\pm}$ plasma and its baryon loading $B \equiv M_B\, c^2/E^{e\pm}_{tot}$, characterizing the source, and the parameters describing the effective CircumBurst medium (CBM) distribution, namely its particle number density ρ and its effective emitting area R. We build a sample of pseudo-GRBs, i.e. a set of theoretically simulated light curves, varying the total energy of the electron-positron plasma $E^{e\pm}_{tot}$ and keeping the same baryon loading; the parametrization used to describe the distribution of the CircumBurst medium is the same as well for all the pseudo-GRBs. The values of these parameters (B, ρ and R) used in this work are equal to the ones assumed to fit GRB050315, a *Swift* burst representing a good example of what in the literature has been addressed as "canonical light curve". For each GRB of the sample we calculate the νF_ν spectrum integrating the theoretically computed light curve over the total time, namely from our T_0, the end of the Proper-GRB (P-GRB), up to the end of our afterglow phase, when the fireshell Lorentz gamma factor is close to unity; we exclude the P-GRB from this spectral computation because, following our "canonical" GRB scenario, this component of the GRB emission is physically different from the other component, that is our afterglow component, so one should take care in no mixing them. We find that the maximum of this spectrum, that is the observed peak energy $E_{p,tot}$, correlates with the initial electron-positron plasma energy $E_{tot}^{e\pm}$ in a way very similar to the Amati one: $E_{p,tot} \propto (E_{tot}^{e\pm})^{0.5}$.

15. R. Guida, M.G. Bernardini, C.L. Bianco, L. Caito, M.G. Dainotti, R. Ruffini; "Theoretical interpretation of the Amati relation within the fireshell model"; in GAMMA-RAY BURSTS 2007: Proceedings of the Santa Fe Conference, Santa Fe (NM, USA), November 2007, M. Galassi, D. Palmer, E. Fenimore, Editors; AIP Conference Proceedings, 1000, 60 (2008).

    We discuss within our theoretical "fireshell" model for Gamma-Ray Bursts (GRBs) the theoretical interpretation of the phenomenological correlation between the isotropic-equivalent radiated energy of the prompt emission E_{iso} and the cosmological rest-frame νF_ν spectrum peak energy E_p observed by Amati and collaborators. Possible reasons for some of the outliers of this relation are given.

16. L. Caito, M.G. Bernardini, C.L. Bianco, M.G. Dainotti, R. Guida, R. Ruffini; "GRB 060614: a Fake Short Gamma-Ray Burst"; in GAMMA-RAY BURSTS 2007: Proceedings of the Santa Fe Conference, Santa Fe (NM, USA), November 2007, M. Galassi, D. Palmer, E. Fenimore, Editors; AIP Conference Proceedings, 1000, 301 (2008).

    The explosion of GRB 060614 produced a deep break in the GRB scenario and opened new horizons of investigation because it can't be traced back to any traditional scheme of classification. In fact, it manifests peculiarities both of long bursts and of short bursts and, above all, it is the first case of long duration near GRB without any bright Ib/c associated Supernova. We will show that, in our canonical GRB scenario, this ”anomalous” situation finds a natural interpretation and allows us to discuss a possible variation to the traditional classification scheme, introducing the distinction between “genuine” and “fake” short bursts.

17. C.L. Bianco, M.G. Bernardini, L. Caito, M.G. Dainotti, R. Guida, R. Ruffini; “Short and canonical GRBs”; in GAMMA-RAY BURSTS 2007: Proceedings of the Santa Fe Conference, Santa Fe (NM, USA), November 2007, M. Galassi, D. Palmer, E. Fenimore, Editors; AIP Conference Proceedings, 1000, 305 (2008).

    Within the “fireshell” model for the Gamma-Ray Bursts (GRBs) we define a “canonical GRB” light curve with two sharply different components: the Proper-GRB (P-GRB), emitted when the optically thick fireshell of electron-positron plasma originating the phenomenon reaches transparency, and the afterglow, emitted due to the collision between the remaining optically thin fireshell and the CircumBurst Medium (CBM). We outline our “canonical GRB” scenario, with a special emphasis on the discrimination between “genuine” and “fake” short GRBs.

18. C.L. Bianco, M.G. Bernardini, L. Caito, M.G. Dainotti, R. Guida, R. Ruffini, G. Vereshchagin, S.-S. Xue; “The Equations of motion of the “fireshell””; in OBSERVATIONAL EVIDENCE FOR BLACK HOLES IN THE UNIVERSE: Proceedings of the 2^{nd} Kolkata Conference, Kolkata (India), February 2008, S.K. Chakrabarti, A.S. Majumdar, Editors; AIP Conference Proceedings, 1053, 259 (2008).

    The Fireshell originating a Gamma-Ray Burst (GRB) encompasses an optically thick regime followed by an optically thin one. In the first one the fireshell self-accelerates from a Lorentz gamma factor equal to 1 all the way to 200-300. The physics of this system is based on the continuous annihilation of electron-positron pairs in an optically thick e^+e^- plasma with a small baryon loading. In the following regime, the optically thin fireshell, composed by the baryons left over after the transparency point, ballistically expands into the CircumBurst Medium (CBM). The dynamics of the fireshell during both regimes will be analyzed. In particular we will re-examine the validity of the constant-index power-law relation between the fireshell Lorentz gamma factor and its radial coordinate, usually adopted in the current literature on the grounds of an “ultrarelativistic” approximation. Such expressions are found to be mathematically correct but only approximately valid in a very limited range of the physical and astrophysical parameters and in an asymptotic regime which is reached only for a very short time, if any.

19. M.G. Bernardini, C.L. Bianco, L. Caito, M.G. Dainotti, R. Guida, R. Ruffini; “The “Canonical” GRBs within the fireshell model”; in OBSERVATIONAL EVIDENCE FOR BLACK HOLES IN THE UNIVERSE: Proceedings of the 2^{nd} Kolkata Conference, Kolkata (India), February 2008, S.K. Chakrabarti, A.S. Majumdar, Editors; AIP Conference Proceedings, 1053, 267 (2008).

    Within the fireshell model we define a “canonical” GRB light curve with two sharply different components: the Proper-GRB (P-GRB), emitted when the optically thick fireshell of electron-positron plasma originating the phenomenon reaches transparency, and the afterglow, emitted due to the collision between the remaining optically thin fireshell and the CircumBurst Medium (CBM). On the basis of the recent understanding of GRB970228 as the prototype for a new class of GRBs with “an occasional softer extended emission lasting tenths of seconds after an initial spikelike emission” we outline our “canonical” GRB scenario, originating from the gravitational collapse to a black hole, with a special emphasis on the discrimination between short GRBs and the ones appearing as such due to their peculiar astrophysical setting.

20. M.G. Dainotti, M.G. Bernardini, C.L. Bianco, L. Caito, R. Guida, R. Ruffini; “GRB 060218: the density mask and its peculiarity compared to the other sources”; in OBSERVATIONAL EVIDENCE FOR BLACK HOLES IN THE UNIVERSE: Proceedings of the 2^{nd} Kolkata Conference, Kolkata (India), February 2008, S.K. Chakrabarti, A.S. Majumdar, Editors; AIP Conference Proceedings, 1053, 283 (2008).

    The Swift satellite has given continuous data in the range 0.3–150 keV from 0 s to 106 s for GRB060218 associated with SN2006aj. It has an unusually long duration ($T_{90} \sim 2100$ s). We plan to fit the complete γ- and X-ray light curves of this long duration GRB, including the prompt emission and we give peculiar attention to the afterglow lightcurve in order to better constrain the density mask. We apply our “fireshell” model based on the formation of a black hole, giving the relevant references. The initial total energy of the electron-positron plasma $E_{e^\pm}^{tot} == 2.32 \times 10^{50}$ erg has a particularly low value similarly to the other GRBs associated with SNe. For the first time we observe a baryon loading $B = 10^{-2}$ which coincides with the upper limit for the dynamical stability of the fireshell. The effective CircumBurst Medium (CBM) density shows a radial dependence $n_{cbm} \propto r^{-a}$ with $1.0 \leq a \leq 1.7$ and monotonically decreases from 1 to 10^{-6} particles/cm^3. Such a behavior is interpreted as due to a fragmentation in the fireshell. Such a fragmentation is crucial in explaining both the unusually large T_{90} and the consequently inferred abnormal low value of the CBM effective density. We present the comparison between the density mask of this source and the ones of a normal GRB 050315 and a fake short, GRB 970228, making some assumptions on the CBM behaviour in the surrounding of the Black hole.

21. L. Caito, M.G. Bernardini, C.L. Bianco, M.G. Dainotti, R. Guida, R. Ruffini; "GRB 060614 in the canonical fireshell model"; in OBSERVATIONAL EVIDENCE FOR BLACK HOLES IN THE UNIVERSE: Proceedings of the 2nd Kolkata Conference, Kolkata (India), February 2008, S.K. Chakrabarti, A.S. Majumdar, Editors; AIP Conference Proceedings, 1053, 291 (2008).

    Gamma-Ray Burst (GRB) 060614 is the first nearby long duration GRB clearly not associated to any bright Ib/c Supernova. The explosion of this burst undermines one of the fundamental assumptions of the standard scenario and opens new horizons and hints of investigation. GRB 060614, hardly classifiable as a short GRB, is not either a "typical" long GRB since it occurs in a low star forming region. Moreover, it presents deep similarities with GRB 970228, which is the prototype of the "fake" short bursts, or better canonical GRBs disguised as short ones. Within the "fireshell" model, we test if this "anomalous" source can be a disguised short GRB.

22. L.J. Rangel Lemos, S. Casanova, R. Ruffini, S.S. Xue; "Fermi's approach to the study of pp interactions"; in OBSERVATIONAL EVIDENCE FOR BLACK HOLES IN THE UNIVERSE: Proceedings of the 2nd Kolkata Conference, Kolkata (India), February 2008, S.K. Chakrabarti, A.S. Majumdar, Editors; AIP Conference Proceedings, 1053, 275 (2008).

    The physics of hadronic interactions found much difficulties for explain the experimental data. In this work we study the approach of Fermi (1950) about the multiplicity of pions emitted in pp interactions and in follow we compare with the modern approach

23. R. Ruffini, A.G. Aksenov, M.G. Bernardini, C.L. Bianco, L. Caito, M.G. Dainotti, G. De Barros, R. Guida, G.V. Vereshchagin, S.-S. Xue; "The canonical Gamma-Ray Bursts and their 'precursors"'; in 2008 NANJING GAMMA-RAY BURST CONFERENCE, Proceedings of the 2008

Nanjing Gamma-Ray Burst Conference, Nanjing (China), June 2008, Y.-F. Huang, Z.-G. Dai, B. Zhang, Editors; AIP Conference Proceedings, 1065, 219 (2008).

The fireshell model for Gamma-Ray Bursts (GRBs) naturally leads to a canonical GRB composed of a proper-GRB (P-GRB) and an afterglow. P-GRBs, introduced by us in 2001, are sometimes considered "precursors" of the main GRB event in the current literature. We show in this paper how the fireshell model leads to the understanding of the structure of GRBs, with precise estimates of the time sequence and intensities of the P-GRB and the of the afterglow. It leads as well to a natural classification of the canonical GRBs which overcomes the traditional one in short and long GRBs.

24. M.G. Bernardini, C.L. Bianco, L. Caito, M.G. Dainotti, R. Guida, R. Ruffini; "Preliminary analysis of GRB060607A within the fireshell model"; in 2008 NANJING GAMMA-RAY BURST CONFERENCE; Proceedings of the 2008 Nanjing Gamma-Ray Burst Conference, Nanjing (China), June 2008, Y.-F. Huang, Z.-G. Dai, B. Zhang, Editors; AIP Conference Proceedings, 1065, 227 (2008).

    GRB060607A is a very distant ($z = 3.082$) and energetic event ($E_{iso} \sim 10^{53}$ erg). Its main peculiarity is that the peak of the near-infrared afterglow has been observed with the REM robotic telescope, allowing to infer the initial Lorentz gamma factor of the emitting system. We present a preliminary analysis of the spectra and light curves of GRB060607A prompt emission within the fireshell model. We show that the N(E) spectrum of the prompt emission, whose behavior is usually described as "simple power-law", can also be fitted in a satisfactory way by a convolution of thermal spectra as predicted by the model we applied. The theoretical time-integrated spectrum of the prompt emission as well as the light curves in the BAT and XRT energy band are in good agreement with the observations, enforcing the plausibility of our approach. Furthermore, the initial value of Lorentz gamma factor we predict is compatible with the one deduced from the REM observations.

25. C.L. Bianco, M.G. Bernardini, L. Caito, M.G. Dainotti, R. Guida, R. Ruffini; "The "fireshell" model and the "canonical GRB" scenario"; in 2008 NANJING GAMMA-RAY BURST CONFERENCE; Proceedings of the 2008 Nanjing Gamma-Ray Burst Conference, Nanjing (China), June 2008, Y.-F. Huang, Z.-G. Dai, B. Zhang, Editors; AIP Conference Proceedings, 1065, 223 (2008).

The Swift observation of GRB 060614, as well as the catalog analysis by Norris & Bonnell (2006), opened the door "on a new Gamma-Ray Bursts (GRBs) classification scheme that straddles both long and short bursts" (Gehrels et al. 2006). Within the "fireshell" model for the Gamma-Ray Bursts (GRBs) we define a "canonical GRB" light curve with two sharply different components: the Proper-GRB (P-GRB), emitted when the optically thick fireshell of electron-positron plasma originating the phenomenon reaches transparency, and the afterglow, emitted due to the collision between the remaining optically thin fireshell and the CircumBurst Medium (CBM). We here outline our "canonical GRB" scenario, which implies three different GRB classes: the "genuine" short GRBs, the "fake" or "disguised" short GRBs and the other (so-called "long") GRBs. We also outline some implications for the theoretical interpretation of the Amati relation.

26. G. De Barros, M.G. Bernardini, C.L. Bianco, L. Caito, M.G. Dainotti, R. Guida, R. Ruffini; "Is GRB 050509b a "genuine" short GRB?"; in 2008 NANJING GAMMA-RAY BURST CONFERENCE; Proceedings of the 2008 Nanjing Gamma-Ray Burst Conference, Nanjing (China), June 2008, Y.-F. Huang, Z.-G. Dai, B. Zhang, Editors; AIP Conference Proceedings, 1065, 231 (2008).

    Within our "fireshell" model we introduced a "canonical" GRB scenario which differentiates physically the "proper GRB" (P-GRB) emission when photons decouple, and the afterglow emission due to interaction of the accelerated baryons with the CircumBurst Medium (CBM). The ratio between energetics of the two components is ruled by the baryon loading of the fireshell. We here analyse the possibility that GRB050509b is the first case of a "genuine" short GRB the ones with smaller baryon loading. In such a case, the GRB050509b "prompt emission" would be dominated by the "proper GRB" and, moreover, the P-GRB total energy would be greater than the afterglow one. Our fit of the afterglow data and of the P-GRB energetics indicates that this source present the smallest baryon loading we ever encountered so far, being on the order of 10^{-4}.

27. G. De Barros, A.G. Aksenov, C.L. Bianco, R. Ruffini, G.V. Vereshchagin; "Fireshell versus Fireball scenarios"; in 2008 NANJING GAMMA-RAY BURST CONFERENCE; Proceedings of the 2008 Nanjing Gamma-Ray Burst Conference, Nanjing (China), June 2008, Y.-F. Huang, Z.-G. Dai, B. Zhang, Editors; AIP Conference Proceedings, 1065, 234 (2008).

We revisit Cavallo and Rees classification based on the analysis of initial conditions in electron-positron-photon plasma which appears suddenly around compact astrophysical objects and gives origin to GRBs. These initial conditions were recently studied in [1,2] by numerical integration of relativistic Boltzmann equations with collision integrals, including binary and triple interactions between particles. The main conclusion is that the pair plasma in GRB sources quickly reaches thermal equilibrium well before its expansion starts. In light of this work we comment on each of the four scenarios proposed by Cavallo and Rees and discuss their applicability to describe evolution of GRB sources.

28. M.G. Bernardini, C.L. Bianco, L. Caito, M.G. Dainotti, R. Guida, R. Ruffini; "GRB970228 as a prototype for the class of GRBs with an initial spikelike emission"; in Proceedings of the Eleventh Marcel Grossmann Meeting on General Relativity, Berlin, Germany, July 2006, H. Kleinert, R.T. Jantzen, Editors; World Scientific, (Singapore, 2008).

    We interpret GRB970228 prompt emission within our "canonical" GRB scenario, identifying the initial spikelike emission with the Proper-GRB (P-GRB) and the following bumps with the afterglow peak emission. Furthermore, we emphasize the necessity to consider the "canonical" GRB as a whole due to the highly non-linear nature of the model we applied.

29. M.G. Bernardini, C.L. Bianco, L. Caito, M.G. Dainotti, R. Guida, R. Ruffini; "GRB980425 and the puzzling URCA1 emission"; in Proceedings of the Eleventh Marcel Grossmann Meeting on General Relativity, Berlin, Germany, July 2006, H. Kleinert, R.T. Jantzen, Editors; World Scientific, (Singapore, 2008).

    We applied our "fireshell" model to GRB980425 observational data, reproducing very satisfactory its prompt emission. We use the results of our analysis to provide a possible interpretation for the X-ray emission of the source S1. The effect on the GRB analysis of the lack of data in the pre-Swift observations is also outlined.

30. C.L. Bianco, M.G. Bernardini, L. Caito, P. Chardonnet, M.G. Dainotti, F. Fraschetti, R. Guida, R. Ruffini, S.-S. Xue; "Theoretical interpretation of 'long' and 'short' GRBs"; in Proceedings of the Eleventh Marcel Grossmann Meeting on General Relativity, Berlin, Germany, July 2006, H. Kleinert, R.T. Jantzen, Editors; World Scientific, (Singapore, 2008).

Within the "fireshell" model we define a "canonical GRB" light curve with two sharply different components: the Proper-GRB (P-GRB), emitted when the optically thick fireshell of electron-positron plasma originating the phenomenon reaches transparency, and the afterglow, emitted due to the collision between the remaining optically thin fireshell and the CircumBurst Medium (CBM). We here present the consequences of such a scenario on the theoretical interpretation of the nature of "long" and "short" GRBs.

31. C.L. Bianco, M.G. Bernardini, P. Chardonnet, F. Fraschetti, R. Ruffini, S.-S. Xue; "Theoretical interpretation of luminosity and spectral properties of GRB 031203"; in Proceedings of the Eleventh Marcel Grossmann Meeting on General Relativity, Berlin, Germany, July 2006, H. Kleinert, R.T. Jantzen, Editors; World Scientific, (Singapore, 2008).

    We show how an emission endowed with an instantaneous thermal spectrum in the co-moving frame of the expanding fireshell can reproduce the time-integrated GRB observed non-thermal spectrum. An explicit example in the case of GRB 031203 is presented.

32. C.L. Bianco, R. Ruffini; "The 'Fireshell' model in the Swift era"; in Proceedings of the Eleventh Marcel Grossmann Meeting on General Relativity, Berlin, Germany, July 2006, H. Kleinert, R.T. Jantzen, Editors; World Scientific, (Singapore, 2008).

    We here re-examine the validity of the constant-index power-law relation between the fireshell Lorentz gamma factor and its radial coordinate, usually adopted in the current Gamma-Ray Burst (GRB) literature on the grounds of an "ultrarelativistic" approximation. Such expressions are found to be mathematically correct but only approximately valid in a very limited range of the physical and astrophysical parameters and in an asymptotic regime which is reached only for a very short time, if any.

33. L. Caito, M.G. Bernardini, C.L. Bianco, M.G. Dainotti, R. Guida, R. Ruffini; "Theoretical interpretation of GRB011121"; in Proceedings of the Eleventh Marcel Grossmann Meeting on General Relativity, Berlin, Germany, July 2006, H. Kleinert, R.T. Jantzen, Editors; World Scientific, (Singapore, 2008).

    GRB 011121, detected by the BeppoSAX satellite, is studied as a prototype to understand the presence of flares observed by Swift in the afterglow of many GRB sources. Detailed theoretical analysis of the GRB 011121 light curves in selected energy bands are presented and compared with observational data. An interpretation of the flare of this source is provided by the introduction of the three-dimensional structure of the CircumBurst Medium(CBM).

34. M.G. Dainotti, M.G. Bernardini, C.L. Bianco, L. Caito, R. Guida, R. Ruffini; "On GRB 060218 and the GRBs related to Supernovae Ib/c"; in Proceedings of the Eleventh Marcel Grossmann Meeting on General Relativity, Berlin, Germany, July 2006, H. Kleinert, R.T. Jantzen, Editors; World Scientific, (Singapore, 2008).

    We study the Gamma-Ray Burst (GRB) 060218: a particularly close source at $z = 0.033$ with an extremely long duration, namely $T_{90} \sim 2000$ s, related to SN 2006aj. This source appears to be a very soft burst, with a peak in the spectrum at 4.9 keV, therefore interpreted as an X-Ray Flash (XRF) and it obeys to the Amati relation. We fit the X- and γ-ray observations by Swift of GRB 060218 in the 0.1–150 keV energy band during the entire time of observations from 0 all the way to 106 s within a unified theoretical model. The details of our theoretical analysis have been recently published in a series of articles. The free parameters of the theory are only three, namely the total energy $E_{e\pm}^{tot}$ of the $e^{\pm}$ plasma, its baryon loading $B = M_B c^2 / E_{e\pm}^{tot}$, as well as the CircumBurst Medium (CBM) distribution. We fit the entire light curve, including the prompt emission as an essential part of the afterglow. We recall that this value of the B parameter is the highest among the sources we have analyzed and it is very close to its absolute upper limit expected. We successfully make definite predictions about the spectral distribution in the early part of the light curve, exactly we derive the instantaneous photon number spectrum N(E) and we show that although the spectrum in the co-moving frame of the expanding pulse is thermal, the shape of the final spectrum in the laboratory frame is clearly non thermal. In fact each single instantaneous spectrum is the result of an integration of thousands of thermal spectra over the corresponding EQuiTemporal Surfaces (EQTS). By our fit we show that there is no basic differences between XRFs and more general GRBs. They all originate from the collapse process to a black hole and their difference is due to the variability of the three basic parameters within the range of full applicability of the theory.

35. R. Guida, M.G. Bernardini, C.L. Bianco, L. Caito, M.G. Dainotti, R. Ruffini; "Theoretical interpretation of GRB060124"; in Proceedings of the Eleventh Marcel Grossmann Meeting on General Relativity, Berlin, Germany, July 2006, H. Kleinert, R.T. Jantzen, Editors; World Scientific, (Singapore,

2008).

We show the preliminary results of the application of our "fireshell" model to GRB060124. This source is very peculiar because it is the first event for which both the prompt and the afterglow emission were observed simultaneously by the three Swift instruments: BAT (15 - 350 keV), XRT (0,2 - 10 keV) and UVOT (170 - 650 nm), due to the presence of a precursor $\sim$ 570 s before the main burst. We analyze GRB060124 within our "canonical" GRB scenario, identifying the precursor with the P-GRB and the prompt emission with the afterglow peak emission. In this way we reproduce correctly the energetics of both these two components. We reproduce also the observed time delay between the precursor (P-GRB) and the main burst. The effect of such a time delay in our model will be discussed.

36. R. Ruffini, M.G. Bernardini, C.L. Bianco, L. Caito, P. Chardonnet, C. Cherubini, M.G. Dainotti, F. fraschetti, A. Geralico, R. Guida, B. Patricelli, M. Rotondo, J. Rueda Hernandez, G. Vereshchagin, S.-S. Xue; "Gamma-Ray Bursts"; in Proceedings of the Eleventh Marcel Grossmann Meeting on General Relativity, Berlin, Germany, July 2006, H. Kleinert, R.T. Jantzen, Editors; World Scientific, (Singapore, 2008).

We show by example how the uncoding of Gamma-Ray Bursts (GRBs) offers unprecedented possibilities to foster new knowledge in fundamental physics and in astrophysics. After recalling some of the classic work on vacuum polarization in uniform electric fields by Klein, Sauter, Heisenberg, Euler and Schwinger, we summarize some of the efforts to observe these effects in heavy ions and high energy ion collisions. We then turn to the theory of vacuum polarization around a Kerr-Newman black hole, leading to the extraction of the blackholic energy, to the concept of dyadosphere and dyadotorus, and to the creation of an electron-positron-photon plasma. We then present a new theoretical approach encompassing the physics of neutron stars and heavy nuclei. It is shown that configurations of nuclear matter in bulk with global charge neutrality can exist on macroscopic scales and with electric fields close to the critical value near their surfaces. These configurations may represent an initial condition for the process of gravitational collapse, leading to the creation of an electron-positron-photon plasma: the basic self-accelerating system explaining both the energetics and the high energy Lorentz factor observed in GRBs. We then turn to recall the two basic interpretational paradigms of our GRB model: 1) the Relative Space-Time Transformation (RSTT) paradigm and

2) the Interpretation of the Burst Structure (IBS) paradigm. These paradigms lead to a "canonical" GRB light curve formed from two different components: a Proper-GRB (P-GRB) and an extended afterglow comprising a raising part, a peak, and a decaying tail. When the P-GRB is energetically predominant we have a "genuine" short GRB, while when the afterglow is energetically predominant we have a so-called long GRB or a "fake" short GRB. We compare and contrast the description of the relativistic expansion of the electron-positron plasma within our approach and within the other ones in the current literature. We then turn to the special role of the baryon loading in discriminating between "genuine" short and long or "fake" short GRBs and to the special role of GRB 991216 to illustrate for the first time the "canonical" GRB bolometric light curve. We then propose a spectral analysis of GRBs, and proceed to some applications: GRB 031203, the first spectral analysis, GRB 050315, the first complete light curve fitting, GRB 060218, the first evidence for a critical value of the baryon loading, GRB 970228, the appearance of "fake" short GRBs. We finally turn to the GRB-Supernova Time Sequence (GSTS) paradigm: the concept of induced gravitational collapse. We illustrate this paradigm by the systems GRB 980425 / SN 1998bw, GRB 030329 / SN 2003dh, GRB 031203 / SN 2003lw, GRB 060218 / SN 2006aj, and we present the enigma of the URCA sources. We then present some general conclusions.

37. R. Ruffini, A.G. Aksenov, M.G. Bernardini, C.L. Bianco, L. Caito, M.G. Dainotti, G. De Barros, R. Guida, G. Vereshchagin, S.-S. Xue; "The canonical Gamma-Ray Bursts: long, 'fake'-'disguised' and 'genuine' short bursts; in PROBING STELLAR POPULATIONS OUT TO THE DISTANT UNIVERSE: CEFALU 2008, Proceedings of the International Conference; Cefalù (Italy), September 2008, G. Giobbi, A. Tornambe, G. Raimondo, M. Limongi, L. A. Antonelli, N. Menci, E. Brocato, Editors; AIP Conference Proceedings, 1111, 325 (2009).

    The Gamma-Ray Bursts (GRBs) offer the unprecedented opportunity to observe for the first time the blackholic energy extracted by the vacuum polarization during the process of gravitational collapse to a black hole leading to the formation of an electron-positron plasma. The uniqueness of the Kerr-Newman black hole implies that very different processes originating from the gravitational collapse a) of a single star in a binary system induced by the companion, or b) of two neutron stars, or c) of a neutron star and a white dwarf, do lead to the same structure for the observed GRB. The recent progress of the numerical integration of the relativistic Boltzmann equations with collision integrals including 2-body and 3-body interactions between the particles offer a powerful conceptual tool in order to differentiate the traditional "fireball" picture, an expanding hot cavity considered by Cavallo and Rees, as opposed to the "fireshell" model, composed of an internally cold shell of relativistically expanding electron-positron-baryon plasma. The analysis of the fireshell naturally leads to a canonical GRB composed of a proper-GRB and an extended afterglow. By recalling the three interpretational paradigms for GRBs we show how the fireshell model leads to an understanding of the GRB structure and to an alternative classification of short and long GRBs.

38. M.G. Bernardini, M.G. Dainotti, C.L. Bianco, L. Caito, R. Guida, R. Ruffini; "Prompt emission and X-ray flares: the case of GRB 060607 A"; in PROBING STELLAR POPULATIONS OUT TO THE DISTANT UNIVERSE: CEFALU 2008, Proceedings of the International Conference; Cefalù (Italy), September 2008, G. Giobbi, A. Tornambe, G. Raimondo, M. Limongi, L. A. Antonelli, N. Menci, E. Brocato, Editors; AIP Conference Proceedings, 1111, 383 (2009).

    GRB 060607A is a very distant and energetic event. Its main peculiarity is that the peak of the near-infrared (NIR) afterglow has been observed with the REM robotic telescope, allowing to estimate the initial Lorentz gamma factor within the fireball forward shock model. We analyze GRB 060607A within the fireshell model. The initial Lorentz gamma factor of the fireshell can be obtained adopting the exact solutions of its equations of motion, dealing only with the BAT and XRT observations, that are the basic contribution to the afterglow emission, up to a distance from the progenitor $r \sim 10^{18}$ cm. According to the "canonical GRB" scenario we interpret the whole prompt emission as the peak of the afterglow emission, and we show that the observed temporal variability of the prompt emission can be produced by the interaction of the fireshell with overdense CircumBurst Medium (CBM) clumps. This is indeed the case also of the X-ray flares which are present in the early phases of the afterglow light curve.

39. C.L. Bianco, M.G. Bernardini, L. Caito, M.G. Dainotti, R. Guida, R. Ruffini; "The 'fireshell' model and the 'canonical GRB' scenario. Implications for the Amati relation"; in PROBING STELLAR POPULATIONS OUT TO THE DISTANT UNIVERSE: CEFALU 2008, Proceedings of the International Conference; Cefalù (Italy), September 2008, G. Giobbi, A. Tornambe, G. Raimondo, M. Limongi, L. A. Antonelli, N. Menci, E. Bro-

cato, Editors; AIP Conference Proceedings, 1111, 587 (2009).

Within the "fireshell" model for GRBs we define a "canonical GRB" light curve with two sharply different components: the Proper-GRB (P-GRB), emitted when the optically thick fireshell reaches transparency, and the extended afterglow, emitted due to the collision between the remaining optically thin fireshell and the CircumBurst Medium (CBM). We here outline our "canonical GRB" scenario, which implies three different GRB classes: the "genuine" short GRBs, the "fake" or "disguised" short GRBs and the other (so-called "long") GRBs. We will also outline the corresponding implications for the Amati relation, which are opening its use for cosmology.

40. R. Ruffini, A.G. Aksenov, M.G. Bernardini, C.L. Bianco, L. Caito, P. Chardonnet, M.G. Dainotti, G. De Barros, R. Guida, L. Izzo, B. Patricelli, L.J. Rangel Lemos, M. Rotondo, J.A. Rueda Hernandez, G. Vereshchagin, S.-S. Xue; "The Blackholic energy and the canonical Gamma-Ray Burst IV: the 'long', 'genuine short' and 'fake – disguised short' GRBs"; in Proceedings of the XIIIth Brazilian School on Cosmology and Gravitation, Mangaratiba, Rio de Janeiro (Brazil), July-August 2008, M. Novello, S.E. Perez Bergliaffa, Editors; AIP Conference Proceedings, 1132, 199 (2009).

    We report some recent developments in the understanding of GRBs based on the theoretical framework of the "fireshell" model, already presented in the last three editions of the "Brazilian School of Cosmology and Gravitation". After recalling the basic features of the "fireshell model", we emphasize the following novel results: 1) the interpretation of the X-ray flares in GRB afterglows as due to the interaction of the optically thin fireshell with isolated clouds in the CircumBurst Medium (CBM); 2) an interpretation as "fake - disguised" short GRBs of the GRBs belonging to the class identified by Norris & Bonnell; we present two prototypes, GRB 970228 and GRB 060614; both these cases are consistent with an origin from the final coalescence of a binary system in the halo of their host galaxies with particularly low CBM density $n_{cbm} \sim 10^{-3}$ particles/cm^3; 3) the first attempt to study a genuine short GRB with the analysis of GRB 050509B, that reveals indeed still an open question; 4) the interpretation of the GRB-SN association in the case of GRB 060218 via the "induced gravitational collapse" process; 5) a first attempt to understand the nature of the "Amati relation", a phenomenological correlation between the isotropic-equivalent radiated energy of the prompt emission E_{iso} with the cosmological rest-frame νF_ν spectrum peak energy $E_{p,i}$. In addition, recent progress on the thermalization of the electron-positron plasma close to their formation phase, as well as the structure of the electrodynamics of Kerr-Newman Black Holes are presented. An outlook for possible explanation of high-energy phenomena in GRBs to be expected from the AGILE and the Fermi satellites are discussed. As an example of high energy process, the work by Enrico Fermi dealing with ultrarelativistic collisions is examined. It is clear that all the GRB physics points to the existence of overcritical electrodynamical fields. In this sense we present some progresses on a unified approach to heavy nuclei and neutron stars cores, which leads to the existence of overcritical fields under the neutron star crust.

41. A.G. Aksenov, M.G. Bernardini, C.L. Bianco, L. Caito, C. Cherubini, G. De Barros, A. Geralico, L. Izzo, F.A. Massucci, B. Patricelli, M. Rotondo, J.A. Rueda Hernandez, R. Ruffini, G. Vereshchagin, S.-S. Xue; "The fireshell model for Gamma-Ray Bursts"; in The Shocking Universe, Proceedings of the conference held in Venice (Italy), September 2009, G. Chincarini, P. D'Avanzo, R. Margutti, R. Salvaterra, Editors; SIF Conference Proceedings, 102, 451 (2010).

    The fireshell model for GRBs is briefly outlined, and the currently ongoing developments are summarized.

42. M.G. Bernardini, C.L. Bianco, L. Caito, L. Izzo, B. Patricelli, R. Ruffini; "The end of the prompt emission within the fireshell model"; in The Shocking Universe, Proceedings of the conference held in Venice (Italy), September 2009, G. Chincarini, P. D'Avanzo, R. Margutti, R. Salvaterra, Editors; SIF Conference Proceedings, 102, 489 (2010)

    The shallow decay emission, revealed by the Swift satellite in the X-ray afterglow of a good sample of bursts, is a puzzle. Within the fireshell model it has been recently proposed an alternative explanation: if we assume that after the prompt phase the system has a range of Lorentz factors, the plateau phase is simply the product of the injection of slower material into the fireshell. This injection produces a modification both in the dynamics of the fireshell and in the spectrum of the emitted radiation. We postulate that this spread in the fireshell Lorentz factor occurs when the fireshell becomes transparent and do not depend on a prolonged activity of the central engine. The aim of this paper is to characterize dynamically the system in order to understand the nature of that material.

43. L. Izzo, M.G. Bernardini, C.L. Bianco, L. Caito, B. Patricelli, R. Ruffini; "GRB 090423 in the fireshell scenario"; in The Shocking Universe, Proceedings of the conference held in Venice (Italy), September 2009, G. Chincarini, P. D'Avanzo, R. Margutti, R. Salvaterra, Editors; SIF Conference Proceedings, 102, 537 (2010).

44. B. Patricelli, M.G. Bernardini, C.L. Bianco, L. Caito, L. Izzo, R. Ruffini, G. Vereshchagin; "A new spectral energy distribution of photons in the fireshell model of GRBs"; in The Shocking Universe, Proceedings of the conference held in Venice (Italy), September 2009, G. Chincarini, P. D'Avanzo, R. Margutti, R. Salvaterra, Editors; SIF Conference Proceedings, 102, 559 (2010).

    The fireshell model of Gamma Ray Bursts (GRBs) postulates that the emission process is thermal in the comoving frame of the fireshell, but this is just a first approximation. We investigate a different spectrum of photons in the comoving frame in order to better reproduce the observed spectral properties of GRB prompt emission. We introduce a modified thermal spectrum whose low energy slope depends on an index α, left as a free parameter. We test it by comparing the numerical simulations with observed BAT spectra integrated over different intervals of time. We find that the observational data can be correctly reproduced by assuming $\alpha = -1.8$.

45. C.L. Bianco, M.G. Bernardini, L. Caito, G. De Barros, L. Izzo, B. Patricelli, R. Ruffini; "Disguised Short Bursts and the Amati Relation"; in Deciphering the ancient universe with Gamma-Ray Bursts, Proceedings of the conference held in Kyoto (Japan), April 2010, N. Kawai, S. Nagataki, Editors; AIP Conference Proceedings, 1279, 299 (2010).

    The class of "Disguised short" GRBs implied by the fireshell scenario is presented, with special emphasis on the implications for the Amati relation.

46. L. Izzo, M.G. Bernardini, C.L. Bianco, L. Caito, B. Patricelli, L.J. Rangel Lemos, R. Ruffini; "On GRB 080916C and GRB 090902B observed by the Fermi satellite"; in Deciphering the ancient universe with Gamma-Ray Bursts, Proceedings of the conference held in Kyoto (Japan), April 2010, N. Kawai, S. Nagataki, Editors; AIP Conference Proceedings, 1279, 343 (2010).

    We propose a possible explanation, in the context of the Fireshell scenario, for the high-energy emission observed in GRB 080916C and GRB 090902B. The physical process underlying this emission consists mainly in the interaction of the baryon in the Fireshell with some high-density region around the burst site. Moreover we associate the observed delay of the onset of the high-energy emission as due to the P-GRB emission.

47. B. Patricelli, M.G. Bernardini, C.L. Bianco, L. Caito, G. De Barros, L. Izzo, R. Ruffini; "Black Holes in Gamma Ray Bursts"; in Deciphering the ancient universe with Gamma-Ray Bursts, Proceedings of the conference held in Kyoto (Japan), April 2010, N. Kawai, S. Nagataki, Editors; AIP Conference Proceedings, 1279, 406 (2010).

    Within the fireshell model, Gamma Ray Bursts (GRBs) originate from an optically thick $e^{\pm}$ plasma created by vacuum polarization process during the formation of a Black Hole (BH). Here we briefly recall the basic features of this model, then we show how it is possible to interpret GRB observational properties within it. In particular we present, as a specific example, the analysis of GRB 050904 observations of the prompt emission light curve and spectrum in the Swift BAT energy band (15-150 keV).

48. M.G. Bernardini, C.L. Bianco, L. Caito, M.G. Dainotti, R. Guida, R. Ruffini; "The GRB classification within the "fireshell" model: short, long and "fake" short GRBs"; in Proceedings of the 3rd Stueckelberg Workshop on Relativistic Field Theories, Pescara, Italy, July 2008, N. Carlevaro, R. Ruffini, G.V. Vereshchagin, Editors; Cambridge Scientific Publishers, (UK, 2011).

49. C.L. Bianco, M.G. Bernardini, L. Caito, M.G. Dainotti, R. Guida, R. Ruffini, G.V. Vereshchagin, S.-S. Xue; "Equations of motion of the "fireshell""; in Proceedings of the 3rd Stueckelberg Workshop on Relativistic Field Theories, Pescara, Italy, July 2008, N. Carlevaro, R. Ruffini, G.V. Vereshchagin, Editors; Cambridge Scientific Publishers, (UK, 2011).

50. L. Caito, M.G. Bernardini, C.L. Bianco, M.G. Dainotti, R. Guida, R. Ruffini; "GRB 060614: another example of "fake" short burst from a merging binary system"; in Proceedings of the 3rd Stueckelberg Workshop on Relativistic Field Theories, Pescara, Italy, July 2008, N. Carlevaro, R. Ruffini, G.V. Vereshchagin, Editors; Cambridge Scientific Publishers, (UK, 2011).

51. G. De Barros, M.G. Bernardini, C.L. Bianco, L. Caito, R. Guida, R. Ruffini; "Analysis of GRB 050509b"; in Proceedings of the 3rd Stueckelberg Workshop on Relativistic Field Theories, Pescara, Italy, July 2008, N. Carlevaro, R. Ruffini, G.V. Vereshchagin, Editors; Cambridge Scientific Publishers, (UK, 2011).

52. R. Ruffini, L. Izzo, A.V. Penacchioni, C.L. Bianco, L. Caito, S.K. Chakrabarti, A. Nandi; "GRB 090618: a possible case of multiple GRB?"; in Proceedings of the 25th Texas Symposium on Relativistic Astrophysics, held in Heidelberg (Germany), December 2010, F.M. Rieger, C. van Eldik, W. Hofmann, Editors; PoS(Texas2010), 101.

53. L.J. Rangel Lemos, C.L. Bianco, H.J. Mosquera Cuesta, J.A. Rueda, R. Ruffini; "Luminosity function of BATSE GRBs dominated by extended afterglow"; in Proceedings of the 25th Texas Symposium on Relativistic Astrophysics, held in Heidelberg (Germany), December 2010, F.M. Rieger, C. van Eldik, W. Hofmann, Editors; PoS(Texas2010), 204.

54. R. Ruffini, A.G. Aksenov, M.G. Bernardini, C.L. Bianco, L. Caito, P. Chardonnet, M.G. Dainotti, G. De Barros, R. Guida, L. Izzo, B. Patricelli, L.J. Rangel Lemos, M. Rotondo, J.A. Rueda Hernandez, G. Vereshchagin, She-Sheng Xue; "Black Holes Energetics and GRBs"; in The Sun, the Stars, the Universe and General Relativity: Proceedings of Sobral 2009; S.E. Perez Bergliaffa, M. Novello , R. Ruffini, Editors; Cambridge Scientific Publishers (UK, 2011).

55. C.L. Bianco, L. Amati, M.G. Bernardini, L. Caito, G. De Barros, L. Izzo, B. Patricelli, R. Ruffini; "The class of 'disguised' short GRBs and its implications for the Amati relation"; in GRBs as probes - from the progenitors environment to the high redshift Universe, Proceedings of the conference held in Como (Italy), May 2011, S. Campana, P. D'Avanzo, A. Melandri, Editors; Mem. S.A.It. Suppl., 21, 139 (2012).

56. A.V. Penacchioni, R. Ruffini, L. Izzo, M. Muccino, C.L. Bianco, L. Caito, B. Patricelli; "Evidences for a double component in the emission of GRB 101023"; in GRBs as probes - from the progenitors environment to the high redshift Universe, Proceedings of the conference held in Como (Italy), May 2011, S. Campana, P. D'Avanzo, A. Melandri, Editors; Mem. S.A.It. Suppl., 21, 230 (2012).

57. M.G. Bernardini, C.L. Bianco, L. Caito, L. Izzo, B. Patricelli, R. Ruffini; "The X-Ray Flares of GRB 060607A within the Fireshell Model"; in Proceedings of the Twelfth Marcel Grossmann Meeting on General Relativity, Paris, France, July 2009, T. Damour, R.T. Jantzen, R. Ruffini, Editors; World Scientific, (Singapore, 2012).

58. L. Izzo, M.G. Bernardini, C.L. Bianco, L. Caito, B. Patricelli, R. Ruffini; "GRB 090423 in the Fireshell Scenario: A Canonical GRB at Redshift 8.2"; in Proceedings of the Twelfth Marcel Grossmann Meeting on General Relativity, Paris, France, July 2009, T. Damour, R.T. Jantzen, R. Ruffini, Editors; World Scientific, (Singapore, 2012).

59. B. Patricelli, M.G. Bernardini, C.L. Bianco, L. Caito, L. Izzo, R. Ruffini, G.V. Vereshchagin; "A New Spectral Energy Distribution of Photons in the Fireshell Model of GRBs"; in Proceedings of the Twelfth Marcel Grossmann Meeting on General Relativity, Paris, France, July 2009, T. Damour, R.T. Jantzen, R. Ruffini, Editors; World Scientific, (Singapore, 2012).

60. C.L. Bianco, M.G. Bernardini, L. Caito, G. De Barros, L. Izzo, M. Muccino, B. Patricelli, A.V. Penacchioni, G.B. Pisani, R. Ruffini; "Needs for a new GRB classification following the fireshell model: "genuine short", "disguised short" and "long" GRBs"; in Proceedings of the Gamma-Ray Bursts 2012 Conference, held in Munich (Germany), May 2012, A. Rau, J. Greiner, Editors; PoS(GRB 2012), 043.

61. A.V. Penacchioni, G.B. Pisani, R. Ruffini, C.L. Bianco, L. Izzo, M. Muccino; "The proto-black hole concept in GRB 101023 and its possible extension to GRB 110709B"; in Proceedings of the Gamma-Ray Bursts 2012 Conference, held in Munich (Germany), May 2012, A. Rau, J. Greiner, Editors; PoS(GRB 2012), 042.

62. B. Patricelli, M.G. Bernardini, C.L. Bianco, L. Caito, L. Izzo, R. Ruffini; "GRB 050904: The study of a high redshift GRB within the Fireshell Model"; in Proceedings of the Twelfth Marcel Grossmann Meeting on General Relativity, Paris, France, July 2009, T. Damour, R.T. Jantzen, R. Ruffini, Editors; World Scientific, (Singapore, 2012).

63. L. Izzo, G.B. Pisani, M. Muccino, J.A. Rueda, Y.Wang, C.L. Bianco, A.V. Penacchioni, R. Ruffini; "A common behavior in the late X-ray after-

glow of energetic GRB-SN systems"; EAS Publications Series, Volume 61, 595-597 (2013).

64. R. Ruffini; "Black Holes, Supernovae and Gamma Ray Bursts"; in Proceedings of the Thirteenth Marcel Grossmann Meeting on General Relativity, Stockholm, Sweden, July 2012, R.T. Jantzen, K. Rosquist, R. Ruffini, Editors; World Scientific, (Singapore, 2015).

65. M. Muccino, R. Ruffini, C.L. Bianco, L. Izzo, A.V. Penacchioni, G.B. Pisani; "GRB 090227B: The missing link between the genuine short and long GRBs"; in Proceedings of the Thirteenth Marcel Grossmann Meeting on General Relativity, Stockholm, Sweden, July 2012, R.T. Jantzen, K. Rosquist, R. Ruffini, Editors; World Scientific, (Singapore, 2015).

66. A.V. Penacchioni, R. Ruffini, C.L. Bianco, L. Izzo, M. Muccino, G.B. Pisani, J.A. Rueda; "The family of the Induced Gravitational Collapse scenario: The case of GRB 110709B"; in Proceedings of the Thirteenth Marcel Grossmann Meeting on General Relativity, Stockholm, Sweden, July 2012, R.T. Jantzen, K. Rosquist, R. Ruffini, Editors; World Scientific, (Singapore, 2015).

67. A.V. Penacchioni, R. Ruffini, C.L. Bianco, L. Izzo, M. Muccino, G.B. Pisani; "GRB 111228, analysis within the Induced Gravitational Collapse scenario and association with a supernova"; in Proceedings of the Thirteenth Marcel Grossmann Meeting on General Relativity, Stockholm, Sweden, July 2012, R.T. Jantzen, K. Rosquist, R. Ruffini, Editors; World Scientific, (Singapore, 2015).

68. G.B. Pisani, L. Izzo, R. Ruffini, C.L. Bianco, M. Muccino, A.V. Penacchioni, J.A. Rueda, Y. Wang; "On a novel distance indicator for Gamma-Ray Bursts associated with supernovae"; in Proceedings of the Thirteenth Marcel Grossmann Meeting on General Relativity, Stockholm, Sweden, July 2012, R.T. Jantzen, K. Rosquist, R. Ruffini, Editors; World Scientific, (Singapore, 2015).

69. M. Muccino, R. Ruffini, C.L. Bianco, L. Izzo, A.V. Penacchioni, G.B. Pisani; "GRB 090510, explosion of a GRB in the highest circumburst medium even inferred: a disguised short GRB"; in Proceedings of the Thirteenth Marcel Grossmann Meeting on General Relativity, Stockholm,

Sweden, July 2012, R.T. Jantzen, K. Rosquist, R. Ruffini, Editors; World Scientific, (Singapore, 2015).

70. L. Izzo, G.B. Pisani, M. Muccino, R. Ruffini, C.L. Bianco, M. Enderli, Y. Wang; "Hints for a physically based GRB distance indicator"; in Proceedings of the Thirteenth Marcel Grossmann Meeting on General Relativity, Stockholm, Sweden, July 2012, R.T. Jantzen, K. Rosquist, R. Ruffini, Editors; World Scientific, (Singapore, 2015).

71. R. Ruffini, Y. Aimuratov, V. Belinski, C.L. Bianco, M. Enderli, L. Izzo, M. Kovacevic, G.J. Mathews, R. Moradi, M. Muccino, A.V. Penacchioni, G.B. Pisani, J.A. Rueda, G.V. Vereshchagin, Y. Wang, S.-S. Xue; Cosmic matrix in the jubilee of relativistic astrophysics; in THE SECOND ICRANET CÉSAR LATTES MEETING: Supernovae, Neutron Stars and Black Holes, Proceedings of the conference held in Rio de Janeiro – Niterói – João Pessoa – Recife – Fortaleza (Brazil), 13-22 April 2015, U. Barres de Almeida, P. Chardonnet, R. Picanco Negreiros, J. Rueda, R. Ruffini, G. Vereshchagin, C. Zen Vasconcellos, Editors; AIP Conference Proceedings, 1693, 020001 (2015).

72. L. Becerra, C.L. Bianco, F. Cipolletta, M. Enderli, C.L. Fryer, L. Izzo, M. Kovacevic, R. Camargo Rodrigues de Lima, M. Muccino, F.G. de Oliveira, A.V. Penacchioni, G.B. Pisani, J.A. Rueda, R. Ruffini, Y. Wang, E. Zaninoni; Black holes, neutron stars and supernovae within the induced gravitational collapse paradigm for GRBs; in THE SECOND ICRANET CÉSAR LATTES MEETING: Supernovae, Neutron Stars and Black Holes, Proceedings of the conference held in Rio de Janeiro – Niterói – João Pessoa – Recife – Fortaleza (Brazil), 13-22 April 2015, U. Barres de Almeida, P. Chardonnet, R. Picanco Negreiros, J. Rueda, R. Ruffini, G. Vereshchagin, C. Zen Vasconcellos, Editors; AIP Conference Proceedings, 1693, 020002 (2015).

73. L.J. Rangel Lemos, C.L. Bianco, R. Ruffini; Applying the luminosity function statistics in the fireshell model; in THE SECOND ICRANET CÉSAR LATTES MEETING: Supernovae, Neutron Stars and Black Holes, Proceedings of the conference held in Rio de Janeiro – Niterói – João Pessoa – Recife – Fortaleza (Brazil), 13-22 April 2015, U. Barres de Almeida, P. Chardonnet, R. Picanco Negreiros, J. Rueda, R. Ruffini, G. Vereshchagin, C. Zen Vasconcellos, Editors; AIP Conference Proceedings, 1693,

070004 (2015).

74. J.A. Rueda, R. Ruffini, J.F. Rodriguez, M. Muccino, Y. Aimuratov, U. Barres de Almeida, L.M. Becerra, C.L. Bianco, C. Cherubini, S. Filippi, M. Kovacevic, R. Moradi, G.B. Pisani, Y. Wang; The binary progenitors of short and long GRBs and their gravitational-wave emission; EPJ Web of Conferences, 168, 01006 (2018).

75. M. Muccino, R. Ruffini, Y. Aimuratov, L.M. Becerra, C.L. Bianco, M. Karlika, M. Kovacevic, J.D. Melon Fuksman, R. Moradi, A.V. Penacchioni, G.B. Pisani, D. Primorac, J.A. Rueda, S. Shakeri, G.V. Vereshchagin, S.-S. Xue, Y. Wang; What can we learn from GRBs?; EPJ Web of Conferences, 168, 01015 (2018).

76. L.M. Becerra, C.L. Bianco, C. Fryer, J.A. Rueda, R. Ruffini; On the Induced Gravitational Collapse; EPJ Web of Conferences, 168, 02005 (2018).

77. G.B. Pisani, R. Ruffini, Y. Aimuratov, C.L. Bianco, M. Karlika, M. Kovacevic, R. Moradi, M. Muccino, A.V. Penacchioni, D. Primorac, J.A. Rueda, Y. Wang; The first ICRANet catalog of Binary-Driven Hypernovae; EPJ Web of Conferences, 168, 04002 (2018).

78. D. Primorac, R. Ruffini, G.B. Pisani, Y. Aimuratov, C.L. Bianco, M. Karlika, J.D. Melon Fuksman, R. Moradi, M. Muccino, A.V. Penacchioni, J.A. Rueda, Y. Wang; GRB 110731A within the IGC paradgm; EPJ Web of Conferences, 168, 04008 (2018).

79. J.D. Melon Fuksman, L.M. Becerra, C.L. Bianco, M. Karlika, M. Kovacevic, R. Moradi, M. Muccino, G.B. Pisani, D. Primorac, J.A. Rueda, R. Ruffini, G.V. Vereshchagin, Y. Wang; Evolution of an electron-positron plasma produced by induced gravitational collapse in binary-driven hypernovae; EPJ Web of Conferences, 168, 04009 (2018).

The Astrophysical Journal, 966:219 (10pp), 2024 May 10 https://doi.org/10.3847/1538-4357/ad2fa9

Probing Electromagnetic Gravitational-wave Emission Coincidence in a Type I Binary-driven Hypernova Family of Long Gamma-Ray Bursts at Very High Redshift

C. L. Bianco[1,2,3,4], M. T. Mirtorabi[1,5], R. Moradi[1,2,6,7], F. Rastegarnia[1,5], J. A. Rueda[1,2,4,8,9], R. Ruffini[1,2,3,10], Y. Wang (王瑜)[1,2,6], M. Della Valle[1,11], Liang Li (李亮)[1,2,6], and S. R. Zhang (张书瑞)[1,8,12,13]

[1] ICRANet, Piazza della Repubblica 10, I-65122 Pescara, Italy; ruffini@icra.it, bianco@icra.it, torabi@alzahra.ac.ir, rmoradi@ihep.ac.cn, fatemeh.rastegarnia@icranet.org, jorge.rueda@icra.it, yu.wang@icranet.org, massimo.dellavalle@inaf.it, liang.li@icranet.org and zhangsr@mail.ustc.edu.cn
[2] ICRA, Dip. di Fisica, Sapienza Università di Roma, Piazzale Aldo Moro 5, I-00185 Roma, Italy
[3] Université de Nice Sophia-Antipolis, Grand Château Parc Valrose, Nice, CEDEX 2, France
[4] INAF, Istituto di Astrofisica e Planetologia Spaziali, Via Fosso del Cavaliere 100, 00133 Rome, Italy
[5] Department of Fundamental Physics, Faculty of Physics, Alzahra University, Tehran, Iran
[6] INAF—Osservatorio Astronomico d'Abruzzo, Via M. Maggini snc, I-64100, Teramo, Italy
[7] Key Laboratory of Particle Astrophysics, Institute of High Energy Physics, Chinese Academy of Sciences, Beijing 100049, People's Republic of China
[8] ICRANet-Ferrara, Dip. di Fisica e Scienze della Terra, Università degli Studi di Ferrara, Via Saragat 1, I–44122 Ferrara, Italy
[9] Dip. di Fisica e Scienze della Terra, Università degli Studi di Ferrara, Via Saragat 1, I–44122 Ferrara, Italy
[10] INAF, Viale del Parco Mellini 84, 00136 Rome, Italy
[11] INAF—Osservatorio Astronomico di Capodimonte, Salita Moiariello 16, I-80131, Napoli, Italy
[12] School of Astronomy and Space Science, University of Science and Technology of China, Hefei 230026, People's Republic of China
[13] CAS Key Laboratory for Research in Galaxies and Cosmology, Department of Astronomy, University of Science and Technology of China, Hefei 230026, People's Republic of China

Received 2023 June 9; revised 2024 February 5; accepted 2024 February 26; published 2024 May 9

Abstract

The repointing time of the X-Ray Telescope (XRT) instrument on the Neil Gehrels Swift Observatory satellite has posed challenges in observing and studying the early X-ray emissions within ≈40 s after a gamma-ray burst (GRB) trigger. To address this issue, we adopt a novel approach that capitalizes on the cosmological time dilation in GRBs with redshifts ranging from 3 to 9. Applying this strategy to Swift/XRT data, we investigate the earliest X-ray emissions of 368 GRBs from the Swift catalog, including short and long GRBs. We compare the observed time delay between the GRB trigger and the initial Swift/XRT observation, measured in the GRB observer frame, and the corresponding cosmological rest-frame time delay (RTD). This technique is here used in the analysis of GRB 090423 at $z = 8.233$ (RTD ∼8.2 s), GRB 090429B at $z \approx 9.4$ (RTD ∼10.1 s), and GRB 220101A at $z = 4.61$ (RTD ∼14.4 s). The cosmological time dilation enables us to observe the very early X-ray afterglow emission in these three GRBs. We thus validate the observation of the collapse of the carbon–oxygen core and the coeval newborn neutron star (νNS) formation triggering the GRB event in the binary-driven hypernova (BdHN) scenario. We also evidence the νNS spin-up due to supernova ejecta fallback and its subsequent slowing down due to the X-ray/optical/radio synchrotron afterglow emission. A brief gravitational-wave signal may separate the two stages owing to a fast-spinning νNS triaxial-to-axisymmetric transition. We also analyze the long GRB redshift distribution for the different BdHN types and infer that BdHNe II and III may originate the NS binary progenitors of short GRBs.

Unified Astronomy Thesaurus concepts: Gamma-ray bursts (629)

Supporting material: machine-readable table

1. Introduction

Important astronomical breakthroughs are often marked by the possibility of studying events occurring in the nearby Universe. There are several prominent examples, e.g., supernova (SN) SN 1987A: its proximity has allowed the first detection of neutrinos (Bionta et al. 1987; Hirata et al. 1987; Alexeyev et al. 1988) and the observation of the shock breakout (Arnett et al. 1989). Another example is gamma-ray burst (GRB) GRB 980425 and SN 1998bw, the prototype of GRB–SN connection (Galama et al. 1998; Patat et al. 2001), which occurred at about 40 Mpc. It is still the closest case of GRB–SN connection observed so far. The problem of the GRB–SN connection has been addressed in Aimuratov et al. (2023), where the binary-driven hypernova (BdHN) model has been illustrated (see also the Appendix in this paper). Again, the most important information has been gained from nearby sources (GRB 190114C with $z = 0.0425$ and $E_{iso} = 2.5 \times 10^{53}$ erg, GRB 171205A with $z = 0.0368$ and $E_{iso} = 5.7 \times 10^{49}$ erg, GRB 190829A with $z = 0.0785$ and $E_{iso} = 2 \times 10^{50}$ erg). Unlike the cases briefly illustrated above, in this work we show how the observation of GRBs at very high redshift, by exploiting the cosmological time dilatation factor $(1 + z)$ as a novel observational tool, can allow us to enter the terra incognita of the very early GRB X-ray emission. This emission is currently inaccessible to Swift's X-Ray Telescope (XRT) detector in nearby events, which paradoxically would be more suitable to be studied. However, the significant instrumental delay of repointing the Swift/XRT detector following the GRB trigger, expressed in the observer's rest frame, prevents their early X-ray emission observations. Cosmology, here used as an observational tool, lets us detect the GRB early X-ray afterglow emission at very high redshift. This is one of the main results presented in this article.

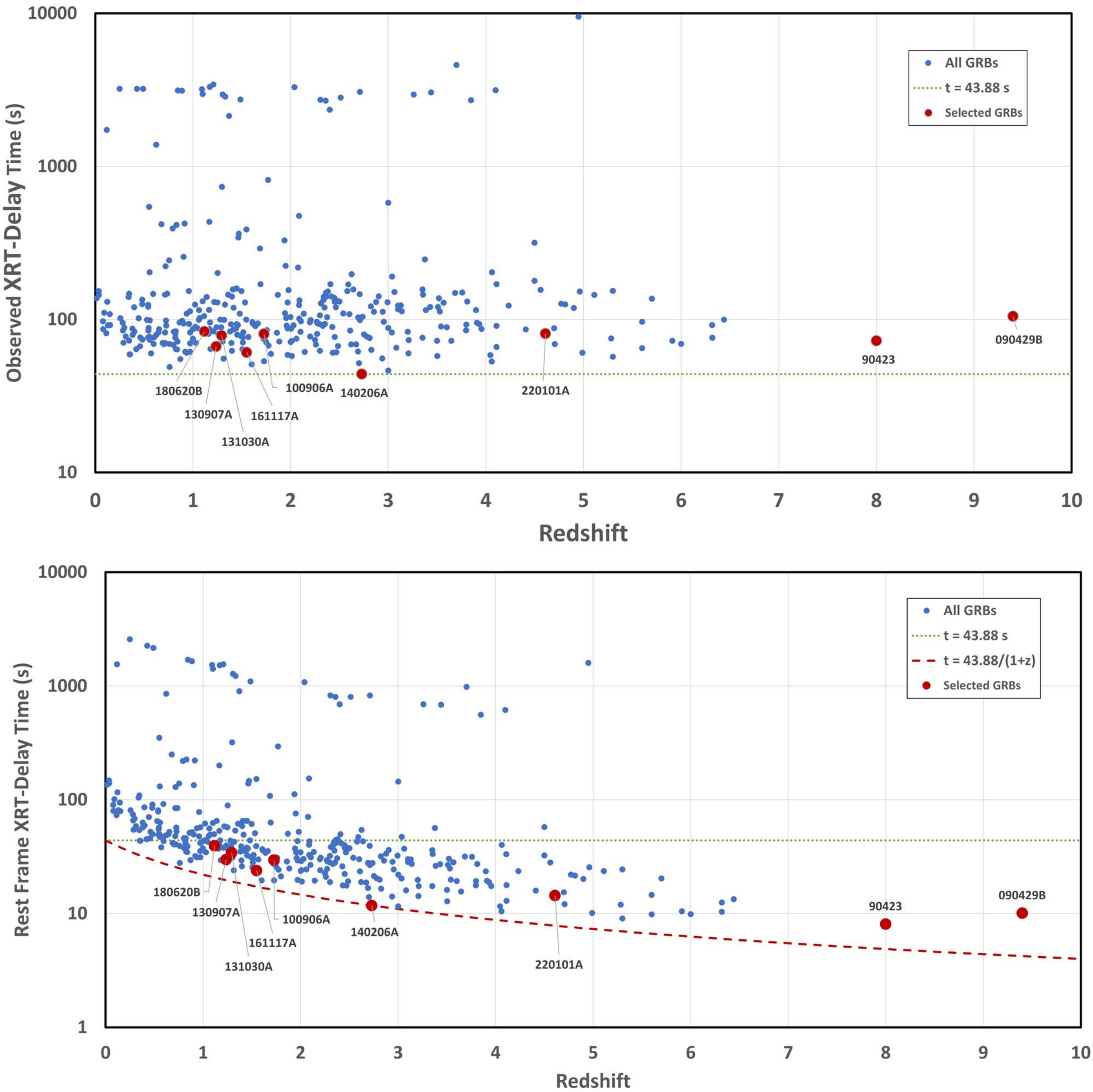

Figure 1. The Swift/XRT time delay in the observer's frame (OTD; top panel) and the cosmological rest-frame (RTD; bottom panel). Red circles mark GRB 220101A at $z = 4.61$, GRB 090423 at $z = 8.2$, GRB 090429B at $z \sim 9.4$, GRB 140206A at $z \sim 2.73$, GRB 100906A at $z \sim 1.727$, GRB 161117 at $z \sim 1.549$, GRB 130907A at $z \sim 1.238$, GRB 180620B at $z \sim 1.118$, and GRB 131030A at $z \sim 1.239$.

For this task, we use the complete sample of 368 GRBs of the Swift GRB database[14] with a measured redshift (see Section 2). The sample includes short and long GRBs. We define the observed time delay (OTD) as the time after the GRB trigger needed by Swift/XRT to repoint the source measured in the observer frame[15] (for details see Section 3 and, e.g., Troja 2020, as well as Gehrels et al. 2004). The minimum OTD in our sample is 43.88 s for GRB 140206A at redshift $z = 2.73$ (marked by a horizontal green line in Figure 1). It becomes clear that Swift/XRT is generally technically unable to observe the X-ray emission in the first tens of seconds after the GRB trigger. Hence, the X-ray emission within ≈40 s of the GRB trigger remains unobservable by the only available instrument, Swift/XRT. This time interval represents an uncharted new X-ray territory. This large OTD can be circumvented by considering the cosmological corrections presented in this article, using the cosmological rest-frame time delay (RTD; see Section 3).

In Section 4, special attention is dedicated to the three prototypes of BdHNe I: GRB 220101A at $z = 4.61$ (Fu et al. 2022; Fynbo et al. 2022; Perley 2022), GRB 090423 at $z = 8.2$ (Salvaterra et al. 2009; Tanvir et al. 2009; Ruffini et al. 2014), and GRB 090429B at a photometric redshift $z \sim 9.4$ (Cucchiara et al. 2011), duly accounting for the k-correction and the 0.3–10 keV luminosity light curves. Their excellent data create the condition to analyze long GRBs' very early X-ray afterglow

[14] https://swift.gsfc.nasa.gov/archive/grb_table/
[15] Namely, the column "XRT Time to First Observation [sec]" in the Swift GRB catalog; see https://swift.gsfc.nasa.gov/archive/grb_table/.

emission, which is a stringent test for all theoretical models. This is particularly relevant in the case of the BdHN model since it allows the analysis of the new physics of the SN rise. This provides a unique opportunity to confirm the observation of Episode I, which corresponds to the carbon–oxygen (CO) core collapse and to the coeval newborn neutron star (νNS) formation, both of which trigger the onset of the BdHN event. We then evidence the observation of Episode II. This allows us to identify the physical processes occurring in the νNS rise as announced in Rueda et al. (2022c) and Aimuratov et al. (2023); see Section 4.

Section 5 discusses the implications of the above findings for the distribution of black holes (BHs) across the Universe.

In Section 6, we finally analyze the redshift distributions of the long GRBs belonging to different BdHN families. We show that their distribution supports the BdHN theoretical prediction, presented in Fryer et al. (2015) and Ruffini et al. (2016, 2018b), that BdHNe II and III may form the NS binary progenitors of short GRBs.

Finally, we summarize our conclusions in Section 7.

2. Our Sample of 368 GRBs and Their Redshift Distribution

For the analysis of the cosmological time dilation, we build our GRB sample including all GRBs (long and short) that respect these three criteria:

1. The GRB is present in the Swift GRB database (see https://swift.gsfc.nasa.gov/archive/grb_table/).
2. The GRB has a measured redshift reported in the Swift GRB database.
3. The GRB has XRT observations with a measured delay between the GRB trigger time determined by Swift/BAT and the moment of the first Swift/XRT observation.

This sample comprises 368 GRBs from 2005 to the end of 2023 (see Table 1).

3. The Swift/XRT Observed Time Delay and the Cosmological Rest-frame Time Delay

We now turn to the main point of this paper and focus on the Swift/XRT time delays in our sample of 368 GRBs as a function of their cosmological redshift. We define the OTD as the time after the GRB trigger needed by Swift/XRT to repoint the source measured in the observer frame (see Gehrels et al. 2004 for more information). We plot this quantity in the top panel of Figure 1. The minimum OTD in our sample is 43.88 s from GRB 140206A at redshift $z = 2.73$ (marked by a horizontal green dotted line in the plot). Table 1 presents the complete list of the 368 GRBs in our sample and their OTD in seconds.

It is then clear that Swift/XRT is generally unable to observe the X-ray emission in the first 43 s after the GRB trigger. This is because it takes at least between 10 and 20 s for the Swift satellite to automatically realize that a Swift/BAT trigger condition occurred, to compute the coordinates of the source, to check whether a slewing to those coordinates is possible, and to start slewing to put the source in the Swift/XRT field of view; the actual slewing time is between 20 and 75 s (for details see, e.g., Troja 2020, and Gehrels et al. 2004). Hence, X-ray events occurring within ≈40 s of the GRB trigger remain unobservable by Swift/XRT, making this time interval an X-ray-uncharted new territory. Our knowledge during this phase, which corresponds to the prompt emission of GRBs, is confined to fewer than 100 detections made by BeppoSAX and HETE-2 (see, e.g., Tamagawa et al. 2003; Costa & Frontera 2011; Frontera 2019).

Table 1
List of GRBs Observed by Swift/XRT and Their Observed Time Delay and Cosmological Rest-frame Time Delay in Seconds

No.	GRB	Redshift	OTD (s)	RTD (s)
1	231215A	2.305	2725.7	824.7
2	231210B	3.13	123.4	29.9
3	231118A	0.8304	413.8	226.1
4	231117A	0.257	101.8	81
5	231111A	1.28	99.6	43.7
6	230818A	2.42	141.1	41.3
7	230506C	3.7	4600	978.7
8	230414B	3.568	128.6	28.1
9	230328B	0.09	110.3	101.2
10	230325A	1.664	94.1	35.3

Note. The delay time is between the initial burst detection and the start time of the first XRT observation. The XRT start time data are sourced from https://swift.gsfc.nasa.gov/archive/grb_table/. The bold GRB names in this table indicate GRBs with an RTD of less than 43.9 s, namely shorter than the minimum OTD.

(This table is available in its entirety in machine-readable form.)

Interestingly, this large OTD can be circumvented by considering the cosmological corrections presented in this article and turning to the cosmological RTD in seconds. This procedure has been routinely applied in our approach (see, e.g., Ruffini et al. 2021, and references therein). Due to the cosmological time dilation, a time interval Δt measured on Earth corresponds to a time interval $\Delta t/(1+z)$ in the cosmological source rest frame, where z is its cosmological redshift. In other words, a phenomenon appearing to our instruments on Earth to last 50 s may last 10 s if the source is at $z = 4$, like if we were observing the phenomenon in slow motion.

Therefore, the OTD needed by Swift/XRT to start its observations after the GRB trigger may correspond to a much shorter actual RTD for sources with a large redshift z, exactly by a factor $(1 + z)$. If, e.g., XRT starts to observe a GRB 60 s after the trigger in the observer frame, it is observing the X-ray signals emitted $60/(1 + z)$ s after the trigger in the rest frame of the source. This corresponds to the possibility of observing 10 s after the trigger for a GRB with $z = 5$: the higher the GRB redshift, the shorter the time Swift/XRT can observe the source after the GRB trigger.

This is clearly shown in the bottom panel of Figure 1, where we present the time delays of the top panel converted in the cosmological rest frame of each source; see also Table 1, where we compare and contrast OTD and RTD. The green dotted line still marks the 43.88 s minimum OTD, and the red dashed line corresponds to this minimum OTD rescaled as a function of the redshift of the source: $43.88/(1 + z)$ s. Many sources, which were observed by Swift/XRT with an OTD greater than 43.88 s, would not have been deemed interesting from the early X-ray emission point of view. However, thanks to their large cosmological redshift, when looking at their RTD, it is clear that they have been observed 10 s after the trigger, allowing us to observe the new physical process in Episode II related to the

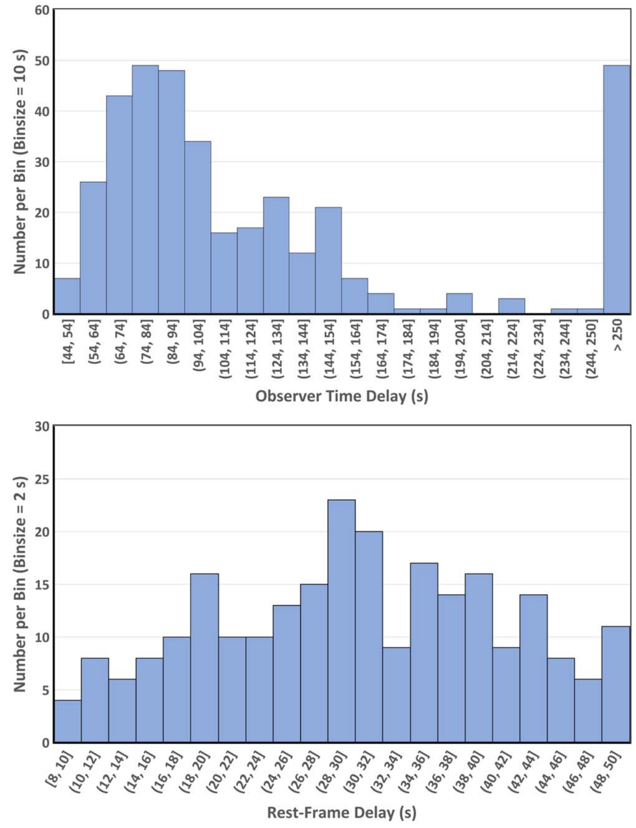

Figure 2. The histogram of Swift-XRT time delays in the observer's frame (OTD; top panel) and the cosmological rest frame (RTD; bottom panel).

νNS rise of GRBs (see the Appendix for a summary of the BdHN model and the emission episodes).

This can also be seen in Figure 2, where we plot the histogram of the OTD (top panel) and of the RTD (bottom panel): the OTD for most GRBs lies between 50 and 170 s and peaks at $\sim$80 s, while the recorded minimum RTD in the sample of 368 GRBs is $\sim$8 s from GRB 090423 at redshift $z = 8.2$, and the RTD range for most of the GRBs is between 8 and 50 s, with a peak at $\sim$30 s.

Therefore, observing GRBs at large z represents an invaluable tool for exploring the early transient X-ray regimes that occur just after the GRB trigger time and poses a stringent test for all GRB theoretical models. This is particularly relevant in the case of the BdHN model (see the Appendix) since, analyzing the transient X-ray regimes occurring just after the SN rise described in Episode I and the GRB trigger, it is possible to unveil the physical processes taking place during the νNS rise (Episode II).

4. The Prototypical Cases of GRB 220101A, GRB 090423, and GRB 090429B

We now turn to the X-ray emission of three high-z BdHNe I, our prototypical cases: GRB 220101A, GRB 090423, and GRB 090429B. The photon index during the early afterglow of a GRB exhibits significant variations, especially in the steep decay or X-ray flare periods, where the photon index can deviate from the average value of $\sim$2 in the afterglow, evolving between approximately 1 and 4. When calculating the GRB luminosity based on the observed flux, we need to consider the k-correction, a function of the photon index. Therefore, we must consider time-resolved k-correction when dealing with early afterglow data. For some bursts, the shape of the luminosity light curve of the early afterglow generated by time-resolved k-correction differs from that generated by time-integrated k-correction (see details in Ruffini et al. 2018c; Wang et al. 2023).

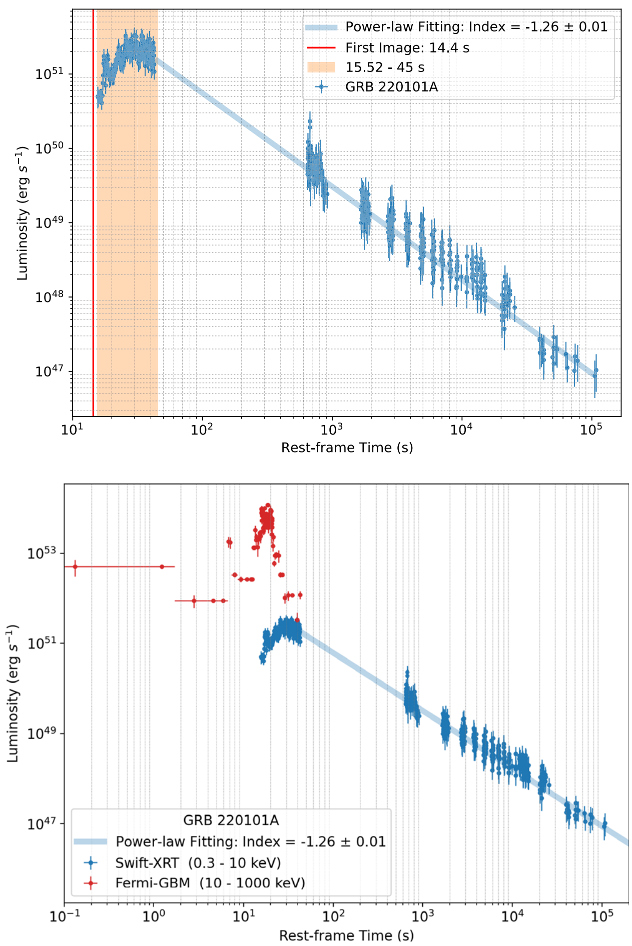

Figure 3. Top panel: the Swift-XRT 0.3–10 keV luminosity of GRB 220101A in the cosmological rest frame. The red line at 14.4 s corresponds to the first observation by XRT while still in Image mode before switching to Windowed Timing (WT) mode (for details, see, e.g., Troja 2020, as well as Gehrels et al. 2004). The orange strip, which extends from 15.52 to 45 s, indicates the data observable thanks to the cosmological effect at $z = 4.61$ duly considered in this article. Other data points between 13.3 and 14.4 s correspond to observations performed while Swift was still slewing to the source location and have not been considered in this paper. The blue line is a power-law fitting function of the form $A_X t^{\alpha}$, whose best-fit parameters are $A_X = (1.80 \pm 0.11) \times 10^{53}$ erg s^{-1} and $\alpha = -1.26 \pm 0.01$. Bottom panel: the same Swift-XRT light curve of the top panel together with the Fermi-GBM 10–10^3 keV light curve indicating CO core and the SN rise (Episode I). This process occurs from -0.18 up to 3.57 s and lasts for 3.57 s, all in the rest frame. The total energy emitted in this event is 1.2×10^{53} erg. The corresponding data for seven additional SN rise events are now available (R. Ruffini et al. 2024, in preparation).

From the above analysis, we conclude the following for the prototypical cases:

1. GRB 220101A has a redshift $z = 4.61$, and the OTD is 80.78 s, corresponding to an RTD of 14.40 s. Swift/XRT 0.3–10 keV luminosity is shown in Figure 3. The orange strip marks the data before $\sim$45 s, which are observable only thanks to the methodology presented in this article

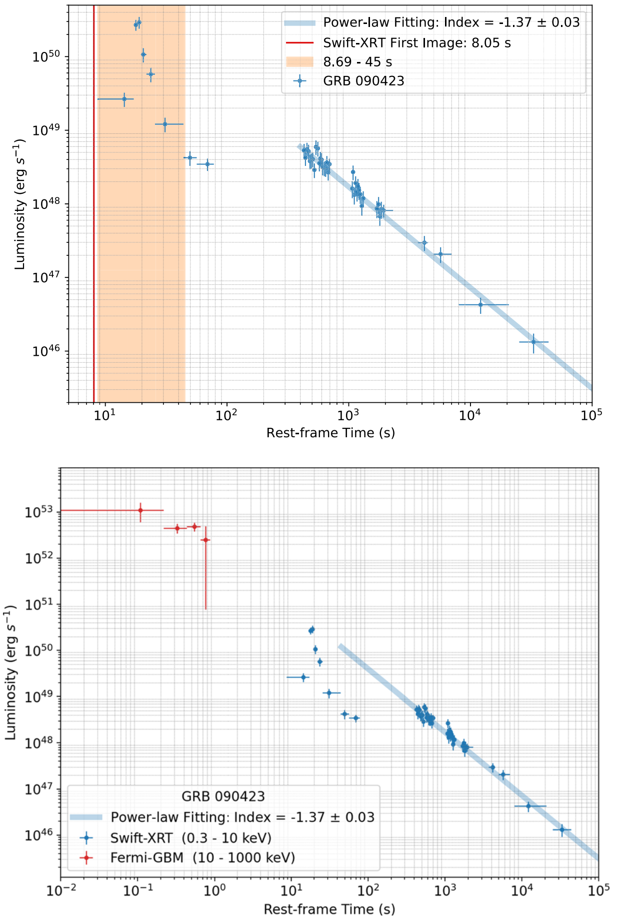

Figure 4. Top panel: the Swift-XRT 0.3–10 keV luminosity of GRB 090423 in the cosmological rest frame. As in Figure 3, the red line corresponds to the first observation by XRT while still in Image mode before switching to Windowed Timing (WT) mode. The orange strip, which extends from 8.69 to 45 s, indicates the data observable owing to the cosmological effect at $z = 8.2$. The blue line is a power-law fitting function of the form $A_X t^{\alpha}$, whose best-fit parameters are $A_X = (2.18 \pm 0.49) \times 10^{52}$ erg s^{-1} and $\alpha = -1.37 \pm 0.03$. Bottom panel: the same Swift-XRT light curve of the top panel and the Fermi-GBM 10–10^3 keV light curve indicating CO core and the SN rise (Episode I). This process occurs from −0.6 to 0.8 s with a duration of 1.4 s, all in the rest frame. The total energy emitted in this event is 1.6×10^{53} erg.

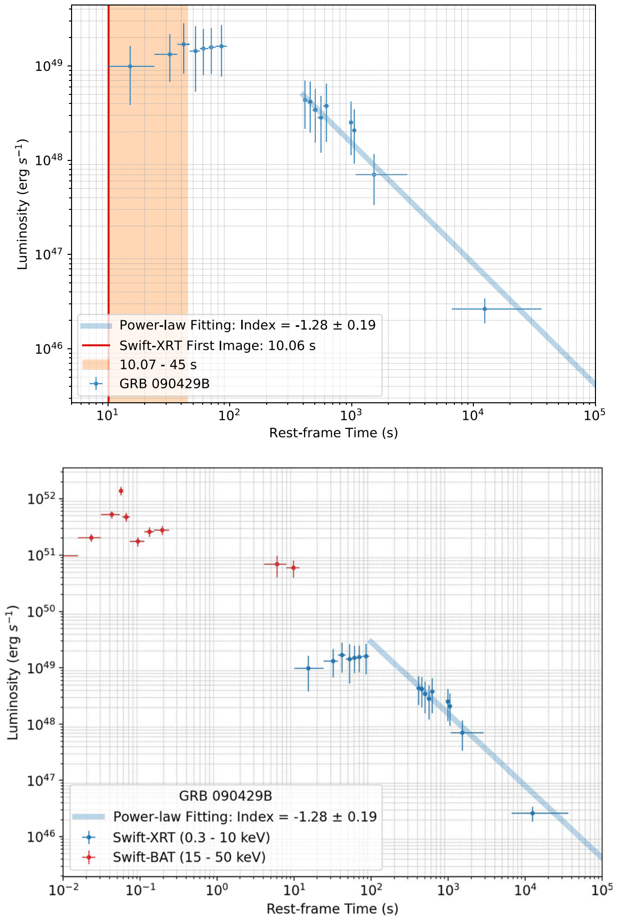

Figure 5. Top panel: the Swift-XRT 0.3–10 keV luminosity of GRB 090429B in the cosmological rest frame. The red line corresponds to the first observation by XRT while still in Image mode before switching to Windowed Timing (WT) mode. The orange strip, which extends from 10.07 to 45 s, indicates the data observable owing to the cosmological effect at $z = 9.4$. The blue line is a power-law fitting function of the form $A_X t^{\alpha}$, whose best-fit parameters are $A_X = (1.05 \pm 0.13) \times 10^{52}$ erg s^{-1} and $\alpha = -1.28 \pm 0.19$. Bottom panel: the same Swift-XRT light curve of the top panel and the Swift-BAT 15–50 keV light curve indicating the CO core and the SN rise (Episode I). This process occurs between 0 and 0.96 s with a duration of 0.96 s in the rest frame. The total energy emitted in this event is 3.5×10^{52} erg.

for high source redshift. The best-fit parameters of the decaying part are $A_X = (1.80 \pm 0.11) \times 10^{53}$ erg s^{-1} and $\alpha = -1.26 \pm 0.01$ representing the X-ray afterglow.

2. GRB 090423 has a redshift $z \sim 8.2$, and the OTD is 72.48 s, corresponding to an RTD of ∼8 s. Swift-XRT 0.3–10 keV luminosity is shown in Figure 4. As in Figure 3, the orange strip marks the data from 8.1 up to ∼45 s. The best-fit parameters of the decaying part are $A_X = (2.18 \pm 0.49) \times 10^{52}$ erg s^{-1} and $\alpha = -1.37 \pm 0.03$ representing the X-ray afterglow.
3. GRB 090429B has a photometric redshift $z \sim 9.4$. The OTD is 104.69 s, corresponding to an RTD of ∼10.1 s. Swift-XRT 0.3–10 keV luminosity is shown in Figure 5. The orange strip marks the data from 10.1 to ∼45 s. The best-fit parameters of the decaying part are $A_X = (1.05 \pm 0.13) \times 10^{52}$ erg s^{-1} and $\alpha = -1.28 \pm 0.19$ representing the X-ray afterglow.

Therefore, the above analysis of the X-ray emission observed by Swift/XRT is a powerful tool to validate the observation of the episodes expected in the BdHN scenario (see the Appendix). For the three prototypes analyzed above, the XRT data show, at the end of the SN rise (Episode I), the presence of Episode II marked by the spin-up phase of the νNS by SN ejecta fallback accretion (Rueda et al. 2022c), followed by its slowing down characterizing the X-ray afterglow (Rueda et al. 2022a, 2022c; Becerra et al. 2022; Wang et al. 2023). These results confirm the sources' BdHN I nature and the formation of stellar-mass BHs up to large cosmological redshifts, $z \sim 10$.

This analysis will be completed by information on emission in all the wavelengths in the GeV and MeV for redshifts smaller than 5, e.g., GRB 220101A (R. Ruffini et al. 2024, in preparation); see Figure 3.

5. Inference for the Cosmological Distribution of the Black Holes

The analysis of GRB 220101A, GRB 090423, and GRB 090429B heralds an important astrophysical message.

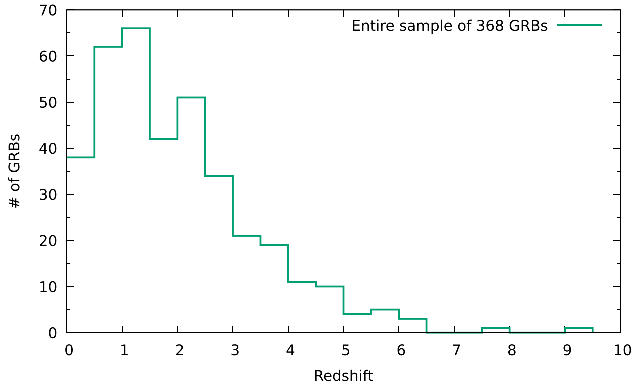

Figure 6. The distribution of the redshifts of the 368 GRBs in our sample (see Table 1).

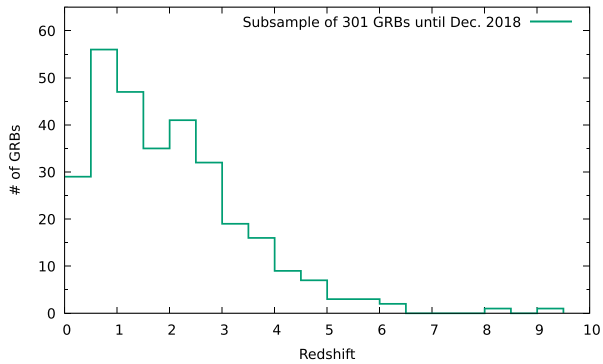

Figure 7. The distribution of the redshifts of the 301 GRBs in the subsample until 2018 December.

We have shown that stellar-mass BHs from BdHNe I occur at a very high redshift, $z \sim 10$, originating from massive binary stars, possibly $\lesssim 25\ M_{\odot}$ each, only a few hundred million years from the Big Bang. This conclusion may suggest revisiting the cosmological and stellar evolution paradigm. Indeed, our results agree with the conclusion by Madau & Dickinson (2014): "it seems premature to tinker further with the (stellar initial mass function) IMF, although if discrepancies remain after further improvements in the measurements and modeling then this topic may be worth revisiting."

The above evidence of stellar-mass BHs formed in GRBs up to redshift $z \sim 10$ complements the daily information being gained by the observations of the James Webb Space Telescope of quasars at high redshift, e.g., at $z \sim 6$–7 (Yang et al. 2021; Yue et al. 2023), and the farthest quasars ever observed at the center of the galaxy UHZ1 at $z \approx 10.3$ (Bogdán et al. 2024) and of GN-z11 at $z \approx 10.6$ (Maiolino et al. 2024). These observations are unveiling a larger population of supermassive BHs at very high redshift than previously thought (see Gilli et al. 2022; Kocevski et al. 2023; Maiolino et al. 2023; Fan et al. 2023, for a recent review), suggesting a possible role of dark matter in their formation (Argüelles et al. 2023, 2024). Therefore, from all the above, it appears that the presence of BHs in the Universe is ubiquitous. Indeed, these two topics are not independent. A new research window has been opened to test whether supermassive BHs at large redshifts may boost the star formation in the early Universe (Mirabel & Rodríguez 2022).

6. The BdHN Model and the Double-peak GRB Redshift Distribution

We turn now to additional information that can be gained from the distribution of GRBs across the Universe. In Figure 6, we present the distribution of the redshifts of the 368 GRBs in our sample (see Table 1). We can see the first peak between $z = 1$ and $z = 1.5$ and the second peak between $z = 2$ and $z = 2.5$. This same double-peak structure in the GRB redshift distribution was also present in the GRB sample considered by Wanderman & Piran (2010) and in the one considered by Lien et al. (2016).

Having determined the redshift distribution of our sample of 368 GRBs detected by Swift since the year 2005 up to the end of the year 2023, including both long and short GRBs, we would like to address the double-peak structure found in Figure 6. We are going to use all available data on different BdHN families.

As indicated in the Appendix (see Table 2 there), the BdHN model identifies several different GRB families (Aimuratov et al. 2023, and references therein), and it is of interest to inquire about the possible difference in the redshift distribution of each family.

A preliminary result was obtained by Ruffini et al. (2021), where a catalog of all BdHNe I observed from the early 1990s until 2018 December is presented. Therefore, we limit our current analysis of the redshift distribution of our sample of 368 GRBs to a subsample of 301 GRBs exploded until 2018 December (see below and Figure 7). What is very interesting is that also, in this distribution, the double-peak structure is maintained. We can then compare and contrast this redshift distribution of Figure 7 with the BdHN I sample published in Ruffini et al. (2021).

1. We build a subsample of our sample of 368 GRBs by selecting all GRBs detected until 2018 December. There are 304 GRBs in this subsample.
2. We look for each of these 304 GRBs in the BdHNe I catalog published by Ruffini et al. (2021). We find 216 of them. We therefore conclude that in our subsample of 304 GRBs exploded until 2018 December there are 216 BdHNe I.
3. We have 88 GRBs in our subsample that still need to be classified.
4. We look to the observed prompt emission duration of all 88 GRBs still needing a classification.
5. We see that 21 GRBs have an observed prompt emission duration $T_{90} < 2$ s and can therefore be classified as short GRBs. They are too few to be further subdivided to build statistically significant redshift distributions of the different families of short GRBs implied by the BdHN model. Therefore, our current analysis considers the cumulative redshift distribution of all 21 of these short GRBs as a single family.
6. We are left with 67 GRBs in our subsample that still need a classification.
7. We find that 64 GRBs have an observed prompt emission duration $T_{90} > 2$ s. Therefore, they are neither short GRBs nor BdHNe I (since they are not in the catalog by Ruffini et al. 2021, albeit exploded before 2018 December). They must be either BdHNe II or BdHNe III. A further subdivision of these 64 GRBs into BdHNe II and BdHNe III requires an extra analysis outside the present paper's scope. Then, in our current analysis, we are considering the cumulative redshift distribution of all

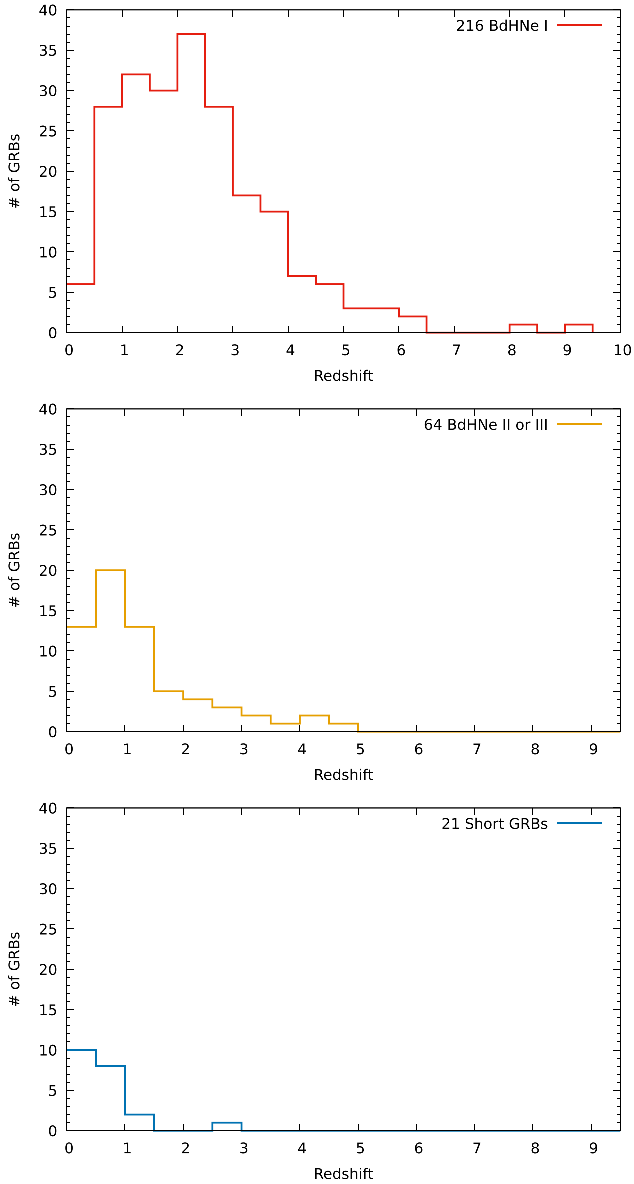

Figure 8. The distributions of the redshifts of the 301 GRBs in our subsample, divided into three groups: BdHNe I (top panel, red line), BdHNe II/III (middle panel, orange line), and short GRBs (bottom panel, blue line).

64 of these BdHNe II or BdHNe III as if they were a single family.

8. We still have three GRBs in our sample with no observed T_{90} duration in the Swift catalog, which we therefore exclude from our current analysis. Our final subsample of GRBs exploded until 2018 December and contains 301 GRBs.

In summary, starting from our sample of 368 GRBs, we built a subsample of 301 GRBs detected until 2018 December. The redshift distribution of the GRBs in this subsample is plotted in Figure 7 to be compared and contrasted with the one of the entire sample of 368 GRBs (Figure 6). We can see that both distributions present the same double-peaked structure at $z \lesssim 2$. Therefore, the results we will obtain by analyzing the distribution of the subsample can be considered valid for the entire sample of 368 GRBs as well.

Following the procedure described above, we have that the subsample of 301 GRBs exploded until 2018 December can be subdivided among the different GRB families indicated by the BdHN model as follows:

1. 216 GRBs are BdHNe I;
2. 64 GRBs are BdHNe II or BdHNe III;
3. 21 GRBs are short GRBs.

Figure 8 shows the distributions of the redshifts of each of these three GRB groups in the subsample. We can see that the redshift distribution of BdHNe I presents a single peak between $z \sim 2$ and $z \sim 2.5$ and a sort of plateau for $0.5 \lesssim z \lesssim 2$, while the distribution of BdHNe II and BdHNe III presents a single peak around $z \sim 1$ and that of short GRBs presents a single peak for $z < 0.5$. The K-S test applied to the distributions shown in Figure 8, BdHNe I (top panel) versus short GRBs (bottom panel), yields a probability $P = 4.5 \times 10^{-10}$, suggesting that there is sufficient statistical evidence to conclude that the redshift distributions of BdHNe I and short GRBs are not identical. The same conclusion can be reached after comparing BdHNe I (top panel) versus BdHNe II and BdHNe III (middle panel), which yields a $P = 5.0 \times 10^{-9}$. On the other hand, the K-S test applied to the redshift distributions of BdHNe II and BdHNe III (middle panel) versus short GRBs (bottom panel) yields a much larger value, $P = 0.011$, indicating that the two distributions do not differ significantly. This similarity in the redshift distributions supports the idea, advanced in Ruffini et al. (2016, 2018b), that BdHNe II and BdHNe III may end up in remnant binary systems that, in turn, at the end of their evolution, can later become progenitors of short GRBs. We can also see that BdHNe I extend to much higher redshifts than BdHNe II, BdHNe III, and short GRBs, but this may be due to a selection effect (BdHNe I, being the most energetic and most luminous of the long GRBs, are easier to detect, even at very high redshift).

We can then conclude that the double-peak structure in the redshift distribution of our sample of 368 GRBs can be explained by the superposition of the redshift distributions of the different BdHN families.

7. Conclusion

We can summarize three main conclusions:

1. In this article, we have introduced the use of the time dilation in high-redshift GRBs to overcome the observed instrumental time delay, greater than 43 s, between the GRB trigger time and the first X-ray observations by Swift/XRT. This time delay has traditionally hampered the observations of Episode I and Episode II in BdHNe (see, e.g., Aimuratov et al. 2023). The methodology has been developed using a sample of 368 GRBs, reported in Table 1, all with an identified redshift. When measured in the observer frame, the time delay (OTD) between the earliest X-ray emission and the GRB trigger time is always larger than 40 s (see the top panels of Figures 1 and 2). In contrast, a substantially shorter time delay is observed in the rest frame of the source (RTD; see the bottom panels of Figures 1 and 2). This new methodology allows the analysis of the very early transient X-ray regimes in GRB afterglows, which pose a stringent test for all GRB theoretical models. Within the context of the BdHN model, we applied it to three BdHNe I at high redshift. This has

allowed us to unveil the occurrence of the spinning-up νNS emission, increasing with time. This emission precedes the traditional X-ray afterglow emission, which decreases in time with a specific power-law index.

2. The most eloquent example is the case of one of the most powerful GRBs ever detected, GRB 220101A, at $z = 4.61$ (R. Ruffini et al. 2024, in preparation). Given the source's high redshift and outstanding luminosity, this source allows the identification of all seven episodes of a BdHN, except for the late radioactive decay of the SN ashes. In particular, GRB 220101A shows the SN rise (Episode I) triggering the entire GRB; see Figure 3 (R. Ruffini et al., 2024, in preparation). Especially significant are the unexpected high-quality data associated with the Swift/XRT observations of the νNS rise (Episode II). The X-ray emission observed by Swift/XRT starts 14.4 s after the trigger, following the end of the SN rise and indicating the spin-up phase of the νNS by the fallback accretion of matter initially ejected by the SN. It is followed by the slowing-down phase starting at 45 s corresponding to the decaying part of the X-ray afterglow (Rueda et al. 2022a, 2022c; Becerra et al. 2022; Wang et al. 2023). The unexpected very high quality data associated with the Swift/XRT observations of the νNS rise (Episode II) also apply to GRB 090423 at $z = 8.2$ (see Figure 4) and GRB 090429B at $z = 9.4$ (see Figure 5): in both cases the first Swift/XRT data show the νNS spin-up phase, extending up to 10^2 s and followed by the slowing-down phase corresponding to the decaying part of the X-ray afterglow. One of the key questions to be addressed is the possibility that, at the end of the spin-up phase, a short time ($\lesssim$1 s) process of gravitational-wave emission occurs as a result of a transition to a triaxial configuration of the fast-spinning νNS, with characteristic strain $h_c \sim 10^{-23}$ at about kHz frequency (see Rueda et al. 2022c, for details).
3. Equally important is the by-product of analyzing the redshift distributions of all 368 GRBs of the sample (see Figure 6), of all 301 GRBs until 2018 December (see Figure 7), and in particular of the 216 BdHNe I, the 64 BdHNe II and BdHNe III, and the 21 short GRBs until 2018 December (see Figure 8). The distribution of the entire sample of 368 sources presents two peaks: the first, dominated by the BdHNe II and BdHNe III, at $z \sim 1$ and the second, dominated by BdHNe I, at $z \sim 2$. Such a two-peak structure of the GRB density rate, which seems not to trace the star formation rate (see, e.g., Madau & Dickinson 2014), is indeed present in the distributions by Wanderman & Piran (2010) and Lien et al. (2016). We have shown here that the different physical properties between BdHNe I, BdHNe II, and BdHNe III explain these two peak distributions. An additional conclusion can be drawn based on the GRB distributions. The similarity between the redshift distribution of BdHNe II and BdHNe III and that of short GRBs supports the hypothesis, advanced in Ruffini et al. (2016, 2018b), that the BdHNe II and BdHNe III remnants, after evolving into binary NS systems, could later become progenitors of short GRBs. This unique prediction of the BdHN scenario deserves further attention from an observational and a theoretical point of view, e.g., recent simulations show that BdHNe lead to bound NS–NS binaries with a wide range of merger times (Becerra et al. 2024).

Indeed, a great opportunity exists for new missions with wide-field-of-view soft X-ray instruments designed to simultaneously observe the GRB X-ray and gamma-ray emissions from 0.3 keV to 10 MeV from the moment of the GRB trigger without any time delay, such as, e.g., THESEUS (Amati et al. 2018, 2021) and HERMES (Fuschino et al. 2019; Fiore et al. 2020).

Acknowledgments

We express our gratitude to an anonymous referee whose suggestions greatly improved the presentation of our results. We are grateful to B. Cenko and J. Kennea for their important clarifications on the timing of the Swift automatic slew system. We also thank Y. Aimuratov, L. Amati, L. M. Becerra, C. Cherubini, M. Karlica, P. Madau, and N. Sahakyan for the fruitful discussions leading to these new results.

Appendix
The Binary-driven Hypernova Model

Within the BdHN model, long GRBs of different energies have a common progenitor: a binary comprising a CO star and an NS companion (Rueda & Ruffini 2012). The CO star is at the end of its thermonuclear evolution. The collapse of the CO star iron core forms a newborn NS (νNS) at the center and produces an SN explosion. The latter triggers various physical phenomena whose occurrence and/or entity depends mostly on the system's orbital period (Fryer et al. 2014, 2015). Numerical, three-dimensional, smoothed particle hydrodynamics simulations of the BdHN scenario (Becerra et al. 2016, 2019, 2022) have led to the definition of three different types of BdHNe, corresponding to the diversity of long GRBs:

1. BdHNe I are the most extreme with energies 10^{52}–10^{54} erg. Their orbital periods are about 5 minutes. In these sources, the material ejected in the SN is easily accreted by the NS companion, so it reaches the point of gravitational collapse, forming a rotating BH. BdHN I examples are GRB 130427A (Ruffini et al. 2019b), GRB 180720B (Rueda et al. 2022a), and GRB 190114C (Moradi et al. 2021a, 2021b).
2. BdHNe II have orbital periods of 20–40 minutes and emit energies 10^{50}–10^{52} erg. The accretion is lower, so the NS remains stable. A BdHN II example is GRB 190829A (Wang et al. 2022).
3. BdHNe III have orbital periods of hours, and the accretion is negligible. They explain GRBs with energies lower than 10^{50} erg. A BdHN III example is GRB 171205A (Wang et al. 2023).

Seven observable episodes characterize the most general BdHN sequence of physical processes. They have spectral signatures in the GRB precursor, MeV prompt, GeV and TeV emissions, X-ray/optical/radio afterglow, and optical SN emission. They involve the physics of the early SN, NS accretion, BH formation, synchro-curvature radiation, and quantum and classic electrodynamics processes to extract the BH rotational energy. Episode I, the SN rise, describes the CO core collapse, generating the νNS and the SN. This episode has been possibly identified in three BdHNe, GRB 090423, GRB 090429B, and GRB 220101A (see Section 4). Episode II, the νNS and NS rise, is due to the SN ejecta accretion onto the νNS, the NS companion, and their consequent spin-up process (Rueda et al. 2022c; Becerra et al. 2022; Wang et al. 2023).

Table 2
Upper: Physical Phenomena Occurring in BdHN I, II, and III, and Their Associated Observations in the GRB Data. Lower: Examples of the GRB Episodes Identified in Some BdHNe I, II, and III

Physical Phenomenon	BdHN Type	GRB Episodes											
		I	II		III	IV	V			VI			VII
		(SN rise)	(νNS rise and NS rise)		(BH rise overcritical)	(BH rise undercritical)	(BH echoes)			(Afterglows)			(SN Ic and HN)
		SN rise	νNS rise	NS rise	UPE	Jetted emission	Cavity	HXF	SXF	X-ray	Opt.	Rad.	Opt. SN and HN
		(X–γ)	(X–γ)	(X–γ)	(X–γ)	(GeV)	(X–γ)	(X–γ)	(X)				
CO core collapse (a)	I,II,III	⊗											
νNS accretion (b)	I,II,III		⊗										
NS accretion (b)	I,II			⊗									
BH QED (d): e^+e^- accel. and transp. (low baryon load)	I				⊗								
BH CED (e): e^- accel. and radiation	I					⊗							
BH QED (f): e^+e^- accel. and transp. (high baryon load)	I						⊗	⊗	⊗				
νNS synchr. and pulsar emission (g)	I,II,III									⊗	⊗	⊗	
Nickel decay and ejecta kinetic energy (h)	I,II,III												⊗
Source	BdHN type	GRB Episodes											
GRB 180720B	I		⊗	⊗	⊗	⊗	⊗	⊗	⊗	⊗	⊗	⊗	⊗
GRB 190114C	I		⊗		⊗	⊗	⊗	⊗	⊗	⊗	⊗	⊗	⊗
GRB 190829A	II		⊗	⊗						⊗	⊗	⊗	⊗
GRB 171205A	III		⊗							⊗	⊗	⊗	⊗

Note. UPE stands for ultrarelativistic prompt emission, SXFs for soft X-ray flares, HXFs for hard X-ray flares, CED for classical electrodynamics, QED for quantum electrodynamics, SN for supernova, and HN for hypernova. We refer to Aimuratov et al. (2023) and references therein for further quantitative details on each episode of these sources.

References. (a) Wang et al. 2019; Rueda et al. 2022c; Wang et al. 2022; (b) Fryer et al. 2014; Becerra et al. 2016; Rueda et al. 2022c; Becerra et al. 2022; Wang et al. 2022; (c) Ruffini et al. 2019b; Moradi et al. 2021a; Moradi et al. 2021b; (d) Bianco et al. 2001; Moradi et al. 2021b; Rastegarnia et al. 2022; (e) Ruffini et al. 2019b; Rueda & Ruffini 2020; Moradi et al. 2021a; Rueda et al. 2022b; (f) Ruffini et al. 2018c; (g) Ruffini et al. 2018a; Wang et al. 2019; Rueda et al. 2020; (h) Cano et al. 2017; Aimuratov et al. 2023.

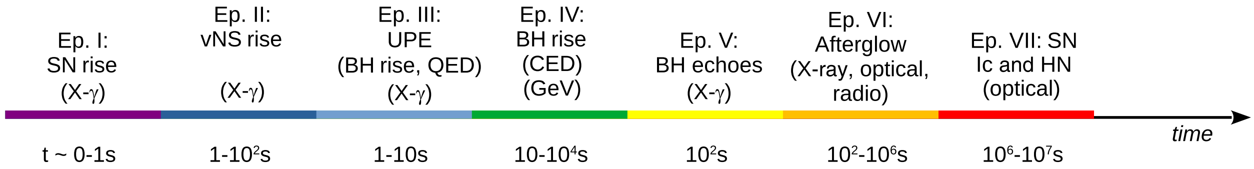

Figure 9. Time sequence of the episodes in BdHNe I, according to Table 2. The times are orders-of-magnitude estimates based on the specific examples of BdHNe I, GRB 180720B (Rueda et al. 2022a; Rastegarnia et al. 2022), and GRB 190114C (Rueda et al. 2020; Moradi et al. 2021a, 2021b), summarized in Aimuratov et al. (2023). Some episodes of BdHNe II and III in Table 2 have also been identified, e.g., in GRB 190829A (Wang et al. 2022) and GRB 171205A (Wang et al. 2023), as summarized in Aimuratov et al. (2023). The acronyms are the same as in Table 2.

Episode III, the ultrarelativistic prompt emission phase, is explained by the radiation by an e^+e^- expanding self-accelerated pair plasma loaded with baryons (Moradi et al. 2021b; Rastegarnia et al. 2022; Li et al. 2023). The pairs are produced by the quantum electrodynamics process of vacuum breakdown by an overcritical electric field. The latter is induced by the interaction of the BH spin with the external magnetic field (inherited by the collapsed NS). Episode IV, the GeV emission, is due to the radiation of electrons accelerated by the induced electric field near the BH (Ruffini et al. 2019b; Rueda & Ruffini 2020; Moradi et al. 2021a; Rueda et al. 2022b). Episode V, called BH echoes, encompasses the emission from the interaction of the expanding e^+e^- pairs with the ultra–low-density region (referred to as the cavity) around the BH (Ruffini et al. 2019a) and along other directions of higher density leading to soft and hard X-ray flares (SXFs and HXFs; Ruffini et al. 2018c). Episode VI, the X-ray, optical, and radio afterglow emission, is due to synchrotron radiation in the expanding ejecta and the νNS pulsar emission (Ruffini et al. 2018a; Wang et al. 2019; Rueda et al. 2020, 2022a). Finally, Episode VII is the optical emission by the SN ejecta, powered by the decay of nickel into cobalt (see Aimuratov et al. 2023, for a recent analysis of the SN associated with long GRBs). Table 2 and Figure 9 summarize the physical processes and associated GRB episodes of each BdHN type, including specific examples; see also Aimuratov et al. (2023) for further details on the BdHN emission episodes.

ORCID iDs

C. L. Bianco https://orcid.org/0000-0001-7749-4078
M. T. Mirtorabi https://orcid.org/0000-0001-9277-3366
R. Moradi https://orcid.org/0000-0002-2516-5894
J. A. Rueda https://orcid.org/0000-0003-4904-0014
R. Ruffini https://orcid.org/0000-0003-0829-8318
Y. Wang (王瑜) https://orcid.org/0000-0001-7959-3387
M. Della Valle https://orcid.org/0000-0003-3142-5020
Liang Li (李亮) https://orcid.org/0000-0002-1343-3089

References

Aimuratov, Y., Becerra, L. M., Bianco, C. L., et al. 2023, ApJ, 955, 93
Alexeyev, E. N., Alexeyeva, L. N., Krivosheina, I. V., & Volchenko, V. I. 1988, PhLB, 205, 209
Amati, L., O'Brien, P., Götz, D., et al. 2018, AdSpR, 62, 191
Amati, L., O'Brien, P. T., Götz, D., et al. 2021, ExA, 52, 183
Argüelles, C. R., Boshkayev, K., Krut, A., et al. 2023, MNRAS, 523, 2209
Argüelles, C. R., Rueda, J. A., & Ruffini, R. 2024, ApJL, 961, L10
Arnett, W. D., Bahcall, J. N., Kirshner, R. P., & Woosley, S. E. 1989, ARA&A, 27, 629
Becerra, L., Bianco, C. L., Fryer, C. L., Rueda, J. A., & Ruffini, R. 2016, ApJ, 833, 107
Becerra, L., Ellinger, C. L., Fryer, C. L., Rueda, J. A., & Ruffini, R. 2019, ApJ, 871, 14
Becerra, L. M., Fryer, C. L., Rueda, J. A., & Ruffini, R. 2024, arXiv:2401.15702
Becerra, L. M., Moradi, R., Rueda, J. A., Ruffini, R., & Wang, Y. 2022, PhRvD, 106, 083002
Bianco, C. L., Ruffini, R., & Xue, S.-S. 2001, A&A, 368, 377
Bionta, R. M., Blewitt, G., Bratton, C. B., et al. 1987, PhRvL, 58, 1494
Bogdán, Á., Goulding, A. D., Natarajan, P., et al. 2024, NatAs, 8, 126
Cano, Z., Wang, S.-Q., Dai, Z.-G., & Wu, X.-F. 2017, AdAst, 2017, 8929054
Costa, E., & Frontera, F. 2011, NCimR, 34, 585
Cucchiara, A., Levan, A. J., Fox, D. B., et al. 2011, ApJ, 736, 7
Fan, X., Bañados, E., & Simcoe, R. A. 2023, ARA&A, 61, 373
Fiore, F., Burderi, L., Lavagna, M., et al. 2020, Proc. SPIE, 11444, 114441R
Frontera, F. 2019, RLSFN, 30, 171
Fryer, C. L., Oliveira, F. G., Rueda, J. A., & Ruffini, R. 2015, PhRvL, 115, 231102
Fryer, C. L., Rueda, J. A., & Ruffini, R. 2014, ApJL, 793, L36
Fu, S. Y., Zhu, Z. P., Xu, D., Liu, X., & Jiang, S. Q. 2022, GCN Circ., 31353, 1
Fuschino, F., Campana, R., Labanti, C., et al. 2019, NIMPA, 936, 199
Fynbo, J. P. U., de Ugarte Postigo, A., Xu, D., et al. 2022, GCN Circ., 31359, 1
Galama, T. J., Vreeswijk, P. M., van Paradijs, J., et al. 1998, Natur, 395, 670
Gehrels, N., Chincarini, G., Giommi, P., et al. 2004, ApJ, 611, 1005
Gilli, R., Norman, C., Calura, F., et al. 2022, A&A, 666, A17
Hirata, K., Kajita, T., Koshiba, M., et al. 1987, PhRvL, 58, 1490
Kocevski, D. D., Onoue, M., Inayoshi, K., et al. 2023, ApJL, 954, L4
Li, L., Rueda, J. A., Moradi, R., et al. 2023, ApJ, 945, 10
Lien, A., Sakamoto, T., Barthelmy, S. D., et al. 2016, ApJ, 829, 7
Madau, P., & Dickinson, M. 2014, ARA&A, 52, 415
Maiolino, R., Scholtz, J., Curtis-Lake, E., et al. 2023, arXiv:2308.01230
Maiolino, R., Scholtz, J., Witstok, J., et al. 2024, Natur, 627, 59
Mirabel, I. F., & Rodríguez, L. F. 2022, NewAR, 94, 101642
Moradi, R., Rueda, J. A., Ruffini, R., & Wang, Y. 2021a, A&A, 649, A75
Moradi, R., Rueda, J. A., Ruffini, R., et al. 2021b, PhRvD, 104, 063043
Patat, F., Cappellaro, E., Danziger, J., et al. 2001, ApJ, 555, 900
Perley, D. A. 2022, GCN Circ., 31357, 1
Rastegarnia, F., Moradi, R., Rueda, J. A., et al. 2022, EPJC, 82, 778
Rueda, J. A., Li, L., Moradi, R., et al. 2022a, ApJ, 939, 62
Rueda, J. A., & Ruffini, R. 2012, ApJL, 758, L7
Rueda, J. A., & Ruffini, R. 2020, EPJC, 80, 300
Rueda, J. A., Ruffini, R., Karlica, M., Moradi, R., & Wang, Y. 2020, ApJ, 893, 148
Rueda, J. A., Ruffini, R., & Kerr, R. P. 2022b, ApJ, 929, 56
Rueda, J. A., Ruffini, R., Li, L., et al. 2022c, PhRvD, 106, 083004
Ruffini, R., Izzo, L., Muccino, M., et al. 2014, A&A, 569, A39
Ruffini, R., Karlica, M., Sahakyan, N., et al. 2018a, ApJ, 869, 101
Ruffini, R., Melon Fuksman, J. D., & Vereshchagin, G. V. 2019a, ApJ, 883, 191
Ruffini, R., Moradi, R., Rueda, J. A., et al. 2019b, ApJ, 886, 82
Ruffini, R., Moradi, R., Rueda, J. A., et al. 2021, MNRAS, 504, 5301
Ruffini, R., Rodriguez, J., Muccino, M., et al. 2018b, ApJ, 859, 30
Ruffini, R., Rueda, J. A., Muccino, M., et al. 2016, ApJ, 832, 136
Ruffini, R., Wang, Y., Aimuratov, Y., et al. 2018c, ApJ, 852, 53
Salvaterra, R., Della Valle, M., Campana, S., et al. 2009, Natur, 461, 1258
Tamagawa, T., Kawai, N., Yoshida, A., et al. 2003, ICRC (Tsukuba), 2741
Tanvir, N. R., Fox, D. B., Levan, A. J., et al. 2009, Natur, 461, 1254
Troja, E. 2020, The Neil Gehrels Swift Observatory Technical Handbook, v17.0, Swift Science Center, https://swift.gsfc.nasa.gov/proposals/tech_appd/swiftta_v17.pdf
Wanderman, D., & Piran, T. 2010, MNRAS, 406, 1944
Wang, Y., Becerra, L. M., Fryer, C. L., Rueda, J. A., & Ruffini, R. 2023, ApJ, 945, 95
Wang, Y., Rueda, J. A., Ruffini, R., et al. 2019, ApJ, 874, 39
Wang, Y., Rueda, J. A., Ruffini, R., et al. 2022, ApJ, 936, 190
Yang, J., Wang, F., Fan, X., et al. 2021, ApJ, 923, 262
Yue, M., Eilers, A.-C., Simcoe, R. A., et al. 2023, arXiv:2309.04614

Long and short GRB connection

J. A. Rueda,[1,2,3,4,5] L. Becerra,[6,1] C. L. Bianco,[1,2,5] M. Della Valle,[7,1] C. L. Fryer,[8,9,10,11,12] C. Guidorzi,[13,14] and R. Ruffini[1,2,15,16,*]

[1]*ICRANet, Piazza della Repubblica 10, I-65122 Pescara, Italy*
[2]*ICRA, Dipartimento di Fisica, Sapienza Università di Roma, Piazzale Aldo Moro 5, I-00185 Roma, Italy*
[3]*ICRANet-Ferrara, Dipartimento di Fisica e Scienze della Terra, Università degli Studi di Ferrara, Via Saragat 1, I-44122 Ferrara, Italy*
[4]*Dipartimento di Fisica e Scienze della Terra, Università degli Studi di Ferrara, Via Saragat 1, I–44122 Ferrara, Italy*
[5]*INAF, Istituto di Astrofisica e Planetologia Spaziali, Via Fosso del Cavaliere 100, 00133 Rome, Italy*
[6]*Centro Multidisciplinario de Física, Vicerrectoría de Investigación, Universidad Mayor, Santiago de Chile 8580745, Chile*
[7]*INAF - Osservatorio Astronomico di Capodimonte, Salita Moiariello 16, I-80131 Napoli, Italy*
[8]*Center for Theoretical Astrophysics, Los Alamos National Laboratory, Los Alamos, New Mexico 87545, USA*
[9]*Computer, Computational, and Statistical Sciences Division, Los Alamos National Laboratory, Los Alamos, New Mexico 87545, USA*
[10]*The University of Arizona, Tucson, Arizona 85721, USA*
[11]*Department of Physics and Astronomy, The University of New Mexico, Albuquerque, New Mexico 87131, USA*
[12]*The George Washington University, Washington, DC 20052, USA*
[13]*INFN - Sezione di Ferrara, Via Saragat 1, 44122 Ferrara, Italy*
[14]*INAF - Osservatorio di Astrofisica e Scienza dello Spazio di Bologna, Via Piero Gobetti 101, 40129 Bologna, Italy*
[15]*Université de Nice Sophia-Antipolis, Grand Château Parc Valrose, Nice, CEDEX 2, France*
[16]*INAF, Viale del Parco Mellini 84, 00136 Rome, Italy*

(Received 17 July 2024; accepted 16 December 2024; published 6 January 2025)

Long and short gamma-ray bursts (GRBs) are thought to arise from different and unrelated astrophysical progenitors. The association of long GRBs with supernovae (SNe) and the difference in the distributions of galactocentric offsets of long and short GRBs within their host galaxies have often been considered strong evidence of their unrelated origins. Long GRBs have been thought to result from the collapse of single massive stars, while short GRBs come from mergers of compact-object binaries. Our present study challenges this conventional view. We demonstrate that the observational properties, such as the association with SNe and the different galactic offsets, are naturally explained within the framework of the binary-driven hypernova model, suggesting an evolutionary connection between long and short GRBs.

DOI: 10.1103/PhysRevD.111.023010

I. INTRODUCTION

The binary nature of short gamma-ray bursts (GRBs) was recognized and widely accepted since the first proposals based on mergers of binaries formed of two neutron stars (NS-NS) or an NS and a black hole (NS-BH; e.g., [1–4]). On the other hand, long GRBs have been mostly considered to arise from the core collapse of a single massive star into a BH (or a magnetar), a "collapsar" [5], surrounded by a massive accretion disk [6,7].

Therefore, the above theoretical models of long and short GRBs have treated them as two different and unrelated classes of astrophysical sources from different progenitors. This assumption has been further enhanced by the fact that only the long GRBs are associated with supernovae (SNe) and by the differences in the observed projected galactocentric offsets of short and long GRBs in the host galaxies. This work shows that such apparent differences are instead explained through an evolutionary connection between the long and the short GRBs that naturally arises when considering the role of binaries in the stellar evolution of massive stars.

Indeed, multiwavelength observations in the intervening years point to a key role of binaries in the evolution of massive stars and GRBs. The BeppoSAX satellite capabilities led to the discovery of the x-ray afterglow of GRBs [8],

[*]Contact author: jorge.rueda@icra.it

and the accurate position, which allowed the optical follow-up by ground-based telescopes, led to two major results: determining the GRB cosmological nature [9] and observing long GRBs in temporal and spatial coincidence with type Ic SNe. The first GRB-SN association was GRB 980425-SN 1998bw [10]. The follow-up by the Neil Gehrels Swift Observatory [11–13] of the optical afterglow has confirmed about twenty GRB-SN associations [14–18]. The SNe Ic associated with the long GRBs show similar optical luminosity and peak time independent of the GRB energetics, which spans nearly 7 orders of magnitude in the sample of GRB-SN (see Ref. [18], for details). Explaining the GRB-SN association is one of the most stringent constraints for GRB models.

GRB-SN systems are related to massive star explosions [19–21], and most massive stars belong to binaries [22,23]. The SN associated with long GRBs are of type Ic, and theoretical models and simulations show that they are more plausibly explained via binary interactions to aid the hydrogen and helium layers of the pre-SN star to be ejected [24–30]. Further discussion on binary and single-star model progenitors of GRB-SNe can be found in Aimuratov *et al.* [18].

The above theoretical and observational considerations suggest that long GRBs associated with SNe likely occur in binaries. A possible crucial role of binaries in GRBs had been envisaged in Fryer *et al.* [31]. The binary-driven hypernova (BdHN) model has proposed a binary progenitor for long GRBs to respond to the above exigences. In this model, the GRB-SN event arises from a binary comprising a carbon-oxygen (CO) star and an NS companion. The collapse of the iron core of the CO star leads to a newborn NS (νNS) and a type Ic SN. The explosion and expelled matter in the presence of the NS companion in a tight orbit triggers a series of physical processes that lead to the observed emission episodes (see, e.g., Refs. [18,32–38] and references therein). Most relevant is the hypercritical accretion of SN ejecta onto the νNS and NS companion [39], allowed by the copious emission of MeV neutrinos [35,40]. The accretion rate, highly dependent on the orbital period, leads to various BdHN types.

In the few-minute-orbital-period CO-NS binaries, the NS reaches the critical mass, collapsing into a rotating (Kerr) BH. These systems are called BdHN I and are the most energetic long GRBs with an energy release $\gtrsim 10^{52}$ erg. Some examples are GRB 130427A [41], GRB 180720B [42], and GRB 190114C [43,44]. The accretion rate is lower in less compact binaries with periods from tens of minutes to hours, so the NS remains stable as a more massive, fast-rotating NS. These systems, called BdHNe II, release energies $\sim 10^{50}$–10^{52} erg. An example is GRB 190829A [45]. Wide CO-NS binaries with periods of up to days, called BdHNe III, release $\lesssim 10^{50}$ erg, such as GRB 171205A [46].

The above picture predicts that BdHN events (long GRBs) may lead to three possible fates of the CO-NS binary: an NS-BH (BdHNe I) and NS-NS (BdHNe II) or two runaway NSs (most BdHNe III). The gravitational wave emission will lead the new compact-object binaries that remain bound to merge, producing short GRBs [33,47–49]. We refer to this evolutionary process as the “long-short GRB connection.” We have recently performed a suite of numerical simulations to determine the binary parameters that form NS-BH, NS-NS, and those that become unbound by BdHN events [50]. Here, we use those new results to assess the long-short GRB connection from the theoretical and observational viewpoint. In particular, we analyze information from the GRB density rates, the distribution as a function of redshift, the host galaxy types, and the projected offset position of long and short GRBs.

Section II summarizes the observational constraints for the long-short GRB connection imposed by the observed GRB populations, density rates, the host galaxies, and the sources’ position projected offsets. Section III shows the main results of the three-dimensional numerical simulations of the BdHN scenario relevant to the analysis of this work. Specifically, we calculate the merger times and the difference of the position offsets between the long and short GRBs, predicted by the BdHN model simulations. In Sec. IV, we discuss our results and draw the main conclusions.

II. OBSERVATIONAL CONSTRAINTS FOR THE LONG-SHORT GRB CONNECTION

A. GRB density rates

A clue for the long-short GRB connection may arise from the GRB occurrence rates. Here, we use the rates estimated in Ruffini *et al.* [47], following the method by Sun *et al.* [51]. Suppose ΔN_i bursts are detected by various instruments in a logarithmic luminosity bin from $\log L$ to $\log L + \Delta \log L$. Thus, the total local density rate between observed minimum and maximum luminosities $L_{\rm min}$ and $L_{\rm max}$ can be estimated as

$$\mathcal{R} = \sum_i \sum_{L_{\rm min}}^{L_{\rm max}} \frac{4\pi}{\Omega_i T_i} \frac{1}{\ln 10} \frac{1}{g(L)} \frac{\Delta N_i}{\Delta \log L} \frac{\Delta L}{L}, \tag{1}$$

where Ω_i and T_i are the instrument field of view and observing time, $g(L) = \int_0^{z_{\rm max}} (1+z)^{-1} dV(z)$, being $V(z)$ the comoving volume given in a flat ΛCDM cosmology by $dV(z)/dz = (c/H_0) 4\pi d_L^2 / [(1+z^2)\sqrt{\Omega_M (1+z)^3 + \Omega_\Lambda}]$, with H_0 the Hubble constant, d_L the luminosity distance, Ω_M and Ω_Λ the cosmology matter and dark energy density parameters, and $z_{\rm max}$ is the maximum redshift at which a burst of luminosity L can be detected. We refer the reader to Sec. X in [47] for further details.

Using a sample of 233 long bursts with $E_{\rm iso} \gtrsim 10^{52}$ erg, peak energy $0.2 \lesssim E_p \lesssim 2$ MeV, and measured redshifts $0.169 \leq z \leq 9.3$, Ruffini *et al.* [47] estimated the observed (isotropic) density rate of BdHN I, $\mathcal{R}_{\rm I} \approx 0.7$–$0.9\ \mathrm{Gpc}^{-3}\,\mathrm{yr}^{-1}$. As expected from the above definitions, this rate agrees with the estimated rate of the so-called high-luminous ($L \gtrsim 10^{50}\ \mathrm{erg\,s^{-1}}$) long GRBs, e.g., 0.6–1.9 [52] and 0.7–0.9 $\mathrm{Gpc}^{-3}\,\mathrm{yr}^{-1}$ [51].

As discussed in [33], the BdHN I subclass can arise from a small subset of the ultrastripped binaries. The rate of ultrastripped binaries, $\mathcal{R}_{\rm USB}$, is expected to be 0.1%–1% of the total SN Ic [53]. The rate of SN Ic (not the total core-collapse SN) has been estimated to be $\mathcal{R}_{\rm SNIc} \approx 2.6 \times 10^4\ \mathrm{Gpc}^{-3}\ \mathrm{yr}^{-1}$ (see, e.g., [54]). This estimate is compatible with more recent estimates, e.g., $\mathcal{R}_{\rm SNIc} \sim 2.4 \times 10^4\ \mathrm{Gpc}^{-3}\ \mathrm{yr}^{-1}$ [55]. Therefore, the rate of ultrastripped binaries may be $\mathcal{R}_{\rm USB} \sim 24$–$240\ \mathrm{Gpc}^3\ \mathrm{yr}^{-1}$, which implies that ∼0.4%–4% of them may explain the BdHNe I observed population.

Turning now to the BdHNe II and III, the above method leads to the total density rate $\mathcal{R}_{\rm II+III} \approx 66$–$145\ \mathrm{Gpc}^{-3}\,\mathrm{yr}^{-1}$, which was estimated in [47] with a sample of 10 long bursts with $E_{\rm iso} \lesssim 10^{52}$ erg, $4 \lesssim E_p \lesssim 200$ keV, and measured redshifts $0.0085 \leq z \leq 1.096$. As expected from the above features, this rate agrees with independent estimates of the density rate of the so-called low-luminous ($L \lesssim 10^{48}\ \mathrm{erg\,s^{-1}}$) long GRBs, e.g., 148–677 [56], 155–1000 [54], ∼200 [57], and 99–262 $\mathrm{Gpc}^{-3}\ \mathrm{yr}^{-1}$ [51]. Therefore, the BdHNe II and III dominate the long GRB rate, i.e., $\mathcal{R}_{\rm long} \equiv \mathcal{R}_{\rm I+II+III} \approx \mathcal{R}_{\rm II+III}$.

Let us now discuss the post-BdHN binaries formed by the BdHNe I, II, and III. The ("pre-BdHN") CO-NS progenitors of BdHNe I have orbital periods of a few minutes, so most of them remain bound after the SN explosion [33,36]. The bursts from the NS-BH mergers formed after BdHNe I are expected to have compact and potentially low-mass disks, leading to very short durations. Hence, they have been called ultrashort GRBs (U-GRBs). The above properties make U-GRBs hard to detect, and it is thought that no U-GRB has been observed [33]. Thus, we can assume the rate of BdHN I as the upper limit to the U-GRBs from NS-BH mergers, i.e., $\mathcal{R}_{\rm U\text{-}GRB} \lesssim \mathcal{R}_{\rm I}$.

In BdHNe II and III, the SN can either disrupt the binary, leading to runaway NSs or, if it remains bound, to an NS-NS binary. The mergers of the NS-NS binaries are expected to produce short GRBs. As for BdHN I and II energy separatrix of $\sim 10^{52}$ erg related to the energy required to bring the NS companion to the critical mass for BH formation, in Ruffini *et al.* [47,48], two subclasses of short bursts from NS-NS mergers have been distinguished. The mergers that overcome the NS critical mass, so those forming a BH, should release an energy $\gtrsim 10^{52}$ erg. These systems have been called authentic short GRBs (S-GRBs). The NS-NS mergers leading to a stable, massive NS have been called short gamma-ray flashes (S-GRFs) and release $\lesssim 10^{52}$ erg. It has been there estimated that $\mathcal{R}_{\rm S\text{-}GRF} \approx 4$ and $\mathcal{R}_{\rm S\text{-}GRB} \approx 0.002\ \mathrm{Gpc}^3\,\mathrm{yr}^{-1}$. Hence, the S-GRFs dominate the rate of short bursts, i.e., $\mathcal{R}_{\rm short} \equiv \mathcal{R}_{\rm S\text{-}GRF} + \mathcal{R}_{\rm S\text{-}GRB} + \mathcal{R}_{\rm U\text{-}GRB} \approx \mathcal{R}_{\rm S\text{-}GRF}$. This implies that NS-NS mergers dominate the observed local short GRB rate. The above estimates agree with independent assessments of the short GRB rate (see Table 2 in [58] for a summary) and the current upper limit of AT 2017gfo kilonovalike events $< 900\ \mathrm{Gpc}^3\,\mathrm{yr}^{-1}$ [59]. We refer to Mandel and Broekgaarden [60] for a recent review.

We summarize in Table I all the above information for the various BdHN and short GRB subclasses. The fact that $\mathcal{R}_{\rm long} > \mathcal{R}_{\rm short}$ supports the expectation that the SN event disrupts a non-negligible fraction of binaries. Indeed, if we require the short-burst population to derive from the long-burst population, the fraction of binaries that remain bound should be $\mathcal{R}_{\rm short}/\mathcal{R}_{\rm long} \approx 2\%$–$8\%$. Thus, the SN explosion would disrupt the 92%–98% of NS-NS binaries from BdHNe II and III. However, the latter dominates the percentage of unbound systems given their much wider pre-SN orbits [50]. Interestingly, this inferred ∼1% fraction of survived NS-NS binaries only based on the GRB rates and the BdHN prediction that short GRBs are long GRB descendants agrees with estimates from population synthesis simulations (see, e.g., [61–65] and references therein). See also Kochanek *et al.* [66], Chrimes *et al.* [67], Luitel and Rangelov [68], and Chrimes *et al.* [69] for more recent analyses. All the above has triggered new observational campaigns searching for bound or ejected companions of SN explosions (see, e.g., [69–74] and references therein).

TABLE I. Summary of some physical and observational properties of the GRB subclasses relevant for this work. The first three columns indicate the GRB subclass name and the corresponding pre-BdHN and post-BdHN binaries. In columns 4 and 5, we list the ranges of peak energy ($E_{\rm p,i}$) and isotropic energy released ($E_{\rm iso}$) (rest frame 1–10^4 keV). Columns 6 and 7 list the maximum observed redshift and the local observed rate $\mathcal{R}$ obtained in Ruffini *et al.* [47].

Subclass	Pre-BdHN	Post-BdHN	$E_{\rm p,i}$ (MeV)	$E_{\rm iso}$ (erg)	$z_{\rm max}$	$\mathcal{R}$ ($\mathrm{Gpc}^{-3}\mathrm{yr}^{-1}$)
BdHN I	CO-NS	NS-BH	∼0.2–2	$\sim 10^{52}$–10^{54}	9.3	$0.77^{+0.09}_{-0.08}$
BdHN II + III	CO-NS	NS-NS	$\lesssim 0.2$	$\sim 10^{48}$–10^{52}	1.096	100^{+45}_{-34}
S-GRF	NS-NS	NS	$\lesssim 2$	$\sim 10^{49}$–10^{52}	2.609	$3.6^{+1.4}_{-1.0}$
S-GRB	NS-NS	BH	$\gtrsim 2$	$\sim 10^{52}$–10^{53}	5.52	$(1.9^{+1.8}_{-1.1}) \times 10^{-3}$
U-GRB	NS-BH	BH	$\gtrsim 2$	$\gtrsim 10^{52}$	$\lesssim z^{\rm I}_{\rm max}$	$\lesssim \mathcal{R}_{\rm I}$

B. GRB redshift distribution

In Bianco *et al.* [75], the redshift distribution of a sample of 301 GRBs observed by Swift before December 2018 was analyzed. Based on the definition of long GRB types within the BdHN scenario and that of short GRBs, the above Swift sample was subdivided into three subsamples: 216 BdHNe I, 64 BdHNe II and III, and 21 short GRBs. The redshift distribution of the BdHNe I subsample shows a single peak between $z \sim 2$ and $z \sim 2.5$ and a sort of plateau for $0.5 \lesssim z \lesssim 2$. The distribution of the subsample formed by BdHNe II and III shows a single peak around $z \sim 1$. Therefore, the distribution of BdHN I + II + III has a double-peak structure [75], which, as expected, agrees with previous analysis of the long GRB population (see, e.g., [52,76] and Fig. 8 in Grieco *et al.* [77]). The sample of short GRBs shows a single peak at $z \lesssim 0.5$. In this paper, we updated this GRB sample by considering 34 additional short GRBs until the end of 2023. The total number of short GRBs in this new sample is, therefore, 55, and the total number of GRBs in the entire sample is 335. Figure 1 shows the distributions of the BdHNe I (upper panel), BdHNe II + III (middle panel), and short GRBs (lower panel) subsamples. It shows the following qualitative features:

(i) The BdHN I population is responsible for the long GRB peak at $z_p^I \sim 2$–2.5 [75]. The BdHN II + III distribution peaks at $z_p^{\mathrm{II+III}} \approx 0.72$. One of the reasons for $z_p^{\mathrm{I}} > z_p^{\mathrm{II+III}}$ is the BdHN I higher energetics, which allows their detection at larger redshifts.

(ii) The distributions of BdHNe II + III and short GRBs show a similar shape [75]. The former is wider than the latter, and their peaks occur at slightly different redshifts. The peak of the short GRB distribution occurs at $z_p^{\mathrm{short}} \approx 0.42$, which is lower than $z_p^{\mathrm{II+III}} \approx 0.72$ by $\Delta z \approx 0.3$.

We have performed a Kolmogorov-Smirnov test on the relation hypothesis between the BdHN I, BdHN II + III, and short GRB distributions. The following conclusions can be drawn:

(i) The p-value testing the BdHN I and short GRB distribution similarity is 4.5×10^{-10}. This very low value suggests their relationship is unlikely.

(ii) The p-value testing the BdHN II + III and short GRB distribution similarity is 0.011. This much larger value indicates similarity. The difference in the position of the peaks dominates the difference in the distributions. In fact, by shifting any of the distributions by the difference of their peaks, $\Delta z \approx 0.3$, the p-value increases to ≈ 0.35.

The above results agree with our previous conclusions based on the GRB density rates: the observed population of short GRBs appears dominated by NS-NS mergers and not by NS-BH mergers, so it is not evolutionarily connected with the BdHN I population but with that of BdHNe II and III, i.e., the latter may form the NS-NS binaries that become the short GRB progenitors. This conclusion finds further support from the estimated merger times. The most recent numerical simulations of the BdHN scenario [50] lead to a wide range of merger timescales $\sim 10^4$–10^9 yr (see Fig. 2 below). The rapidly merging binaries are those of short orbital periods, so they are mostly NS-BH, which have merger times $\tau_{\mathrm{merger}} \sim 10$ kyr [33]. As we discussed above, those NS-BH are post-BdHN I products. Thus, given the peak of the BdHN I distribution at $z \sim 2$ and the NS-BH short merging times, these binaries should not be expected to contribute to the short GRB population at low redshifts.

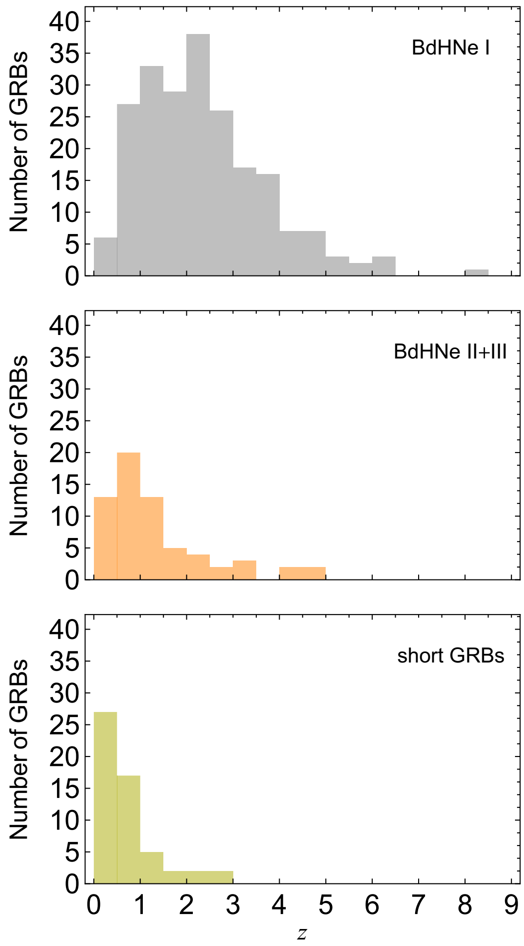

FIG. 1. Distributions of a sample of 335 GRBs as a function of the cosmological redshift. The sample is divided into three subsamples: BdHNe I (upper panel, 216 sources, gray), BdHNe II + III (middle panel, 64 sources, orange), and short GRBs (lower panel, 55 sources, green). This GRB sample is an updated version, with 34 additional short GRBs until the end of 2023, of the one considered by Bianco *et al.* [75]. We refer to Sec. VI of Bianco *et al.* [75] for additional details on the definition of the sample.

C. GRB host galaxies and projected offsets

Concerning the short GRB host galaxies, Nugent *et al.* [78] shows that 84% are star forming, like long GRB hosts. This

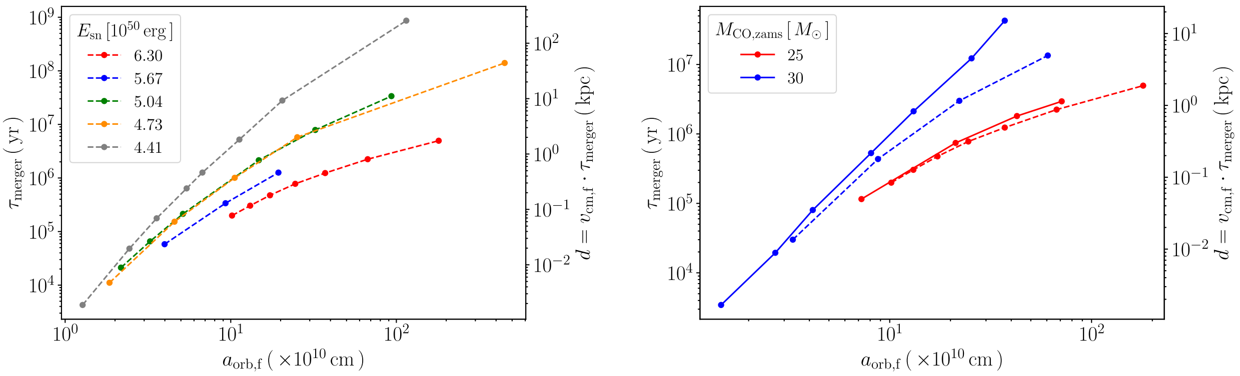

FIG. 2. Characteristic merger time by gravitational-wave emission (left axis) and distance travel (right axis) for the binary systems that remain bound (negative total energy) after a BdHN event as a function of the final binary separation. Left: the initial binary comprises a CO-evolved star from a ZAMS progenitor of $M_{zams} = 25M_\odot$ and a $2M_\odot$ NS companion and the curves correspond to selected SN explosion energies. Right: simulations for the SN explosion energy 6.30×10^{50} erg for two CO-evolved stars from ZAMS progenitors: $M_{zams} = 25M_\odot$ (red) and $30M_\odot$ (blue). The dashed (solid) curves correspond to symmetric (asymmetric) SN explosions (see [50] for details).

fraction decreases significantly at low redshift ($z \lesssim 0.25$), in line with galaxy evolution. Interestingly, high-mass galaxies are less abundant among the short GRB hosts than field galaxies, which becomes more evident at $z \gtrsim 0.5$ and more similar to the analogous distribution for long GRB hosts. Moreover, they found evidence for both a short delay-time population, mostly for star-forming hosts at $z > 1$, and a long delay-time one, which becomes prevalent at lower redshift in quiescent hosts.

The projected physical offsets from the host galaxy center of short GRBs are, on average, larger than those of long GRBs. Recent work by Fong *et al.* [79] including 90 short GRB host galaxies, the majority of which are robust associations, finds offsets ranging from a fraction of kiloparsec to ≈60 kpc, with a median offset value 5–8 kpc (see also O'Connor *et al.* [80]). These values must be compared with the median value of long GRBs of 1.28 kpc. Indeed, 90% of long GRB offsets are < 5 kpc [81].

The above observational properties evidence that, for long and short GRBs to share a common progenitor, the delay-time distribution of the compact-object binary mergers must include short and long values. We shall discuss these points in the next section.

III. POST-BdHN NS-NS/NS-BH TIME AND DISTANCE TRAVELED TO MERGER

We have recently presented in Becerra *et al.* [50] a new set of numerical simulations performed with the SN-SPH code [82] of the evolution of the binary system from the CO star SN explosion. The code follows the structure evolution of the νNS and the NS companion as they move and accrete matter from the SN ejecta. The initial setup has been described in detail in Becerra *et al.* [36] (see also [38]).

The code tracks the SN ejecta and point-mass particles' position and velocity. The total energy of the evolving νNS-NS system, E_{tot}, is given by the sum of the total kinetic energy relative to the binary's center of mass and the gravitational binding energy. The system is bound if $E_{tot} < 0$. In that case, the orbital separation can be determined from the binary total energy, the orbital period from Kepler's law, and the eccentric from the orbital angular momentum (see [50] for further details).

To examine the conditions under which the binary remains bound, we perform simulations for various initial orbital periods, keeping fixed the initial mass of the NS companion, $M_{NS,i} = 2M_\odot$, the zero-age main-sequence (ZAMS) of the CO star ($M_{zams} = 25M_\odot$), and the SN explosion energy. The pre-SN CO star has a total mass of $M_{CO} = 6.8M_\odot$ and leaves a νNS of $M_{\nu NS,i} = 1.8M_\odot$. Thus, it ejects $M_{ej} \approx 5M_\odot$ in the SN explosion. We recall that $M_{CO} = M_{\nu NS,i} + M_{ej}$. We record the final values of the νNS mass $M_{\nu NS,f}$, the NS companion mass $M_{NS,f}$, orbital separation $a_{orb,f}$, orbital period $P_{orb,f}$, and eccentricity e_f. Another key quantity is the final binary center of mass velocity $v_{c.m.,f}$. We end the simulation when most of the ejecta have left the system, i.e., when the mass gravitationally bound to the stars (νNS and NS) is gravitationally negligible, e.g., $\lesssim 10^{-3} M_\odot$.

The final total energy of the systems in the simulations is well fitted by the following polynomial function:

$$E_{tot,f} \approx -\frac{1}{2}\frac{GM_{CO}M_{ns,i}}{a_{orb,i}}(a + bx + cx^2), \qquad x \equiv \frac{a_{orb,i}P_{orb,i}}{v_{sn}}, \tag{2}$$

where $v_{sn} = \sqrt{2E_{sn}/M_{ej}}$ is an indicative average expansion velocity of the SN ejecta of mass M_{ej}. For the present binary, $a = 0.294$, the constants b and c depend on the SN explosion energy and are listed in Table 2 of Becerra *et al.* [50]. For example, for $E_{sn} = 6.3 \times 10^{50}$ erg, $b = -3.153$ and

$c = 5.219$. The maximum initial period for the system to hold bound is obtained by setting the final total energy to zero. In the present example, the energy becomes zero at $x = 0.115$, which implies $P_{\mathrm{orb,max}} \approx 7.15$ min.

The final bound systems will be compact binary systems (NS-NS or NS-BH), which will eventually merge through the emission of gravitational waves. The time to merger is given by (see, e.g., [83])

$$\tau_{\mathrm{merger}} = \frac{c^5}{G^3} \frac{5}{256} \frac{a_{\mathrm{orb}}^4}{\mu M^2} F(e), \tag{3}$$

$$F(e) = \frac{48}{19} \frac{1}{g(e)^4} \int_0^e \frac{g(e)^4 (1-e^2)^{5/2}}{e(1 + \frac{121}{304} e^2)} de, \tag{4}$$

where $g(e) = e^{12/19}(1-e^2)^{-1}(1 + 121e^2/304)^{870/2299}$, being $M = m_1 + m_2$, $\mu = m_1 m_2/M$, and e the orbit total mass, reduced mass, and eccentricity.

We have calculated the time to merger from Eq. (3), using the parameters obtained from the numerical simulations, i.e., $a_{\mathrm{orb}} = a_{\mathrm{orb,f}}$, $m_1 = M_{\nu\mathrm{NS,f}}$, $m_2 = M_{\mathrm{NS,f}}$, and $e = e_f$. With this information, the distance traveled by the newly formed compact-object binary from the BdHN event location to the merger site is

$$d = v_{\mathrm{c.m.,f}} \tau_{\mathrm{merger}}. \tag{5}$$

Figure 2 shows τ_{merger} (left axis) and d (right axis) as a function of $a_{\mathrm{orb,f}}$. We show the results when the CO star's companion is an NS of $M_{\mathrm{NS},i} = 2M_\odot$, while we adopt two models for the CO star. The first is the model of the previous example, i.e., a CO-evolved star from a ZAMS progenitor of $M_{\mathrm{zams}} = 25M_\odot$; $M_{\mathrm{CO}} = M_{\nu\mathrm{NS},i} + M_{\mathrm{ej}} \approx 6.8M_\odot$, where $M_{\nu\mathrm{NS},i} \approx 1.8M_\odot$ and $M_{\mathrm{ej}} \approx 5M_\odot$. The second model is the CO star from a $M_{\mathrm{zams}} = 30M_\odot$; $M_{\mathrm{CO}} \approx 8.9M_\odot$, where $M_{\nu\mathrm{NS},i} = 1.7M_\odot$ and $M_{\mathrm{ej}} \approx 7.2M_\odot$. Each point in each curve corresponds to a different value of the parameter x defined in Eq. (2), so for fixed initial component masses, ejecta mass, and SN explosion energy, it explores a range of orbital periods $P_{\mathrm{orb,i}}$ (or, equivalently, $a_{\mathrm{orb,i}}$). In the right panel plot, we compare the results for a symmetric and asymmetric SN explosion of the same energy.

For the various SN explosion energies, the left panel of Fig. 2 shows a range of merger times $\tau_{\mathrm{merger}} = 10^4$–$10^9$ yr. Correspondingly, we obtain systemic velocities $v_{\mathrm{c.m.,f}} \sim 10$–$100\ \mathrm{km\,s^{-1}}$ for those newly formed binaries. From the above, we find that the distance traveled by these binaries (NS-NS or NS-BH) after the BdHN event ranges $d = 0.01$–100 kpc.

The measured projected offsets of long and short GRBs in the host galaxies differ about 1 order of magnitude (see [79] and Sec. II B). While most long GRBs have offsets < 5 kpc, with a median value $\sim$1 kpc, short GRBs show an equally broad distribution but shifted to larger values by about one decade, that is, from a fraction of kiloparsec to $\approx$70 kpc. The short GRB offset median is $\approx$8 or $\approx$5 kpc for the golden sample of the most robust associations. The offsets of the short GRBs in the sample of Fig. 1 are 0.15–70.19 kpc. This range of values strikingly agrees with that obtained for the distance traveled by the NS-NS and NS-BH binaries produced by BdHNe.

It is worth mentioning that the above conclusions have been obtained within the model's hypotheses and are limited to the parameter space we have explored. Such a parameter space (e.g., CO star mass and orbital period) is not arbitrary; it corresponds to the conditions that, from our simulations, lead to the three subclasses of BdHNe (I, II, III). However, these conditions may vary according to the various physical conditions in population synthesis simulations leading to the pre-BdHN CO-NS binaries. Such simulations are still missing in the literature and represent an interesting new research topic.

IV. DISCUSSION AND CONCLUSIONS

We have reached the following conclusions:

(1) GRB rates. The inequality $\mathcal{R}_{\mathrm{short}} < \mathcal{R}_{\mathrm{long}}$ is explained as follows (see Sec. II A). First and foremost, the short GRB is dominated by NS-NS mergers, and only a subset of the BdHNe can produce NS-NS (BdHNe II and III). Thus, the subset leading to short GRBs is given by the BdHNe II and III that lead to bound NS-NS binaries [50]. Further, BdHNe I lead to NS-BH binaries. These binaries can produce short GRBs only if the BH is low enough mass; otherwise, tidal disruption of the NS by the BH is more likely to occur.

(2) Redshift distribution. First, we have shown in Sec. II B that $z_p^{\mathrm{I}}(\approx 2$–$2.5) > z_p^{\mathrm{II+III}}(\approx 0.72)$ (see also Fig. 1), which reflects the higher energetics of the BdHN I relative to BdHN II and III that allows their observation at higher redshifts. Then, we showed that the short GRB distribution peaks at $z_p^{\mathrm{short}} \approx 0.42$. The inequality $z_p^{\mathrm{short}} \ll z_p^{\mathrm{I}}$ suggests that BdHN I remnant binaries have a negligible role in the distribution of short GRBs. Indeed, in the BdHN scenario, BdHNe I produce compact-orbit NS-BH binaries, rapidly merging on timescales $< 10^5$ yr [33]. At the peak redshift of the BdHN I distribution, $z_p^I \approx 2$–2.5, such a timescale implies a negligible redshift interval, so their contribution at $z_p^{\mathrm{short}} \approx 0.42$ is negligible. On the other hand, the distribution of BdHN II + III shows similarities with that of the short GRBs, and $z_p^{\mathrm{II+III}} \approx 0.72$, which differs from z_p^{short} by $\Delta z = 0.3$. The merger timescales of NS-NS products by BdHN II and III (see Fig. 2) could explain the time delay (redshift difference) between the two distributions. The above analysis suggests a link between the NS-NS

remnant binaries from BdHN II and III as possible progenitors of the short GRBs. Thus, further detailed calculations are needed to deepen this connection, such as simulating the merger time-delay distribution accounting for the occurrence rate and intrinsic distribution of binary periods at different redshifts and the cosmological expansion. Such a calculation goes beyond the exploratory character of the present article and is left for future analyses.

(3) Host galaxies. Short-GRB host stellar-population ages support the picture of a short delay-time population within young and star-forming galaxies at $z > 0.25$, along with a long delay-time population which characterizes older and quiescent galaxies at lower z [78]. The above observations suggest compact-orbit NS-NS binaries should be more abundant in the former galaxies, while wide-orbit NS-NS binaries dominate in the latter. This suggestive information deserves further attention from combined cosmology and population synthesis models, which, combined with the BdHN simulations, could be used to estimate the expected galactocentric offsets and circum-merger conditions for NS-NS merging systems (see, e.g., [84]).

(4) Galactocentric offsets. The NS-NS produced by BdHNe II and III have a distribution of binary periods, eccentricities, and systemic velocities, which predict a wide distribution of systemic velocities 10–100 $\mathrm{km\,s^{-1}}$ and merger times 10^4–10^9 yr, leading to distances of 0.01–100 kpc traveled by these systems from the BdHN site to their merger site at which the short GRBs are expected to be produced (see Fig. 2). In the BdHN scenario, this distance traveled by the post-BdHN binary directly measures the distance separating the long and short GRB occurrence sites. Therefore, our modeling does not give information on the offset of the long or the short GRB but on their relative offset. Indeed, most long GRBs have offsets < 5 kpc, while short GRB offsets span from a fraction of kiloparsec to $\approx$70 kpc. This difference in the offset of about a decade agrees with the BdHN numerical simulations presented here.

There are additional consequences of the present scenario. Current distributions of merger times and large systemic postformation velocities are in tension with observations of short GRBs in dwarf galaxies. The velocities larger than the galaxy escape velocities and the long merger times predict offsets larger than observed would impede the r-process enrichment of the galaxy [85]. In this regard, our results imply two possibilities. First, a population of short-merger-time binaries ($<$ 100 kyr) do not have time to move outside the dwarf galaxy, even for velocities larger than the galaxy's escape velocity. Second, there are binaries with longer merger times but with velocities lower than the galaxy's escape velocity. The present results, combined with future detailed population studies, may determine the relative relevance of these systems to explain these observations.

In summary, we have shown that observations of the GRB density rates and density distribution, the host galaxy types, and the sources' projected position offsets agree with the expectations from the BdHN scenario and numerical simulations. This constitutes a strong test of the surprising conclusion, as it may sound: short GRBs are long GRB descendants.

All the above implies, at the same time, the binary progenitor nature of long GRBs and, consequently, the associated preceding binary stellar evolution. Therefore, further theoretical and observational scrutiny from the GRB, x-ray binaries, population synthesis, stellar evolution, and cosmology communities is highly encouraged.

ACKNOWLEDGMENTS

The simulations were performed on LANL HPC resources provided under the Institutional Computing program.

[1] J. Goodman, Astrophys. J. Lett. **308**, L47 (1986).
[2] B. Paczynski, Astrophys. J. Lett. **308**, L43 (1986).
[3] David Eichler, Mario Livio, Tsvi Piran, and David N. Schramm, Nature (London) **340**, 126 (1989).
[4] R. Narayan, T. Piran, and A. Shemi, Astrophys. J. Lett. **379**, L17 (1991).
[5] S. E. Woosley, Astrophys. J. **405**, 273 (1993).
[6] P. Mészáros, Annu. Rev. Astron. Astrophys. **40**, 137 (2002).
[7] T. Piran, Rev. Mod. Phys. **76**, 1143 (2004).
[8] E. Costa, F. Frontera, J. Heise, M. Feroci, J. in't Zand, F. Fiore, M. N. Cinti, D. Dal Fiume, L. Nicastro, M. Orlandini *et al.*, Nature (London) **387**, 783 (1997).
[9] M. R. Metzger, S. G. Djorgovski, S. R. Kulkarni, C. C. Steidel, K. L. Adelberger, D. A. Frail, E. Costa, and F. Frontera, Nature (London) **387**, 878 (1997).
[10] T. J. Galama, P. M. Vreeswijk, J. van Paradijs, C. Kouveliotou, T. Augusteijn, H. Böhnhardt, J. P. Brewer, V. Doublier, J. F. Gonzalez, B. Leibundgut *et al.*, Nature (London) **395**, 670 (1998).

[11] S. D. Barthelmy, L. M. Barbier, J. R. Cummings, E. E. Fenimore, N. Gehrels, D. Hullinger, H. A. Krimm, C. B. Markwardt, D. M. Palmer, A. Parsons *et al.*, Space Sci. Rev. **120**, 143 (2005).
[12] D. N. Burrows, J. E. Hill, J. A. Nousek, J. A. Kennea, A. Wells, J. P. Osborne, A. F. Abbey, A. Beardmore, K. Mukerjee, A. D. T. Short *et al.*, Space Sci. Rev. **120**, 165 (2005).
[13] P. W. A. Roming, T. E. Kennedy, K. O. Mason, J. A. Nousek, L. Ahr, R. E. Bingham, P. S. Broos, M. J. Carter, B. K. Hancock, H. E. Huckle *et al.*, Space Sci. Rev. **120**, 95 (2005).
[14] S. E. Woosley and J. S. Bloom, Annu. Rev. Astron. Astrophys. **44**, 507 (2006).
[15] M. Della Valle, Int. J. Mod. Phys. D **20**, 1745 (2011).
[16] J. Hjorth and J. S. Bloom, The gamma-ray burst—supernova connection, in *Gamma-Ray Bursts*, edited by C. Kouveliotou, R. A. M. J. Wijers, and S. Woosley, Cambridge Astrophysics Series Vol. 51 (Cambridge University Press, Cambridge, England, 2012), Chap. 9, pp. 169–190.
[17] Z. Cano, S.-Q. Wang, Z.-G. Dai, and X.-F. Wu, Adv. Astron. **2017**, 8929054 (2017).
[18] Y. Aimuratov, L. M. Becerra, C. L. Bianco, C. Cherubini, M. Della Valle, S. Filippi, L. Li, R. Moradi, F. Rastegarnia, J. A. Rueda *et al.*, Astrophys. J. **955**, 93 (2023).
[19] A. S. Fruchter, A. J. Levan, L. Strolger, P. M. Vreeswijk, S. E. Thorsett, D. Bersier, I. Burud, J. M. Castro Cerón, A. J. Castro-Tirado, C. Conselice *et al.*, Nature (London) **441**, 463 (2006).
[20] C. Raskin, E. Scannapieco, J. Rhoads, and M. Della Valle, Astrophys. J. **689**, 358 (2008).
[21] P. L. Kelly, R. P. Kirshner, and M. Pahre, Astrophys. J. **687**, 1201 (2008).
[22] H. A. Kobulnicky and C. L. Fryer, Astrophys. J. **670**, 747 (2007).
[23] H. Sana, S. E. de Mink, A. de Koter, N. Langer, C. J. Evans, M. Gieles, E. Gosset, R. G. Izzard, J. B. Le Bouquin, and F. R. N. Schneider, Science **337**, 444 (2012).
[24] K. Nomoto and M. Hashimoto, Phys. Rep. **163**, 13 (1988).
[25] K. Iwamoto, K. Nomoto, P. Höflich, H. Yamaoka, S. Kumagai, and T. Shigeyama, Astrophys. J. Lett. **437**, L115 (1994).
[26] C. L. Fryer, P. A. Mazzali, J. Prochaska, E. Cappellaro, A. Panaitescu, E. Berger, M. van Putten, E. P. J. van den Heuvel, P. Young, A. Hungerford *et al.*, Publ. Astron. Soc. Pac. **119**, 1211 (2007).
[27] S.-C. Yoon, S. E. Woosley, and N. Langer, Astrophys. J. **725**, 940 (2010).
[28] N. Smith, W. Li, J. M. Silverman, M. Ganeshalingam, and A. V. Filippenko, Mon. Not. R. Astron. Soc. **415**, 773 (2011).
[29] S.-C. Yoon, Pub. Astron. Soc. Aust. **32**, e015 (2015).
[30] H.-J. Kim, S.-C. Yoon, and B.-C. Koo, Astrophys. J. **809**, 131 (2015).
[31] C. L. Fryer, S. E. Woosley, and D. H. Hartmann, Astrophys. J. **526**, 152 (1999).
[32] J. A. Rueda and R. Ruffini, Astrophys. J. Lett. **758**, L7 (2012).
[33] C. L. Fryer, F. G. Oliveira, J. A. Rueda, and R. Ruffini, Phys. Rev. Lett. **115**, 231102 (2015).
[34] L. Becerra, F. Cipolletta, C. L. Fryer, J. A. Rueda, and R. Ruffini, Astrophys. J. **812**, 100 (2015).
[35] L. Becerra, C. L. Bianco, C. L. Fryer, J. A. Rueda, and R. Ruffini, Astrophys. J. **833**, 107 (2016).
[36] L. Becerra, C. L. Ellinger, C. L. Fryer, J. A. Rueda, and R. Ruffini, Astrophys. J. **871**, 14 (2019).
[37] J. A. Rueda, R. Ruffini, L. Li, R. Moradi, J. F. Rodriguez, and Y. Wang, Phys. Rev. D **106**, 083004 (2022).
[38] L. M. Becerra, R. Moradi, J. A. Rueda, R. Ruffini, and Y. Wang, Phys. Rev. D **106**, 083002 (2022).
[39] C. L. Fryer, J. A. Rueda, and R. Ruffini, Astrophys. J. Lett. **793**, L36 (2014).
[40] L. Becerra, M. M. Guzzo, F. Rossi-Torres, J. A. Rueda, R. Ruffini, and J. D. Uribe, Astrophys. J. **852**, 120 (2018).
[41] R. Ruffini, R. Moradi, J. A. Rueda, L. Becerra, C. L. Bianco, C. Cherubini, S. Filippi, Y. C. Chen, M. Karlica, N. Sahakyan *et al.*, Astrophys. J. **886**, 82 (2019).
[42] J. A. Rueda, L. Li, R. Moradi, R. Ruffini, N. Sahakyan, and Y. Wang, Astrophys. J. **939**, 62 (2022).
[43] R. Moradi, J. A. Rueda, R. Ruffini, L. Li, C. L. Bianco, S. Campion, C. Cherubini, S. Filippi, Y. Wang, and S. S. Xue, Phys. Rev. D **104**, 063043 (2021).
[44] R. Moradi, J. A. Rueda, R. Ruffini, and Y. Wang, Astron. Astrophys. **649**, A75 (2021).
[45] Y. Wang, J. A. Rueda, R. Ruffini, R. Moradi, L. Li, Y. Aimuratov, F. Rastegarnia, S. Eslamzadeh, N. Sahakyan, and Y. Zheng, Astrophys. J. **936**, 190 (2022).
[46] Y. Wang, L. M. Becerra, C. L. Fryer, J. A. Rueda, and R. Ruffini, Astrophys. J. **945**, 95 (2023).
[47] R. Ruffini, J. A. Rueda, M. Muccino, Y. Aimuratov, L. M. Becerra, C. L. Bianco, M. Kovacevic, R. Moradi, F. G. Oliveira, G. B. Pisani *et al.*, Astrophys. J. **832**, 136 (2016).
[48] R. Ruffini, J. Rodriguez, M. Muccino, J. A. Rueda, Y. Aimuratov, U. Barres de Almeida, L. Becerra, C. L. Bianco, C. Cherubini, S. Filippi *et al.*, Astrophys. J. **859**, 30 (2018).
[49] L. M. Becerra, C. Fryer, J. F. Rodriguez, J. A. Rueda, and R. Ruffini, Universe **9**, 332 (2023).
[50] L. M. Becerra, C. L. Fryer, J. A. Rueda, and R. Ruffini, arXiv:2401.15702.
[51] H. Sun, B. Zhang, and Z. Li, Astrophys. J. **812**, 33 (2015).
[52] D. Wanderman and T. Piran, Mon. Not. R. Astron. Soc. **406**, 1944 (2010).
[53] T. M. Tauris, N. Langer, and P. Podsiadlowski, Mon. Not. R. Astron. Soc. **451**, 2123 (2015).
[54] D. Guetta and M. Della Valle, Astrophys. J. Lett. **657**, L73 (2007).
[55] C. Frohmaier, C. R. Angus, M. Vincenzi, M. Sullivan, M. Smith, P. E. Nugent, S. B. Cenko, A. Gal-Yam, S. R. Kulkarni, N. M. Law *et al.*, Mon. Not. R. Astron. Soc. **500**, 5142 (2021).
[56] E. Liang, B. Zhang, F. Virgili, and Z. G. Dai, Astrophys. J. **662**, 1111 (2007).
[57] F. J. Virgili, E.-W. Liang, and B. Zhang, Mon. Not. R. Astron. Soc. **392**, 91 (2009).
[58] M. Della Valle, D. Guetta, E. Cappellaro, L. Amati, M. T. Botticella, M. Branchesi, E. Brocato, L. Izzo, M. A. Perez-Torres, and G. Stratta, Mon. Not. R. Astron. Soc. **481**, 4355 (2018).

[59] I. Andreoni, M. W. Coughlin, E. C. Kool, M. M. Kasliwal, H. Kumar, V. Bhalerao, A. S. Carracedo, A. Y. Q. Ho, P. T. H. Pang, D. Saraogi *et al.*, Astrophys. J. **918**, 63 (2021).
[60] I. Mandel and F. S. Broekgaarden, Living Rev. Relativity **25**, 1 (2022).
[61] M. Dominik, K. Belczynski, C. Fryer, D. E. Holz, E. Berti, T. Bulik, I. Mandel, and R. O'Shaughnessy, Astrophys. J. **759**, 52 (2012).
[62] K. A. Postnov and L. R. Yungelson, Living Rev. Relativity **17**, 3 (2014).
[63] M. Dominik, E. Berti, R. O'Shaughnessy, I. Mandel, K. Belczynski, C. Fryer, D. E. Holz, T. Bulik, and F. Pannarale, Astrophys. J. **806**, 263 (2015).
[64] C. L. Fryer, K. Belczynski, E. Ramirez-Ruiz, S. Rosswog, G. Shen, and A. W. Steiner, Astrophys. J. **812**, 24 (2015).
[65] K. Belczynski, S. Repetto, D. E. Holz, R. O'Shaughnessy, T. Bulik, E. Berti, C. Fryer, and M. Dominik, Astrophys. J. **819**, 108 (2016).
[66] C. S. Kochanek, K. Auchettl, and K. Belczynski, Mon. Not. R. Astron. Soc. **485**, 5394 (2019).
[67] A. A. Chrimes, A. J. Levan, A. S. Fruchter, P. J. Groot, P. G. Jonker, C. Kouveliotou, J. D. Lyman, E. R. Stanway, N. R. Tanvir, and K. Wiersema, Mon. Not. R. Astron. Soc. **513**, 3550 (2022).
[68] S. Luitel and B. Rangelov, Res. Not. Am. Astron. Soc. **6**, 13 (2022).
[69] A. A. Chrimes, A. J. Levan, J. J. Eldridge, M. Fraser, N. Gaspari, P. J. Groot, J. D. Lyman, G. Nelemans, E. R. Stanway, and K. Wiersema, Mon. Not. R. Astron. Soc. **522**, 2029 (2023).
[70] M. Ogata, R. Hirai, and K. Hijikawa, Mon. Not. R. Astron. Soc. **505**, 2485 (2021).
[71] O. D. Fox, S. D. Van Dyk, B. F. Williams, M. Drout, E. Zapartas, N. Smith, D. Milisavljevic, J. E. Andrews, K. A. Bostroem, A. V. Filippenko *et al.*, Astrophys. J. Lett. **929**, L15 (2022).
[72] T. Moore, S. J. Smartt, M. Nicholl, S. Srivastav, H. F. Stevance, D. B. Jess, S. D. T. Grant, M. D. Fulton, L. Rhodes, S. A. Sim *et al.*, Astrophys. J. Lett. **956**, L31 (2023).
[73] H.-P. Chen, S.-J. Rau, and K.-C. Pan, Astrophys. J. **949**, 121 (2023).
[74] P. Chen, A. Gal-Yam, J. Sollerman, S. Schulze, R. S. Post, C. Liu, E. O. Ofek, K. K. Das, C. Fremling, A. Horesh *et al.*, Nature (London) **625**, 253 (2024).
[75] C. L. Bianco, M. T. Mirtorabi, R. Moradi, F. Rastegarnia, J. A. Rueda, R. Ruffini, Y. Wang, M. Della Valle, L. Li, and S. R. Zhang, Astrophys. J. **966**, 219 (2024).
[76] A. Lien, T. Sakamoto, S. D. Barthelmy, W. H. Baumgartner, J. K. Cannizzo, K. Chen, N. R. Collins, J. R. Cummings, N. Gehrels, H. A. Krimm *et al.*, Astrophys. J. **829**, 7 (2016).
[77] V. Grieco, F. Matteucci, G. Meynet, F. Longo, M. Della Valle, and R. Salvaterra, Mon. Not. R. Astron. Soc. **423**, 3049 (2012).
[78] A. E. Nugent, W.-F. Fong, Y. Dong, J. Leja, E. Berger, M. Zevin, R. Chornock, B. E. Cobb, L. Z. Kelley, C. D. Kilpatrick *et al.*, Astrophys. J. **940**, 57 (2022).
[79] W.-f. Fong, A. E. Nugent, Y. Dong, E. Berger, K. Paterson, R. Chornock, A. Levan, P. Blanchard, K. D. Alexander, J. Andrews *et al.*, Astrophys. J. **940**, 56 (2022).
[80] B. O'Connor, E. Troja, S. Dichiara, P. Beniamini, S. B. Cenko, C. Kouveliotou, J. B. González, J. Durbak, P. Gatkine, A. Kutyrev *et al.*, Mon. Not. R. Astron. Soc. **515**, 4890 (2022).
[81] P. K. Blanchard, E. Berger, and W.-f. Fong, Astrophys. J. **817**, 144 (2016).
[82] C. L. Fryer, G. Rockefeller, and M. S. Warren, Astrophys. J. **643**, 292 (2006).
[83] M. Maggiore, *Gravitational Waves. Vol. 1: Theory and Experiments* (Oxford University Press, New York, 2007), ISBN 9780198570745, 9780198520740.
[84] B. K. Wiggins, C. L. Fryer, J. M. Smidt, D. Hartmann, N. Lloyd-Ronning, and C. Belcynski, Astrophys. J. **865**, 27 (2018).
[85] A. E. Nugent, W.-f. Fong, C. Castrejon, J. Leja, M. Zevin, and A. P. Ji, Astrophys. J. **962**, 5 (2024).

Astronomy & Astrophysics manuscript no. simple
June 6, 2024

Ten Supernova-rise in Binary Driven Gamma-ray Bursts

R. Ruffini[1234], C. L. Bianco[1254], Liang Li (李亮)[126], M. T. Mirtorabi[17], R. Moradi[1268], F. Rastegarnia[17], J. A. Rueda[129105], S. R. Zhang (张书瑞)[191112], and Y. Wang (王瑜)[216]

[1] ICRANet, Piazza della Repubblica 10, I-65122 Pescara, Italye-mail: yu.wang@icranet.org, liang.li@icranet.org, ruffini@icra.it
[2] ICRA, Dip. di Fisica, Sapienza Università di Roma, Piazzale Aldo Moro 5, I-00185 Roma, Italy
[3] INAF, Viale del Parco Mellini 84, 00136 Rome, Italy
[4] Université de Nice Sophia-Antipolis, Grand Château Parc Valrose, Nice, CEDEX 2, France
[5] INAF, Istituto di Astrofisica e Planetologia Spaziali, Via Fosso del Cavaliere 100, 00133 Rome, Italy
[6] INAF, Osservatorio Astronomico d'Abruzzo, Via M. Maggini snc, I-64100, Teramo, Italy
[7] Department of Fundamental Physics, Faculty of Physics, Alzahra University, Tehran, Iran
[8] Key Laboratory of Particle Astrophysics, Institute of High Energy Physics, Chinese Academy of Sciences, Beijing 100049, People's Republic of China
[9] ICRANet-Ferrara, Dip. di Fisica e Scienze della Terra, Università degli Studi di Ferrara, Via Saragat 1, I–44122 Ferrara, Italy
[10] Dip. di Fisica e Scienze della Terra, Università degli Studi di Ferrara, Via Saragat 1, I–44122 Ferrara, Italy
[11] School of Astronomy and Space Science, University of Science and Technology of China, Hefei 230026, China
[12] CAS Key Laboratory for Research in Galaxies and Cosmology, Department of Astronomy, University of Science and Technology of China, Hefei 230026, China

June 6, 2024

ABSTRACT

The observation of a gamma-ray burst (GRB) associated with a supernova (SN) coincides remarkably with the energy output from a binary system comprising a very massive carbon-oxygen (CO) core and an associated binary neutron star (NS) by the Binary-Driven Hypernova (BdHN) model. The dragging effect in the late evolution of such systems leads to co-rotation, with binary periods on the order of minutes, resulting in a very fast rotating core and a binary NS companion at a distance of $\sim 10^5$ km. Such a fast-rotating CO core, stripped of its hydrogen and helium, undergoes gravitational collapse and, within a fraction of seconds, leads to a supernova (SN) and a newly born, fast-spinning neutron star (νNS), we name the emergence of the SN and the νNS as the SN-rise and νNS-rise. Typically, the SN energies range from 10^{51} to 10^{53} erg. We address this issue by examining 10 cases of Type-I BdHNe, the most energetic ones, in which SN accretion onto the companion NS leads to the formation of a black hole (BH). In all ten cases, the energetics of the SN events are estimated, ranging between 0.18 and 12×10^{52} erg. Additionally, in all 8 sources at redshift z closer than 4.61, a clear thermal blackbody component has been identified, with temperatures between 6.2 and 39.99 keV, as a possible signature of pair-driven SN. The triggering of the X-ray afterglow induced by the νNS-rise are identified in three cases at high redshift where early X-ray observations are achievable, benefits from the interplay of cosmological effects.

1. Introduction

Supernovae (SNe) and gamma-ray bursts (GRBs) are among the most violent stellar events in the universe due to their luminosity and energy. These cataclysmic phenomena not only reshape their immediate cosmic neighborhood but also offer vital clues about the life cycle of stars, the interstellar medium, and the dynamics of galaxy evolution. A particularly intriguing subclass of these events involves the simultaneous occurrence of a Type Ic supernova (SN Ic) and a long-duration gamma-ray burst (Aimuratov et al. 2023; Woosley & Bloom 2006), a scenario that challenges our understanding of stellar evolution and explosion mechanisms.

Historically, simultaneous observation of SN Ic and GRBs has been rare, in total around 30 events up to now, with the first case being GRB 980425 / SN 1998bw (Galama et al. 1998). These events have prompted intense observational campaigns and theoretical efforts to understand the connection between supernovae and GRBs. The BdHN model, in particular, provides a framework to interpret these observations, suggesting that the co-evolution of a CO core and a neutron star (NS) in a close binary system can lead to such dual explosions (Rueda & Ruffini 2012; Fryer et al. 2014; Becerra et al. 2015; Fryer et al. 2015; Becerra et al. 2016; Cipolletta et al. 2017; Becerra et al. 2018, 2019; Rueda et al. 2021).

The BdHN process, which includes the formation of a Type Ic supernova (SN Ic) and the associated gamma-ray burst (GRB), is initiated by the gravitational collapse of the carbon-oxygen (CO) core of a massive star. This event's early detection, specifically the first emergence of the supernova linked to the CO core collapse (termed as the SNrise), is referred to as Episode I.

This initial episode possesses a lower luminosity, ranging from 10^{51} to 10^{52} erg s^{-1} , compared to subsequent episodes. It precedes the remaining episodes by a time interval varying from a few seconds to around 100 seconds. The specific characteristics of this event depend on numerous factors, such as the GRB's energy, the distance to the source, and notably the functionality of the multi-wavelength detectors at the unpredictable moment when the gravitational collapse occurs.

In the previous paper (Ruffini et al. 2021), we suggested that this episode one signal might have been present in three specific GRBs (GRB 160625B , GRB 221009A and GRB 220101A). In this article, we extend our study to cover 10 sources, here indicated by their time of appearance, and perform a comprehensive spectral analysis to further confirm and investigate this phenomenon.

The article is structured as follows: Section 2 presents a review of the physical background underlying the BdHN model, including three types of BdHNe and the seven episodes of BdHN. Section 3 describes the observational data and the analysis of each GRB, we focus on the thermal component found in the SN-rise. Section 4 summarizes this study and outlines potential directions for future research.

2. Binary Driven Hypernova

The BdHN suggests that GRBs originate from a binary system comprising a carbon-oxygen star and a neutron star. When the carbon-oxygen core collapses, it triggers a hypernova, resulting in a fast-spinning new neutron star at the center. Depending on the orbital separation of the binary system, different types of BdHN events occur, characterized by varying energy outputs and mechanisms.

1. **BdHN I**: Occurs in systems with very short orbital periods (approximately 4-5 minutes) and involves extremely high energies ranging from 10^{52} to 10^{54} ergs. The high energy is due to the accretion of supernova ejecta onto a companion NS, leading to the formation of a BH. BdHN I is typically associated with hypernova (HN) with energy around 10^{52} ergs (Ruffini et al. 2015).
2. **BdHN II**: Characterized by longer orbital periods (about 20 minutes) and lower energy outputs ranging from 10^{50} to 10^{52} ergs. In these systems, the NS does not undergo collapse into a black hole, given the comparatively slower accretion rates. This type still leads to significant energetic outputs but at a scale less than that of BdHN I (Rueda et al. 2021).
3. **BdHN III**: Involves even longer orbital periods, up to several hours, and the lowest energy range, below 10^{50} ergs. The accretion rate is minimal, preventing any significant alteration to the neutron star, and likely does not lead to black hole formation. BdHN III events typically occur in systems where the supernova explosion disrupts the binary, with the energy mainly contributed by interactions between the supernova ejecta and the neutron star (Wang et al. 2022).

The BdHN model outlines seven distinct emission episodes. These episodes cover a range of phenomena from the initial SN-rise to later afterglow emissions that follow the major burst even. Each type of BdHN (I, II, III) exhibits a subset of these seven episodes. Seven episodes include:

1. **SN-rise (Episode I)**: This episode involves the gravitational collapse of the Carbon-Oxygen core, leading to a SN explosion and the formation of a new neutron star (ν NS) (Ruffini et al. 2021).
2. **ν NS-rise and SN Ejecta Accretion (Episode II)**: Following the SN, the supernova ejecta begins to accrete onto the newly formed ν NS and the existing neutron star (Wang et al. 2022).
3. **Ultra-high-energy Prompt Emission (UPE) Phase - BH Overcritical (Episode III)**: Hypercritical accretion can cause the existing neutron star in the binary system to accumulate sufficient mass to form a BH. The formation of the BH triggers ultra-relativistic prompt emission, due to the overcritical field near the BH (Ruffini et al. 2015; Moradi et al. 2021).
4. **BH GeV Emission - Undercritical (Episode IV)**: After the UPE phase, the environment near the newly formed BH transitions to a state where high-energy GeV emissions are observable, driven by synchrotron radiation from charged particles accelerated in the undercritical magnetic fields near the BH (Ruffini et al. 2021).
5. **BH Echoes (Episode V)**: Following the BH formation, the environment stabilizes somewhat, allowing for observable emissions known as "BH echoes" which are interactions of the emitted radiation with surrounding matter (Ruffini et al. 2019).
6. **Multiwavelength Afterglow (Episode VI)**: This episode involves the extended emission of X-rays, optical, and radio waves as the ejected material from the supernova interacts with the interstellar medium (Ruffini et al. 2015; Rueda et al. 2020).
7. **The optical SN Emission (Episode VII)**: this episode involves the optical emission from the supernova ejecta powered by the decay of nickel to cobalt Wang et al. (2019b); Aimuratov et al. (2023).

A detailed analysis of 24 Type Ic SNe that are spectroscopically well-identified and associated with long GRBs are analysed in Aimuratov et al. (2023). The SNe display consistent peak luminosities and timing relative to the onset of their associated GRBs. This consistency occurs despite the wide range of energies and redshifts among the GRBs, suggesting a predictable underlying mechanism dictated by the dynamics of the binary systems in the BdHN model.

3. Analysis of Supernova-rise

3.1. GRB 090423

GRB 090423 was detected on April 23, 2009, and it has been classified as one of the most distant cosmic explosions ever observed. With a redshift of z = 8.2, it happened when the universe was just about 630 million years old (or roughly 4% of its current age).

Swift-BAT triggered on GRB 090423 at 07:55:19 UT. The event had a double-peaked structure with a duration of about 20 seconds and a peak count rate of 2000 counts/sec in the 15-350 keV range (see top panel of Fig. 1). Swift's X-Ray Telescope (XRT) began observations 72.5 seconds post-trigger, identifying a fading X-ray source (Krimm et al. 2009) (see Fig. 2). The *Fermi* Gamma-Ray Burst Monitor (GBM) triggered on GRB 090423 as well, with a light curve showing a single structured peak with a duration (T_{90}) of about 12 seconds (von Kienlin 2009a).

The initial discussion on the redshift of GRB 090423 was approximately $z \sim 9$ based on early NIR observations and spectral analysis (Cucchiara et al. 2009b,a). However, more refined measurements and analyses have determined the redshift of GRB 090423 more accurately to be $z = 8.2$ through spectroscopic observations (Tanvir et al. 2009; Riechers et al. 2009). This makes GRB 090423 one of the most distant cosmic explosions ever observed and a highly significant object for understanding the early universe. The isotropic equivalent energy ($E_{\rm iso}$) in the $8-1000$ keV band was calculated as $(1.0\pm0.3)E{+}53$ ergs (von Kienlin 2009a,b)

Due to the high redshift, it fell outside the capacity of LAT for high energy observation and the optical telescopes for the confirmation of supernova. However, due to the high brightness of early X-rays, the Swift-XRT remains capable of detecting the radiation from high-redshift GRBs. Additionally, because the universe's expansion stretches the timescale of high-redshift GRBs in the observer's frame, Swift has sufficient time to reorient and capture the initial tens of seconds radiation measured in the rest-frame, see more examples in Bianco et al. (2023).

A first analysis of GRB 090423 within the BdHN model was presented in Ruffini et al. (2014).

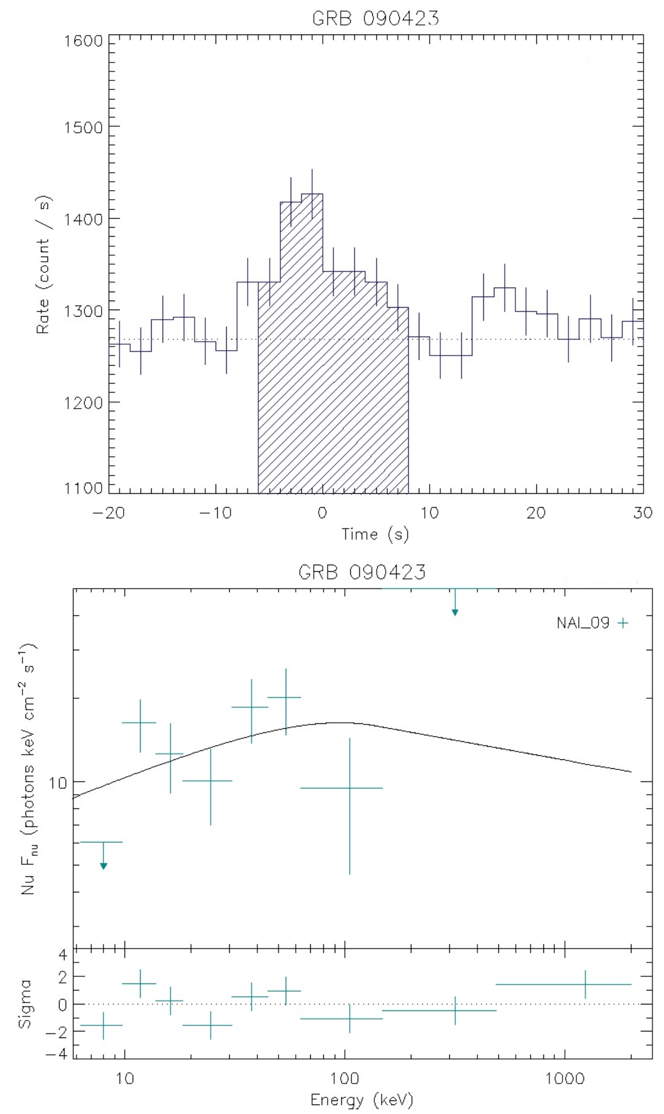

Fig. 1. Top: GRB 090423 light-curve, shadow part indicates the period of episode 1. Bottom: the spectrum of episode 1, fitted by a cutoff power-law function.

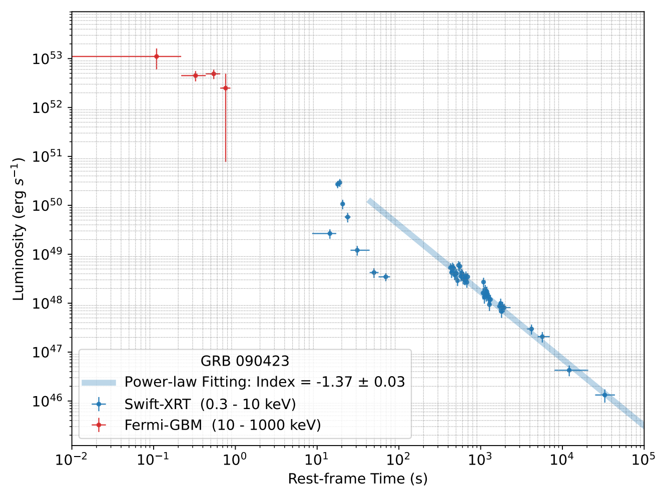

Fig. 2. Luminosity light-curve of GRB 090423, including the prompt emission and the afterglow, observed by Fermi-GBM and Swift-XRT, respectively.

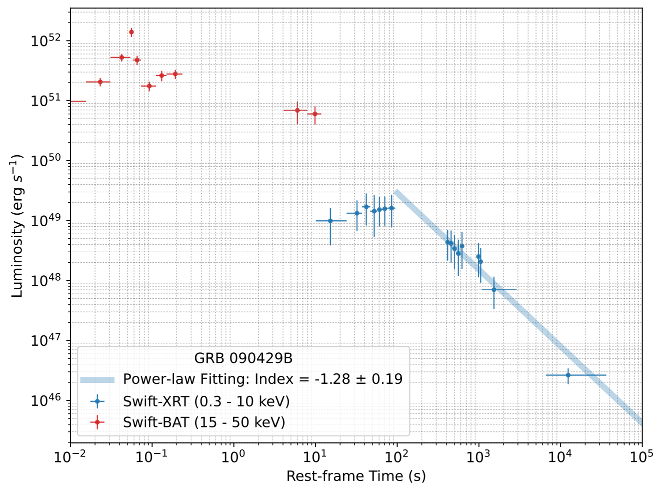

Fig. 3. Luminosity light-curve of GRB 090429B, including the prompt emission and the afterglow, observed by Swift-BAT and Swift-XRT, respectively.

GRB 090423 exhibits its first SN-rise episode takes place from approximately -5.5 to 7.4 seconds in the observed frame, which corresponds to -0.6 to 0.8 seconds in the cosmological rest frame, lasting 1.4 seconds. The spectrum is best fitted by a cutoff power-law function peaking at 80 keV. The isotropic equivalent energy released during the supernova rise is 1.6×10^{53} ergs. The black body temperature is not recognized due to its high redshift (see Fig. 1).

3.2. GRB 090429B

GRB 090429B was detected on April 29, 2009, by the Swift satellite. The burst duration was short among the long GRBs, just about 5 seconds, yet it was extremely bright (Ukwatta et al. 2009). Although the optical afterglow was faint, the Gemini-North telescope was able to capture its near-infrared spectrum (Cucchiara et al. 2009c; Levan et al. 2009). The GROND (Gamma-Ray burst Optical/Near-Infrared Detector) at the MPG/ESO 2.2-meter telescope in La Silla, Chile, carried out multicolor imaging (Levan et al. 2009). This burst was not detected by Fermi.

Analysis of 8.9 ks of XRT data, covering from 104 s to 29.9 ks post the BAT trigger, reveals an initial light curve ascent fitted by a power-law index of $0.89^{+0.36}_{-0.46}$, transitioning at $T + 642$ s to a decay phase with an index of $1.20^{+0.11}_{-0.10}$ (see Fig. 3). Spectral fitting indicates an absorbed power-law photon index of $2.00^{+0.15}_{-0.24}$, with absorption exceeding Galactic levels (Rowlinson & Ukwatta 2009).

The key discovery related to GRB 090429B was its estimated redshift. Due to the faintness of the afterglow and the lack of spectral features, it was impossible to determine the redshift directly through spectroscopic methods. Instead, the photometric redshift estimation is applied, a technique that uses the broad-band colors to estimate its redshift. The photometric data strongly suggested a high redshift for this burst, with an initial estimation of z = 9.4, which would place the GRB's origin just 520 million years after the Big Bang (Cucchiara et al. 2011). This high redshift implies that GRB 090429B can provide valuable insights into the early universe, including the formation of the first stars and galaxies.

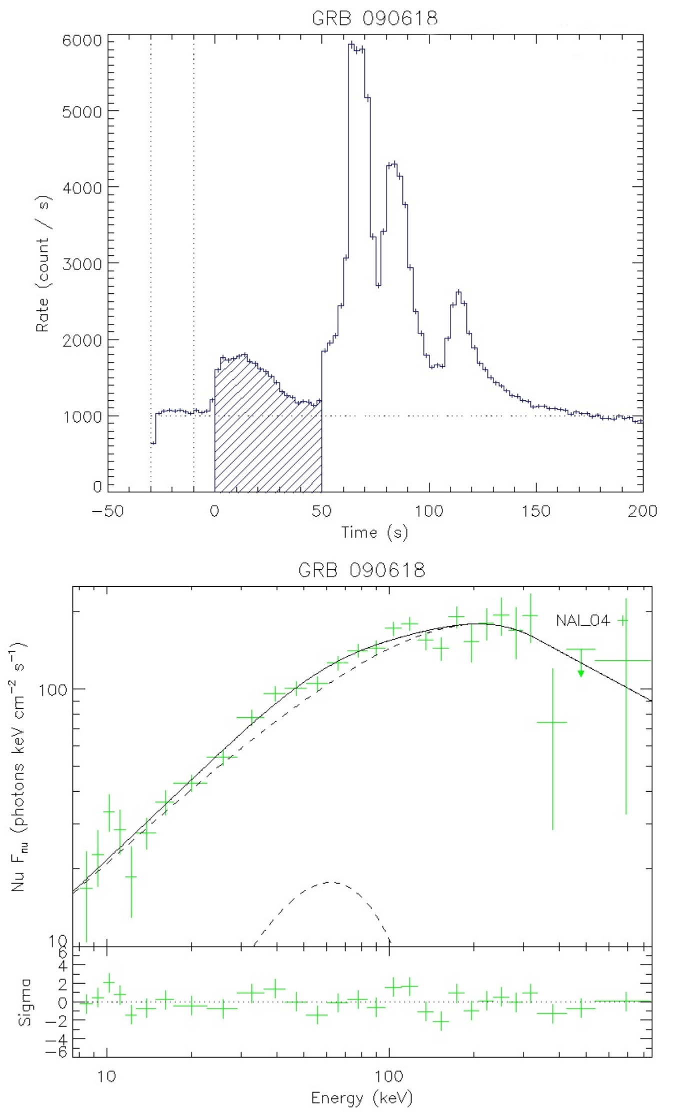

Fig. 4. Top: GRB 090618 light-curve, shadow part indicates the period of episode 1. Bottom: the spectrum of episode 1, fitted by the Band function plus a blackbody component, the observed temperature is 15.86 keV.

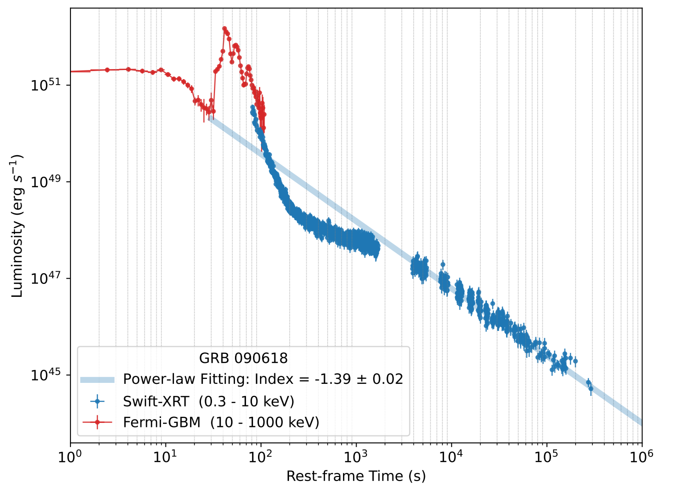

Fig. 5. Luminosity light-curve of GRB 090618, including the prompt emission and the afterglow, observed by Fermi-GBM and Swift-XRT, respectively.

This GRB shows its SN-rise episode lasting 0.96 seconds in the rest frame, spanning 0 to 10 seconds observed. It's spectrum is fitted by a cutoff powerlaw function and isotropic energy released is 3.5×10^{52} ergs. The black body component has not been resolved due to its high redshift.

3.3. GRB 090618

GRB 090618 was initially detected by the Swift satellite, Swift-BAT observation shows the multi-peak structure of its light curve, indicating a duration of about 130 seconds with a peak count rate of $\sim$ 40000 counts/s (15-350 keV) at 80 sec after the trigger (see top panel of Fig. 4). Swift-XRT observed this source at 120.9 seconds after the BAT trigger (see Fig. 5). Swift-UVOT observations identified the optical afterglow with an estimated magnitude of 14.36 in the white filter, 128 seconds post-trigger (Schady et al. 2009).

The time-averaged spectrum from T_0 to T_0 + 140 s from Fermi observation can be adequately fit by a Band function, with a peak energy $E_{\rm peak}$ = 155.5 keV, a low-energy photon index $\alpha = -1.26$, and a high-energy photon index $\beta = -2.50$ (McBreen 2009) (see Fig. 5). This suggests significant spectral evolution within the observed time interval. The isotropic energy ($E_{\rm iso}$) estimated from the GBM data is $2.0E + 53$ erg in the 8-1000 keV band, positioning GRB 090618 as one of the energetically significant bursts observed by Fermi. The boresight angle of Fermi-LAT is 133 degrees, out of capacity of detecting GeV photons (McBreen 2009).

The AGILE satellite detected GRB 090618 with its MCAL instrument, providing a complementary spectral analysis: The total MCAL spectrum between T_0 and T_0 + 120 sec could be fit by a simple power law with a photon index of 3.16, in the 0.5-10 MeV energy range, highlighting the burst's brightness below a few MeV and the lack of significant gamma-ray emission above 30 MeV (Longo et al. 2009).

This burst has been extensively studied within the context of the BdHN model, as elucidated by Izzo et al. (2012b,a, 2013). Their analysis divides the GRB into two distinctive episodes: an initial spike due to the supernova explosion and neutron star formation, a later phase associated with the formation of the black hole.

This GRB's first episode spans 0 to 47.7 seconds in the observed frame, which translates to 0 to 31 seconds in the rest frame and lasts 31 seconds, of which the spectrum is best fitted by the Band function plus a blackbody component, the integrated isotropic energy is 3.61×10^{52} ergs, and the observed black body temperature is 15.86 keV (see Fig. 4).

3.4. GRB 130427A

GRB 130427A, detected on April 27, 2013, was one of the most energetic and brightest GRBs ever observed as of 2021. It was initially detected by the Neil Gehrels Swift Gamma-Ray Burst Mission (Maselli et al. 2013), Fermi Gamma-ray Space Telescope (von Kienlin 2013), and INTEGRAL (INTErnational Gamma-Ray Astrophysics Laboratory) (Pozanenko et al. 2013), and subsequently observed across multiple wavelengths by numerous ground and space-based observatories around the world. Using the Gemini-North / GMOS telescope, the observed high-quality spectra revealed absorption lines for Ca H and K, Mg I, and the Mg II doublet at a redshift of z=0.34 (Levan et al. 2013).

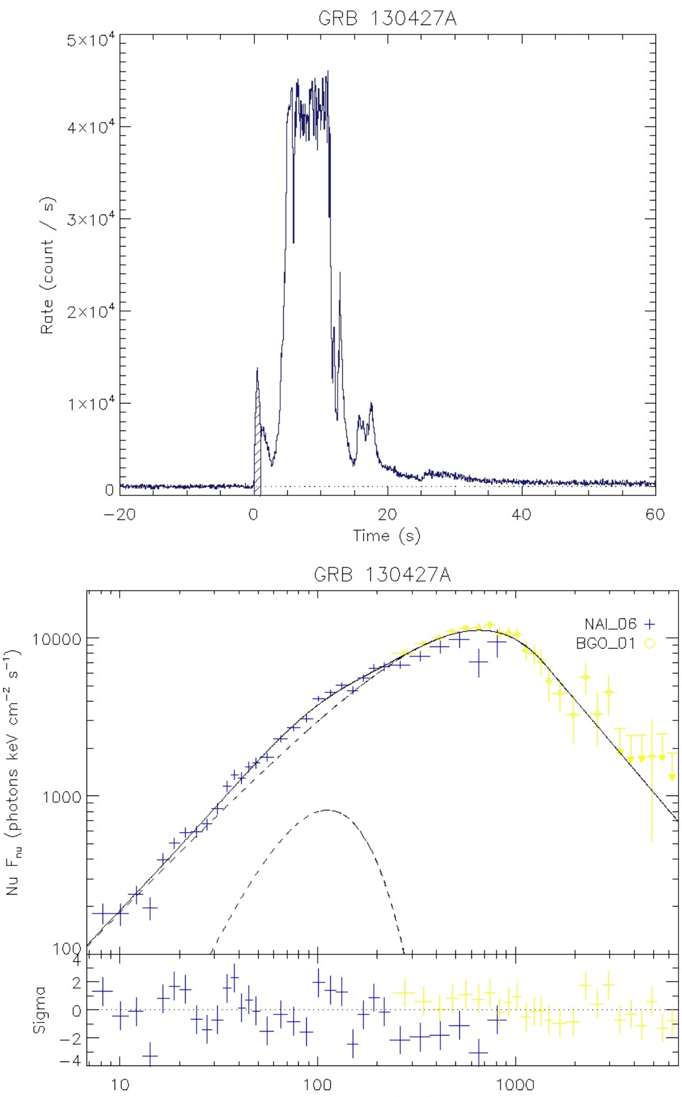

Fig. 6. Top: GRB 130427A light-curve, shadow part indicates the period of episode 1. Bottom: the spectrum of episode 1, fitted by the Band function plus a blackbody component, the observed temperature is 28.66 keV.

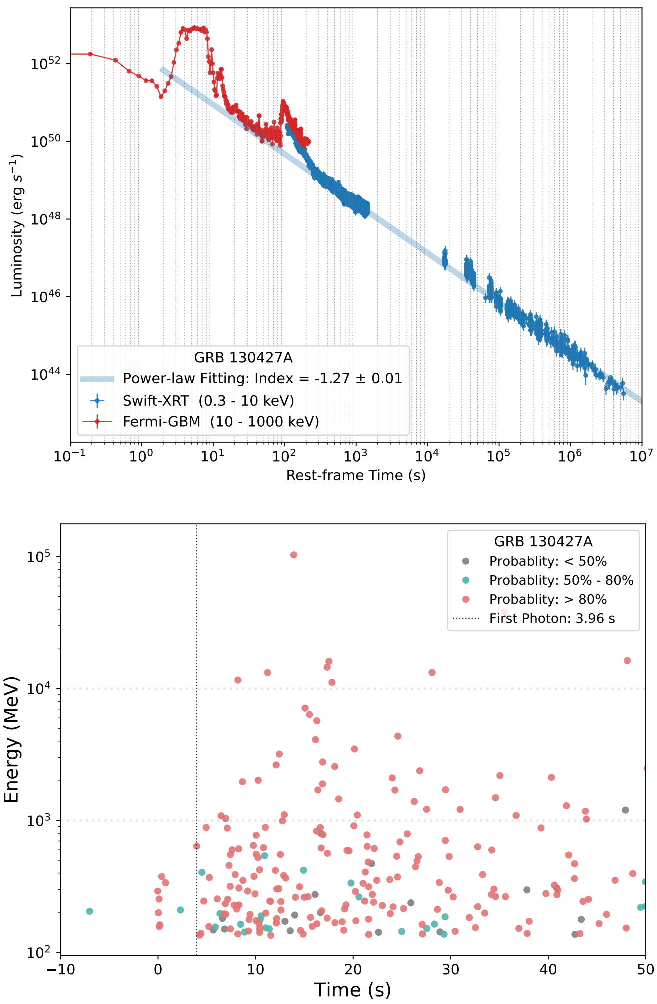

Fig. 7. Top: Luminosity light-curve of GRB 130427A, including the prompt emission and the afterglow, observed by Fermi-GBM and Swift-XRT, respectively. Bottom: GeV photons observed by Fermi-LAT.

The GBM light curve features a bright structured peak and a FRED-like (Fast Rise Exponential Decay) pulse approximately 120 seconds after the trigger. The overall duration (T_{90}) of the burst, covering the energy range 50-300 keV, is about 138 seconds (see top panel of Fig. 6 and top panel of Fig. 7)). Spectral analysis using a Band function fit for the interval from $T_0+0.002$ s to $T_0 + 18.432$ s provided parameters of $E_{\rm peak} = 830 \pm 5$ keV, $\alpha = -0.789 \pm 0.003$, and $\beta = -3.06 \pm 0.02$. However, due to the burst's brightness, systematic effects were significant, and no single model was found to adequately fit the data. The fluence in the 10-1000 keV range for the specified time interval is reported as $(1.975 \pm 0.003) \times 10^{-3}$ erg/cm^2, and the 1.024-second peak photon flux starting from $T_0 + 7.48808$ s in the 8-1000 keV band is $10^{52} \pm 2$ photons/s/cm^2. An isotropic-equivalent radiated energy of $(1.05 \pm 0.15) \times 10^{54}$ erg (1-10000 keV cosmological rest-frame) is obtained (see bottom panel of Fig. 6). These measurements indicate that GRB 130427A is the most intense and fluent GRB detected by Fermi GBM up to that point (von Kienlin 2013; Amati et al. 2013).

At the time of the trigger, the burst was approximately 47 degrees from the LAT boresight but remained within the LAT's field of view for the subsequent 700 seconds. The Fermi LAT data revealed a multi-peaked light curve that aligns with the GBM trigger, with more than 200 photons above 100 MeV observed within the first 100 seconds, boasting a Test Statistic (TS) of greater than 1000. Remarkably, the highest energy photon recorded by the LAT for this burst had an energy of 94 GeV (Zhu et al. 2013) (see bottom panel of Fig. 7).

These comprehensive observations across the electromagnetic spectrum, from radio to gamma-rays, have made GRB 130427A one of the best-studied GRBs, providing a wealth of data for theoretical models like the binary-driven hypernova (BdHN) model (see, e.g., Ruffini et al. 2015; Wang et al. 2019b; Rueda et al. 2020; Li et al. 2023, and references therein), to explain the complex processes during and after the explosion.

The SN-rise episode of this GRB lasts only 0.65 seconds in the rest frame, occurring from 0 to 0.9 seconds observed, in which the spectrum is best fitted by a Band function plus a blackbody component. It releases a modest 0.65×10^{52} ergs of energy, with a notably high black body temperature of 28.66 keV (see Fig. 6).

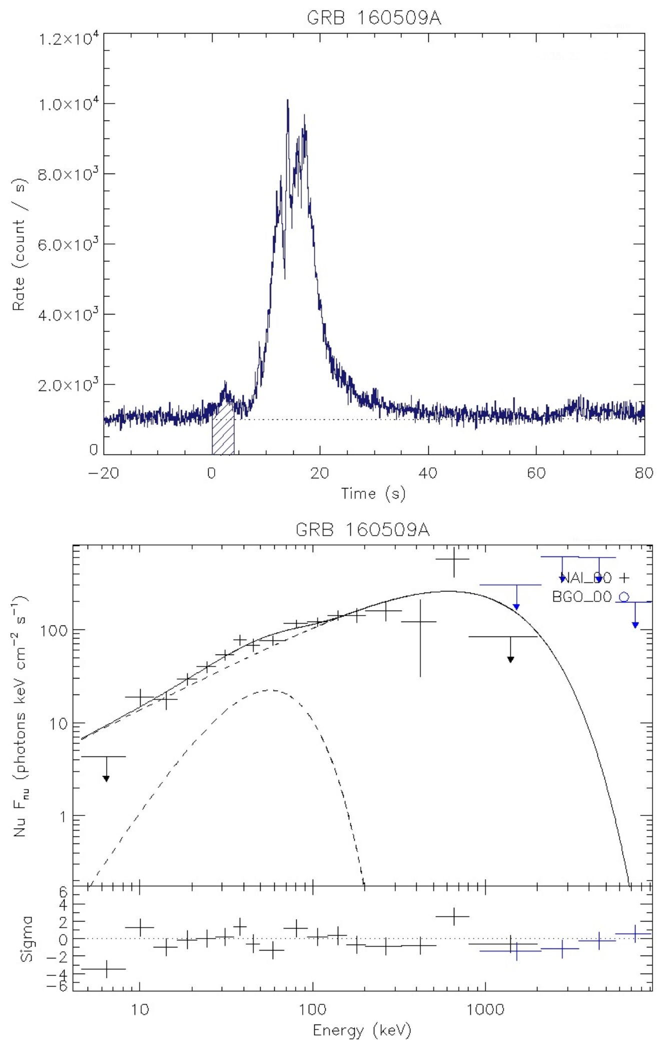

Fig. 8. Top: GRB 160509A light-curve, shadow part indicates the period of episode 1. Bottom: the spectrum of episode 1, fitted by the cutoff power-law plus a blackbody component, the observed temperature is 14.43 keV.

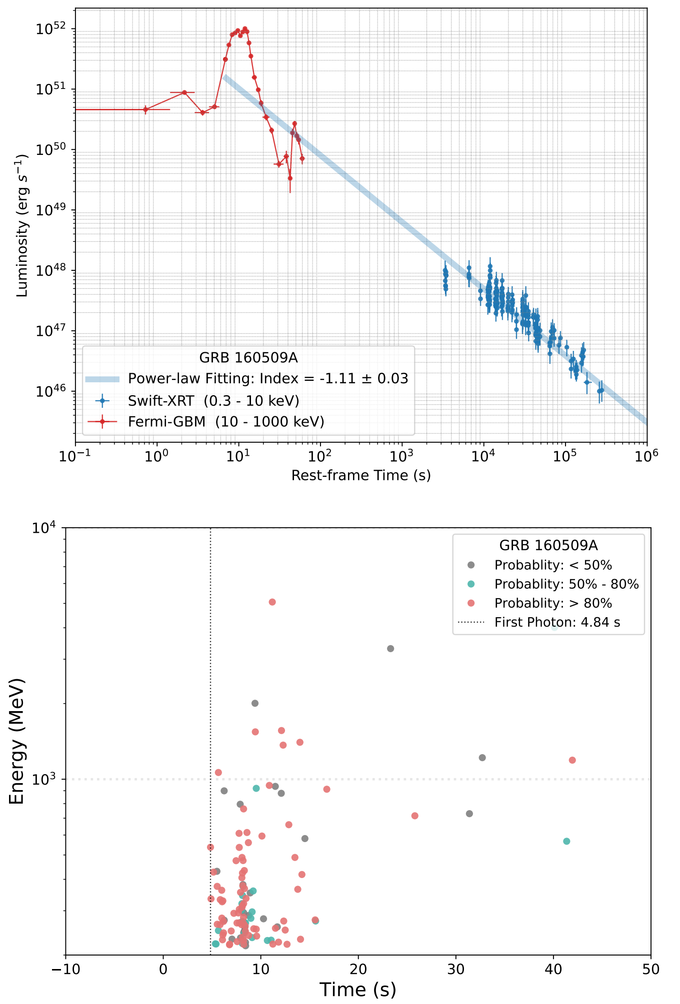

Fig. 9. Top: Luminosity light-curve of GRB 160509A, including the prompt emission and the afterglow, observed by Fermi-GBM and Swift-XRT, respectively. Bottom: GeV photons observed by Fermi-LAT.

3.5. GRB 160509A

GRB 160509A is a long gamma-ray burst detected at 08:59:04.36 UTC on May 09, 2016 by Fermi-LAT (Longo et al. 2016a). It also triggered Fermi-GBM (Roberts et al. 2016) and Swift (Kennea et al. 2016) (see top panel of Fig. 8). It shows two gamma-ray pulses separated at about 3 second and has an afterglow lasting weeks.

The Fermi GBM light curve displayed multiple peaks over a duration (T90) of about 371 seconds. The time-averaged spectrum of the initial bright 40 s was best fit by a Band function, with $E_{\rm peak}$ = 370 ± 7 keV, *alpha* = −0.89 ± 0.01, and *beta* = −2.11 ± 0.02. The event's fluence (10-1000 keV) was $(1.51 \pm 0.01) \times 10^{-4}$ erg cm^{-2}, and the peak photon flux was 75.5 ± 0.6s cm^{-2} (Roberts et al. 2016).

Swift-XRT conducted follow-up observations on GRB 160509A in a series of 7 tiles totaling 1.7 ks of exposure time, with the longest single exposure being 560 seconds (see top panel of Fig. 9). The spectrum obtained from PC mode data fits an absorbed power-law model with a photon spectral index of 1.7 ± 0.3 and an absorption column density of $4.6^{+2.3}_{-1.8} \times 10^{21}$ cm^{-2} (Kennea et al. 2016).

Utilizing Fermi-LAT events of greater than 100 MeV from 0 until 2660 seconds after the trigger, refined the burst's localization and detected a 52 GeV photon, 77 seconds post-trigger (see bottom panel of Fig. 9). The high-energy emission was characterized by a soft power-law with an index of −3.4 ± 0.2 during the main GBM emission episode, transitioning to a harder index of −2.0 ± 0.1 afterwards (Longo et al. 2016b).

The analysis of GRB 160509A within the BdHN model has been presented in Rueda et al. (2020); Li et al. (2023).

The first episode of this burst is observed from 0 to 4.0 seconds , translating to 0 to 1.84 seconds in the rest frame, with a duration of 1.84 seconds. The spectrum of this episode is fitted by a cutoff power-law plus a thermal component. It releases 1.47×10^{52} ergs of energy, and the observed black body temperature is 14.43 keV (see Fig. 8).

3.6. GRB 160625B

On June 25, 2016, at 22:40:16.28 UT, the NASA Fermi Gamma-ray Space Telescope's GBM was triggered by GRB 160625B (Burns 2016a) (see top panel of Fig. 10). The Fermi-LAT started its observation 188.54 seconds post-trigger, detecting over 300 photons with energy exceeding 100 MeV, with the highest photon energy around 15 GeV (Dirirsa et al. 2016) (see bottom panel

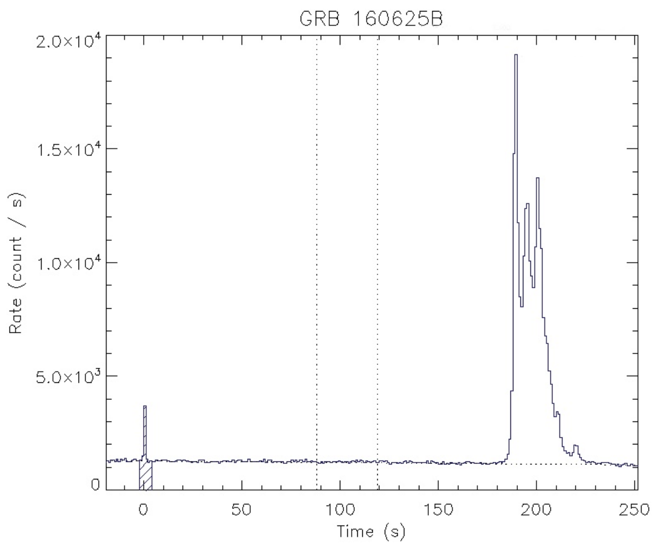

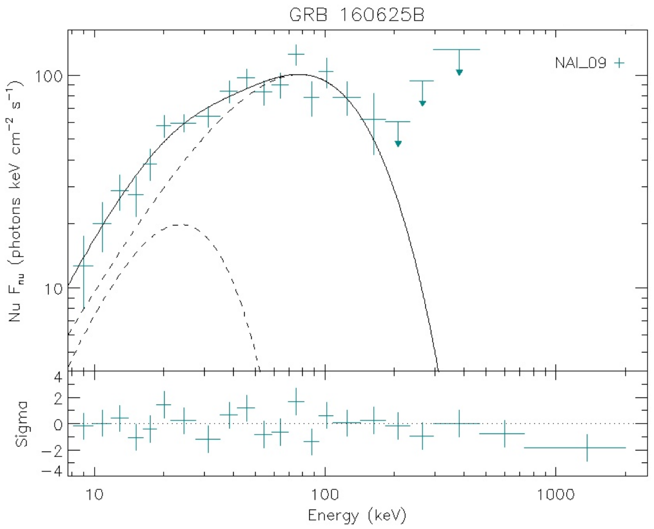

Fig. 10. Top: GRB 160625B light-curve, shadow part indicates the period of episode 1. Bottom: the spectrum of episode 1, fitted by the cutoff power-law plus a blackbody component, the observed temperature is 6.025 keV.

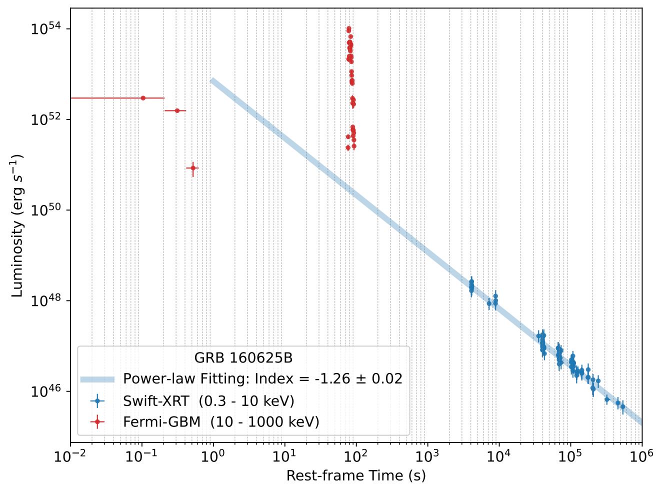

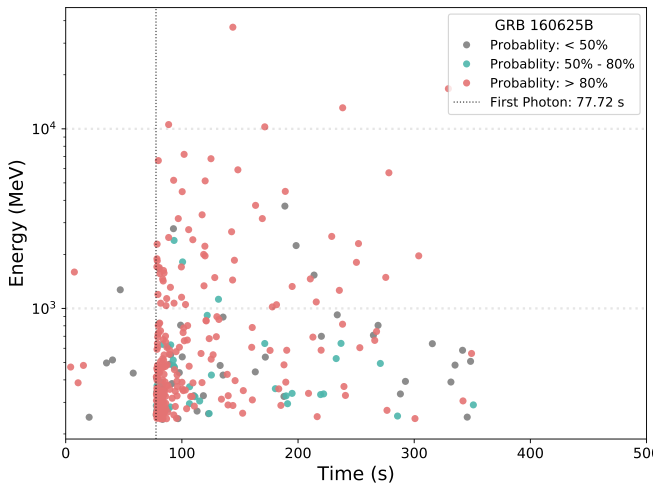

Fig. 11. Top: Luminosity light-curve of GRB 160625B, including the prompt emission and the afterglow, observed by Fermi-GBM and Swift-XRT, respectively. Bottom: GeV photons observed by Fermi-LAT.

of Fig. 11). The Swift-XRT began its observation later, discovering a power-law behavior with a decaying index of approximately -1.25 (Melandri et al. 2016). The redshift $z = 1.406$ is reported (Xu et al. 2016; D'Elia et al. 2016) (see top panel of Fig. 11). GRB 160625B is among the most energetic GRBs, with an isotropic energy of about $3{\times}10^{54}$ erg (Xu et al. 2016). GRB 160625B is a bright GRB with detectable polarization (Troja et al. 2017). Due to its high redshift, $z > 1$, there is no associated supernova confirmation.

The GBM light curve of GRB 160625B showcases multiple peaks, with a total T_{90}

duration of approximately 460 seconds in the 50-300 keV range (see top panel of Fig. 10). The initial GBM trigger was due to a soft peak lasting about 1 second. Spectral analysis of this phase reveals a power-law function with an exponential cutoff, characterized by a power-law index of -0.2 ± 0.1 and a cutoff energy ($E_{\rm peak}$) of 68 ± 1 keV. The fluence during this interval was $(1.65 \pm 0.03) \times 10^{-6}$ erg/cm^2. The main peak, responsible for the LAT trigger, extended for about 25 seconds. Its spectrum fits well with a Band function, showing an $E_{\rm peak}$ of 657 ± 5 keV, an alpha of -0.74, and a beta of 2.36 ± 0.01. The fluence in this period was $(5.00 \pm 0.01) \times 10^{-4}$ erg/cm^2 (Burns 2016b) (see bottom panel of Fig. 10).

The early emission can be categorized into three episodes as suggested by several independent studies: a short precursor (G_1), a main burst (G_2), and a long-lasting tail (G_3). A significant and variable linear optical polarization in G_2 was detected, and it was inferred that the GRB outflows might be dominated by Poynting flux, where the magnetic energy dissipates quickly before the magnetic reconnection, resulting in bright gamma rays. A meticulous time-resolved analysis revealed an evolution of the thermal component in G_1. The bright G_2 episode was divided into 71 slices, each with at least 2500 net counts, for a detailed time-resolved spectral analysis. All slices fit a Band function; no thermal component was determined. G_3 is faint, and its time-resolved spectra were fitted by a single power law or cutoff power laws. The spectral evolution from thermal to nonthermal suggests a transition of the outflow from fireball to Poynting-flux-dominated.

The analysis of GRB 160625B within the BdHN model has been presented in Rueda et al. (2020); Li et al. (2023).

The SN-rise episode of this GRB lasts from -1.2 to 3.1 seconds observed (-0.5 to 1.3 seconds in the rest frame), lasting 0.75 seconds. The burst emits 1.04×10^{52} ergs and has a lower black body temperature of 6.025 keV (see Fig. 10).

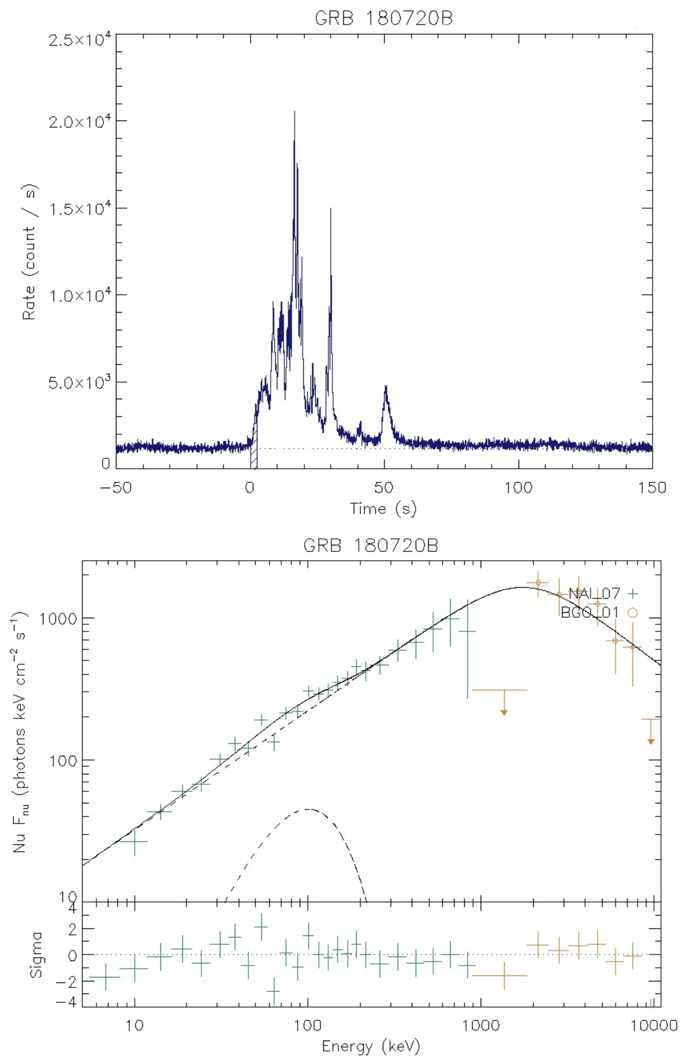

Fig. 12. Top: GRB 180720B light-curve, shadow part indicates the period of episode 1. Bottom: the spectrum of episode 1, fitted by the Band function plus a blackbody component, the observed temperature is 17.67 keV.

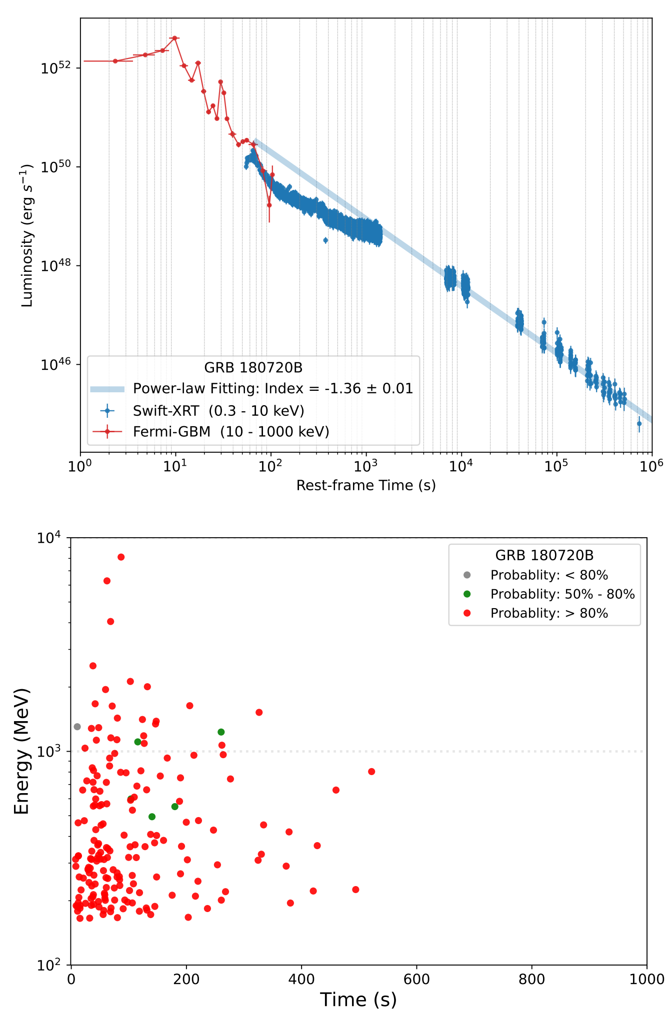

Fig. 13. Top: Luminosity light-curve of GRB 180720B, including the prompt emission and the afterglow, observed by Fermi-GBM and Swift-XRT, respectively. Bottom: GeV photons observed by Fermi-LAT.

3.7. GRB 180720B

GRB 180720B was detected by Swift BAT on July 20, 2018, at 14:21:44 UT. BAT shows a multi-peaked light curve with a duration of ∼ 150 s and a peak count rate of $\sim 5 \times 10^4$ counts/s (see top panel of Fig. 12). XRT observation began 86.5 s after BAT trigger, locating the X-ray afterglow at RA = 00h 02m 6.70s, Dec = -02d 55' 01.2", with an uncertainty of 5.0 arcseconds (Siegel et al. 2018) (see top panel of Fig. 13). An optical counterpart within the XRT error circle with a magnitude of $R \sim 9.4$ mag 73 s after the trigger by Kanata telescope at Higashi-Hiroshima Observatory, indicating a bright optical afterglow (Sasada et al. 2018). The absorption features were identified corresponding to a redshift of $z = 0.654$ by ESO's VLT/X-shooter (Vreeswijk et al. 2018).

The Fermi GBM triggered almost simultaneously with Swift BAT, providing a detailed light curve and spectral analysis of the burst (Roberts & Meegan 2018). The GBM light curve displayed a very bright, FRED-like peak with numerous overlapping pulses, lasting a duration (T90) of 49 s in the 50-300 keV range. Spectral analysis from GBM data revealed a time-averaged spectrum best fit by a Band function, with peak energy $E_p = 631 \pm 10$ keV, lower photon index $\alpha = -1.11 \pm 0.01$, and higher photon index $\beta = -2.30 \pm 0.03$. The event's fluence (10-1000 keV) over the T90 interval was reported as $(2.985 \pm 0.001)10^{-4} erg\ cm^{-2}$. The 1-sec peak photon flux measured starting from T0+4.4 s in the 10-1000 keV band was $125 \pm 1 s^{-1} cm^{-2}$. The isotropic energy released is $E_{iso} = 6.82(-0.22, 0.24) \times 10^{53}$ erg (Cherry et al. 2018).

The Very-High-Energy (VHE) emission from GRB 180720B was first announced by Ruiz-Velasco at the 1st International CTA Symposium in May 2019. The High Energy Stereoscopic System (H.E.S.S.) observations revealed a new gamma-ray source ranging from 100-440 GeV at time about 10 hours post-burst, pinpointing the emission's origin close to the identified GRB location at other wavelengths. Follow-up observations under similar conditions 18 days later showed a background-consistent sky map, effectively ruling out associations with steady gamma ray emitters like active galactic nuclei or persistent systematic effects, thereby reinforcing the link between the VHE emission and GRB 180720B (Wang et al. 2019a; Abdalla et al. 2019) (see bottom panel of Fig. 13).

The analysis of GRB 180720B within the BdHN model has been presented in Rueda et al. (2022); Ruffini (2022).

This GRB's first episode spans 0 to 2.5 seconds observed, translating to 0 to 1.51 seconds in the rest frame, and lasts 1.51

seconds. Its spectrum is fitted by a Band function plus a blackbody. It releases $1.6 \pm 0.3 \times 10^{52}$ ergs of energy, with a black body temperature of 17.67 keV (see Fig. 12).

3.8. GRB 190114C

GRB 190114C was detected on January 14, 2019 (Gropp et al. 2019), and sparked significant interest due to its brightness and the detection of high-energy emissions, including VHE gamma-ray emissions observed by the MAGIC telescope (Mirzoyan et al. 2019).

The Swift Burst Alert Telescope (BAT) triggered on the burst at 20:57:03 UT, locating it with coordinates RA = 03h 38m 02s, Dec = -26d 56' 18" (J2000). Swift's X-Ray Telescope (XRT) began observing 64.0 seconds after the BAT trigger, identifying a bright X-ray source within the BAT error circle. The Ultraviolet/Optical Telescope (UVOT) detected a candidate afterglow in its imaging (Gropp et al. 2019). Optical telescopes, including MASTER, Nordic Optical Telescope (NOT), and others, provided early-time optical observations and spectroscopy, identifying the optical counterpart and determining a redshift of $z = 0.42$ (Selsing et al. 2019; Castro-Tirado et al. 2019). Observations in the radio, infrared, and sub-millimeter bands were conducted, including with the VLA, ALMA, and ATCA, providing multi-wavelength coverage of the afterglow.

The GBM light curve for GRB 190114C reveals a highly luminous, multi-peaked structure extending to 15 s, succeeded by a less intense pulse from roughly 15 s to 25 s (see top panel of Fig. 14). Fainter emissions are discernible up to about 200 s. The duration, T_{90}, is estimated at approximately 116 s. The time-averaged spectrum from 0 s to 38.59 s can be accurately modeled by a Band function, with $E_{\rm p} = 998.6 \pm 11.9$ keV, $\alpha = -1.058 \pm 0.003$, and $\beta = -3.18 \pm 0.07$. The fluence for the event, within the 10-1000 keV energy band for this time interval, is $(3.99 \pm 0.00081) \times 10^{-4} erg\ cm^{-2}$. The peak photon flux measured starting from $T_0 + 3.84$ seconds in the 10-1000 keV band is $246.86 \pm 0.86\ s^{-1} cm^{-2}$. Utilizing the Band spectral fit and the redshift measurement of $z = 0.42$ (Selsing et al. 2019), the isotropic energy release in gamma-rays, $E_{\rm iso}$, is estimated to be 3×10^{53} erg, and the isotropic peak luminosity, $L_{\rm iso}$, is calculated to be $\sim 10^{53}$erg s^{-1} , within the 1 keV to 10 MeV energy band (Hamburg et al. 2019). Fermi/LAT detected a significant increase in the event rate that is spatially correlated with the GBM trigger with high significance. The highest-energy photon is a 22.9 GeV event which is observed 15 s after the GBM trigger (Kocevski et al. 2019).

The afterglow of GRB 190114C exhibited a power-law decay across X-ray, optical, and radio wavelengths, indicative of synchrotron radiation origination. X-ray observations by Swift-XRT identified a fading afterglow with a decay index of $\alpha_X \approx 1.34 \pm 0.01$, fitting the typical afterglow emission model. The initial X-ray flux, measured 64 seconds post-trigger, was 7.39×10^{-8} erg cm^{-2}s^{-1} in the 0.3-10 keV range (D'Elia et al. 2019) (see top panel of Fig. 15). Optical follow-up revealed that late-time light curve was influenced by an emerging supernova component (Melandri et al. 2019). This supernova, associated with the GRB, peaked at approximately $r \approx 23.9$ mag (AB) in the rest frame, about 15 days post-burst.

GRB 190114C has been extensively studied within the BdHN model (see, e.g., Ruffini et al. 2019; Rueda et al. 2020; Moradi et al. 2021; Ruffini 2022; Li et al. 2023, and references therein).

The SN-rise of this burst spanning 0 to 1.1 seconds observed (0 to 0.79 seconds in the rest frame), and lasts 0.79 seconds,

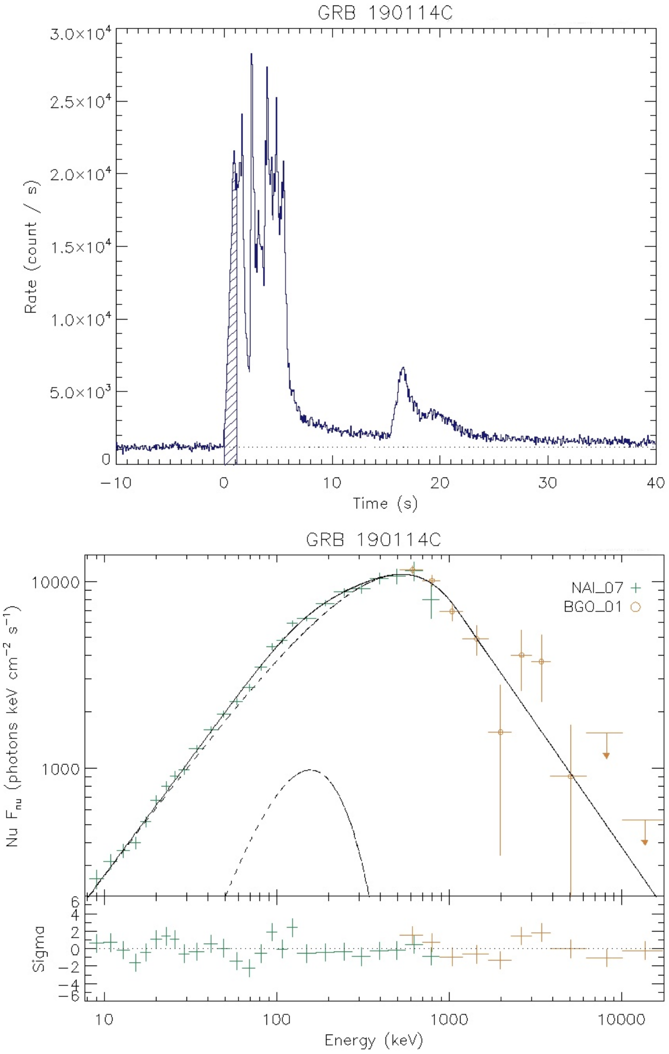

s

Fig. 14. Top: GRB 190114C light-curve, shadow part indicates the period of episode 1. Bottom: the spectrum of episode 1, fitted by the Band function plus a blackbody component, the observed temperature is 39.99 keV.

described by the Band function plus a blackbody component. It emits $3.5 \pm 0.2 \times 10^{52}$ ergs of energy, with a particularly high black body temperature of 39.99 keV (see Fig. 14).

3.9. GRB 220101A

The Swift-BAT detected GRB 220101A at 05:09:55, January 1, 2022 UT. The peak count rate was 7000 counts/s in the 15-350 keV range, approximately 89 seconds after the trigger (see top panel of Fig. 16). The X-Ray Telescope (XRT) began observations 80.8 seconds after the trigger, identifying a bright, uncatalogued X-ray source at RA = 00h 05m 25.46s, Dec = +31d 46' 12.7" with an uncertainty of 4.7 arcseconds (see top panel of Fig. 17). The Ultraviolet/Optical Telescope (UVOT) identified a candidate afterglow with a magnitude of 14.60 in the white filter (Tohuvavohu et al. 2022).

The spectral analysis by Fermi-GBM indicated a best fit with a power law function with an exponential high-energy cutoff, where the power law index was -1.09 ± 0.02, and the cutoff energy ($E_{\rm c}$) was 330 ± 15 keV. A Band function fit was equally well with parameters $E_{\rm p} = 290 \pm 18$ keV, $\alpha = -1.06 \pm 0.02$, and $\beta = -2.3 \pm 0.2$ (Lesage et al. 2022a) (see bottom panel of

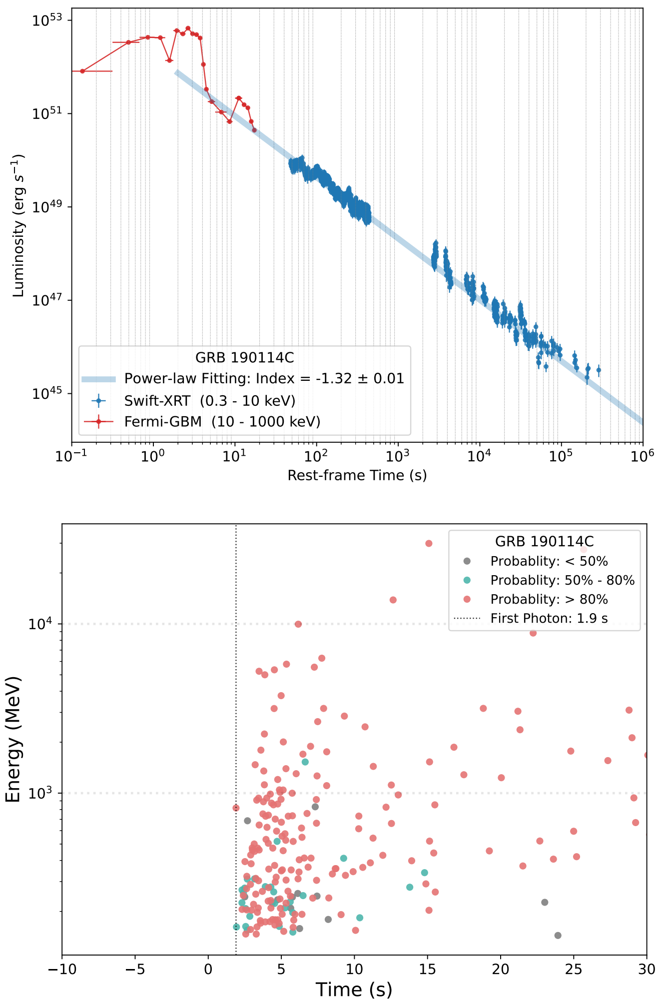

Fig. 15. Top: Luminosity light-curve of GRB 190114C, including the prompt emission and the afterglow, observed by Fermi-GBM and Swift-XRT, respectively. Bottom: GeV photons observed by Fermi-LAT.

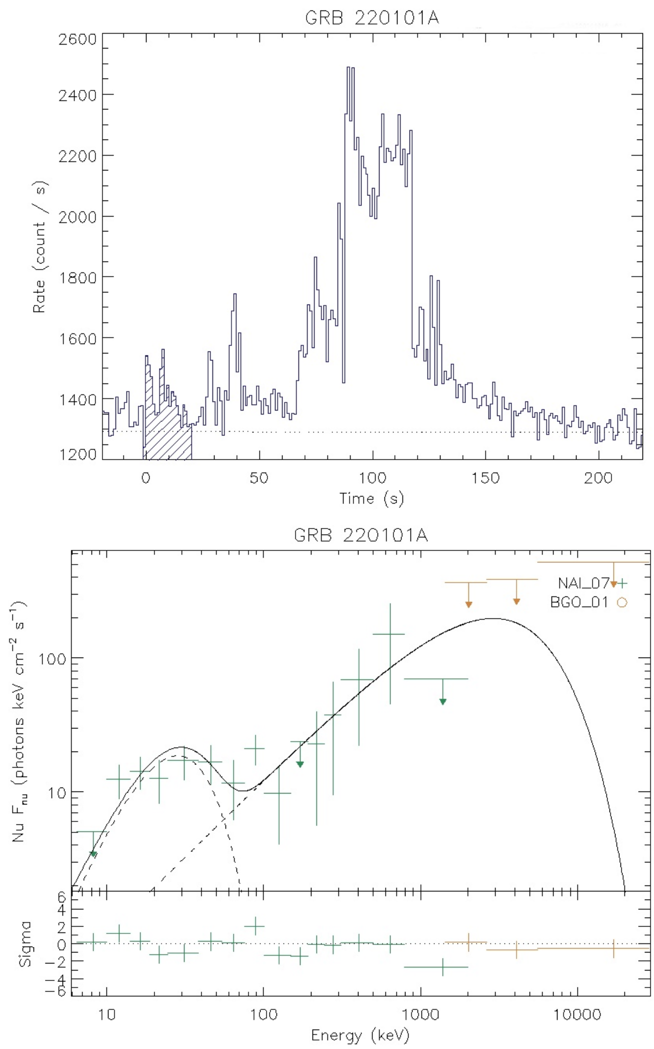

Fig. 16. Top: GRB 220101A light-curve, shadow part indicates the period of episode 1. Bottom: the spectrum of episode 1, fitted by the cutoff power-law plus a blackbody component, the observed temperature is 7.215 keV.

Fig. 16). The GRB has been detected also by AGILE (Ursi et al. 2022). The isotropic energy ($E_{\rm iso}$) was calculated to be approximately 3.7×10^{54} ergs, equating to one of the highest measured isotropic energies for GRBs to date (Atteia 2022; Tsvetkova et al. 2022; Tsvetkova & Konus-Wind Team 2022).

The *Fermi-LAT* detected high-energy emission from GRB 220101A with a photon flux above 100 MeV of $2.5\times10^{-5} \pm 5\times10^{-6}$ph/cm^2/s in the time interval 0-600s after the Swift trigger. The estimated photon index was -2.46 ± 0.25 (Arimoto et al. 2022) (see bottom panel of Fig. 17).

The redshift of GRB 220101A was determined to be z = 4.61, based on spectroscopic observations using the Xinglong-2.16m telescope and the Nordic Optical Telescope (NOT), identifying a broad absorption feature likely corresponding to Lyman-alpha absorption (Fu et al. 2022; Fynbo et al. 2022).

For a preliminary analysis of GRB 220101A within the BdHN model see Bianco et al. (2023).

The first episode of this GRB ranges from -1.0 to 20.0 seconds observed (-0.18 to 3.57 seconds in the rest frame), lasting 3.75 seconds. The spectrum of this episode is fitted by the Band function plus a blackbody component. It releases 1.2×10^{53} ergs of isotropic energy, with a black body temperature of 7.215 keV (see Fig. 16).

3.10. GRB 221009A

The Swift-BAT detected GRB 221009A, initially named Swift J1913.1+1946, on October 9 of 2022 at 14:10:17 UT (see top panel of Fig. 18). Swift-XRT began observing the field 143 seconds after the BAT trigger, identifying a bright, fading X-ray source at RA = 19h 13m 3.43s, Dec = +19d 46' 16.3" with an uncertainty of 5.6 arcseconds (see Fig. 19). The Swift-UVOT took an exposure 179 seconds after the BAT trigger, identifying a candidate counterpart with an estimated magnitude of 16.63 (Dichiara et al. 2022).

The Fermi-GBM team reported (Lesage et al. 2022b) that the time-averaged spectrum for the first emission episode is best fitted by a power-law function with an exponential high-energy cutoff. The photon index was found to be -1.70 ± 0.02, the exponential cutoff is at 375 ± 87 keV. The fluence in the 10-1000 keV range for this time interval was reported as $(2.12 \pm 0.05) \times 10^{-5}$ erg/cm^2.

For the high-energy observations made by Fermi LAT, Bissaldi et al. (2022) detailed the detection. The initial boresight angle was 94 degrees then the satellite rotated to point to the source. The spectral fitting from LAT observations revealed that in the time interval 500-3500 s after the Swift trig-

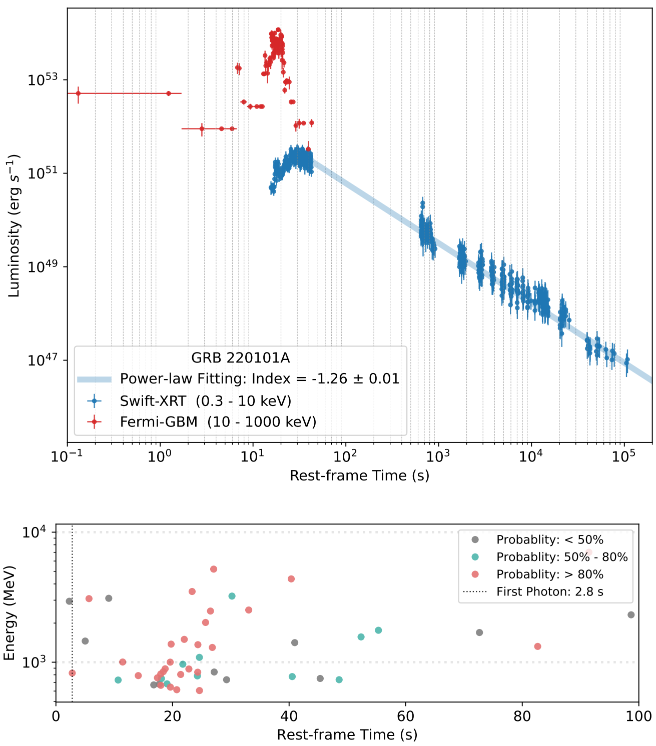

Fig. 17. Top: Luminosity light-curve of GRB 220101A, including the prompt emission and the afterglow, observed by Fermi-GBM and Swift-XRT, respectively. Bottom: GeV photons observed by Fermi-LAT.

ger, the photon flux in the range of 100 MeV - 1 GeV is $(1.27 \pm 0.16) \times 10^{-5}$ cm^2/s. The estimated photon index above 100 MeV is -2.12 ± 0.11. LAT observed a highest-energy photon of 7.8 GeV 766 seconds after the Swift trigger.

Observations of X-shooter instrument at ESO's Very Large Telescope began 11.55 hours after the Fermi GBM trigger and 10.66 hours after the Swift BAT trigger. The spectrum showed a very red continuum with absorption features corresponding to CaII, CaI, and NaID. These absorption features were used to determine a redshift of $z = 0.151$. Using this redshift and the GBM fluence, an $E_{\rm iso}$ value of 2×10^{54} erg is determined, placing GRB 221009A within the upper end of GRB energetics de Ugarte Postigo et al. (2022).

LHAASO detected GRB 221009A with significant findings that by LHAASO-WCDA above 500 GeV and LHAASO-KM2A, marking the first detection of photons above 10 TeV from GRBs. Above 100 standard deviations (s.d.) for LHAASO-WCDA and about 10 s.d. for LHAASO-KM2A. The highest photon energy reached 18 TeV (Huang et al. 2022).

Spectra of the afterglow of GRB 221009A were also obtained with JWST/NIRSpec under DDT program 2784 (P.I. Blanchard) on 2023 April 20, 193 observer-frame days after the burst. The spectrum, differing significantly from the earlier power-law continuum observed, indicates a considerable contribution from the SN/host galaxy. JWST/NIRSpec detected a feature centered at 1 micron, consistent with the Ca II IR triplet from a SN. Prominent narrow lines were also observed (Blanchard et al. 2023).

This GRB's SN-rise episode lasts from 0 to 15.0 seconds observed (0 to 13 seconds in the rest frame), with a duration of 13 seconds, of which the spectrum is best fitted by the Band function plus a blackbody component. It releases a much lower

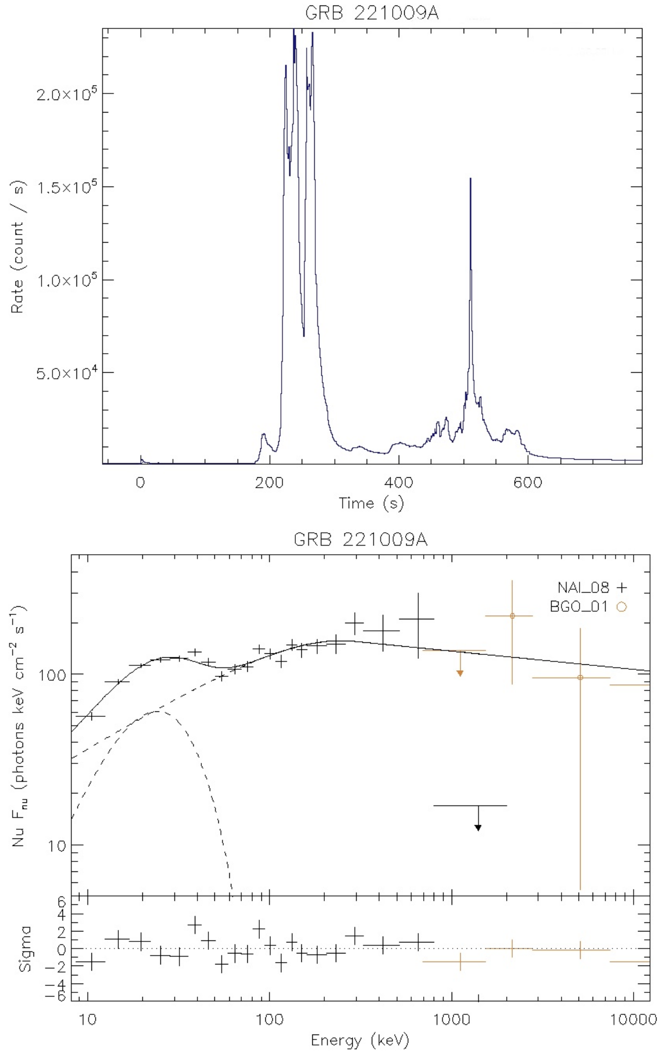

Fig. 18. Top: GRB 221009A light-curve, shadow part indicates the period of episode 1. Bottom: the spectrum of episode 1, fitted by the Band function plus a blackbody component, the observed temperature is 6.169 keV.

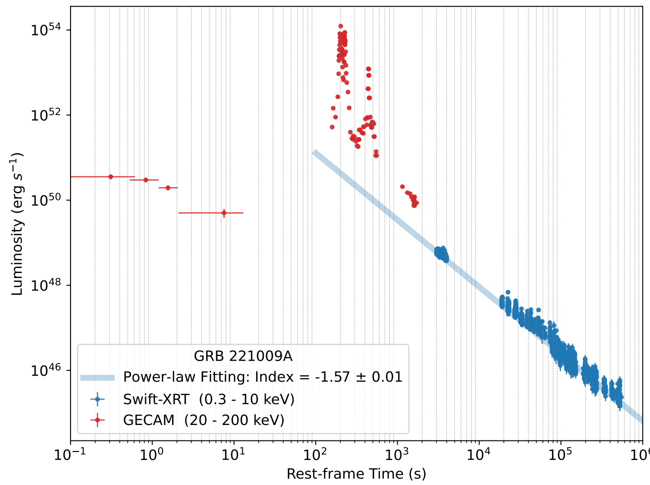

s

Fig. 19. Luminosity light-curve of GRB 221009A, including the prompt emission and the afterglow, observed by GECAM and Swift-XRT, respectively.

Table 1. GRB SN-rise properties: For each GRB Episode 1 is given its Trigger number, its redshift, its starting time t_s and ending time t_e both in the observed frame and in the GRB cosmological rest frame, its duration in the GRB cosmological rest frame, its isotropic equivalent energy $E_{iso}^{SN-rise}$, and its observed black body temperature.

GRB name	Trigger number	z	Episode	$t_s \sim t_e$ (s, obs.)	$t_s \sim t_e$ (s, rest)	Duration (s, rest)	$E_{iso}^{SN-rise}$ (10^{52}erg)	BB Temp. (keV, obs.)
090423	090423330	8.2	1 (SN-rise)	-5.5 ~ 7.4	-0.6~0.8	1.4	16	—
090429B	350854	9.4	1 (SN-rise)	0 ~ 10	0~0.96	0.96	3.5	—
090618	090618353	0.54	1 (SN-rise)	0 ~ 47.7	0~31	31	3.61	15.86
130427A	130427324	0.34	1 (SN-rise)	0 ~ 0.9	0~0.65	0.65	0.65	28.66
160509A	160509374	1.17	1 (SN-rise)	0 ~ 4.0	0~1.84	1.84	1.47	14.43
160625B	160625945	1.406	1 (SN-rise)	-1.2 ~ 3.1	-0.5~1.3	0.75	1.04	6.025
180720B	180720598	0.653	1 (SN-rise)	0 ~ 2.5	0~1.51	1.51	1.6 ± 0.3	17.67
190114C	190114873	0.425	1 (SN-rise)	0 ~ 1.1	0~0.79	0.79	3.5 ± 0.2	39.99
220101A	220101215	4.61	1 (SN-rise)	-1.0 ~ 20.0	-0.18~3.57	3.75	12	7.215
221009A	221009553	0.151	1 (SN-rise)	0 ~ 15.0	0~13	13	0.18 ± 0.01	6.169

$0.18 \pm 0.01 \times 10^{52}$ ergs of energy, with a black body temperature of 6.169 keV (see Fig. 18).

3.11. Challenges in Detecting Thermal Components of High Redshift GRBs

For GRBs at high redshifts, the detection of their thermal components becomes notably challenging compared to those at lower redshifts. This phenomenon can be attributed to two primary factors:

1. **Data Quality and Model Complexity**
   Introducing a thermal component to the fitting models introduces two additional degrees of freedom. Consequently, constraining the models with an additional thermal component mandates high-quality observational data.
   Considering GRBs at significant redshifts, like those at $z = 5$, the luminosity distance is magnified to be seven times that of GRBs situated at $z = 1$. This translates to a drastic reduction, about 50-fold, in the number of photons that can be observed. Moreover, if the selected time bin is small, there will be even fewer accumulated photons, making it more difficult to constrain a model that includes a thermal component.
2. **Cosmic Expansion and Energy Range Limitations**
   The universe's ongoing expansion plays a role in redshifting the thermal component of the GRB. This redshifting can push the thermal component towards, or even beyond, the peripheries of a telescope's bandwidth.
   Typically, the temperature of a GRB's thermal component hovers around tens of keV. Several GRBs in this article have temperatures ranging between 20-50 keV in their rest frames. Such temperatures, when emitting from a high redshift location like $z = 5$, undergo redshifting to fall between 3-8 keV by the time they reach Earth. The peak of a blackbody spectrum is situated at 2.82 times its temperature. This means the most discernible region of the thermal component lies between 10-25 keV. Given the Fermi-GBM NaI detector's energy bandwidth of 8-900 keV, the thermal component is located at the spectrum's lower energy edge. The blackbody spectrum, especially its ascent, might not be wholly observable. Adding another layer of difficulty to detect and fit the thermal component.

An illustrative example from this article is GRB 090423, which has a redshift of 8.2. The spectral data from its SN-rise phase (depicted in Figure 1) clearly reflects the aforementioned challenges. The spectrum has a limited number of data points, with a mere 4 points lying below 30 keV, which is not adequate to constrain an additional thermal component. While the spectrum fitting in Figure 1 employs the CPL model, this is more of a compromise due to sparse data. We cannot justify the presence of a thermal component in the intrinsic spectrum.

4. Conclusion

The duration, energetics and thermal component of the SN-rise for the ten sources are summarized in Table 1. The thermal component identified in the analysis of GRBs associated with supernovae is a significant aspect of these observations. This thermal component has been detected in all the 8 sources at redshifts less than 5. The temperatures of these thermal components range between 6.23 keV and 39.99 keV. These observations suggest a possible signature of pair-driven supernovae, indicative of the immense energy and the high-density environment in which these bursts occur. Such thermal emissions provide crucial insights into the physical conditions prevailing during the explosive events, contributing to our understanding of the mechanisms driving supernovae and associated GRBs.

References

Abdalla, H., Adam, R., Aharonian, F., et al. 2019, Nature, 575, 464
Aimuratov, Y., Becerra, L. M., Bianco, C. L., et al. 2023, ApJ, 955, 93
Amati, L., Dichiara, S., Frontera, F., & Guidorzi, C. 2013, GRB Coordinates Network, 14503, 1
Arimoto, M., Scotton, L., Longo, F., & Fermi-LAT Collaboration. 2022, GRB Coordinates Network, 31350, 1
Atteia, J. L. 2022, GRB Coordinates Network, 31365, 1
Becerra, L., Bianco, C. L., Fryer, C. L., Rueda, J. A., & Ruffini, R. 2016, ApJ, 833, 107
Becerra, L., Cipolletta, F., Fryer, C. L., Rueda, J. A., & Ruffini, R. 2015, ApJ, 812, 100
Becerra, L., Ellinger, C. L., Fryer, C. L., Rueda, J. A., & Ruffini, R. 2019, ApJ, 871, 14
Becerra, L., Guzzo, M. M., Rossi-Torres, F., et al. 2018, ApJ, 852, 120
Bianco, C. L., Mirtorabi, M. T., Moradi, R., et al. 2023, arXiv e-prints, arXiv:2306.05855
Bissaldi, E., Omodei, N., Kerr, M., & Fermi-LAT Team. 2022, GRB Coordinates Network, 32637, 1
Blanchard, P. K., Villar, V. A., Chornock, R., et al. 2023, GRB Coordinates Network, 33676, 1
Burns, E. 2016a, GRB Coordinates Network, 19581, 1
Burns, E. 2016b, GRB Coordinates Network, 19587, 1
Castro-Tirado, A. J., Hu, Y., Fernandez-Garcia, E., et al. 2019, GRB Coordinates Network, 23708, 1

Cherry, M. L., Yoshida, A., Sakamoto, T., et al. 2018, GRB Coordinates Network, 23042, 1
Cipolletta, F., Cherubini, C., Filippi, S., Rueda, J. A., & Ruffini, R. 2017, Phys. Rev. D, 96, 024046
Cucchiara, A., Fox, D. B., & Berger, E. 2009a, GRB Coordinates Network, 9213, 1
Cucchiara, A., Fox, D. B., & Berger, E. 2009b, GRB Coordinates Network, 9209, 1
Cucchiara, A., Levan, A., Tanvir, N., Fox, D. B., & Berger, E. 2009c, GRB Coordinates Network, 9286, 1
Cucchiara, A., Levan, A. J., Fox, D. B., et al. 2011, ApJ, 736, 7
de Ugarte Postigo, A., Izzo, L., Pugliese, G., et al. 2022, GRB Coordinates Network, 32648, 1
D'Elia, V., D'Ai, A., Sbarufatti, B., et al. 2019, GRB Coordinates Network, 23706, 1
D'Elia, V., Melandri, A., & Malesani, D. 2016, GRB Coordinates Network, 19601, 1
Dichiara, S., Gropp, J. D., Kennea, J. A., et al. 2022, GRB Coordinates Network, 32632, 1
Dirirsa, F., Vianello, G., Racusin, J., & Axelsson, M. 2016, GRB Coordinates Network, 19586, 1
Fryer, C. L., Oliveira, F. G., Rueda, J. A., & Ruffini, R. 2015, Physical Review Letters, 115, 231102
Fryer, C. L., Rueda, J. A., & Ruffini, R. 2014, ApJ, 793, L36
Fu, S. Y., Zhu, Z. P., Xu, D., Liu, X., & Jiang, S. Q. 2022, GRB Coordinates Network, 31353, 1
Fynbo, J. P. U., de Ugarte Postigo, A., Xu, D., et al. 2022, GRB Coordinates Network, 31359, 1
Galama, T. J., Vreeswijk, P. M., van Paradijs, J., et al. 1998, Nature, 395, 670
Gropp, J. D., Kennea, J. A., Klingler, N. J., et al. 2019, GRB Coordinates Network, 23688, 1
Hamburg, R., Veres, P., Meegan, C., et al. 2019, GRB Coordinates Network, 23707, 1
Huang, Y., Hu, S., Chen, S., et al. 2022, GRB Coordinates Network, 32677, 1
Izzo, L., Bianco, C. L., Muccino, M., Penacchioni, A. V., & Ruffini, R. 2013, International Journal of Modern Physics Conference Series, 23, 202
Izzo, L., Rueda, J. A., & Ruffini, R. 2012a, A&A, 548, L5
Izzo, L., Ruffini, R., Penacchioni, A. V., et al. 2012b, A&A, 543, A10
Kennea, J. A., Roegiers, T. G. R., Osborne, J. P., et al. 2016, GRB Coordinates Network, 19408, 1
Kocevski, D., Omodei, N., Axelsson, M., et al. 2019, GRB Coordinates Network, 23709, 1
Krimm, H. A., Beardmore, A. P., Evans, P. A., et al. 2009, GRB Coordinates Network, 9198, 1
Lesage, S., Meegan, C., & Fermi Gamma-ray Burst Monitor Team. 2022a, GRB Coordinates Network, 31360, 1
Lesage, S., Veres, P., Roberts, O. J., et al. 2022b, GRB Coordinates Network, 32642, 1
Levan, A., Warwick, U., Cucchiara, A., et al. 2009, GRB Coordinates Network, 9306, 1
Levan, A. J., Cenko, S. B., Perley, D. A., & Tanvir, N. R. 2013, GRB Coordinates Network, 14455, 1
Li, L., Rueda, J. A., Moradi, R., et al. 2023, ApJ, 945, 10
Longo, F., Bissaldi, E., Bregeon, J., et al. 2016a, GRB Coordinates Network, 19403, 1
Longo, F., Bissaldi, E., Vianello, G., et al. 2016b, GRB Coordinates Network, 19413, 1
Longo, F., Moretti, E., Barbiellini, G., et al. 2009, GRB Coordinates Network, 9524, 1
Maselli, A., Beardmore, A. P., Lien, A. Y., et al. 2013, GRB Coordinates Network, 14448, 1
McBreen, S. 2009, GRB Coordinates Network, 9535, 1
Melandri, A., D'Avanzo, P., D'Elia, V., et al. 2016, GRB Coordinates Network, 19585, 1
Melandri, A., Izzo, L., D'Avanzo, P., et al. 2019, GRB Coordinates Network, 23983, 1
Mirzoyan, R., Noda, K., Moretti, E., et al. 2019, GRB Coordinates Network, 23701, 1
Moradi, R., Rueda, J. A., Ruffini, R., et al. 2021, Phys. Rev. D, 104, 063043
Pozanenko, A., Minaev, P., & Volnova, A. 2013, GRB Coordinates Network, 14484, 1
Riechers, D. A., Walter, F., Bertoldi, F., et al. 2009, GRB Coordinates Network, 9322, 1
Roberts, O. J., Fitzpatrick, G., & Veres, P. 2016, GRB Coordinates Network, 19411, 1
Roberts, O. J. & Meegan, C. 2018, GRB Coordinates Network, 22981, 1
Rowlinson, A. & Ukwatta, T. N. 2009, GRB Coordinates Network, 9298, 1
Rueda, J. A., Li, L., Moradi, R., et al. 2022, ApJ, 939, 62
Rueda, J. A. & Ruffini, R. 2012, ApJ, 758, L7
Rueda, J. A., Ruffini, R., Karlica, M., Moradi, R., & Wang, Y. 2020, ApJ, 893, 148
Rueda, J. A., Ruffini, R., Moradi, R., & Wang, Y. 2021, International Journal of Modern Physics D, 30, 2130007
Ruffini, R. 2022, Astronomical and Astrophysical Transactions, 33, 191
Ruffini, R., Izzo, L., Muccino, M., et al. 2014, A&A, 569, A39
Ruffini, R., Melon Fuksman, J. D., & Vereshchagin, G. V. 2019, ApJ, 883, 191
Ruffini, R., Moradi, R., Rueda, J. A., et al. 2021, MNRAS, 504, 5301
Ruffini, R., Wang, Y., Enderli, M., et al. 2015, ApJ, 798, 10
Sasada, M., Nakaoka, T., Kawabata, M., et al. 2018, GRB Coordinates Network, 22977, 1
Schady, P., Baumgartner, W. H., Beardmore, A. P., et al. 2009, GRB Coordinates Network, 9512, 1
Selsing, J., Fynbo, J. P. U., Heintz, K. E., & Watson, D. 2019, GRB Coordinates Network, 23695, 1
Siegel, M. H., Burrows, D. N., Deich, A., et al. 2018, GRB Coordinates Network, 22973, 1
Tanvir, N., Levan, A., Wiersema, K., et al. 2009, GRB Coordinates Network, 9219, 1
Tohuvavohu, A., Gropp, J. D., Kennea, J. A., et al. 2022, GRB Coordinates Network, 31347, 1
Troja, E., Lipunov, V. M., Mundell, C. G., et al. 2017, Nature, 547, 425
Tsvetkova, A., Frederiks, D., Lysenko, A., et al. 2022, GRB Coordinates Network, 31433, 1
Tsvetkova, A. & Konus-Wind Team. 2022, GRB Coordinates Network, 31436, 1
Ukwatta, T. N., Barthelmy, S. D., Evans, P. A., et al. 2009, GRB Coordinates Network, 9281, 1
Ursi, A., Menegoni, E., Longo, F., et al. 2022, GRB Coordinates Network, 31354, 1
von Kienlin, A. 2009a, GRB Coordinates Network, 9229, 1
von Kienlin, A. 2009b, GRB Coordinates Network, 9251, 1
von Kienlin, A. 2013, GRB Coordinates Network, 14473, 1
Vreeswijk, P. M., Kann, D. A., Heintz, K. E., et al. 2018, GRB Coordinates Network, 22996, 1
Wang, X.-Y., Liu, R.-Y., Zhang, H.-M., Xi, S.-Q., & Zhang, B. 2019a, ApJ, 884, 117
Wang, Y., Rueda, J. A., Ruffini, R., et al. 2019b, ApJ, 874, 39
Wang, Y., Rueda, J. A., Ruffini, R., et al. 2022, ApJ, 936, 190
Woosley, S. E. & Bloom, J. S. 2006, ARA&A, 44, 507
Xu, D., Malesani, D., Fynbo, J. P. U., et al. 2016, GRB Coordinates Network, 19600, 1
Zhu, S., Racusin, J., Kocevski, D., et al. 2013, GRB Coordinates Network, 14471, 1